The effect of *Cyclopia maculata* extract on β-cell function, protection against oxidative stress and cell survival

by

Nireshni Chellan

Dissertation presented for the degree of *Doctor of Philosophy
(Medical Physiology) in the Faculty of Medicine and Health Sciences
at Stellenbosch University*

Supervisor: Dr C.J.F. Muller

Co-supervisors: Prof H. Strijdom and Prof E. Joubert

December 2014

Declaration

By submitting this thesis, I declare that the entirety of the work contained therein is my own, original work, that I am the sole author thereof (save to the extent explicitly otherwise stated), that reproduction and publication thereof by Stellenbosch University will not infringe any third party rights and that I have not previously in its entirety or in part submitted it for obtaining any qualification.

Nireshni Chellan

September 2014

II

ABSTRACT

Insights into the role of oxidative stress and pancreatic β-cell dysfunction in the pathogenesis of type 2 diabetes (T2D) reveals an opportunity for the development of novel therapeutics that directly protect and preserve β-cells. The protective role of dietary antioxidants, such as plant polyphenols, against oxidative stress induced diseases, including T2D, is increasingly under scrutiny. Polyphenol-rich extracts of *Cyclopia* spp, containing mangiferin, may provide novel therapeutics. An aqueous extract of unfermented *Cyclopia maculata*, containing more than 6 % mangiferin, was assessed for its protective effect in pancreatic β-cells *in vitro, ex vivo* and *in vivo* under conditions characteristic of T2D. The effect of mangiferin was also evaluated *in vitro* and *ex vivo*, with *N*-acetyl cysteine (NAC) as an antioxidant control.

In this study, we established *in vitro* toxicity models in RIN-5F insulinoma cells based on conditions β-cells are exposed to in T2D; i.e. lipotoxicity, inflammation and oxidative stress conditions. To achieve this, cells were exposed to the following stressors: palmitic acid (PA), a pro-inflammatory cytokine combination and streptozotocin (STZ), respectively. Thereafter, the ability of the *C. maculata* extract, mangiferin and NAC to protect RIN-5F cells from the effects of these stressors was assessed by measuring β-cell viability, function and oxidative stress. Cell viability was assessed using the 3-(4,5-dimethylthiazol-2-yl)-2,5-diphenyltetrazolium bromide, adenosine triphosphate and annexin-V and propidium iodide assays. Cell function was evaluated by measuring glucose stimulated insulin secretion, cell proliferation and cellular calcium. To assess oxidative stress in the RIN-5F cells, diaminofluorescein-FM and dihydroethidium fluorescence, and superoxide dismutase enzyme activity were measured. The *in vitro* findings were then verified in isolated pancreatic rat islets using methods and models established in the RIN-5F experiments. The protective effect of the extract, NAC and metformin was assessed in STZ induced diabetic Wistar rats, using two treatment regimes, i.e. by treating rats with established diabetes and by pretreating rats prior to induction of diabetes by STZ. Glucose metabolism, oxidative stress and pancreatic morphology were assessed by performing an oral glucose tolerance test, measuring serum insulin, triglycerides, nitrites, catalase and glutathione. Hepatic thiobarbituric acid reactive substances and nitrotyrosine were also assessed. Immunohistochemical labelling of pancreata with insulin, glucagon and MIB-5 was used for morphological assessment.

The extract improved β-cell viability, function and attenuated oxidative stress, most apparently in STZ and PA induced toxicity models comparable with NAC both *in vitro* and in isolated islets. Mangiferin was not as effective, showing only marginal improvement in RIN-5F cell and islet function, and oxidative stress. Pretreatment of STZ induced diabetic Wistar rats with extract was as effective as, if not better than, metformin in improving glucose tolerance, hypertriglyceridaemia and pancreatic islet morphology related to improved β-cell function.

This study demonstrated that the aqueous extract of unfermented *C. maculata* was able to protect pancreatic β-cells from STZ and PA induced toxicity *in vitro* and *ex vivo*. *In vivo,* pretreatment with the extract improved glucose metabolism and pancreatic islet morphology in STZ induced diabetic Wistar rats.

OPSOMMING

Insigte oor die rol wat oksidatiewe stres en pankreas β-sel disfunksie in die patogenese van tipe 2-diabetes (T2D) speel, bied 'n geleentheid vir die ontwikkeling van nuwe terapeutiese middels wat β-selle direk daarteen beskerm. Die beskermende rol van antioksidante in die dieët soos plantaardige polifenole teen oksidatiewe stres geinduseerde siektes soos T2D, is toenemend onder die soeklig. Polifenolryk ekstrakte van *Cyclopia spp* wat mangiferin bevat mag nuwe terapeutiese middels lewer. 'n Waterekstrak van ongefermenteerde *Cyclopia maculata* wat meer as 6% mangiferin bevat, is ondersoek vir sy beskermende effek op pankreas ß-selle *in vitro, ex vivo* en *in vivo* teen kondisies kenmerkend aan T2D. Die effek van mangiferin is ook *in vitro* en *ex vivo* geëvalueer, met *N*-asetielsistien (NAC) as 'n antioksidant kontrole.

In hierdie studie is *in vitro* toksisiteitsmodelle in RIN-5F insulinoomselle gevestig. Die modelle is gebaseer op toestande waaraan β-selle blootgestel word tydens T2D; d.w.s. lipotoksisiteit, inflammasie en oksidatiewe stres. Hiervoor is die selle aan die volgende stressors blootgestel: palmitiensuur (PA), 'n pro-inflammatoriese sitokien mengsel en streptozotosien (STZ). Vervolgens is die vermoë van die *C. maculata* ekstrak, mangiferin en NAC om die RIN-5Fselle teen hierdie stressors te beskerm, beoordeel deur die meting van β-sellewensvatbaarheid, funksie en oksidatiewe stres. Sellewensvatbaarheid is bepaal met 3-(4,5-dimetielthiazol-2-yl)-2,5-difenieltetrazolium bromied, adenosientrifosfaat en anneksien-V and propidium jodied toetse. Selfunksie is geëvalueer d.m.v. glukose gestimuleerde insuliensekresie, selproliferasie en sellulêre kalsium bepaling. Oksidatiewe stres in die RIN-5Fselle is geëvalueer d.m.v. diaminofluorescein-FM en dihidroethidium fluoressensie bepalings, asook meting van superoksied dismutase ensiemaktiwiteit. Die *in vitro* bevindings is daarna in geïsoleerde rot pankreaseilande bevestig deur die metodes en modelle wat in die RIN-5F eksperimente gebruik is. Die antidiabetiese effekte van die ekstrak, NAC en metformien in STZ-geïnduseerde diabetiese Wistar rotte is bepaal d.m.v. twee behandlingsregimes, d.w.s. die behandeling van rotte met gevestigde diabetes of deur die behandeling voor die induksie van diabetes te begin. Glukose metabolisme, oksidatiewe stres en veranderinge in die pankreasmorfologie is ondersoek d.m.v. orale glukose toleransie toetse en die bepaling van serum insulien, trigliseriedes, nitriete, katalase en glutationien. Hepatiese tiobarbituursuur reaktiewe stowwe en nitrotirosien is ook geëvalueer. Immunohistochemiese kleuring van pankreas snitte is gebruik vir morfologiese assessering van insulien, glukagon en MIB-5.

Die ekstrak het mees opvallend β-sel lewensvatbaarheid en funksie verbeter, terwyl oksidatiewe stres verminder is in die STZ- en PA-geïnduseerde toksisiteitmodelle. Bogenoemde effekte van die ekstrak *in vitro* en in die geïsoleerde eilande was vergelykbaar met die van NAC. Mangiferin was minder effektief, met slegs 'n marginale verbetering in die funksie van RIN-5Fselle en eilande, asook t.o.v. oksidatiewe stres. Behandeling van die Wistar rotte met die ekstrak voor induksie van diabetes met STZ was net so effektief, of selfs beter as metformien in terme van verbeterde glukosetoleransie, trigliseriedvlakke en die morfologie van pankreas eilande wat verband gehou het met β-sel funksie.

Hierdie studie het getoon dat die waterekstrak van ongefermenteerde *C. maculata* pankreas β-selle teen veral STZ- en PA-geïnduseerde toksisiteit *in vitro* en *ex vivo* beskerm het. *In vivo* het behandeling met die ekstrak voor en na induksie van diabetes, glukosemetabolisme en die morfologie van pankreas eilande in STZ-geïnduseerde diabetiese Wistar rotte verbeter.

VI

ACKNOWLEDGEMENTS

The completion of this doctoral degree would not have been possible without the assistance, support, collaboration and contributions of the following people and/or institutes:

I would like to dedicate the dissertation herewith to my parents,

Ronald & Ranjeni Chellan;

I love you both and appreciate everything you have sacrificed for and given to me.

TABLE OF CONTENTS

X

LIST OF FIGURES

Chapter 4

XVII

Chapter 5

LIST OF TABLES

ABBREVIATIONS

ADP -	Adenosine diphosphate
AGE -	Advanced glycation end product
ALT -	Alanine transaminase
AMPK -	5'-Adenosine monophosphate-activated protein kinase
ANOVA -	Analysis of variance
AP -	Alkaline phosphatase
AST -	Aspartate aminotransferase
ATP -	Adenosine triphosphate
AUC -	Area under the curve
BCL-2 -	β-cell lymphoma-2
BSA -	Bovine serum albumin
C. mac. -	*Cyclopia maculata*
cAMP -	Cyclic adenosine monophosphate
CAT-	Catalase
CM -	Cytokine mixture
CO_2 -	Carbon dioxide
DAF -	Diaminofluorescein-FM diacetate
DHE -	Dihydroethidium
DMNQ -	2,3-dimethoxy-1,4-naphthoquinone
DMSO -	Dimethyl sulphoxide
DNA -	Deoxyribonucleic acid
DPBS -	Dulbecco's phosphate buffered saline
DPP-IV -	Dipeptidyl peptidase-4
EDTA -	K2 ethylenediaminetetraacetic acid
EGCG -	Epigallocatechin gallate
ELISA -	Enzyme-linked immunosorbent assay
ER -	Endoplasmic reticulum
Ex/em -	Excitation/emission
FA -	Fatty acid
FAS -	Fatty acid synthase
FBS -	Fetal bovine serum
Fe -	Iron

FITC - Fluorescein isothiocyanate

Fluo3-AM - N-[4-[6-[(acetyloxy)methoxy]-2,7-dichloro-3-oxo-3H-xanthen-9-yl]-2-[2-[2-[bis[2-[(acetyloxy)methoxy]-2-oxyethyl]amino]-5-methylphenoxy]ethoxy]phenyl]-N-[2-[(acetyloxy)methoxy]-2-oxyethyl]-(acetyloxy)methyl ester

G6Pase - Glucose-6-phosphatase

GK - Glucokinase

GLP-1 - Glucagon-like peptide-1

GLUT-2 - Glucose transporter-2

GLUT-4 - Glucose transporter-4

GPDH - Glycerol-3-phosphate dehydrogenase

GSH - Glutathione

GSIS - Glucose stimulated insulin secretion

HBSS - Hanks balanced salt solution

HGP - Hepatic glucose production

HOMA-IR - Homeostatic model of assessment of insulin resistance

HPLC-DAD - High performance liquid chromatography with diode-array detection

IDF - International Diabetes Federation

IFN-γ - Interferon-γ

IL-1β - Interleukin-1β

IL-6 - Interleukin-6

IL-8 - Interleukin-8

INS - Insulin

IRS - Insulin receptor substrate

IVGTT - Intravenous glucose tolerance test

JNK - c-Jun N-terminal kinase

KRBH - Krebs-Ringer bicarbonate-HEPES buffer

LC_{50} - Lethal concentration 50

LC-CoA - Long-chain acyl coenzyme A

MAPK - Mitogen-activated protein kinase

MCP-1 - Monocyte chemotactic protein-1

mRNA - Messenger ribonucleic acid

MS - Multi-stressor

MTT - 3-(4,5-dimethylthiazol-2-yl)-2,5-diphenyltetrazolium bromide tetrazolium

NAC - _N_-acetyl cysteine

NAD(P)$^+$ - Nicotinamide adenine dinucleotide phosphate

NAD(P)H$^+$ - Nicotinamide adenine dinucleotide phosphate (reduced)

NaOH - Sodium hydroxide

NEFA - Non-esterified fatty acid

NF-κB - Nuclear factor-kappa B

OGTT - Oral glucose tolerance test

PA - Palmitic acid

PDX-1 - Pancreatic duodenal homeobox-1

PEPCK - Phosphoenolpyruvate carboxykinase

PI3K - Phosphatidylinositol-3-kinase

PMSF - Phenylmethanesulfonyl fluoride

PPAR - Peroxisomal proliferator-activated receptor

PUDAC - Primate Unit and Delft Animal Centre

PVDF - Polyvinylidene difluoride

RC/DC - Reducing agent compatible and detergent compatible

RNS - Reactive nitrogen species

ROS - Reactive oxygen species

RPMI1640 - Roswell Park Memorial Institute 1640 media

SDS - Sodium dodecyl sulphate

SDS-PAGE - Sodium dodecyl sulphate-polyacrylamide gel electrophoresis

SGLT - Sodium-glucose co-transporter

SOD - Superoxide dismutase

SST - Serum separating tube

STZ - Streptozotocin

T2D - Type 2 diabetes

TBARS - Thiobarbituric acid reactive substances

TBST - Tris buffered saline containing Tween®20 detergent

TCA - Tricarboxylic acid

TG - Triglycerides

TNF- α - Tumour necrosis factor-α

TZD - Thiazolidinedione

UCP-2 - Uncoupling protein-2

UPR - Unfolded protein response

WST-1 -   Water soluble tetrazolium salt-1

ZAR -   South African Rand

α -   Alpha

β -   Beta

γ -   Gamma

δ -   Delta

˙OH -   Hydroxyl radical

CHAPTER 1

INTRODUCTION

The incidence of type 2 diabetes (T2D) is dramatically increasing (Shaw *et al.*, 2010), not only globally, but also here in South Africa (Bertram *et al.*, 2013). The socio-economic burden of this disease epidemic is not only direct (i.e. treatment of hyperglycemia), but is further exacerbated by health complications associated with this metabolic disease (Kirigia *et al.*, 2009; Bertram *et al.*, 2013). These complications include retinopathy, nephropathy, neuropathy, cardiovascular diseases, as well as physical disability due to surgical amputation of limbs as a result of vascular insufficiency (Bertram *et al.*, 2013). In Africa, the economic burden of this disease was estimated at 11 431.60 international dollars (i.e. Geary-Khamis dollars) per T2D patient per year (Kirigia *et al.*, 2009). With over nine percent of adults over thirty being diagnosed as T2D, and still a further estimated 55 % of undiagnosed cases (Bertram *et al.*, 2013), austere strain is added to an already challenged national health system in South Africa. New therapeutic avenues in treating T2D are needed to avoid or delay the onset of the co-morbidities associated with T2D. New insights into the role of oxidative stress and pancreatic β-cell dysfunction in the pathogenesis of T2D offers opportunities for novel therapeutics (Kaneto *et al.*, 1999; Lee *et al.*, 2011). Increasingly, the protective role of dietary antioxidants against oxidative stress-induced degenerative and age-related diseases is under scrutiny in order to find candidates that could ameliorate T2D associated β-cell dysfunction (Frei, 2004; Scalbert *et al.*, 2005; Lee *et al.*, 2011).

The progression of T2D has typically been described as a steady decline in insulin action (insulin resistance), followed by the inability of pancreatic β-cells to compensate for the higher insulin demand required to maintain glucose homeostasis (Porte, 1991; Arora, 2010; Aziz and Wheatcroft, 2011). Pancreatic β-cell dysfunction has recently been proposed as a putative mechanism, and may, in fact, play a bigger role in the earlier stages of T2D than originally thought (Meier and Bonadonna, 2013). This said, protecting the vulnerable β-cell is becoming increasingly important, making it a high priority therapeutic target. Much emphasis has been placed in preserving β-cell number/mass, which has been shown to be severely reduced in autopsy studies of T2D patients (Butler *et al.*, 2003). Concomitant preservation of β-cell function is also necessary since chronic β-cell stress (e.g. insulin hyper-secretory demand, hyperglycemia, and hypertriglyceridemia) has been shown to cause β-cell dysfunction and eventual failure (Meier and Bonadonna, 2013). Hence, preservation of the *functional* β-cell mass and not just β-cell number should be a priority. As Bertram *et al.* (2013) concluded in their study, "Some of the attributed burden (of T2D) can be prevented through early detection and treatment". The question thus arises if efforts to

26

preserve functional β-cell mass could improve treatment success and reduce the burden of T2D not just here in South Africa, but also globally.

Previous studies have demonstrated that T2D patients have elevated levels of oxidative stress (Johansen *et al.*, 2005; Houstis *et al.*, 2006). Pancreatic β-cells are particularly sensitive to oxidative stress due to their low cellular levels of free-radical quenching enzymes such as glutathione peroxidase and superoxide dismutase (Abdollahi *et al.*, 2004). Long term complications of T2D may be exacerbated by oxygen-free radical activity (e.g. reactive nitrogen species) which can initiate peroxidation of lipids and the associated deleterious downstream effects thereof (Baynes, 1991).

Current clinical T2D therapies include biguanides, sulfonylureas and thiazolidinediones (TZDs), which act predominantly by enhancing insulin action (Seufert *et al.*, 2004). Recently, newer therapeutic approaches, including incretin mimetics and dipeptidyl peptidase-IV (DPP-IV) inhibitors, have been introduced either exclusively in a few cases, or more commonly, in combination with current clinical therapies (Vinik, 2007). Apart from a few negative side-effects, including gastrointestinal upsets, current therapies have been effective in the management of T2D; albeit limited in long-term treatment, with many patients resorting to insulin therapy. A key factor to consider is protection of the functional β-cell mass by increasing the efficacy of T2D treatment in the long-term. The biguanide metformin has been shown to indirectly improve β-cell function in the short term (Wiernsperger and Bailey, 2009). Similar to metformin, TZDs appear to exert beneficial effects on β-cell function. There is, however, no current clinical evidence of direct protection of β-cells by these therapies. Since metformin generally tends to target catabolic pathways (i.e. glycolysis) and TZDs tend to target anabolic pathways (i.e. glycogenesis), a synergy in the combination of the two has been demonstrated (Seufert *et al.*, 2004). With integrated combination therapies being so multifaceted, they are now being promoted in the clinical treatment and management of T2D (Tibaldi, 2014). Coupling classical clinical therapies such as biguanides, sulfonylureas and TZDs with newer incretin based therapies has proved beneficial since both incretin mimetics and DPP-IV inhibitors have been shown to exert both pancreatic and extra-pancreatic glucoregulatory effects (Bosi *et al.*, 2008). Exploiting the incretin hormones and enteroinsular axis have been shown to assist in the preservation of both β-cell mass and function (Bosi *et al.*, 2008; Tibaldi, 2014). Safety in the long-term and

high cost implications are still major concerns facing the use of incretin based therapies (Tibaldi, 2014).

A window of opportunity presents itself for the development of therapeutic agents specifically and directly targeting the protection and preservation of a functional pancreatic β-cell mass. Apart for the enormous health benefits, such an agent developed indigenously will provide much needed socio-economic benefits locally. The World Health Organisation (WHO) developed the "Traditional Medicine Strategy" to better manage traditional medicines and their usage, and outlined the interest in plant-derived medicines, as well as the need for proper safety and scientific validation (World Health Organisation, 2002). Plant polyphenols have been described as possessing both anti-inflammatory and antioxidative properties (Hanhineva *et al.*, 2010) and are increasingly pursued as alternatives to pharmaceutical intervention (Ding *et al.*, 2013). As far back as 1980, Logani and Davies suggested that supplementation with non-toxic antioxidants may have a chemoprotective role in T2D by ameliorating oxidative stress. Antioxidants (*N*-acetyl cysteine and vitamins C and E) have been shown to preserve β-cell function *in vivo* (Kaneto *et al.*,1999). The second generation sulphonylurea, glibenclamide, has also been shown to be effective in treating moderate hyperglycemia, not just by reducing elevated blood glucose levels, but also by restoring antioxidant activities in the tissues of diabetic animals (Rahimi *et al.*, 2005). The efficacy of various South African plant-derived traditional medicines used to treat T2D has been verified both in *in vitro* and *ex vivo* experimentation (Deutschlander *et al.*, 2009). Their efficacy was assessed in terms of glucose uptake and utilisation, with no emphasis on potential amelioritive or protective effects in pancreatic β-cells. South African herbal teas, in particular rooibos and honeybush (*Cyclopia* spp.), have become well-known for their antioxidant properties, associated with their phenolic constituents (Joubert *et al.*, 2008). The ubiquitous presence of the xanthone mangiferin in *Cyclopia* spp. not only contribute to their *in vitro* antioxidant activity (Joubert et al., 2008), but most likely promote the anti-diabetic effects observed for *C. intermedia* (Muller *et al.*, 2011). In addition to its antioxidant properties (Sanchez *et al.*, 2000; Leiro *et al.*, 2003), several studies have demonstarted anti-diabetic actions of mangiferin (Ichiki *et al.*, 1998; Miura *et al.*, 2001; Muruganandan *et al.*, 2002; Sellamuthu *et al.*, 2013).

In this study, we developed a range of *in vitro* and *ex vivo* experimental models in which to assess the efficacy of an aqueous extract from unfermented *C. maculata,* one of the

28

Cyclopia spp. showing commercial potential as a cultivated crop, in protecting pancreatic β-cells exposed to conditions mimicking that of T2D. The major phenolic constituents of the extract, including the mangiferin content, were determined by high-performance liquid chromatography coupled to diode-array detection. A model of streptozotocin (STZ)-induced diabetes was used to determine the *in vivo* effect in rats.

In vitro, the RIN-5F pancreatic β-cell model in this study incorporated stressors associated with T2D such as hyperlipidemia, exogenous cytotoxins and inflammation. Elevated levels of palmitic acid (PA) were used to induce hyperlipidemic conditions, STZ was used as an exogenous cytotoxin and inflammation was induced by a combination of inflammatory cytokines (i.e. TNF-α, IFN-γ and IL-1β). The *ex vivo* model in this study involved the isolation of pancreatic islets from Wistar rats and the treatment thereof based on the findings of the *in vitro* experiments. The efficacy of the *C. maculata* extract in terms of β-cell protection in the RIN-5F cells and the isolated islets was tested under these conditions and compared to *N*-acetyl cysteine (NAC), as well as mangiferin.

RIN-5F cell viability was assessed by measuring mitochondrial dehydrogenase (MDH) activity using the MTT assay and by quantifying cellular ATP. Furthermore, apoptosis and necrosis were assessed by annexin-V and propidium iodide fluorescent staining. The function of RIN-5F cells was evaluated in terms of cellular calcium, proliferation and insulin secretion. The antioxidant status of these cells was assessed by measuring cellular antioxidant enzymes, as well as reactive oxygen species (ROS) and nitrogen species (RNS) staining with fluorescent probes. Cellular proteins associated with apoptosis and β-cell function were assessed by Western blot analysis. Cell viability of isolated pancreatic islets was measured by annexin-V and propidium iodide fluorescent staining, β-cell function using an insulin secretion assay, and antioxidant status by measuring ROS, RNS and cellular antioxidant enzymes. To assess the *in vivo* efficacy of the *C. maculata* extract, rats were treated with the extract, metformin and NAC either before induction of diabetes with STZ or after. Glucose tolerance was assessed by means of an oral glucose tolerance test (OGTT) and by measuring serum insulin. Other blood parameters measured, included serum triglycerides, alkaline phosphatase (AP), aspartate aminotransferase (AST) and alanine aminotransferase (ALT). In addition, the oxidative status of the rats was extensively studied using the following assays: serum nitrites, catalase (CAT) and glutathione (GSH), as well as liver thiobarbituric acid reactive substances (TBARS) and nitrotyrosine (ρNK-β). The

pancreases of the rats were assessed by immunohistochemical staining using insulin and glucagon double labelling, as well as the proliferation marker MIB-5. Using the parameters mentioned above, our objective was to determine the potential protective effect of an aqueous extract of unfermented *C. maculata* on pancreatic β-cells.

CHAPTER 2

LITERATURE REVIEW

1. Type 2 diabetes mellitus

Type 2 diabetes (T2D) is by far the most prominent form of diabetes mellitus, accounting for approximately 90 % of all cases according to the International Diabetes Federation (IDF). Other forms of diabetes mellitus, such as type 1, type 3, secondary and gestational diabetes, account for most of the remaining 10 % of cases (IDF, 2013). The incidence and prevalence of T2D are dramatically increasing both globally (Shaw *et al.*, 2010; IDF, 2013) as well as locally, in South Africa (Bertram *et al.*, 2013). This disease has been described as one of the greatest challenges to healthcare systems and has previously been underrated as a threat to global public health (Alberti and Zimmet, 2014). According to the IDF, 382 million people worldwide are living with diabetes (Fig. 1), with a further 46 % of the international population still undiagnosed (IDF, 2013). At the current rate at which T2D is increasing globally, one in ten adults will be afflicted with this disease by 2035 (IDF, 2013). In Africa, approximately 56 % of diabetic cases are undiagnosed (IDF, 2013). Just under five percent of the global population of diabetic patients are found in Africa (regional prevalence = 4.8 %), with South Africa tipping the scale with a national prevalence of over seven percent (IDF, 2013).
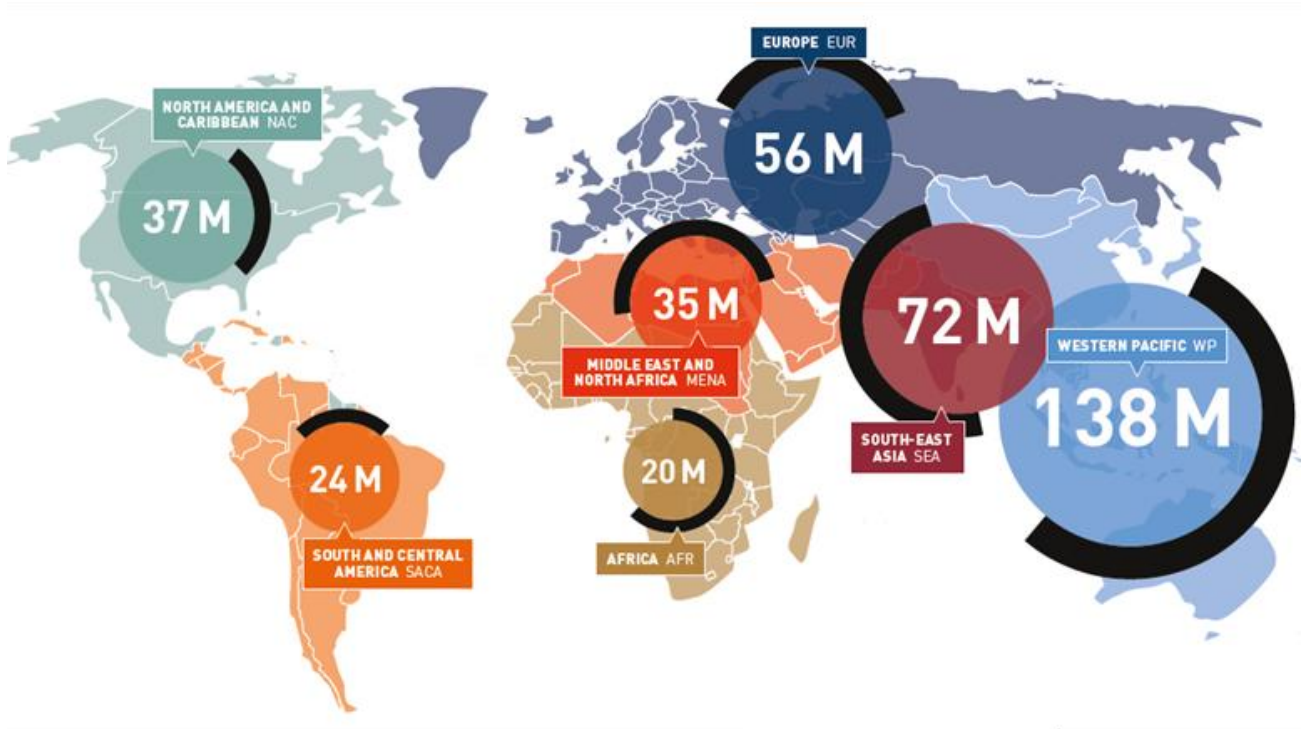
Figure 1. Prevalence of T2D worldwide.

The prevalence of T2D is increasing worldwide, with 20 million T2D patients in Africa. Western Pacific countries contribute the highest number of T2D patients (138 million) to the global prevalence of 382 million (from IDF, 2013).

32

1.1. Burden of disease

The burden of this disease epidemic on low- and middle-income countries is substantial as these countries account for approximately 80 % of T2D patients worldwide (Shaw *et al*., 2010; IDF, 2013). The socio-economic burden of T2D is already significant in Africa and as lifestyle changes and urbanisation increase so too is the prevalence of T2D predicted to increase dramatically over the next 20 years by approximately 109 %. With such a high percentage of undiagnosed cases in Africa, the financial burden of the disease is exacerbated since the benefits of early diagnosis are lost (Kirigia *et al*., 2009; IDF, 2013). The financial cost of T2D is two-fold, loss of economic and social productivity, as well as increased health costs (IDF, 2013). According to Statistics South Africa, T2D was amongst the top ten leading causes of death in South Africa in 2010, accounting for approximately 21 deaths in 1000 (Statistics South Africa, 2010). Health costs are further exacerbated by complications associated with this metabolic disease (Kirigia *et al*., 2009; Bertram *et al*., 2013). These complications include retinopathy, nephropathy, neuropathy, poor oral health and micro- and macro-vascular diseases, including coronary heart and cerebrovascular diseases (Fig. 2) (Bertram *et al*., 2013; IDF, 2013). Physical disability due to surgical amputation of limbs as a result of peripheral vascular insufficiency is also a confounding element (Bertram *et al*., 2013).

In Africa, the economic burden of T2D was estimated at 11 431.60 international dollars (i.e. Geary-Khamis dollars, which is a hypothetical currency with the same purchasing power parity as the US dollar) per T2D patient per annum in 2000 (Kirigia *et al*., 2009), which equates to approximately ZAR 120 760. According to the latest published statistics, there were 1 283 000 T2D patients in South Africa in 2010 (Statistics South Africa, 2010 and Bertram *et al*., 2013), which means that at ZAR 120 760 per person per annum, the cost of T2D alone far exceeds the budget allocated to South African National Healthcare. Not even the 2014/15 budget of ZAR 145.7 billion is sufficient to compensate for 2010 diabetes costs (South African National Treasury, 2014).
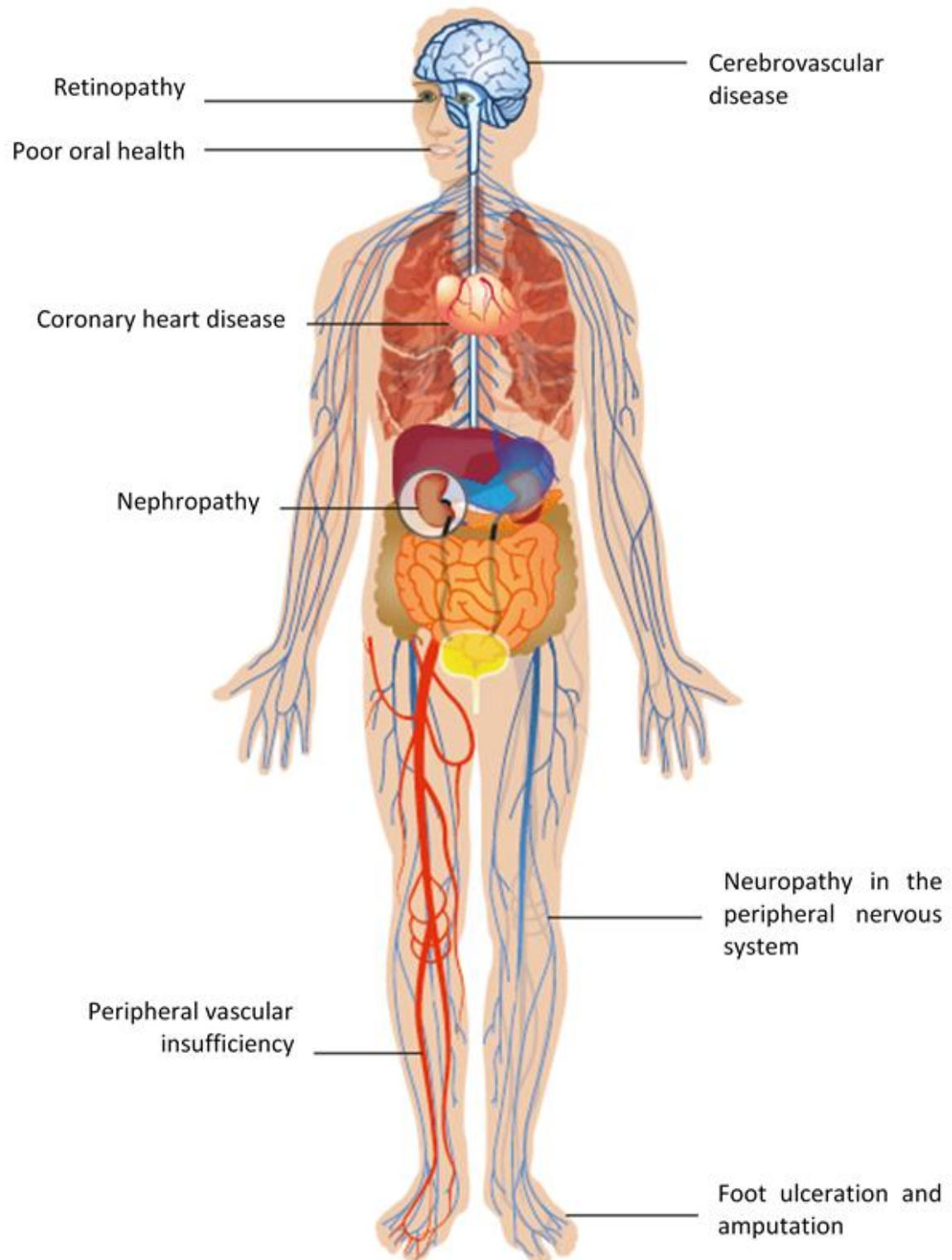
Figure 2.Type 2 diabetes-associated complications.

Several health complications are associated with T2D, and they include cerebrovascular disease, neuropathy, foot ulcerations, peripheral vascular insufficiency, nephropathy, coronary heart disease, poor oral health and retinopathy (adapted from IDF, 2013).

1.2. Pathophysiology of type 2 diabetes

Typically in T2D, insulin action steadily declines, followed by the inability of pancreatic β-cells to compensate for the higher insulin demand required to maintain glucose homeostasis (Porte, 1991; Arora, 2010; Aziz; Wheatcroft, 2011). In the insulin resistant state, β-cells compensate by hypersecretion of insulin, hypertrophy and hyperplasia; failure of these cells to adequately compensate results in hyperglycaemia (Weir and Bonner-Weir, 2004; Arora, 2010; Quan *et al.,* 2013). Chronic hyperglycaemia, hypoinsulinaemia and disturbances in carbohydrate, lipid and protein metabolism are characteristic of T2D (Kahn *et al.,* 2006). Fundamental in the progression of this disease are the deleterious effects of inflammation and oxidative stress, which exacerbate the insulin resistant state and both directly and indirectly influence the failure of β-cells (Kahn *et al.,* 2014). Furthermore, compensatory failure of β-cells is often followed by a reduction in β-cell mass as a result of increased cell death and reduced cell renewal (either by proliferation or neogenesis) (Bonner-Weir and O'Brien, 2008; Meier and Bonadonna, 2013).

1.2.1. Defective insulin signalling

Insulin signalling defects play significant roles in many metabolic diseases, including T2D (Rask-Madsen and Kahn, 2012). Insulin is a peptide hormone, produced by pancreatic β-cells, that regulates carbohydrate, protein and lipid metabolism, as well as vascular compliance (Nedachi and Kanzaki, 2006). Insulin binds to the insulin receptor on cell surfaces, thereby activating the receptor and initiating a cascade of phosphorylation events, second messenger generation, and protein-protein interactions heterogeneously throughout various tissue types (Meerza *et al.,* 2013). Under normal conditions, insulin regulates the hypothalamus, hepatocytes, adipocytes, cardiac and skeletal muscle, macrophages, endothelial cells, and the very β-cells that produce the hormone (Fig. 3) (Rask-Madsen and Kahn, 2012). In the hypothalamus, insulin binding to its receptor on neuronal cells suppresses appetite which is, in part, mediated by melanocortin. Suppression of melanocortin activity and increased appetite was observed in obese individuals (Benoit *et al.,* 2002). Another important function of insulin in the hypothalamus is suppression of hepatic glucose production (HGP), which is mediated by the vagal nerve (Rask-Madsen and Kahn, 2012). Insulin also has direct effects on hepatocytes, which include the suppression of gluconeogenesis (glucose production) and glycogenolysis (glycogen breakdown), and the stimulation of glucose uptake and glycogenesis (glycogen synthesis). Insulin is also responsible for stimulation of lipogenesis as well as the inhibition of lipoprotein lipase (Rask-

35

Madsen and Kahn, 2012; Meerza *et al.,* 2013). Defective insulin signalling results in a significant increase in HGP, as well as circulating non-esterified fatty acids (NEFAs) and triglycerides. The ability of insulin to increase glucose uptake and glycogenesis in skeletal muscle is impaired in T2D and insulin resistant states, and, in conjunction with increased HGP, results in hyperglycaemia (Nedachi and Kanzaki, 2006; Rask-Madsen and Kahn, 2012; Meerza *et al.,* 2013). The inability of insulin to suppress lipolysis and stimulate lipogenesis in insulin resistant adipose tissue and the liver results in further increased levels of circulating NEFAs and triglycerides. In addition, defective insulin signalling results in the accumulation of macrophages, as a result of an increase in the chemotactic response, in adipose tissue, exacerbating obesity associated insulin resistance and inflammation (Rask-Madsen and Kahn, 2012; Meerza *et al.,* 2013). Insulin increases blood flow by vasodilation and capillary perfusion, thereby contributing to increased delivery of both insulin and glucose to tissues such as skeletal muscle and adipose tissues. Elevated insulin stimulates transendothelial transport of the hormone to target tissues (Laakso *et al.,* 1990; Rask-Madsen and Kahn, 2012). The insulin-producing β-cells are also responsive to the secreted hormone; under normal conditions, insulin promotes β-cell proliferation and glucose sensing ability (via glucokinase regulation), and reduces apoptosis (Leibiger *et al.,* 2002; Rask-Madsen and Kahn, 2012). Insulin dependent increase in cytosolic calcium is responsible for the rapid and sustained exocytosis of insulin during the first phase of secretion (Leibiger *et al.,* 2002). This autocrine effect of insulin involves the regulation of downstream first phase insulin secretion via the activation of phosphatidylinositol-3-kinase (PI3-K) and regulation of gene transcription and translation (e.g. pancreatic homeobox-1 - PDX-1) (Leibiger *et al.,* 2002). The role of insulin on β-cell potassium channels is still not clearly illucidated, however it is suggested that insulin activation of PI3-K may be responsible for opening of these channels, thus modulating insulin secretion (Leibiger *et al.,* 2002). The inability of β-cells to secrete stored insulin in response to a glucose challenge, as observed in impaired glucose tolerance tests, may be as a result of defective insulin signalling in the β-cells themselves. Insulin signalling defects in the β-cell also result in failure of compensatory hyperplasia, and, in fact, increases β-cell death by apoptosis (Rask-Madsen and Kahn, 2012).
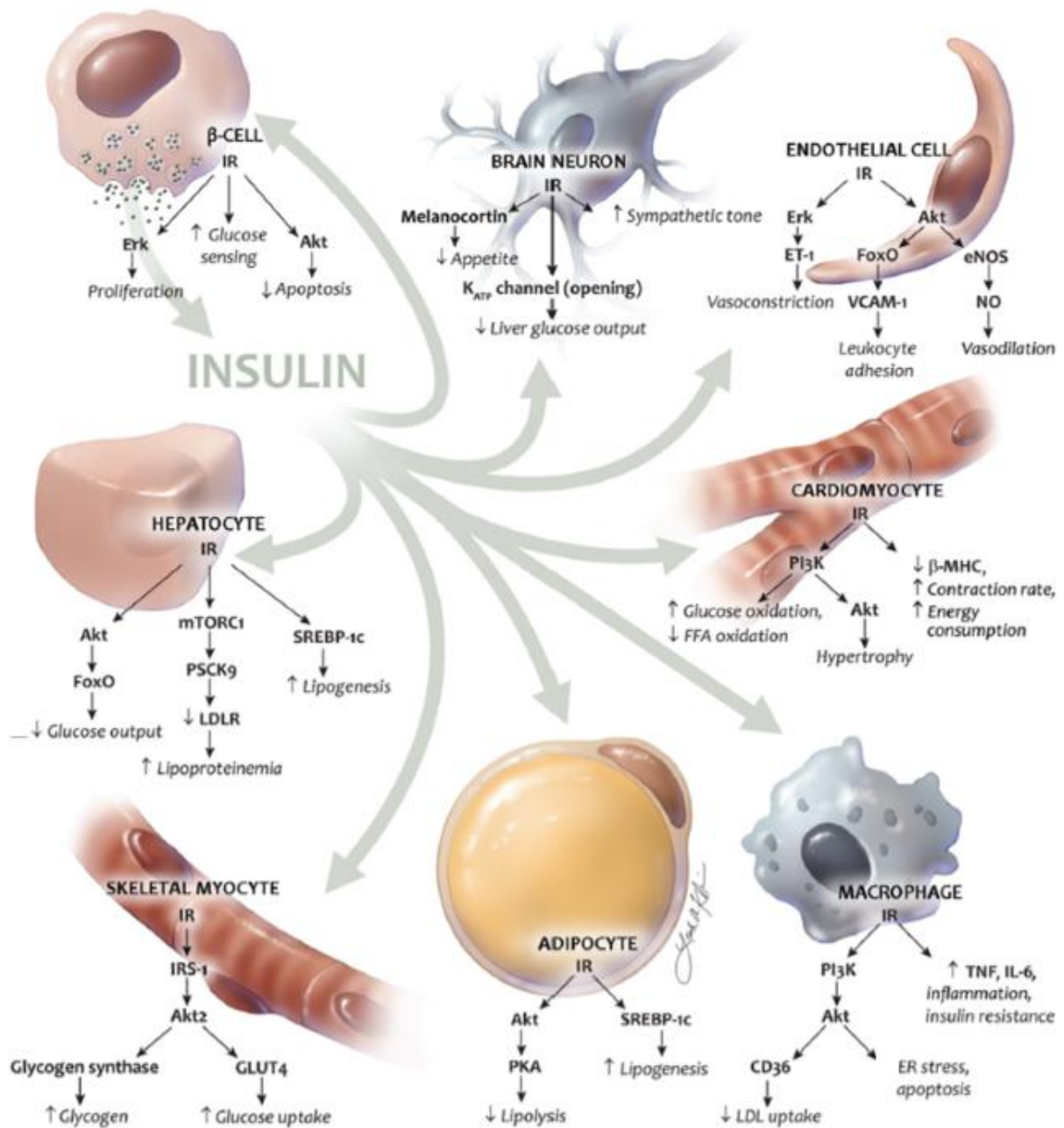
Figure 3. Insulin signalling mechanisms.

Insulin is a stimulus for several important signalling pathways in various cell types, including neurons, endothelial cells, cardiomyocytes, macrophages, adipocytes, skeletal myocytes, hepatocytes and pancreatic β-cells (adapted from Rask-Madsen and Kahn, 2012). (Akt – protein kinase B; Akt2 – protein kinase B2 gene; CD36 – cluster of differentiation 36 (fatty acid translocase); ENOS – endothelial nitric oxide synthase; ER – endoplasmic reticulum; Erk - extracellular signal-regulated kinases; ET1 – endothelin 1 receptor; FFA – free fatty acid; FoxO - forkhead box protein O; GLUT-4 - glucose transporter-4; IR – insulin receptor; IL-6 – interleukin-6; IRS-1 – insulin receptor substrate-1; K_{ATP} – potassium adenosine triphosphate gated channel; LDL – low density lipoprotein; LDLR – low density lipoprotein receptor; mTORC1 - mammalian target of rapamycin complex 1; NO – nitric oxide; PI3-K - phosphatidylinositol-3-kinase; PKA – protein kinase A; PSCK9 - proprotein convertase subtilisin/kexin 9; SREBP-1C - sterol regulatory element binding protein-1C; TNF – tumour necrosis factor; VCAM1 - vascular cell adhesion molecule 1; β-MHC – beta myosin heavy chain).

37

1.2.2. Role of oxidative stress and inflammation in type 2 diabetes

Several factors contribute to the initiation and progression of T2D. These factors include decreased energy expenditure, increased calorie intake of energy dense foods, human microbiota, as well as environmental chemicals, such as nicotine, bisphenol A and pesticides (Kahn *et al.,* 2014). In combination with genetic predispositions, these dynamics contribute to the global increase in obesity and the associated increase in T2D (Kahn *et al.,* 2014). The association of obesity with T2D has been described as devastating, mainly due to the role of elevated NEFAs and pro-inflammatory cytokines in obese subjects, which induce insulin resistance and impair β-cell function (Rask-Madsen and Kahn, 2012; Quan *et al.,* 2013; Kahn *et al.,* 2014). Obesity and a sedentary lifestyle are associated with approximately 80 % of T2D cases (Venables and Jeukendrup, 2009). Clinical and experimental evidence suggests that there is a strong association between T2D, inflammation and oxidative stress, with diabetics having increased levels of free radicals associated with a decline of antioxidant defence mechanisms (Johansen *et al.*, 2005; Houstis *et al.*, 2006).

Elevated free radicals contribute to both insulin resistance as well as dysfunctional insulin secretion in T2D (Houstis *et al.,* 2006). An alteration in primary sites of superoxide formation, such as the mitochondrial complex one and ubiquinone complex three interface, is associated with T2D, resulting in the excessive generation of free radicals (Valko *et al.,* 2007). Increased lipoxygenase expression in T2D results in the release of free radicals by eicosanoid formation (Brash, 1999). *In vitro* studies have also demonstrated the formation of hydroxyl radicals from the reaction of glucose with hydrogen peroxide (Robertson *et al.,* 2003). The deleterious effects of free radicals, including both reactive oxygen species (ROS) and reactive nitrogen species (RNS), are proposed to be mediated by intracellular pathways that interact directly with insulin signalling via serine/threonine inhibitory phosphorylation of insulin receptor substrate (IRS) (Johansen *et al.*, 2005; Bastard *et al.*, 2006). The competitive phosphorylation of IRS inhibits the insulin signalling pathway, causing a reduction in the stimulatory capacity of secreted insulin, thereby inducing insulin resistance (Johansen *et al.*, 2005; Bastard *et al.*, 2006). Free radicals also directly damage deoxyribonucleic acids (DNA), proteins and other biological components through the removal of hydrogen atoms, electron transfer and addition reactions (Zhang *et al.*, 2010). Long term complications of T2D are exacerbated by oxygen-free radical activity (e.g. RNS), which can initiate peroxidation of lipids and the deleterious downstream effects thereof,

which include microvascular complications, particularly associated with diabetic nephropathy that results in renal disease (Baynes, 1991).

Inflammatory mediators have been shown to be increased in T2D patients, as well as in states of obesity and insulin resistance (Dandona *et al.,* 2004; Shoelsen *et al.,* 2006). Activation of inflammatory responses in adipose tissue due to obesity and associated ectopic adipose deposition, together with recruited immune cells, such as macrophages, increases the production of cytokines and chemokines (Dandona *et al.,* 2004; Moser and Williman, 2004; Shoelsen *et al.,* 2006; Lin and Sun, 2010). These pro-inflammatory cytokines, including tumour necrosis factor-α (TNF-α), and chemokines, such as monocyte chemotactic protein-1 (MCP-1), create a systemic inflammatory predisposition that promotes insulin resistance in tissues, such as skeletal muscle and liver, and atherogenesis in the vasculature (Shoelsen *et al.,* 2006). Although inflammation is well known to contribute to T2D, the state of insulin resistance itself promotes inflammation since the anti-inflammatory effects of insulin are also suppressed (Dandona *et al.,* 2004).

2. The diabetic pancreas

Pancreatic islets, also known as islets of Langerhans, comprise a mere 1-2% of the total pancreas (Fig. 4), yet they contain insulin-producing cells that are responsible for global glucose uptake and metabolism (Feldman *et al.*, 2009). Main islet cell types include insulin-producing β-cells, glucagon-producing α-cells, as well as pancreatic polypeptide-producing γ- and somatostatin-producing δ-cells (Brissova *et al.,* 2005; Feldman *et al.*, 2009). Many different islet profiles exist amongst mammalians, with rodent islets having a core cluster of β-cells, with α-, γ- and δ-cells on the periphery. Human and non-human primate islets are arranged with β- and α-cells in close relationship with each other throughout the islet cluster (Elayat *et al.*, 1995; Brissova *et al.*, 2005).
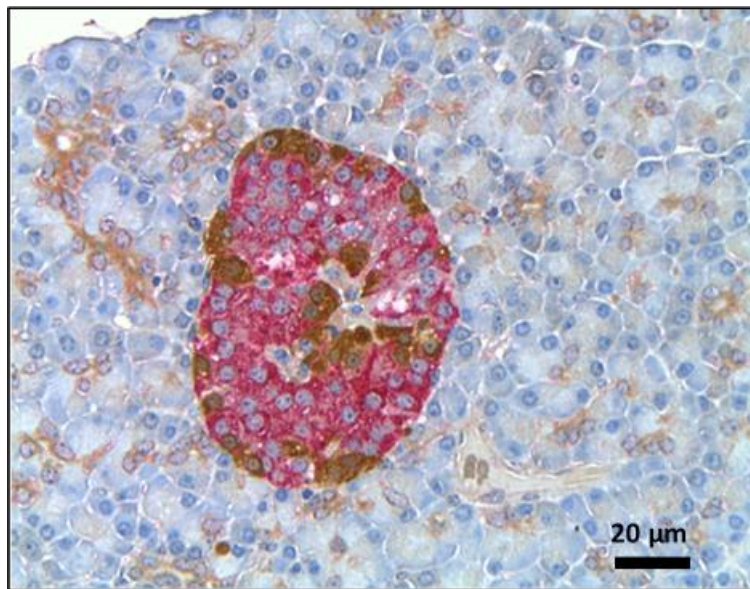
Figure 4. Immunolabelled islets of Langerhans in vervet monkey pancreas.

Pancreatic islets, the endocrine portion of the pancreas, are comprised of 65-85 % of insulin-producing β-cells (pink), with α-cells (brown) comprising 15-20 % (courtesy of the Diabetes Discovery Platform, SA Medical Research Council).

Pancreatic β-cell dysfunction has recently been proposed as a putative mechanism of T2D, and may, in fact, play a bigger role in the earlier stages of T2D than originally thought (Meier and Bonadonna, 2013). Progressive β-cell dysfunction in a large number of T2D patients on antidiabetic treatment was observed in the UK Prospective Diabetes Study, with many patients eventually requiring additional oral antidiabetic medication and even insulin treatment (Turner, 1998). Amyloid deposition and a reduction in β-cell number are observed in islets from long-standing T2D patients (Bonner-Weir and O'Brien, 2008). Initially, as previously mentioned, a compensatory increase in β-cell mass is observed in islets from

pre-diabetic and early diabetic patients, with eventual decreased β-cell mass as a result of an imbalance in loss and renewal of β-cells due to dysfuntion and exhaustion (Butler *et al*., 2003; Bonner-Weir and O'Brien, 2008; Meier and Bonadonna, 2013). Poor metabolic control has been shown to promote glycogen (Toreson, 1951; Liu *et al.,* 2008) and lipid (Lee *et al.,* 1994) accumulation in islets. Patients with T2D also have elevated levels of oxidative stress (Tanaka *et al.,* 2002; Johansen *et al.*, 2005; Houstis *et al.*, 2006). Pancreatic β-cells are particularly sensitive to oxidative stress due to their low cellular levels of free radical quenching enzymes such as glutathione peroxidase and superoxide dismutase (Sakuraba *et al.,* 2002; Tanaka *et al.,* 2002; Abdollahi *et al.*, 2004).

Under normal physiological conditions, the β-cell secretes insulin in response to elevated blood glucose levels. Glucose transporter-2 (GLUT-2), along with the high affinity glucose sensor, glucokinase, facilitates the sensing and transport of glucose into the β-cell. The $NAD(P)H^+$: $NAD(P)^+$ ratio increases, followed by an increase in mitochondrial matrix calcium levels and adenosine triphosphate (ATP) synthase activity (De Marchi *et al.,* 2014). This increase in glucose oxidation results in an increase in the ATP: adenosine diphosphate (ADP) ratio, which in turn inactivates the ATP-gated potassium channels, resulting in depolarization of the β-cell membrane. Calcium channels open, increasing cellular calcium ion concentration which leads to exocytosis of insulin from storage granules (Fig. 5), with calcium being a strong and necessary trigger for oscillatory insulin exocytosis (Cartailler, 2001; Stumvoll *et al.*, 2005). This oscillatory insulin secretion is dependent on intracellular calcium concentrations, rather than β-cell metabolism (Gilon *et al.,* 2002). Glucose mediated calcium influx is essential for first phase insulin secretion and is thus an indicator of normal β-cell function, since it is known to be attenuated in T2D (Henquin *et al.,* 2003).
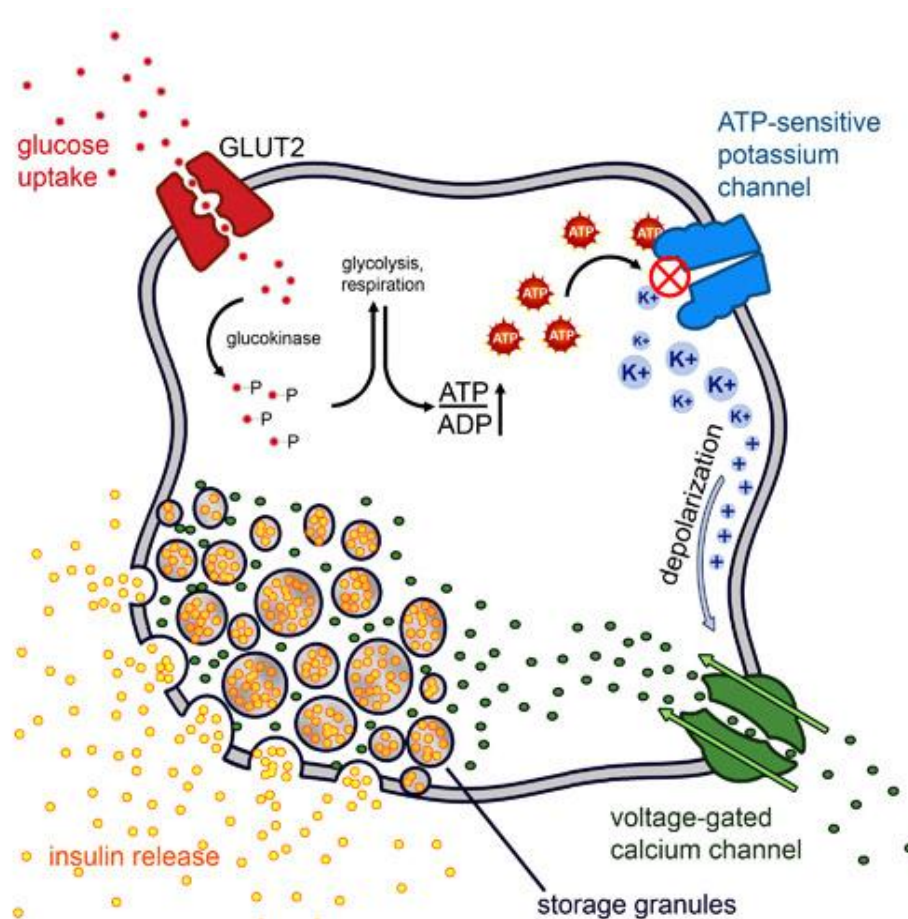
Figure 5. Glucose stimulated insulin secretion in pancreatic β-cells.

Glucose sensing by GLUT-2 and glucokinase triggers a cascade of cellular events in β-cells that result in stored insulin release (from Cartailler, 2001).

This process of insulin secretion is disrupted in dysfunctional β-cells as a result of irreversible damage to cellular components of insulin production over time, such as the endoplasmic reticulum (ER) and mitochondria (Stumvoll *et al.*, 2005). Several factors have been directly linked to defective insulin production and secretion, and thus β-cell dysfunction that includes glucotoxicity, lipotoxicity and inflammation, which are all associated with an increase in oxidative stress (Stumvoll *et al.*, 2005; Maedler, 2008; Biden *et al.*, 2014).

2.1. Glucotoxicity and the β-cell

Glucotoxic conditions (i.e. chronic hyperglycaemia) disrupt the secretion of insulin by β-cells, as well as the synthesis thereof (Maedler, 2008). During short exposures, elevated glucose in culture media was shown to increase β-cell proliferation in human islets, however this effect was lost during chronic exposure to high glucose, with a concomitant increase in β-cell apoptosis (Maedler *et al.,* 2001). Pancreatic β-cells have a high affinity for glucose as is

42

evident in the high level of expression of GLUT-2 and glucokinase (Montane *et al.,* 2014). Although glucose is an important physiological fuel for the β-cell, as well as a trigger for insulin secretion, persistently elevated levels of glucose have been reported to cause a direct reaction between glucose and free amine groups on proteins and lipids, yielding a group of harmful compounds known as advanced glycation end products (AGEs) (Ling *et al.,* 2001; Maedler, 2008). These compounds act via mitochondrial complex three, resulting in increased ROS production in response to hyperglycaemia. Hyperglycaemia increases the rate of glucose oxidation in β-cells thereby stimulating one of the main sources of ROS in the β-cell, namely the mitochondrial electron transport chain (Gurgul *et al.,* 2004). It is the excessive amount of hyperglycaemia induced ROS in β-cells that damages cellular components (Stumvoll *et al.*, 2005). ER stress also plays a role in hyperglycaemia induced β-cell dysfunction, although to a lesser extent as observed in lipotoxicity (discussed in section 2.2. below). The unfolded protein response (UPR) is initiated in order to resolve ER stress and has a key role in adjusting pro-insulin (the peptide precursor to insulin) biosynthesis to acute variations in glucose concentration (Lipson *et al.,* 2006; Maedler, 2008; Biden *et al.,* 2014). Chronically elevated glucose desensitises β-cells to glucose. These conditions also disrupt the UPR processing of pro-insulin and increase the synthesis of misfolded proteins by depleting ER lumenal calcium ion concentrations (Fig. 6) (Lipson *et al.,* 2006; Maedler, 2008; Biden *et al.,* 2014). Protein misfolding in the ER due to glucotoxicity induced overload, caused by the imbalance in the rate of protein synthesis exceeding that of protein exit from the ER, is a contributing factor to ER dysfunction (Biden *et al.,* 2014). Glucotoxicity in β-cells has also been shown to activate the Fas ligand apoptotic pathway as well as stimulate production of the inflammatory cytokine interleukin-1β (IL-1β) (Maedler *et al.,* 2002). Other mechanisms have also been described in the dysfunction of pancreatic β-cells as a result of glucotoxicity. These include the impairment of insulin gene transcription and activation of members of the mitogen-activated protein kinase (MAPK) family (Maedler, 2008). PDX-1 is a transcription factor necessary for pancreatic development and β-cell maturation. Binding activity of PDX-1 is reduced by glucotoxic conditions in the β-cell (Marshak *et al.,* 1999). Hyperglycaemia induced increases in glucokinase synthase activity in β-cells have also been shown to suppress PDX-1 activity (Liu *et al.,* 2008). Co-secretion of amylin with insulin by β-cells has also been implicated in hyperglycaemia induced β-cell dysfunction due to cytotoxic aggregations of islet amyloid polypeptide (Stumvoll *et al.*, 2005).
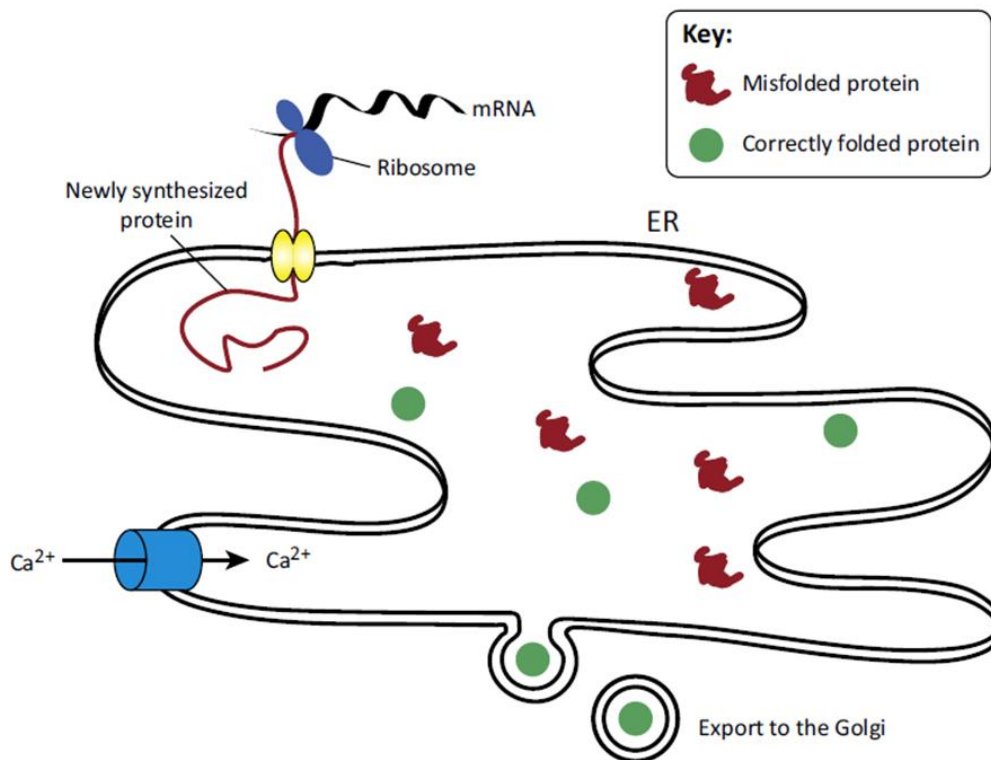
Figure 6. Protein misfolding in the ER.

Gluco- and lipo-toxicity results in increased protein misfolding in the ER with diminished lumenal calcium and protein overload induced ER dysfunction (from Biden *et al.,* 2014).

2.2. Lipotoxicity and the β-cell

Lipotoxic conditions are induced in β-cells during chronic exposure to elevated levels of NEFAs, which is characteristic of obesity and T2D (Kahn *et al.,* 2014). Although demonstrated to increase insulin secretion in β-cells in acute experiments, exposure to chronically elevated NEFAs inhibits insulin secretion (Robertson *et al.,* 2004). One of the more deleterious effects of elevated NEFAs on β-cells is the accumulation of long-chain acyl coenzyme A (LC-CoA). This occurs as a result of elevated glucose inhibiting fatty acid oxidation (Robertson *et al.,* 2004; Stumvoll *et al.*, 2005). The accumulation of LC-CoA directly inhibits insulin secretion by opening β-cell potassium channels and reduces ATP formation by increasing the expression of uncoupling protein-2 (UCP-2) (Stumvoll *et al.*, 2005). Furthermore, NEFA disruption of protein trafficking from the ER to the Golgi, particularly by saturated fatty acids like palmitate has been proposed to cause protein overload induced ER stress (Fig. 7). In addition, the disruption of ER lipid raft composition by NEFAs also disrupts protein trafficking (Boslem *et al.,* 2013). ER stress induced by NEFAs increases protein misfolding and ER overload, further increasing β-cell dysfunction and death (Laybutt *et al.,* 2007; Biden *et al.,* 2014). High levels of lipid exposure not only

increase islet inflammation, but also exacerbate oxidative stress in T2D; direct inhibition of β-cell proliferation by lipotoxicity was also demonstrated (Sharma and Alonso, 2014).
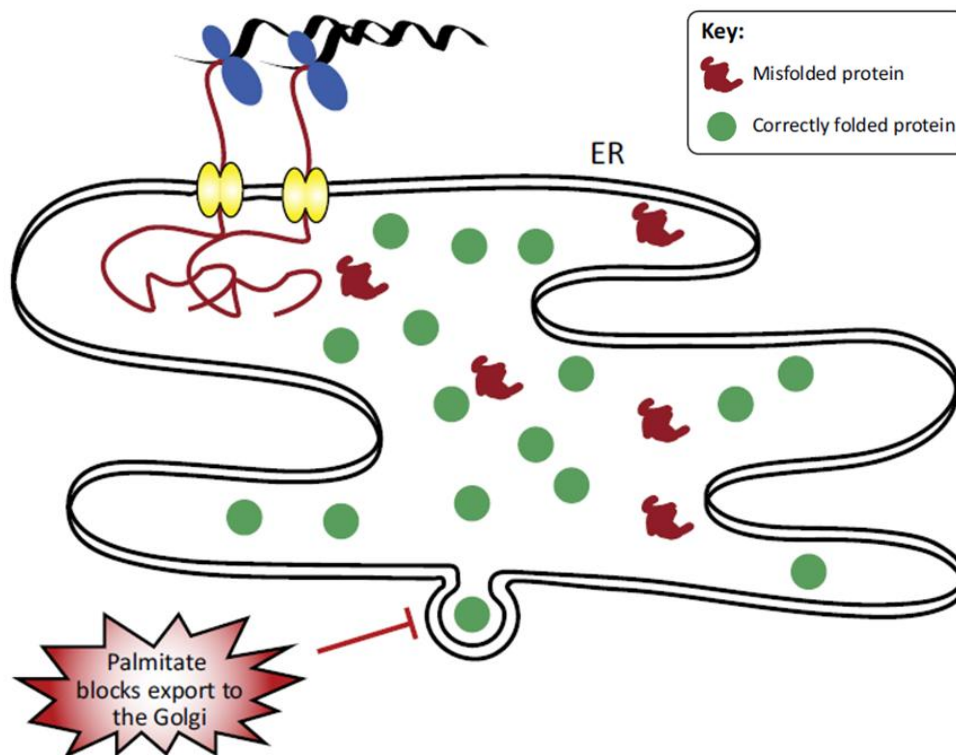
Figure 7. Protein overload the ER.

Lipotoxicity impairs protein export from the ER to the Golgi, resulting in protein overload (from Biden *et al.,* 2014).

2.3. Inflammation and the β-cell

Islet inflammation is well characterised as part of the pathogenesis of T2D (Quan *et al.,* 2013; Montane *et al.,* 2014). Pro-inflammatory cytokines from adipose tissue, cellular cholesterol, islet amyloid peptide, glucotoxicity and lipotoxicity induce β-cell inflammation by activating ER and oxidative stress pathways (Montane *et al.,* 2014). The UPR is activated under conditions of ER stress. Inflammatory pathways involving c-Jun N-terminal kinases (JNKs) and nuclear factor kappa B (NF-κB) are triggered causing increased expression of pro-inflammatory molecules such as interleukin-6 (IL-6), interleukin-8 (IL-8), MCP-1 and TNF-α in the β-cell (Li *et al.,* 2005; Montane *et al.,* 2014). These locally produced pro-inflammatory molecules attract macrophages to the islets, thereby exacerbating inflammation (Ehses *et al.,* 2007). Stimulation of the JNK pathway also promotes insulin resistance in the β-cell, as well as in peripheral tissues (Hirosumi *et al.,* 2002; Lanuza-Masdeu *et al.,* 2013; Montane *et al.,* 2014). Increased activation of the NF-κB pathway

further exacerbates islet inflammation via inflammasome-mediated pro-inflammatory cytokine production (Dixit, 2013). Increased inflammation-induced apoptosis in β-cells is also mediated by increased NF-κB activation in response to elevated ROS (Stumvoll *et al.*, 2005). Elevated ROS also activates MCP-1 and pro-inflammatory cytokine production (Montane *et al.,* 2014). Furthermore, increased nitric oxide is generated, thus exacerbating oxidative stress, in response to pro-inflammatory cytokines, as a result of NF-κB induced increase in inducible nitric oxide synthase activity (Kharroubi *et al.,* 2004). In *in vitro* simulations of inflammation in β-cells, a combination of IL-1β, TNF-α and interferon-γ (IFN-γ) is typically used (Tabatabaie *et al.*, 2000; Barbu *et al.,* 2002), since these cytokines initiate β-cell death by several mechanisms, similar to that observed in T2D (Fig. 8) (Vincenz *et al.,* 2011; Vetere *et al.* 2014). NF-κB is the main mediator of both IL-1β and TNF-α signalling in β-cells (Kwon *et al.,* 1995; Flodstrom *et al.,* 1996; Ortis *et al.,* 2006). In addition, IL-1β also activates suppressor of cytokine signalling-3 (SOCS-3) which potentiates the activation of NF-κB, and suppresses insulin receptor auto-phosphorylation, IRS tyrosine phosphorylation and PI3-K activation (Emanuelli *et al.,* 2004). Signalling of IFN-γ in β-cells is primarily mediated by the Janus kinase/signal transducer and activator of transcription-1 (JAK/STAT-1) pathway (Takeda & Akira, 2000; Vincenz *et al.,* 2011). The effects of these cytokines culminate in the loss of β-cell function, induction of cell stress and eventually, β-cell death.
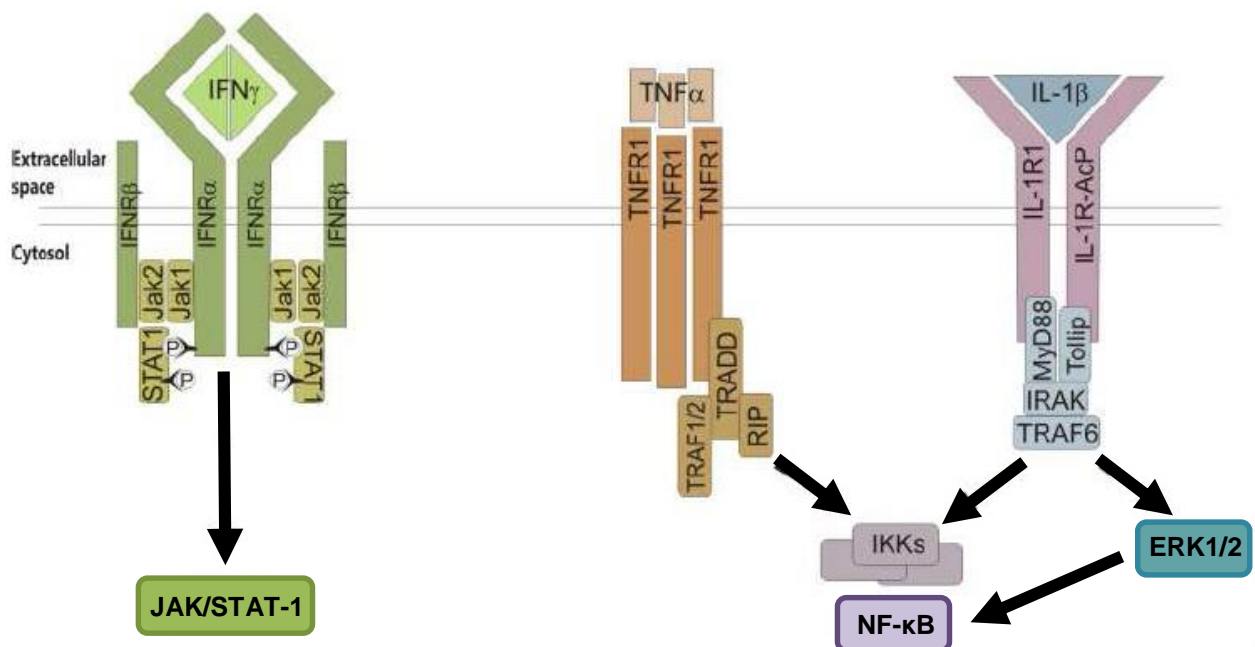
Figure 8. IL-1β, TNF-α and IFN-γ signalling in β-cells.

The cytokine combination of IL-1β, TNF-α and IFN-γ induce signalling cascades which lead to β-cell dysfunction and death (adapted from Vincenz *et al.,* 2011).

In addition, the IL-1β, TNF-α and IFN-γ cytokine combination is known to activate inducible nitric oxide synthase, elevating nitric oxide and oxidative stress (Kacheva *et al.,* 2011). The extrinsic apoptotic pathway is also activated in response to cytokine combinations such as IL-1β, TNF-α and IFN-γ, with the activation of Fas by cytokine induced elevations in nitric oxide and increased cell death by necrosis (Stassi *et al.,* 1997). RIN-5F insulinoma cells were observed to have higher expression of Fas following exposure to a pro-inflammatory cytokine combination which consisted of IL-1β, TNF-α and IFN-γ, as well as streptozotocin (STZ), which thereby induced apoptosis in these cells (Lin *et al.,* 2003).

2.4. Streptozotocin and β-cell death

Oxidative stress contributes significantly to the pathogenesis of T2D, thus the glucosamine-nitrosourea, STZ, is frequently used to induce diabetes in experimental systems since its cytotoxic action is associated with the generation of ROS (Szkudelski, 2001). The STZ compound is specifically taken up by pancreatic β-cells via GLUT-2, inducing cell death mainly by DNA alkylation (Wang and Gleichmann, 1995; Elsner *et al.,* 2000). Due to effects on mitochondria, which include decreasing mitochondrial oxygen usage and limiting ATP generation, as well as by increasing the activity of xanthine oxidase, STZ generates ROS, which contributes to an increase in oxidative stress and DNA fragmentation (Kroncke *et al.,* 1995; Szkudelski, 2001). Since STZ is a nitric oxide donor, nitric oxide generated from STZ metabolism exacerbates the pro-oxidative state of the cell and, in combination with ROS, forms highly toxic and reactive peroxynitrites (Szkudelski, 2001). STZ also reduces cellular ATP, thereby inhibiting insulin synthesis and secretion (Nukatsuka *et al.,* 1990).

2.5. Mechanisms of β-cell death

As a result of the deleterious effects of T2D associated inflammation and oxidative stress on the pancreatic β-cells, cell death processes are initiated when these cells are no longer able to compensate. Programmed cell death, apoptosis, is an energy dependent process that constitutes the largest proportion of β-cell death under both normal and, even more so, in diseased conditions, with necrosis and the atypical apoptosis like form of programmed cell death, "necroptosis" (Cnop *et al.,* 2005; Donath *et al.,* 2005; Elmore, 2007; Cerf, 2013; Yang and Johnson, 2013).

Apoptotic β-cell death can be initiated by both intrinsic and extrinsic signalling pathways that culminate in, what is known as, the execution pathway of cell death via the activation of

caspases, particularly caspase-3, -6 and -7 (Cnop *et al.,* 2005; Elmore, 2007). The intrinsic pathway is not mediated by receptor activation, but rather by intracellular signalling that triggers mitochondrial outer membrane permeabilisation, the release of cytochrome c and the execution of cell death (Saelens *et al.,* 2004; Elmore, 2007). The extrinsic signalling pathway, however, is receptor mediated, involves death receptors that transmit the death signal from the β-cell surface to intracellular signalling pathways (Donath *et al.,* 2005; Elmore, 2007). The Fas receptor, as well as the TNF-α receptor are the main triggers of β-cell apoptosis via the extrinsic pathway (Locksley *et al.*, 2001). Necrotic β-cell death, induced by external activation, is associated with an increase in inflammation as cells rupture and scavenger macrophages are attracted to the islet (Zeiss, 2003). The concept of necroptotic cell death involves β-cell death via a pathway that does not follow the classic definition of apoptosis, and mimics necrotic cell death at the same time (Yang and Johnson, 2013).

3. Current type 2 antidiabetic therapies

Over the past 20 years, the introduction of new classes of antidiabetic drugs has rapidly escalated (Fig. 9) (Kahn *et al.,* 2014). Apart from a few negative side effects, including gastrointestinal upsets and weight gain, current T2D therapies have been effective in the management of T2D, albeit limited in long-term treatment, with many patients requiring exogenous insulin therapy (Seufert *et al.*, 2004).
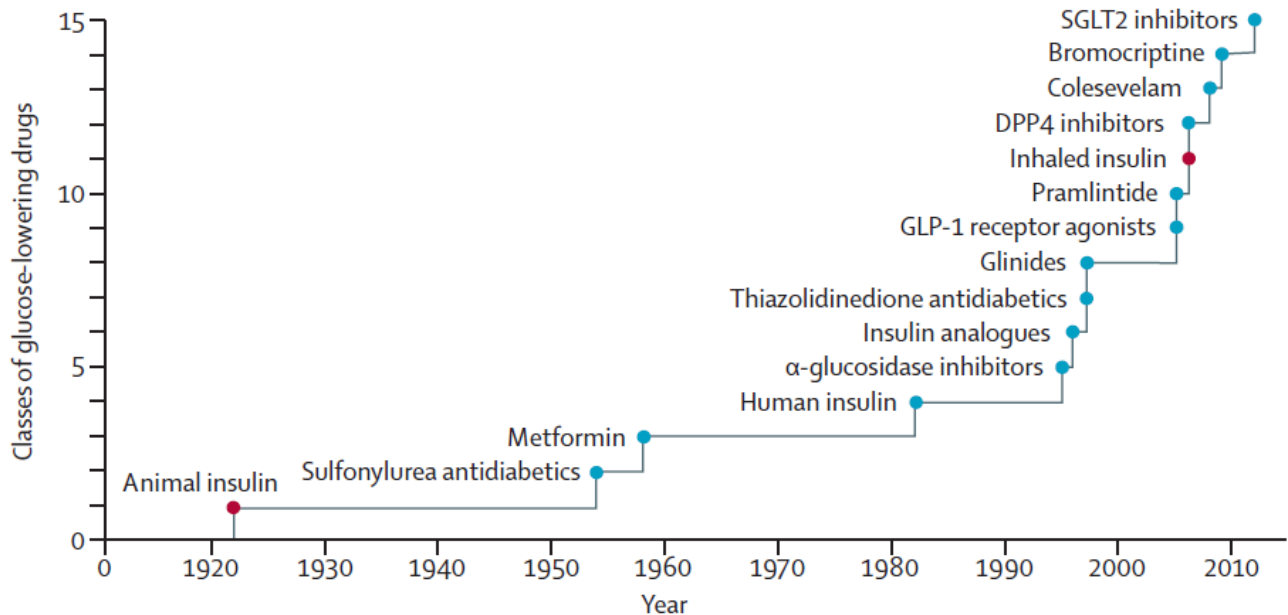
Figure 9. Current antidiabetic therapeutics.

An escalation in new classes of antidiabetic drugs has been observed in the last 20 years, with the discontinuation of both animal and inhaled* insulins due to safety concerns (marked in red) (from Kahn *et al.,* 2014). *Note: As of July 2014, the FDA has approved an improved inhaled insulin, Afrezza®, by Pfizer.

3.1. Conventional antidiabetic therapeutics

Current conventional oral antidiabetic therapeutics include thiazolidinediones (TZDs), sulfonylureas and biguanides, which act predominantly by enhancing insulin action (Seufert *et al.*, 2004; Stumvoll *et al.,* 2005; Kahn *et al.,* 2014). Injectable exogenous insulin therapy was typically initiated only in advanced stages of T2D, when oral antidiabetic agents no longer maintained glucose homeostasis (Stumvoll *et al.,* 2005; McLellan *et al.,* 2014). Recently, however, earlier intervention with basal insulin therapy is being used to restore glucose regulation in prediabetic patients, with a concomitant reduction in micro-vascular disease (Perreault *et al.,* 2012).

As peroxisome proliferator-activated receptor-gamma (PPAR-γ) agonists, TZDs primarily alter adipose tissue metabolism and distribution, resulting in enhanced insulin sensitivity, a

49

reduction in elevated blood glucose, improved vascular function and improved lipid and inflammatory profiles in T2D patients (Yki-Jarvinen, 2004; Stumvoll *et al.,* 2005). The insulin sensitising and anti-inflammatory properties of TZDs are associated with a drug induced increase of adiponectin and reduction of leptin (Kim and Ahn, 2004). By sequestering NEFAs in less lipolytic subcutaneous compartments, TZDs reduce circulating NEFAs and the associated pro-inflammatory cytokines, such as TNF-α (Stumvoll *et al.,* 2005; Kahn *et al.,* 2014). Furthermore, TZDs have been shown to increase the expression of two isoforms of IRS, IRS-1 and IRS-2, thereby increasing insulin sensitivity and glucose uptake in skeletal muscle and the liver (Iwata *et al.,* 2001; Smith *et al.,* 2001). In addition to insulin sensitising effects in adipose tissue and skeletal muscle, TZDs suppress HGP by sensitising hepatocytes to glucose via PPAR-γ (Kim and Ahn, 2004). Generally, TZDs are better tolerated by T2D patients than other oral hypoglycaemic drugs, with fewer gastro-intestinal side effects, however, weight gain and fluid retention are associated with this drug (Nesto *et al.,* 2003; Stumvoll *et al.,* 2005). Congestive heart failure as a result of fluid retention is also a concern in the use of TZDs (Nesto *et al.,* 2003). By ameliorating insulin resistance and thus the secretory demand on β-cells, TZDs offer some protection to pancreatic β-cells (Buchanan *et al.,* 2002). In addition, activation of PPAR-γ in β-cells is known to improve their function and morphology by increasing their glucose sensing ability via GLUT-2 and glucokinase (Kim and Ahn, 2004).

Sulfonylureas decrease blood glucose by closing potassium channels, resulting in stimulated insulin secretion from β-cells (Stumvoll *et al.,* 2005; Del *et al.,* 2007). The use of sulfonylureas has also been associated with a reduction in the risk for the occurrence of both micro- and macro-vascular disease (United Kingdom Prospective Diabetes Study Group, 1998). Although successful in reducing glycaemia in the short term, sulfonylureas have several negative side effects, which include hypoglycaemic episodes, weight gain and β-cell dysfunction due to overstimulation of insulin secretion (Rendell, 2004). In addition, it has been proposed that sulfonylureas accelerate β-cell loss via increased deposition of islet amyloid (Rachman *et al.,* 1998), as well as closure of inwardly rectifying potassium channels in β-cells (Maedler *et al.,* 2005).

The biguanide, metformin, has an insulin sparing effect since it works independently of the pancreas by improving hepatic and peripheral sensitivity to insulin (Stumvoll *et al.,* 2005; Wiernsperger and Bailey, 2009). Metformin suppresses hepatic gluconeogenesis by

stimulating 5'-adenosine monophosphate-activated protein kinase (AMPK) and potentiating the effect of insulin while decreasing the effect of glucagon (Knowler *et al.*, 2002). In addition, metformin increases functional properties of insulin and glucose sensitive transporters, thus improving insulin stimulated glucose uptake in skeletal muscle (Reddi and Jyothirmayi, 1992). Reduced hypertriglyceridaemia has also been observed in metformin treated T2D patients, which is attributed to the suppression of lipolysis in adipose tissue, the suppression of hepatic lipid synthesis, as well as increased re-esterification of triglycerides in adipose tissue (Giannarelli *et al.,* 2003). Metformin therapy has been described as less robust as that of TZDs, but T2D patients treated with this biguanide have a much lower risk of overt hypoglycaemia and are not subject to the weight gain associated with TZDs (Stumvoll *et al.,* 2005; Wiernsperger and Bailey, 2009). Metformin has been shown to indirectly improve β-cell function, albeit in the short term only (Wiernsperger and Bailey, 2009). Metformin has acute beneficial effects on β-cells by improving glucose stimulated insulin secretion in islets isolated from T2D patients (Marchetti *et al.,* 2004). In addition, metformin acutely improved glucose metabolism and responsiveness of isolated human islets exposed to lipotoxic conditions by the reduction of fatty acid oxidation (Lupi *et al.,* 2002). Metformin therapy alone in T2D patients is yet to be shown to prevent the long term deterioration of pancreatic β-cell function (Wiernsperger and Bailey, 2009).

Recently, newer therapeutic approaches, including incretin mimetics and dipeptidyl peptidase-4 (DPP-IV) inhibitors, have been introduced either exclusively in a few cases, or more commonly, in combination with current conventional clinical therapies, such as biguanides, sulfonylureas and TZDs (Vinik, 2007). The incretin hormone glucagon-like peptide-1 (GLP-1) increases insulin sensitivity in both α- and β-cells, thereby stimulating insulin secretion in a glucose dependent manner and concomitantly decreasing glucagon secretion (Toft-Nielsen *et al.,* 2001). The role of DPP-IV inhibitors is to prevent degradation of GLP-1, thus prolonging the effect of the hormone. Together, incretin mimetics and DPP-IV inhibitors have been shown to exert both pancreatic and extrapancreatic glucoregulatory effects; i.e. increase in β-cell mass and insulin gene expression, inhibition of acid secretion in and slowing of gastric emptying from the stomach, decreasing food intake by increasing satiety in the brain and promoting insulin sensitivity (Bosi *et al*., 2008; Tibaldi, 2014). Safety in the long term and high cost implications are still major concerns facing the use of incretin based therapies (Tibaldi, 2014).

3.2. Less conventional antidiabetic therapeutics

Less conventional antidiabetic therapies include α-glucosidase inhibitors and sodium-glucose co-transporter-2 (SGLT-2) inhibitors (Stumvoll *et al.,* 2005; Kahn *et al.,* 2014; McLellan *et al.,* 2014). The inhibition of α-glucosidase in the gastrointestinal tract delays the breakdown of complex carbohydrates, thereby reducing glucose absorption and postprandial hyperglycaemia (Kahn *et al.,* 2014; McLellan *et al.,* 2014). Another antidiabetic therapeutic dependent on the gastrointestinal tract is pramlintide, an amylin agonist, which slows gastric emptying and inhibits glucagon secretion (Schmitz *et al.,* 2004; Younk *et al.,* 2011). Specific inhibitors of SGLT-2, such as dapagliflozin, increase urinary excretion of glucose by blocking glucose reabsorption in the proximal convoluted tubules of the kidneys without affecting glucose uptake (i.e. SGLT-1 transporters) in the gut (Liu *et al.,* 2012).

Bromocriptine is a dopamine receptor agonist that is conventionally used in the treatment of pituitary tumours, Parkinson's disease, hyperprolactinaemia, neuroleptic malignant syndrome, and since 2009, T2D (Holt *et al.,* 2010). Bromocriptine is the only approved antidiabetic therapy that acts via the central nervous system, by restoring circadian rhythm, thereby improving insulin resistance (Pijl *et al.,* 2000; Holt *et al.,* 2010). Inhibition of glucose stimulated insulin secretion in INS-1E β-cells and in C57Bl6/J mice by bromocriptine has been proposed to promote β-cell rest by reducing insulin hypersecretion which is characteristic of early or pre-T2D (De Leeuw van Weenen *et al.,* 2010).

4. Plant polyphenols and human diseases

Polyphenols are secondary plant metabolites, which have unique physical and chemical behaviours, including antioxidative properties (Scalbert *et al.,* 2005). They are derived from a variety of dietary sources, including fruit, such as apples, grapes and berries, beverages, such as tea, coffee and wine, and vegetables, such as red onion and spinach (Scalbert *et al.,* 2000). Edible plants provide the human diet with more than 8000 different polyphenols (Fraga *et al.*, 2010). Chemically, polyphenols are characterised as having one or more hydroxyl groups attached to a benzene ring; compounds with diverse chemical structures are categorised as polyphenols (Fraga *et al.*, 2010). Well known bioactive polyphenols include the flavonoids quercetin, catechin, hesperetin, cyanidin and proanthocyanidins, and phenolic acids, caffeic acid, chlorogenic acid and ferulic acid (Scalbert *et al.,* 2005). The antioxidative properties of polyphenols may limit the risk of degenerative diseases such as cancer, cardiovascular disease, T2D and neurodegenerative disease, which are characterised by oxidative stress (Pandey and Rizvi, 2009). Polyphenols may increase antioxidant capacity in humans by directly scavenging free radicals, by acting in synergy with other antioxidants, by having a sparing effect on endogenous antioxidants or by limiting the absorption of pro-oxidative components (Rice-Evans *et al.,* 1995; Scalbert *et al.,* 2005; Pandey and Rizvi, 2009). Polyphenols have been shown to decrease plasma phospholipid peroxides and plasma concentrations of malondialdehyde in humans (Nakagawa *et al.,* 1999; Young *et al.,* 1999). Consumption of polyphenol rich food and beverages has been associated with reduced oxidative damage to lymphocyte DNA and pronounced reduction in oxidised DNA bases (Lampe, 1999; Leighton *et al.,* 1999).

4.1. Plant polyphenols and type 2 diabetes

The protective role of dietary antioxidants in degenerative and age related diseases is under scrutiny in order to find candidates that could ameliorate T2D and the associated β-cell dysfunction (Frei, 2004, Scalbert *et al.*, 2005; Lee *et al.*, 2011). Plant polyphenols have been shown to influence glycaemia in experimental animal models of T2D and, in conjunction with *in vitro* data, have been shown to decrease digestion and absorption of dietary carbohydrates, regulate metabolism of carbohydrates, improve glucose uptake and disposal in muscle and fat, as well as improve β-cell function and insulin action (Tiwari and Rao, 2002; Scalbert *et al.,* 2005; Bahadoran *et al.,* 2013). Caffeic and isoferulic acids, both found in tea and coffee, improved intravenous glucose tolerance tests (IVGTTs) in STZ induced diabetic and insulin resistant rats (Hsu *et al.,* 2000; Liu *et al.,* 2000). Diacetylated

53

anthocyanins, present in grapes and pomegranates, have been shown to have hypoglycaemic effects in rats by inhibiting α-glucosidase, thereby inhibiting glucose absorption in the gut (Preedy, 2013). The inhibition of intestinal glucose transporters (SGLT-1 and 2) by green tea catechins and epicatechins, chlorogenic acids, ferulic acids, caffeic and tannic acids, quercetin and naringenin decrease intestinal absorption of glucose, thus regulating postprandial hyperglycaemia (Bahadoran *et al.,* 2013). Some polyphenols, such as phlorizin from the bark of fruit trees including pear, apple and cherry, exert hypoglycaemic effects by limiting glucose reabsorption in the kidney, typically by SGLT-2 inhibition (Rossetti *et al.,* 1987; Dimitrakoudis *et al.,* 1992). Polyphenols have also been shown to regulate carbohydrate metabolism in the liver by inhibiting HGP, as in the case of the tea catechin epigallocatechin gallate (EGCG) (Waltner-Law *et al.,* 2002), which may also activate AMPK thereby inhibiting hepatic gluconeogenic enzymes (Collins *et al.,* 2007). Other green tea catechins have also been shown to down regulate the expression of liver glucokinase and up regulate phosphoenolpyruvate carboxykinase (PEPCK), thus providing an additional mechanism by which HGP can be lowered (Waltner-Law *et al.,* 2002). The flavanones hesperidin and naringenin, improved glycaemic control in diabetic mice by increasing hepatic glycogen content and reducing HGP; an improvement in hyperlipidaemia was also observed (Jung *et al.,* 2004; Mahmoud *et al.,* 2012). Peripheral uptake and metabolism of glucose were observed in skeletal muscle and adipose tissue, where caffeic acid stimulated *in vitro* glucose uptake in an insulin mimetic and/or insulin sensitising manner (Cheng *et al.,* 2000). Other polyphenolic compounds, such as quercetin, EGCG and resveratrol, were also reported to stimulate peripheral glucose uptake in muscle and fat *in vitro* via activation of AMPK and GLUT-4 translocation. Direct benefits to pancreatic β-cells were observed in the ability of genistein, an isoflavone found in soy beans and coffee, to stimulate insulin secretion *in vitro* in MIN6 β-cells (Ohno *et al.,* 1993). Enhanced secretion of GLP-1 in humans by chlorogenic acid, found in coffee, has also been demonstrated (Johnston *et al.,* 2003). Increased GLP-1 secretion infers benefits to β-cells as well as plays a role in delaying glucose absorption (Park *et al.,* 2007; Zhang *et al.,* 2011). Resveratrol was shown to reduce pancreatic β-cell loss by reducing islet oxidative stress (Szkudelski and Szkudelsk, 2011). It has also been proposed that resveratrol preserves β-cell mass by reducing chronic overstimulation of the β-cells (Bahadoran *et al.,* 2013).

Polyphenols from a herbal tea brewed from *Aspalathus linearis* (Rooibos), which is endemic to South Africa, were demonstrated to stimulate glucose uptake and improve insulin

resistance *in vitro* in cultured myocytes (Kawano *et al.,* 2009; Mazibuko *et al.,* 2013), with the phenylpropenoic glucoside, enolic phenylpyruvic acid-2-*O*-glucoside, demonstrating improved glucose tolerance *in vivo* in obese insulin-resistant rats (Muller *et al.,* 2013). *In vivo* studies in leptin deficient *ob/ob* mice demonstrated that the rooibos dihydrochalcone *C*-glucoside, aspalathin, improved glucose tolerance by mechanisms including reductions in serum thiobarbituric acid reactive substances (TBARS), serum triglycerides and HGP (Son *et al.,* 2013). Aspalathin, which is unique to Rooibos, has been shown to inhibit α-glucosidase *in vitro* (Muller *et al.,* 2013). In *in vitro* studies in RIN-5F pancreatic β-cells, aspalathin has been shown to stimulate insulin secretion (Kawano *et al.,* 2009), as well as to protect against AGEs (Son *et al.,* 2013).

The beneficial effects of plant derived polyphenols, including gallic, ferulic and chlorogenic acids, in T2D were summarised by Joubert *et al.* (2012) (Fig. 10). In addition to antioxidative properties, such as the up regulation of antioxidant enzymes and scavenging of free radicals, these phenolic acids have been shown to increase glucose uptake in peripheral tissues such as adipose and skeletal muscle, decrease HGP and reduce glucose absorption in the gut. Gallic acid offered substantial benefit in not only demonstrating the ability to increase insulin secretion from β-cells, but also by decreasing apoptosis and up regulating cellular antioxidant enzymes (Joubert *et al.,* 2012). With plant polyphenols having the potential to ameliorate T2D by a large variety of mechanisms, a prodigious opportunity presents itself for further research into the ability of specific polyphenols in the protection and preservation of functional β-cell mass in addition to the amelioration of peripheral insulin insensitivity and glucose intolerance.

Excessive nutrient absorption

Dysfunctional pancreatic islets

Inhibition of α-glucosidase, α-amylase and pancreatic lipase

Dysfunctional hepatic glucose and lipid metabolism

↑ Antioxidant enzyme activity
↑ β-cell number
↓ Apoptosis
↑ Insulin (PDX-1 and INS)

Micro- and macro-vascular damage

↓ Lipid accumulation (↓ FAS)
↑ Antioxidant enzyme activity (↓ TBARS, ↓ H_2O_2)
↑ Glycogen (↑ GK, normalised G6Pase)
↓ Glucose production (↓ PEPCK)
↑ Glucose uptake, ↑ FA β-oxidation

Dysfunctional adipose glucose and lipid metabolism

↓ TBARS, ↓ H_2O_2

Dysfunctional skeletal muscle glucose and lipid metabolism

↑ Glucose uptake (↑ GLUT4, PI3K, AMPK)
↓ Lipid accumulation

↓ Leptin, ↑ adiponectin
↓ Adipogenesis, ↓ Lipid peroxidation
↑ Glucose uptake, ↓ Intracellular TG

Figure 10. Summary of the effects of phenolic acids on T2D associated aberrations.

The ameliorative effects of phenolic acids (green) on T2D are multifaceted and act in a variety of tissues, including metabolic aberrations (red) in the liver, pancreas, skeletal muscle, gastro-intestinal tract and in blood vessels (adapted from Kahn *et al.,* 2006; Joubert *et al.,* 2012, Kahn *et al.,* 2014). (FA – fatty acid; FAS – fatty acid synthase; GK – glucokinase; GLUT4 – glucose transporter-4; G6Pase – glucose-6-phosphatase; INS – insulin gene; PDX-1 – pancreatic duodenal homeobox-1; PEPCK – phosphoenolpyruvate carboxykinase; PI3K – phosphatidylinositol-3-kinase; PPAR – peroxisomal proliferator-activated receptor; TBARS – thiobarbituric acid reactive substances; TG – triglycerides).

4.2. *Cyclopia spp.*

Cyclopia species are members of the leguminous Fabaceae family, and are endemic to South Africa, growing exclusively in the Cape Floristic region (fynbos area) (Fig. 12). The deep yellow flowers (Fig. 13 B), with an indented calyx, and leaves that are trifoliate (Fig. 11) are characteristic of *Cyclopia* spp. A number of species, i.e. *C. genistoides*, *C. sessiliflora*, *C. intermedia* and *C. subternata* have been commercialised in recent years to meet the local and global demand for production of herbal tea, well known as honeybush. Commercialisation of other species are also presently under investigation. These include *C. longifolia* and *C. maculata*. Most of the annual harvest is processed to produce the "fermented" product, but a demand also exists for "unfermented" plant material (Joubert *et al.,* 2011). "Fermentation", a high temperature oxidation process, which is required for the formation of the characteristic sweet flavour and brown colour of the infusion, decreases the polyphenolic content of extracts, including that of the antidiabetic xanthone, mangiferin (Joubert *et al.*, 2008).
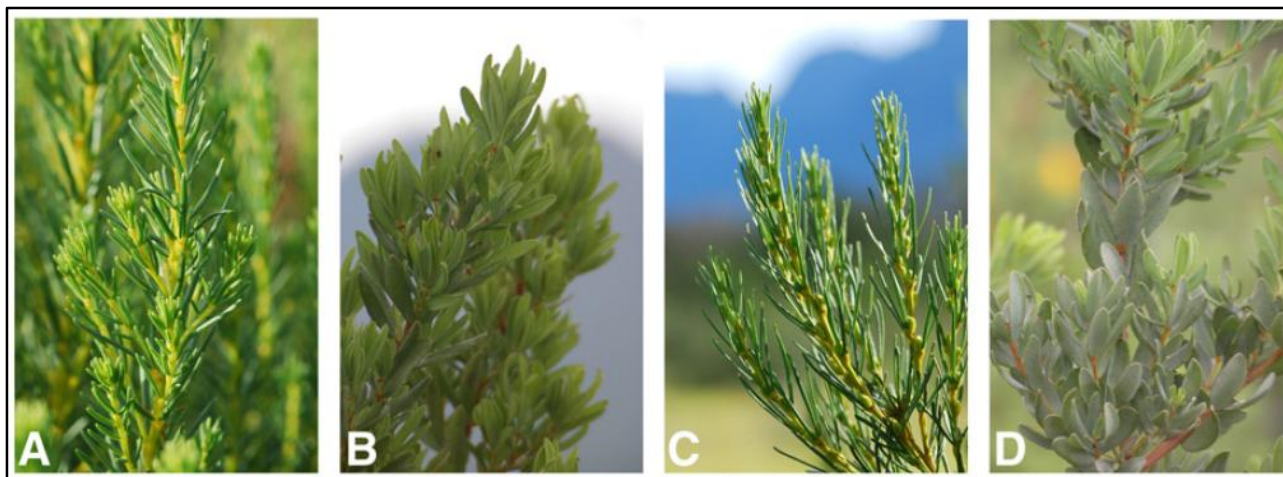
Figure 11. Leaves of *C. genistoides* (A), *C. intermedia* (B), *C. maculata* (C) and *C. subternata* (D).

Cyclopia spp. plants have characteristic trifoliate leaves (from Joubert *et al.,* 2011).
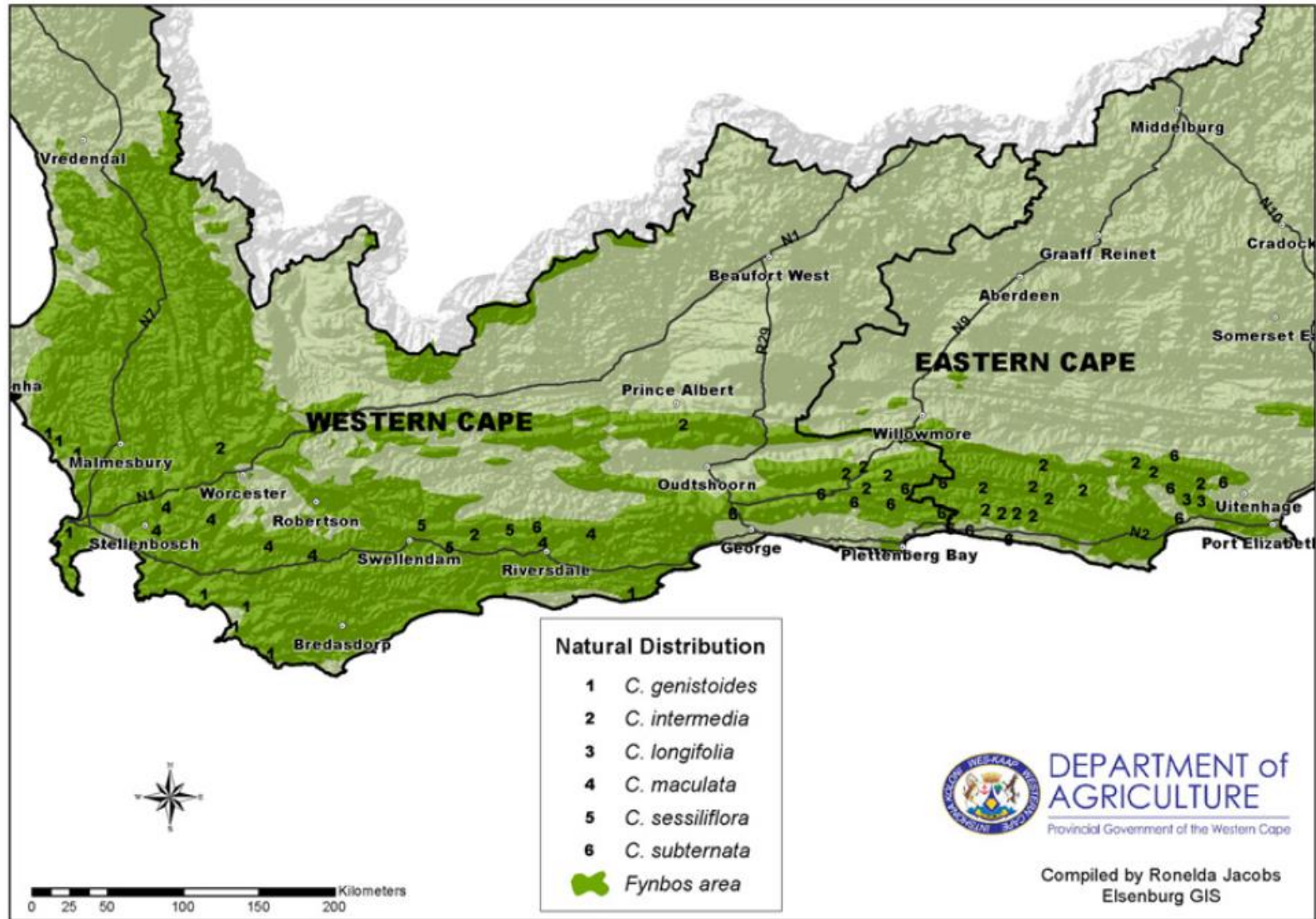
Figure 12. Natural distribution of *Cyclopia* spp. of commercial importance.

Cyclopia spp. occur naturally in the mountainous and coastal regions of the Eastern and Western Cape Provinces of South Africa   (from Joubert *et al.,* 2011).

58

Phenolic composition and biological properties of honeybush tea have gained the interest of medical research as potential therapeutic agents for several degenerative and lifestyle diseases (Joubert *et al.,* 2008; Dudhia *et al.*, 2013; Louw *et al.,* 2013; Pheiffer *et al.*, 2013). Bioactive and antioxidative polyphenols characteristically present in *Cyclopia* spp. include the xanthones mangiferin and isomangiferin (the 4-*C*-glucoside isomer of mangiferin) and the flavanone, hesperidin (an *O*-rutinoside of hesperetin) (De Beer and Jourbert, 2010). To date the research focus was largely on antioxidant, anticancer and phytoestrogenic properties of *C. intermedia, C. genistoides* and/or *C. subternata*, as reviewed by Joubert *et al.* (2008) and Louw *et al.* (2013). Additional therapeutic potential for *Cyclopia* spp. was demonstrated by Muller *et al.* (2011) when an aqueous extract of the unfermented plant material of *C. intermedia* showed antidiabetic potential in both STZ and obese, insulin resistant rats. Furthermore, an aqueous extract of unfermented *C. maculata* (Fig. 13) was shown to have inhibitory effects on adipogenesis *in vitro* in 3T3-L1 adipocytes (Dudhia *et al.,* 2013), as well as lipolytic effects in the same cell line (Pheiffer *et al.,* 2013). As far as we are aware, no other significant scientific research has been conducted using *C. maculata* in relation to lifestyle diseases, specifically T2D, despite this plant having a relatively high polyphenolic content and in particular, a high mangiferin content (Dudhia *et al.,* 2013).
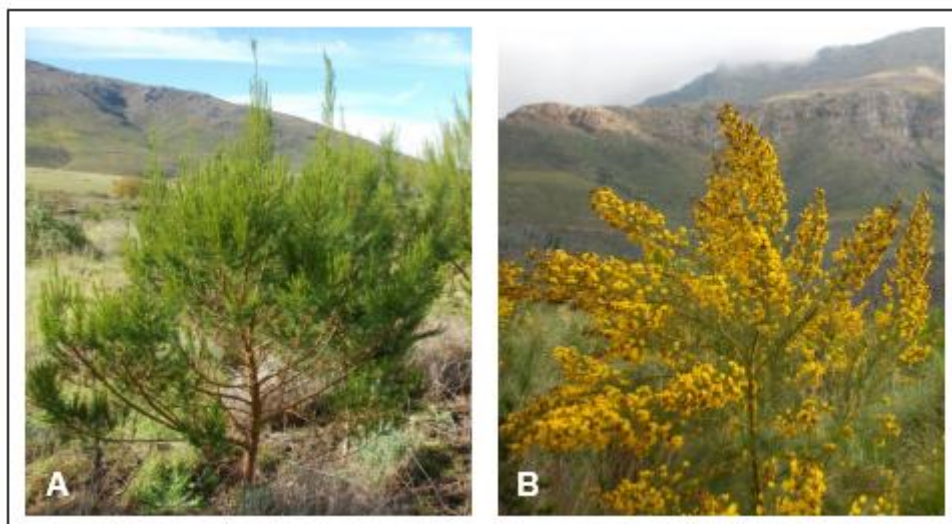
Figure 13. Non-flowering (A) and flowering (B) mature *C. maculata* bushes.

Naturally occurring *C. maculata* bushes grow to approximately 2 m in height and have characteristic yellow flowers during Spring (September–October) (courtesy of the Agricultural Research Council of South Africa, Infruitec-Nietvoorbij and the South African Honeybush Tea Association, 2012, respectively)

The unfermented aqueous extract of *C. maculata* used by Dudhia *et al.* (2013) and Pheiffer *et al.* (2013) was characterised by high performance liquid chromatography with diode-array detection (HPLC-DAD) and was used in this PhD study (Fig. 14). The major polyphenols in this unfermented *C. maculata* extract included mangiferin (6.19 %), isomangiferin (2.08 %), the benzophenone, iriflophenone-3-*C*-glucoside (1.13 %), the dihydrochalcone, phloretin-3',5'-di-*C*-glucoside (0.17 %) and the flavanones, hesperidin (0.80 %) and eriocitrin (0.42 %) (Dudhia *et al.,* 2013).
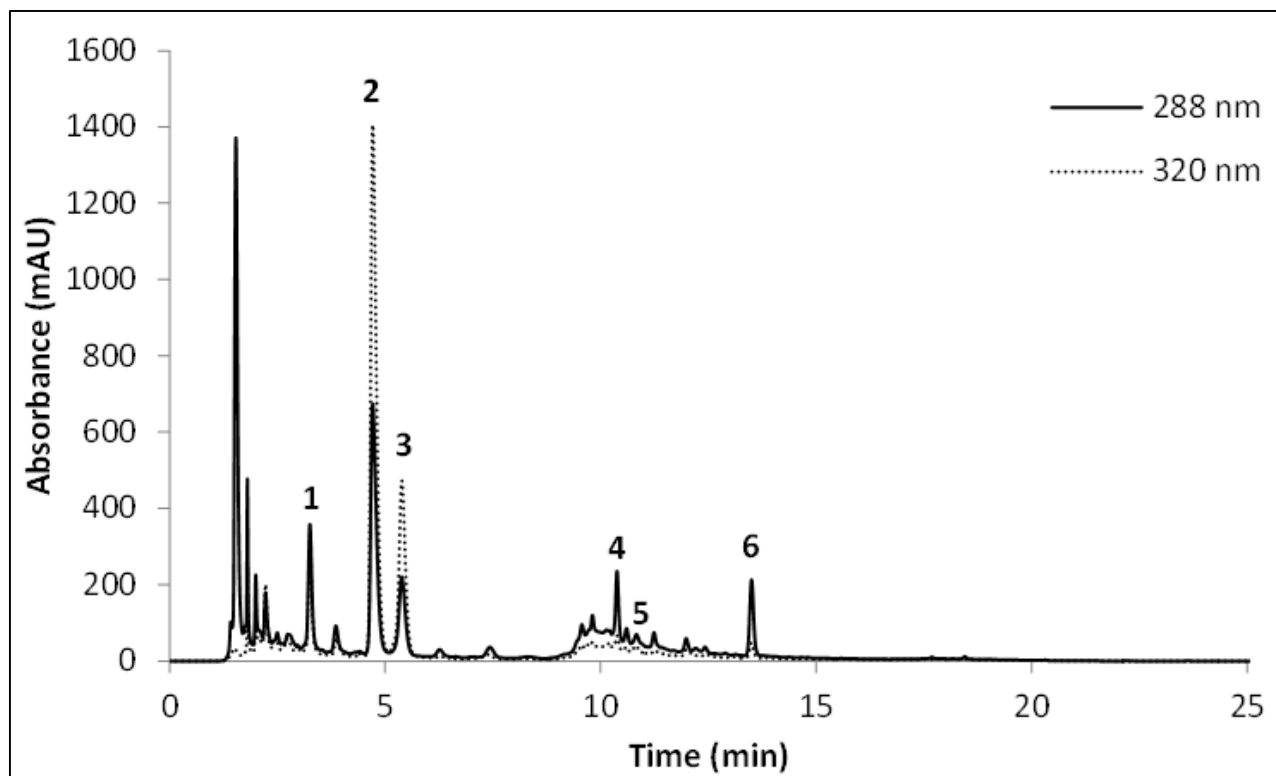
Figure 14. High performance liquid chromatography with diode-array detection chromatogram of the aqueous extract of unfermented *C. maculata*.

This unfermented extract contains high concentrations of polyphenols, with mangiferin (peak 2) being the most abundant. This extract was used by Dudhia *et al.* (2013), Pheiffer *et al.* (2013) and in this PhD study (adapted from Dudhia *et al.,* 2013). (**1-** iriflophenone-3-C-glucoside; **2-** mangiferin; **3-** isomangiferin; **4-** eriocitrin; **5-** phloretin-3',5'-di-C-glucoside; **6-** hesperidin).

Further insight into minor phenolic constituents present in aqueous extract of *C. maculata* was recently provided by Schulze (2013). The flavones, scolymoside and apigenin-6,8-di-*C*-glucoside (vicenin-2), and the benzophenone, maclurin-3-*C*-glucoside, have been positively identified, while hydroxy derivatives of mangiferin and isomangiferin have been tentatively identified, amongst others (Schulze, 2013).

Plant polyphenols with antioxidant activity, as detected in this extract, could either scavenge free radicals or inhibit their generation, and thus be beneficial in pancreatic β-cell protection prior to and/or during hyperglycaemia and β-cell stress. Of particular interest is the presence of mangiferin and its high levels in the extract, since this xanthone is a strong antioxidant (Sanchez *et al.*, 2000; Leiro *et al.*, 2003) and has also been shown to have antidiabetic properties, which include reduced plasma glucose and insulin levels in diabetic rats and mice, as well as suppresed HGP (Ichiki *et al.*, 1998; Miura *et al.*, 2001; Muruganandan *et al.*, 2002; Anitha and Rose 2013; Wan *et al.* 2013). The catechol moiety on mangiferin enables it to form stable mangiferin-Fe^{2+}/Fe^{3+} complexes, thus preventing lipid peroxidation in addition to itself scavenging ROS (Leiro *et al.,* 2003; Andreu *et al.,* 2005). Recently, the peroxyl radical scavenging activity of mangiferin was compared with that of two other major polyphenols found in this extract of unfermented *C. maculata* and the relative order of activity was isomangiferin > mangiferin > iriflophenone-3-*C*-glucoside (Malherbe *et al.,* 2014). Immunoregulatory capabilities of mangiferin have been demonstrated, via the reduction of TNF-α, the inhibition of NF-κB, which is mainly due to its antioxidant ability and the preservation of glutathione (GSH), as well as the suppression of other downstream pro-inflammatory cytokines in macrophages (Leiro *et al.,* 2004; Sarker *et al.,* 2004). An aglycone of mangiferin, norathyriol, improved glucose homeostasis and insulin sensitivity in obese C57BL/6J *ob/ob* mice (Ding *et al.,* 2014). A recent study proposes that the antioxidative properties of mangiferin could protect β-cells in STZ induced diabetic rats (Sellamuthu *et al.,* 2013). Thus, due to the high polyphenolic and, specifically, mangiferin content of this unfermented *C. maculata* extract, there is immense potential for this extract to not only ameliorate peripheral factors involved in T2D, but also offer protection to pancreatic β-cells, thus meriting its investigation.

With an increasing trend towards the use of natural products in the treatment of chronic diseases, either as a primary or as an adjunctive therapy with conventional therapeutics, (Frei, 2004, Scalbert *et al.*, 2005; Lee *et al.*, 2011), verification of the potential efficacy and safety using appropriate research methodology to provide adequate evidence based data is needed. Since β-cell failure is a putative and crucial step in the onset and deterioration of T2D, natural supplementation of current T2D therapy could potentially protect vulnerable pancreatic β-cells and thus improve and prolong quality of life in T2D patients, with a reduction in long-term associated disease complications.

5. Study objectives

I.   Establish an oxidative stress model *in vitro* in RIN-5F insulinoma cells that mimics pancreatic β-cell stress in T2D.

II. Assess the potential protective function of an aqueous, unfermented *C. maculata* extract and its major polyphenol, mangiferin, in RIN-5F cells.

III. Demonstrate the effect of the *C. maculata* extract and mangiferin on cell viability, glucose stimulated insulin secretion and oxidative stress in pancreatic islets isolated from Wistar rats.

IV. Assess the effect of the *C. maculata* extract *in vivo* on glucose metabolism, islet morphology and oxidative stress in the pancreata of STZ-induced diabetic Wistar rats.

CHAPTER 3

METHODOLOGY

In this study, we assessed the potential protective effect of an aqueous extract from unfermented *C. maculata* in protecting pancreatic β-cells exposed to conditions mimicking that of T2D. Both *in vitro* (in RIN-5F cells; section 1) and *ex vivo* (in isolated rat islets; section 2) experimentation were used to assess the effect(s) on β-cell viability function and oxidative stress. A model of STZ induced diabetes in Wistar rats was used to determine the *in vivo* effect (section 3). The aqueous extract of unfermented *C. maculata* used in this study was produced and kindly supplied by Prof E. Joubert of the Post-Harvest and Wine Technology Division at the Agricultural Research Council, Infruitec Nietvoorbij, Stellenbosch. The preparation and analysis of this extract was previously described by Dudhia *et al.* (2013). Briefly, unfermented *C. maculata* plant material was extracted with purified water at a ratio of 1:10 (m/v) at 93 °C for 30 minutes. The extraction was then filtered, allowed to cool to room temperature and freeze-dried. Upon receipt, the extract was stored under silica gel desiccation at room temperature, in the dark. The HPLC chromatogram of the extract is depicted in Fig. 14, in Chapter 2. The normal control referred to in this study represents cells/islets/rats exposed to the same reagents and conditions as the experimental conditions, with the exception of the specific agent(s) (either stressor or treatment) being tested. All reagents and equipment used in this study are listed in Addendum 3.

1. *In vitro* experimental design

The RIN-5F rat islet tumour cell line was used in this *in vitro* component of the study to assess the potential protective effect of the unfermented *C. maculata* extract, as well as mangiferin on this pancreatic β-cell line exposed to conditions characteristic of T2D (i.e. glucotoxicity, lipotoxicity, inflammation and oxidative stress). The protective effect on β-cells of a known antioxidant, *N*-acetyl cysteine (NAC) was also assessed as a positive control. This cell line has previously been used by several researchers to study the effects of T2D associated stress on β-cells (Tabatabaie *et al.*, 2000; Wang *et al.,* 2010; Son *et al.,* 2012 and 2014; Hu *et al.,* 2014). In our study, RIN-5F cells were cultured under standard conditions (section 1.1. below) and were seeded into multi-well plates for assay purposes (Fig. 15). The initial step was to optimise the concentration of each of the T2D associated stressors needed to result in approximately 50 % cell death (LC_{50}). Following 24 hours exposure to a range of concentrations of each stressor (glucotoxicity, lipotoxicity, inflammation and oxidative stress) cell viability was assessed using the 3-(4,5-dimethylthiazol-2-yl)-2,5-diphenyltetrazolium bromide tetrazolium (MTT) reduction assay (section 1.3.1.). After exposure to the optimised stressor concentrations, RIN-5F cells were

treated with a concentration range of *C. maculata* extract, mangiferin and NAC for 24 hours to ascertain the optimal effective concentration of each of these treatments; this was assessed using both the MTT (section 1.3.1.) and ATP (section 1.3.2.) assays. Both the MTT and ATP assays were used since plant polyphenols have previously been reported to interact with the MTT assay (Maioli *et al.,* 2009; Wang *et al.,* 2010). In addition, measurement of cellular ATP has been shown to be more than ten times more sensitive than the MTT assay (Petty *et al.,* 2005). Thus the MTT was a first line of screening, verified using the ATP assay. The efficacy of the optimised concentrations of each of the treatments against stressor induced β-cell dysfunction and death were then assessed in terms of cell viability (section 1.3.1.), cell function (section 1.4.) and oxidative stress (section 1.5.). Western blot analysis (section 1.7.) was also performed in order to determine the treatment effects on proteins involved in β-cell function and apoptosis. Treatment of cells with the extract, mangiferin and NAC for 24 hours was subsequent to exposure of these cells to the stressors for 24 hours, and said treatment period did not include the stressor. Stressors were omitted from the treatment period in order to negate the potential direct effect of any of the treatments on the stressor(s) itself or vice versa i.e. the stressor interacting directly with the treatment. It is important to note that the deleterious effect(s) of each of the stressors was still evident when each of the assays was performed. Standard aseptic conditions were maintained.
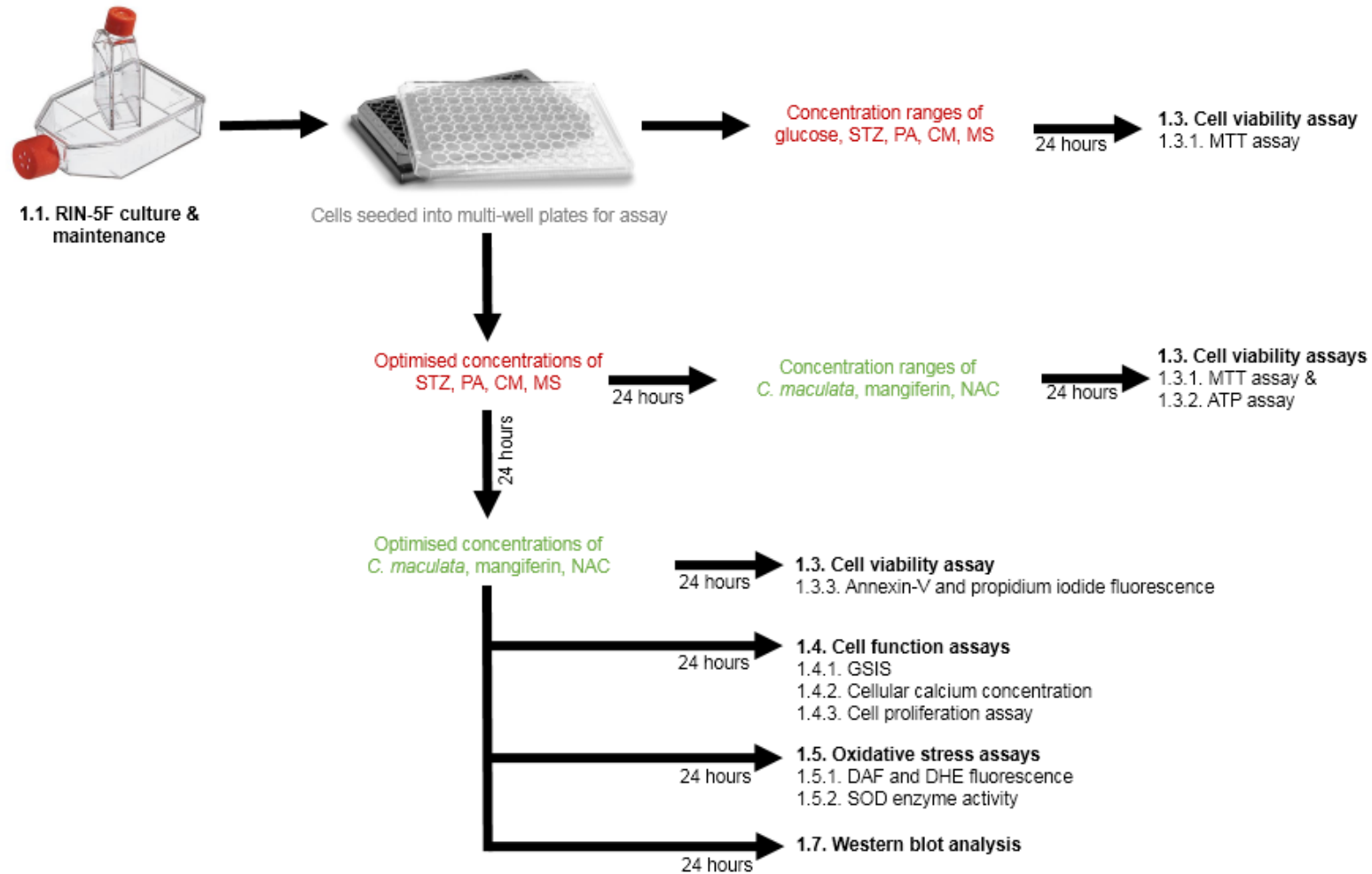
Figure 15. *In vitro* experimental design overview.

RIN-5F cells were cultured under standard conditions and were assayed in terms of cell viability, cell function and oxidative stress following exposure to T2D associated stressors and subsequent treatment with *C. maculata* extract, mangiferin and NAC. (ATP – adenosine triphosphate; CM – cytokine mixture; DAF - diaminofluorescein-FM diacetate; DHE – dihydroethidium; GSIS – glucose stimulated insulin secretion; MS – multi-stressor; MTT - 3-(4,5-dimethylthiazol-2-yl)-2,5-diphenyltetrazolium bromide tetrazolium; NAC – *N*-acetyl cysteine; PA – palmitic acid; SOD – superoxide dismutase STZ – streptozotocin).

1.1. Cell culture and maintenance

1.1.1. Thawing of RIN-5F cells

One 2 mL cryogenic vial containing 1 mL of Roswell Park Memorial Institute 1640 media (RPMI1640) supplemented with 10 % fetal bovine serum (FBS) and 7 % dimethyl sulphoxide (DMSO) containing 2×10^6 RIN-5F cells, stored in a Dewer cryogenic liquid nitrogen container in the vapour phase, was retrieved and placed in a pre-warmed water bath at 37°C. When 80 % of the cell suspension was liquid, the vial was transferred to a biohazard safety cabinet, where the 1 mL cell suspension was transferred into a 75 cm^2 cell culture flask containing 18 mL pre-warmed (37°C) RPMI1640 supplemented with 10 % FBS. One millilitre of the cell suspension was removed into a 2 mL tube in order to determine the number of viable cells, as described in section 1.1.3. The flask of cells (Fig. 16) was incubated at 37 °C in humidified air containing 5 % carbon dioxide (CO_2) for two days, whereafter media was refreshed. Following an additional three days of incubation at 37 °C in humidified air containing 5 % CO_2, the RIN-5F cell clusters at approximately 80 % confluence, were sub-cultured as described in section 1.1.2. If the number of viable cells, as determined by the trypan blue exclusion assay, was less than 70 %, the cells were considered to be compromised and were discarded, and a new vial of cells was thawed.
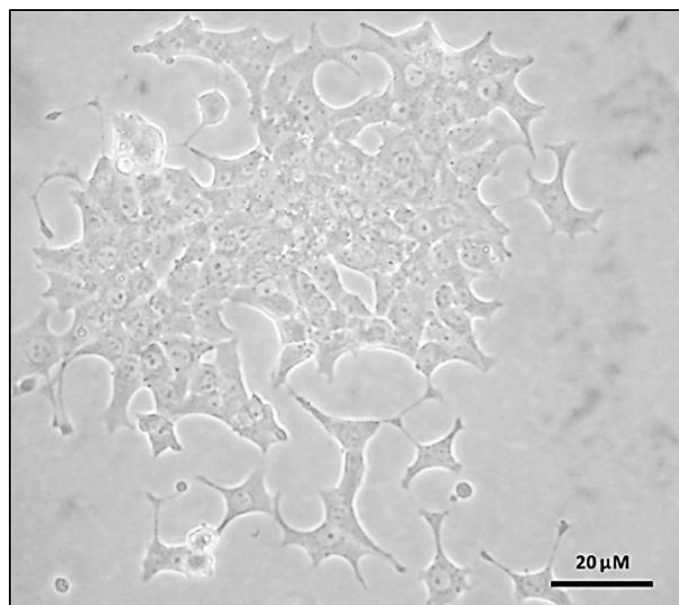
Figure 16. RIN-5F cell cluster in culture.

RIN-5F cells were incubated at 37 °C in humidified air containing 5 % CO_2 in RPMI1640 media supplemented with 10 % FBS. (x 400 magnification).

1.1.2. Sub-culture of RIN-5F cells

Sub-cultures of RIN-5F cells were produced by aspirating the RPMI1640 media off the semi-confluent (approximately 80 %) cells in the 75 cm^2 cell culture flasks and washing the cells with Dulbecco's phosphate buffered saline (DPBS) by adding 8 mL pre-warmed (37°C) DPBS, gently agitating the flask three times and then aspirating the DPBS. Cells were detached from the cell culture flask by incubating the cells at 37 °C in humidified air containing 5 % CO_2 with 2 mL of trypsin-versene for a minimum of seven minutes. After seven minutes, cells were observed under an inverted microscope at 30 second intervals to ensure adequate detachment had occurred. To inhibit the action of the trypsin-versene, 8 mL of pre-warmed (37°C) RPMI1640 supplemented with 10 % FBS was added to the detached cells and a 10 mL serological pipette was used to further dissociate and disperse the cells. Thereafter, the number of viable cells were counted as described in section 1.1.3., and new cell culture dishes were seeded. Cell culture flasks (75 cm^2) were seeded at 9 x 10^5 cells per flask in 18 mL pre-warmed (37°C) RPMI1640 supplemented with 10 % FBS and multi-well plates, for assay purposes, were seeded at 2.63 x 10^4 cells per cm^2. Sub-cultured cells were incubated at 37 °C in humidified air containing 5 % CO_2 for two days, upon which media was refreshed. Following a total of five days of incubation, sub-cultured cells in multi-well plates were used for assay purposes.

1.1.3. Trypan blue exclusion assay

The trypan blue exclusion assay used in this study was based on the principle of viable cells, with intact cell membranes excluding the trypan blue dye, as described by Strober (2001). Equal volumes of the cell suspension and a 0.4 % solution of trypan blue in phosphate buffered saline (PBS) (Fig. 17 C) were mixed and 10 µL of the resultant trypan blue/cell solution was added to one of the chamber ports of the chamber slide (Fig. 17 B). The chamber slide was then inserted in to the Countess^{TM} Automated Cell Counter (Fig. 17) and the total number of viable (live) and dead cells were counted as described by Malinouski *et al.* (2011). The total number of viable cells was then calculated as cells/mL and, in the case of sub-culturing, the required cell seeding densities were prepared.

Figure 17. The Countess^{TM} Automated Cell Counter.

The Countess^{TM} Automated Cell Counter was used to determine the number of viable RIN-5F cells using the trypan blue exclusion assay. This automated cell counter counts the equivalent of four $1\ mm^2$ squares on a standard haemocytometer, which equates to a sample/trypan blue solution volume of 0.4 µL. (From Invitrogen, 2009).

1.2. RIN-5F toxicity models

In order to assess the potential protective effect of the *C. maculata* extract and mangiferin against the deleterious conditions β-cells are exposed to in T2D, we developed toxic conditions to mimic glucotoxicity, lipotoxicity, inflammation and oxidative stress by exposing the cells to the following stressors for 24 hours, i.e. glucose, palmitic acid (PA), a cytokine mixture (CM) consisting of TNF-α, IL-1β and IFN-γ, and streptozotocin (STZ), respectively. In addition, a multi-stressor (MS) combination was derived, which included PA, CM and STZ. The approximate LC_{50} was determined by measuring mitochondrial dehydrogenase activity using the MTT assay (section 1.3.1.). Thereafter, the efficacy of the optimised concentrations of each of the treatments (i.e. *C. maculata* extract, mangiferin and NAC) against stressor induced β-cell dysfunction and death were assessed in terms of cell viability (section 1.3.1.), cell function (section 1.4.) and oxidative stress (section 1.5.). The stressors as well as the treatments were solubilised directly in the RPMI1640 cell culture media, with the exception of PA and NAC. In order to produce a 613 mM stock solution of NAC, 1 g of NAC was solubilised in 10 mL of cell culture tested water in a 37 °C water bath, dilutions of this filter-sterilised solution were used. Due to the hydrophobic nature of PA, we conjugated

69

this fatty acid to BSA to produce an aqueous-soluble reagent using a method modified from Schulz *et al.* (2013). A 50 mM stock solution of PA was prepared by dissolving 128.22 mg PA in 10 mL ethanol at 75 °C. The final concentrations of PA were prepared by adding the required amount of PA stock to a 2 % fatty acid-free bovine serum albumin (BSA) solution at 37 °C. To compensate for the potential cytotoxic effect of the ethanol, the normal control for all PA experiments contained the same amount of ethanol as the final concentration(s) of PA did. Although STZ is soluble in aqueous solutions up to a concentration of 50 mg/mL, it is unstable at neutral pH and rapidly degrades into its α- and β-anomers, therefore STZ was prepared immediately before use in all experiments.

1.3. Cell viability

1.3.1. The MTT assay

The MTT assay used in this study is based on the original description by Mossman (1983). Following exposure to the respective stressors for 24 hours and/or consecutive treatments of the RIN-5F cells, the 96 well cell culture plate wells were aspirated and the cells washed with pre-warmed (37 °C) DPBS. Thereafter, 100 μL of pre-warmed (37 °C) MTT solution (2 mg/mL DPBS) was added to each well and cells were incubated at 37 °C in humidified air containing 5 % CO_2 for 30 minutes. The formazan crystals formed during this incubation period were then dissolved in 200 μL DMSO and 25 μL Sorensen's glycine buffer (pH 10.5). The absorbance of the resulting purple formazan solution then measured on an absorbance BioTek microplate reader (ELX800) at 570 nm, controlled by Gen5 software.

1.3.2. The ATP assay

Cellular ATP, as a result of oxidative metabolism, was measured in RIN-5F cells using the ViaLight[TM] plus kit as described by Crouch *et al.* (1998). Following consecutive exposure of the RIN-5F cells to each of the stressors as well as a range of concentrations of either the extract, mangiferin or NAC, media from the cells in 96 well, flat bottomed, white walled cell culture plates were aspirated and the cells washed with pre-warmed (37 °C) DPBS. Thereafter, the cells were lysed by adding cell lysis reagent (provided in the ViaLight[TM] plus kit) to each well and incubating the cells at 37 °C in humidified air containing 5 % CO_2 for 10 minutes. Once lysed, a 10 μL sample of the lysate was transferred to a clean 96 well assay plate in order determine protein concentrations as described in section 1.3.2.1. To the cell lysate remaining in the culture plate, reconstituted ATP monitoring reagent (provided in the ViaLight[TM] plus kit) was added to the lysate in each well and the luminescence was

70

measured after two minutes on a fluorescent BioTek microplate reader (FLX800) controlled by Gen5 software. As described by the manufacturer, the cellular ATP was normalised to the protein content of each well.

1.3.2.1. Bradford protein quantification assay

Protein determinations were performed using the Bradford method (Bradford, 1976). A 10 µL sample of cell lysate from each well, as well as BSA standards were added to wells of a 96 well assay plate, followed by 250 µL of Bradford reagent. Plates were incubated in the dark for 10 minutes and absorbance was measured at 570 nm on a microplate reader (BioTek, ELX800). The actual protein concentration was determined by extrapolation from the BSA standard curve.

1.3.3. Annexin-V and propidium iodide fluorescence

In order to assess the effect of extract, mangiferin and NAC on stressor exposed RIN-5F cells, an adapted version of the annexin-V and propidium iodide fluorescent staining method described by Vermes *et al.* (1995) was used. As cellular apoptosis initiates, a phosphotidylserine switch from the inner leaflet to the outer leaflet of the cell membrane bilayer occurs, to which annexin-V binds due to its high affinity to said protein. The annexin-V used in this study was conjugated to fluorescein isothiocyanate (FITC) allowing us to quantify its binding using fluorescent detection. The addition of the DNA stain propidium iodide allowed us to also quantify late apoptotic and necrotic cells since this membrane impermeable dye will only intercalate between DNA bases once the cell membrane has been disrupted. In our study, following consecutive exposure of the RIN-5F cells to each of the stressors as well as an optimised concentrations of either the extract, mangiferin or NAC, media from the cells in 96 well, flat bottomed, black walled cell culture plates were aspirated and the cells washed with pre-warmed (37 °C) DPBS. Thereafter, cells were incubated with 2 µg/mL of annexin-V FITC conjugate and 1 µg/mL of propidium iodide in DPBS for 30 minutes at 37 °C in humidified air containing 5 % CO_2. Following incubation with the fluorescent markers, the cells were then washed with pre-warmed (37 °C) DPBS. After washing the cells, fresh pre-warmed (37 °C) DPBS was added to each well and annexin-V fluorescence was measured at excitation/emission (ex/em) of 488/530 nm (green) and propidium iodide at 540/608 nm (red) on a fluorescent microplate reader (BioTek, FLX800) controlled by Gen5 software.

1.4. Cell function

1.4.1. Glucose stimulated insulin secretion

The response of the RIN-5F cells to glucose stimulation was used to assess the function of these cells by means of a method adapted from Mabley *et al.* (2001) and Henningsson *et al.*, (2002). Following consecutive exposure of the RIN-5F cells to each of the stressors as well as an optimised concentration of either the extract, mangiferin or NAC, media from the cells in 96 well, flat bottomed, clear walled cell culture plates was aspirated and the cells were washed with pre-warmed (37 °C) DPBS. The RIN-5F cells were then incubated at 37 °C in humidified air containing 5 % CO_2 for two hours in Krebs-Ringer bicarbonate-HEPES buffer (KRBH) containing 5.5 mM glucose. Basal insulin secretion was determined by incubating the cells in fresh KRBH containing 5.5 mM glucose for 90 minutes at 37 °C in humidified air containing 5 % CO_2. The KRBH from each of the wells was carefully removed to a clean 96 well plate and frozen at -20 °C for enzyme-linked immunosorbent assay (ELISA) analysis. Subsequently, to determine the insulin secreted in response to glucose, fresh KRBH was added to the cells containing 35 mM glucose and cells were incubated for a further 90 minutes at 37 °C in humidified air containing 5 % CO_2. After 90 minutes KRBH was collected from each of the wells and frozen at -20 °C for ELISA analysis. The cells remaining in the plate were lysed by adding 0.1 M sodium hydroxide (NaOH) (supplemented with 1 % sodium dodecyl sulphate (SDS)) to each well and incubating the cells at 37 °C for 30 minutes. Protein concentration of the lysates were determined (as described in section 1.3.2.1.) in order to normalise insulin secretion concentrations as determined by ELISA in section 1.4.1.1.

1.4.1.1. Insulin concentration determination

A rat/mouse insulin sandwich ELISA kit was used to quantify the amount of insulin secreted by the RIN-5F cells into the media (KRBH) according to the manufacturer's instructions. Briefly, the media samples stored at -20 °C were brought to room temperature and were, along with insulin standards provided in the kit, added to the pre-coated ELISA plate. The pre-coating of the ELISA plate with monoclonal mouse anti-rat insulin antibodies allowed for the capture of insulin molecules from the samples and standards to the wells of the plate. Bound insulin was detected using biotinylated polyclonal antibody, horseradish peroxidase and 3,3',5,5'-tetramethylbenzidine substrate detection by measuring absorbency at 450 nm on a microplate reader. Due to acidification of formed products the absorbency at 450 nm was corrected using the absorbency at 590 nm. Actual sample insulin concentrations were

72

extrapolated from the standard curve generated. The insulin concentrations used for the standard curve were 0.2, 0.5, 1.0, 2.0, 5.0 and 10.0 ng/mL.

1.4.2. Cellular calcium determination

Since cellular calcium is crucial to normal functioning of pancreatic β-cells, both in terms of insulin secretion as well as ER function, we modified the method described by Lee *et al.* (2010) in order measure cellular calcium in the RIN-5F cells, the cells were seeded into flat bottomed, black walled 96 well cell culture plates and cellular calcium was determined by incubating the cells with 5 µM of glycine, N-[4-[6-[(acetyloxy)methoxy]-2,7-dichloro-3-oxo-3H-xanthen-9-yl]-2-[2-[2-[bis[2-[(acetyloxy)methoxy]-2-oxyethyl]amino]-5-methylphenoxy]ethoxy]phenyl]-N-[2-[(acetyloxy)methoxy]-2-oxyethyl]-,(acetyloxy)methyl ester (fluo3-AM) in DPBS at 37 °C in humidified air containing 5 % CO_2 for 30 minutes Following the 30 minute incubation, the cells were washed with pre-warmed (37 °C) DPBS, fresh pre-warmed (37 °C) DPBS was added to each well and fluorescence was measured on a fluorescent microplate reader (BioTek, FLX800) controlled by Gen5 software at ex/em of 506/526 nm.

1.4.3. Cell proliferation

The incorporation of tritiated thymidine into the DNA of dividing RIN-5F cells was used to determine cell proliferation. The methods previously described by Harkonen *et al.* (1990) and Buteau *et al.* (2001) were modified in this study. Following exposure of the RIN-5F cells to each of the stressors, a final concentration of 1 µCi/mL of tritiated thymidine was added to each well (2 µL/well) during the last four hours of treatment with the optimised concentration of either the extract, mangiferin or NAC. Media from the cells in 24 well, flat bottomed, clear walled cell culture plates was then aspirated and the cells washed with pre-warmed (37 °C) DPBS. The cells were then lysed by adding 0.1 M NaOH (supplemented with 1 % SDS) to each well and incubating the cells at 37 °C for 30 minutes. Lysate from each well was then transferred to scintillation vials containing distilled water and ULTIMA Gold scintillation fluid. After allowing the samples to equilibrate for one hour, radioactivity was measured on a scintillation counter. The remaining cell lysate was used to determine protein concentrations using the Bradford assay, as described in section 1.3.2.1. Data was normalised to protein concentrations as a measure of cell number per well.

1.5. Oxidative stress

1.5.1. Diaminofluorescein-FM diacetate and dihydroethidium fluorescence

The generation of RNS and ROS was detected using diaminofluorescein-FM diacetate (DAF) and dihydroethidium (DHE) fluorescent probes. The DAF fluorescent probe used in this study is transformed by intracellular esterases into a highly water-soluble fluorescent dye which traps nitric oxide produced in the cell. The DHE fluorescent probe reacts with superoxide anions and forms fluorescent ethidium, which intercalates with DNA. The methods described by Kojima *et al.* (1999) and Chen *et al.* (2013) were combined and modified in this study. A known inducer of ROS, 2,3-dimethoxy-1,4-naphthoquinone (DMNQ), was used as a positive control and was found to not only increase ROS (Fig. 18) in the RIN-5F cells, but also RNS (Fig. 19). RIN-5F cells seeded in 96 well flat bottomed, black walled cell culture plates were exposed to 100 µM DMNQ for 120 minutes, after which cells were washed with pre-warmed (37 °C) DPBS and incubated with 10 µM DAF and 5 µM DHE in DPBS at 37 °C in humidified air containing 5 % CO_2 for 30 minutes. The cells were then washed with pre-warmed (37 °C) DPBS and fluorescent intensities for DAF and DHE were measured on a fluorescent microplate reader controlled by Gen5 software at ex/em 495/515 nm and 518/605 nm, respectively.
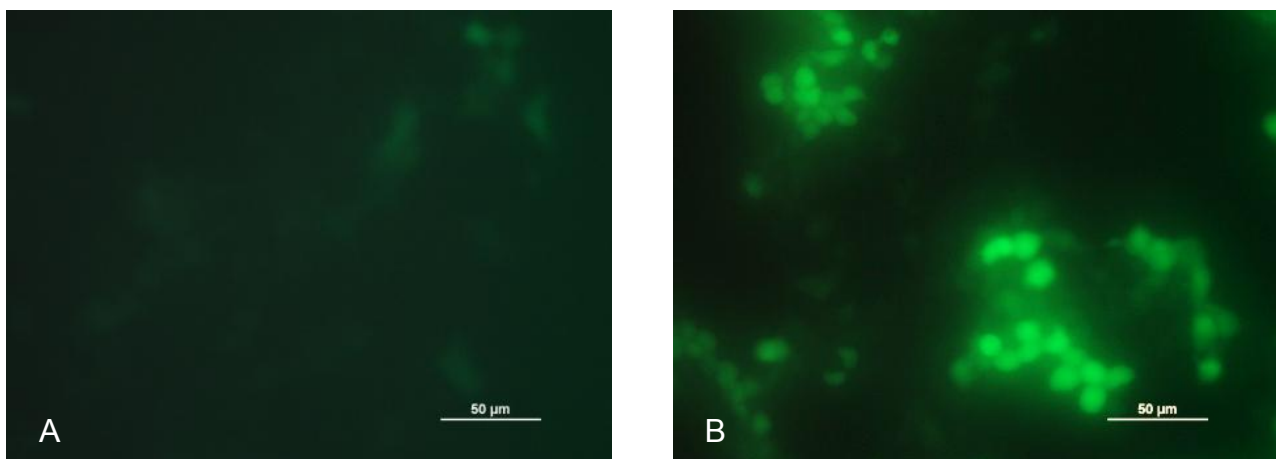
Figure 18. DMNQ induced increase of DAF fluorescence.

Exposure of RIN-5F cells to 100 µM DMNQ for 120 minutes resulted in visual and measurable increases in DAF fluorescence (B) compared to the normal control (A). (x 400 magnification).
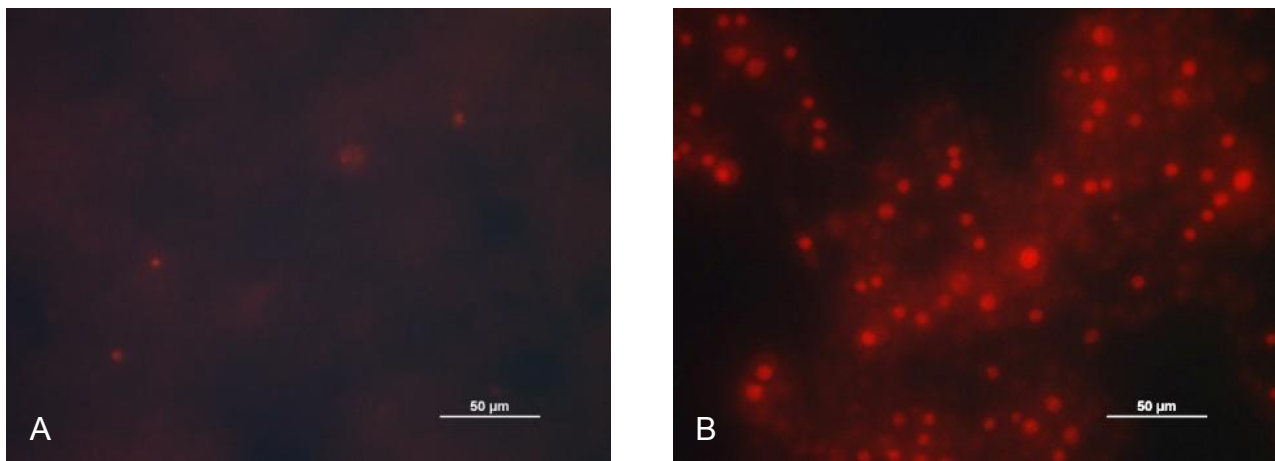
Figure 19. DMNQ induced increase of DHE fluorescence.

Exposure of RIN-5F cells to 100 µM DMNQ for 120 minutes resulted in visual and measurable increases in DHE fluorescence (B) compared to the normal control (A). (x 400 magnification).

1.5.2. Superoxide dismutase enzyme activity

The superoxide dismutase (SOD) enzyme catalyses the dismutation of the superoxide anion into hydrogen peroxide and molecular oxygen. SOD activity was assessed using a SOD assay kit from BioVision® based on a method adapted from Kanter *et al.* (2004). Following consecutive exposure of the RIN-5F cells seeded in 96 well flat bottomed, clear walled cell culture plates to each of the stressors, as well as an optimised concentration of either the extract, mangiferin or NAC, cells were washed with pre-warmed (37 °C) DPBS and 0.1 M Tris/HCl (pH 7.4) buffer containing 0.5 % Triton X-100, 5 mM β-mercaptoethanol and 0.1 mg/ml phenylmethanesulfonyl fluoride (PMSF) protease inhibitor was added to each well. Addition of the Tris/HCl buffer lysed the cells and simultaneously preserved cellular SOD. Three blanks were prepared in a 96 well assay plate; blank 1 contained all reagents except the sample, blank 2 contained all reagents except the enzyme working solution and blank 3 contained all reagents except the both sample and enzyme working solution. Ten microliters of cell lysate was added to the assay plate. The addition of water soluble tetrazolium salt-1 (WST-1; 2-(4-iodophenyl)-3-(4-nitrophenyl)-5-(2,4-disulfophenyl)-2H-tetrazolium monosodium salt) produced a water-soluble formazan dye upon reduction by superoxide anion, which was measured at 450 nm on a microplate reader (BioTek, ELX800) controlled by Gen5 software.

The percentage inhibition of superoxide was calculated using the following formula:

Percent inhibition (SOD activity) = $\frac{(A_{blank1} - A_{blank3}) - (A_{sample} - A_{blank2})}{(A_{blank1} - A_{blank3})}$ x 100

1.6. Extract mitogenicity determination

The potential mitogenic effect of the *C. maculata* extract used in this study was determined by measuring the incorporation of tritiated thymidine into RIN-5F cells treated with a range of extract concentrations (0.01 µg/mL – 100 µg/mL) as described in section 1.4.3. In addition, the effect of the extract on normal proliferation of RIN-5F cells was verified using crystal violet staining as described by Yusta *et al.* (2006). The resultant absorbance due to crystal violet staining of cells was measured at 570 nm on a microplate reader (BioTek, ELX800) controlled by Gen5 software.

1.7. Western blot analysis

Western blot analysis was used to determine the effects on selected proteins involved in β-cell function and apoptosis using a method modified from Mahmood and Yang (2012).

1.7.1. Cell collection and protein extraction

Following consecutive exposure of the RIN-5F cells seeded in 75 cm^2 culture flasks to each of the stressors, as well as an optimised concentration of either the extract, mangiferin or NAC, cells were washed with pre-warmed (37 °C) DPBS and were then collected using a cell scraper in 5 mL cold (4 °C) DPBS that was added to each flask, on ice. The scraped cells in DPBS were then transferred to a clean 15 mL tube and were centrifuged at 600 x g for 5 minutes. The cell pellet was then resuspended in 300 µL of commercial cell lysis buffer and the suspension transferred to a clean 2 mL Eppendorf tube. The cell suspension was then mechanically lysed by adding a steel bead to each Eppendorf tube and homogenising the samples at 25 Hz for 1 minute, with a rest interval on ice for 1 minute; samples were homogenised five times. The cell lysate was then centrifuged at 13 000 rpm at 4 °C for 10 minutes and the supernatant removed into a clean 2 mL Eppendorf tube. The reducing agent compatible and detergent compatible (RC/DC) protein concentration determination kit, based on the Lowry principle (Lowry *et al.,* 1951), was used to quantify sample protein concentration. Five microliters each of a range of BSA standards as well as 5 µL of a 1:20 dilution of each sample was transferred to a clean 96 well assay plate. Kit reagents A' and B were consecutively added to each well and the plate was agitated for 10 seconds before measuring absorbance at 685 nm on a microplate reader (BioTek, ELX800) controlled by Gen5 software. Actual protein concentration of the samples was determined by extrapolating the values from the BSA standard curve generated.

1.7.2. Separation of proteins by electrophoresis

The protein samples were diluted 3:1 with sample buffer (four times concentrate) and were then heated at 95 ℃ for 5 minutes on a heating block to denature proteins. Twenty micrograms of protein for each sample was loaded into a 10 % SDS-polyacrylamide gel electrophoresis (SDS-PAGE) precast gel, along with two molecular weight standard markers; one to monitor the progression of the protein movement through the gel (PageRuler marker) and the other for identifying proteins of interest following chemiluminescent detection (Cruz Marker). The gels were run for approximately 45 minutes (or until the protein front reached the bottom of the gel; Fig. 20) at 150 V in a mini protein tetra cell tank filled with running buffer.
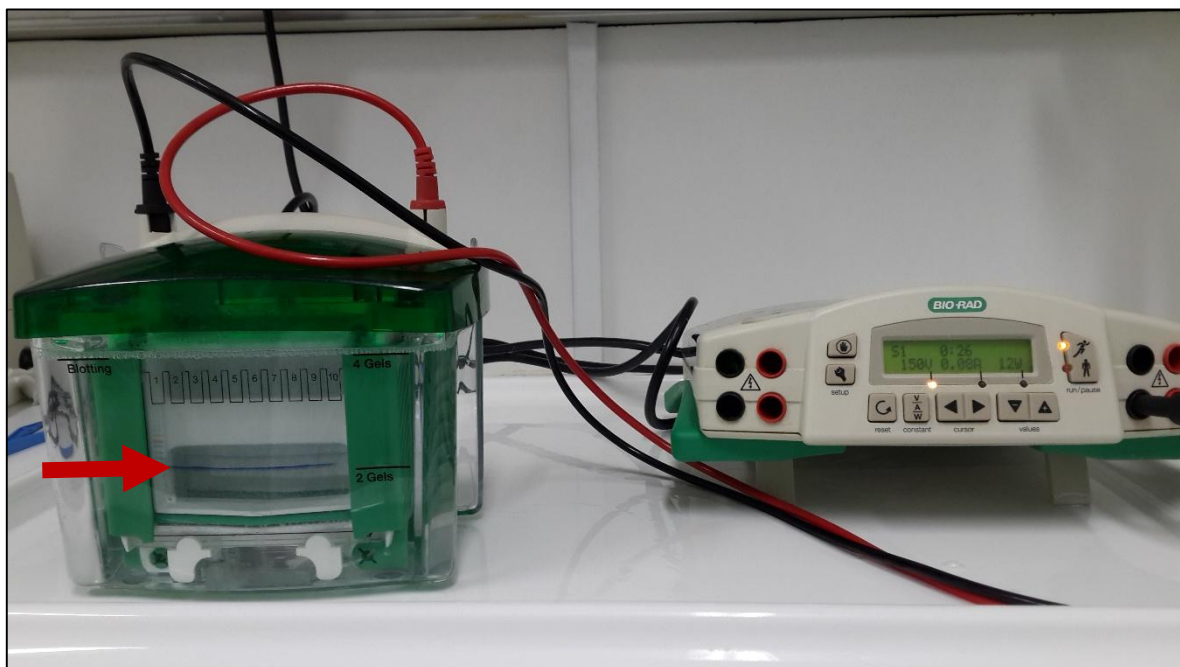
Figure 20. Sodium dodecyl sulphate polyacrylamide gel electrophoresis.
Proteins extracted from RIN-5F cells were separated using SDS-PAGE. The arrow indicates the protein front.

1.7.3. Protein sandwich transfer of gel to membrane

Proteins separated in the SDS-PAGE gels were then transferred to polyvinylidene difluoride (PVDF) membranes. Briefly, Whatman filter paper and PVDF membranes were cut to size (8 x 6 cm) and the membranes were activated by gently shaking in 100 % methanol for 1 minute. The filter paper and membranes, along with transfer fibre pads, were equilibrated in transfer buffer by gently shaking for 20 minutes. The transfer sandwich was then assembled as illustrated in Fig. 21 in the transfer cassette in the following order from cathode (negative terminal) to anode (positive terminal): fibre pad, filter paper, SDS-PAGE gel, PVDF

membrane, filter paper and fibre pad. Care was taken to eliminate air bubbles during transfer assembly.
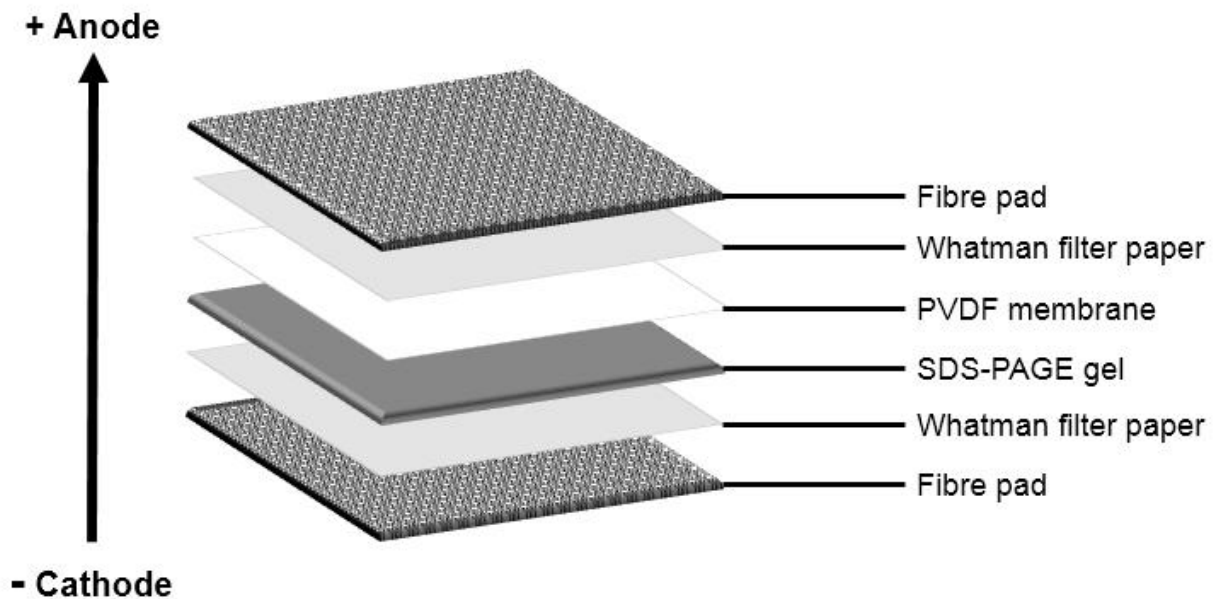
Figure 21. Western blot sandwich transfer assembly.

The transfer sandwich was assembled from cathode to anode by placing a fibre pad down and consecutively layering filter paper, SDS-PAGE gel, PVDF membrane, filter paper and another fibre pad.

The assembled cassette, along with an ice pack to regulate temperature, was placed between the electrodes in the transfer tank, with the respective terminals of the cassette corresponding with that of the tank (i.e. cathode to cathode, and anode to anode). The tank was filled with transfer buffer and proteins were transferred for 75 minutes at 160 V at 4 °C. To confirm transfer of proteins to the PVDF membrane, Ponceau S stain was applied to the membrane after transfer for 5 minutes, with gentle agitation. Once proteins were positively visualised, the membrane was washed with Tris buffered saline containing Tween®20 detergent (TBST) to de-stain the membrane.

1.7.4. Primary and secondary antibody incubations

To minimise nonspecific antibody binding, the PVDF membrane was blocked in TBST containing 5 % non-fat milk powder for two hours with gentle agitation. Four millilitre primary antibody diluted in TBST (Table 1) was applied to each membrane and incubated for 16 hours at 4 °C. Thereafter, the membrane was washed three times by gently agitation in TBST for 10 minutes. The membrane was then incubated with the secondary antibody (anti-rabbit IgG) at a 1:4000 dilution in TBST containing 2.5 % non-fat milk powder for 90 minutes

with gentle agitation. The blot was again washed three times by gently agitation in TBST for 10 minutes.

Table 1. Primary antibody dilutions

Primary antibody	Dilution	Catalogue No.	Manufacturer
Glucose transporter-2 (GLUT-2)	1:500	ab54460	Abcam; Cambridge Incorporated, MA, USA
β-cell lymphoma-2 (BCL-2)	1:1000	2870	Cell Signalling Technology; Danvers, MA, USA
Nuclear factor-kappa β (NF-κB)	1:1000	3033L	Cell Signalling Technology
Pancreatic duodenal homeobox-1 (PDX-1)	1:1000	5679S	Cell Signalling Technology
Caspase-3	1:1000	9662S	Cell Signalling Technology

1.7.5. Chemiluminescent detection

A chemiluminescent substrate detection kit was used to visualise proteins of interest by incubating the membrane in chemiluminescent substrate for 60 seconds in the dark. Excess substrate was drained off the membrane and images were captured using the ChemiDoc XRS imaging system, with 40 exposures for 0.1 seconds. Quantity One 1-D software was used to identify and quantify proteins of interest.

1.7.6. Housekeeping protein detection

In order to detect the housekeeping protein (i.e. β-tubulin), the respective membranes were stripped of the previously detected proteins by immersing the washed (in TBST for 10 minutes) membrane in stripping buffer for 13 minutes with gentle agitation. Thereafter the membrane was blocked in TBST containing 5 % non-fat milk powder for two hours with gentle agitation. The β-tubulin antibody was diluted in TBST (1:1000) and each membrane was incubated with 4 mL thereof for 16 hours at 4 °C. Thereafter, β-tubulin labelling was detected as described in sections 1.7.4 and 1.7.5. Proteins of interest were normalised to β-tubulin, which was used as a protein loading reference control, in order to determine the relative expression thereof.

2. *Ex vivo* experimental design

In order to verify the protective effects observed *in vitro* in RIN-5F cells exposed to STZ and PA, we isolated pancreatic islets from adult, male Wistar rats (section 2.1.1.) and replicated the experiments where the extract had the most marked beneficial effects (Fig. 22). The islets were seeded into multi-well culture plates and exposed to 10 mM STZ and 750 µM PA for 24 hours. Thereafter, the RPMI1640 media containing the stressor(s) was aspirated and fresh RPMI1640 containing either 10 µg/mL of the extract, 100 µg/mL of mangiferin or 0.01 mM NAC was added and the islets incubated for a further 24 hours. The viability of the isolated islets was then assessed using the annexin-V and propidium iodide assay (section 2.2.1.). Islet function was determined by measuring the insulin secretory response of the islets to glucose stimulation (section 2.3.1.), and oxidative stress in the islets was assessed using the DAF/DHE fluorescent assay (section 2.4.1.) and by measuring SOD enzyme activity (section 2.4.2.). All animal procedures were performed in accordance with the ethical code of conduct as prescribed by the latest South African Medical Research Council "Guidelines on ethics for medical research: use of animals in research" as well as The South African National Standard for the Care and Use of Animals for Scientific Purpose (SANS 10386:2008). Ethical approval for this component of the study was obtained from the Research Ethics Committee: Animal Care and Use of Stellenbosch University (Approval no: 11GK_CHE01).
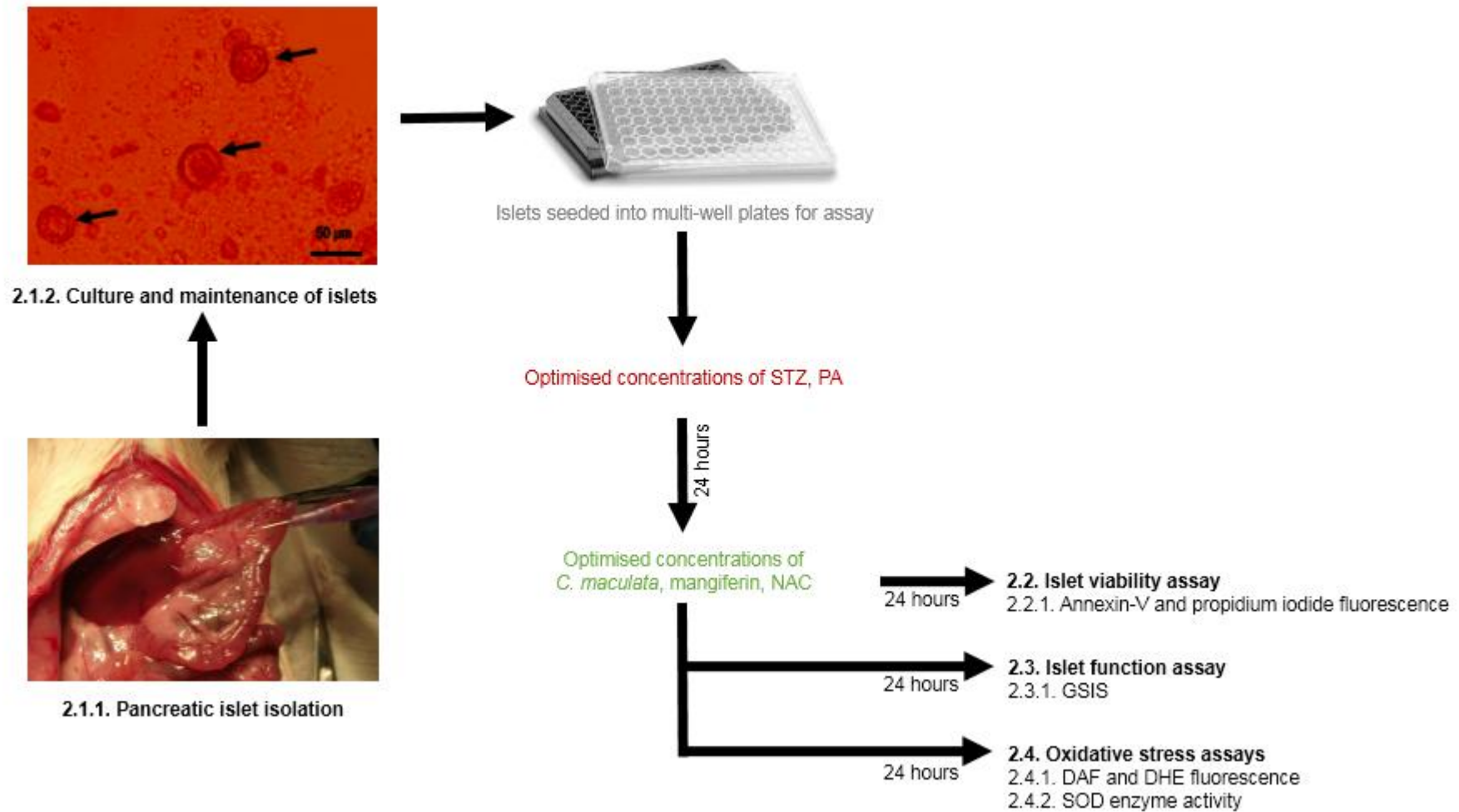
Figure 22. *Ex vivo* experimental design overview.

Pancreatic islets were cultured under standard conditions and were assayed in terms of cell viability, cell function and oxidative stress following exposure to T2D associated stressors and subsequent treatment with *C. maculata* extract, mangiferin and NAC. (ATP – adenosine triphosphate; CM – cytokine mixture; DAF - diaminofluorescein-FM diacetate; DHE – dihydroethidium; GSIS – glucose stimulated insulin secretion; MS – multi-stressor; MTT - 3-(4,5-dimethylthiazol-2-yl)-2,5-diphenyltetrazolium bromide tetrazolium; NAC – *N*-acetyl cysteine; PA – palmitic acid; SOD – superoxide; dismutase STZ – streptozotocin).

81

2.1. Pancreatic islet isolation, culture and maintenance

A total of 54 age-matched adult (three month old) Wistar rats of similar body weight (250 g – 300 g) were housed and maintained under standard conditions (12 hour light/dark cycle at 22 ± 2 °C) at the Primate Unit and Delft Animal Centre (PUDAC) at the South African Medical Research Council. The modified methods of Takaki and Ono (1985) and Kinasiewicz *et al.* (2004) were used to isolate pancreatic islets from these Wistar rats. For each experiment a total of 18 rats were anaesthetised by intra-peritoneal injection with 35 mg/kg sodium pentobarbitone. The main pancreatic duct was identified by making a mid-line abdominal incision and by reflecting the duodenal loop, thereby exposing the main pancreatic duct and ampullae (Fig. 23).
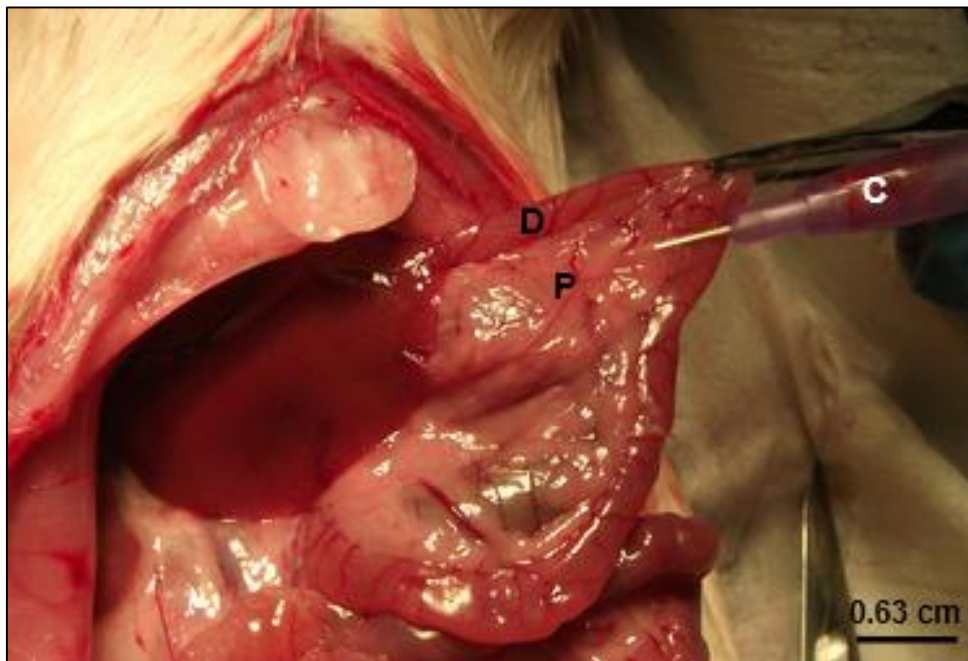
Figure 23. Cannulation of the main pancreatic duct.

A neonatal cannula was used to intubate the main pancreatic duct in order to fully distend the organ with collagenase P solution. (D – duodenum; P – pancreas; C – cannula).

Rat pancreata were fully distended by injecting 6 ml ice cold Hanks balanced salt solution (HBSS) containing 1 mg/mL collagenase P into the main pancreatic duct using a 26 gauge neonatal cannula under a stereo microscope. Special care was taken when excising the distended pancreata to avoid rupture of the digestive tract. The excised pancreata were transferred into a sterile 50 ml tube containing an additional 5 mL of collagenase P solution and was placed on ice. Rats were not allowed to recover from anaesthesia and were euthanised by exsanguation and cardiac snip. The pooled pancreata were digested at 37

°C in a circulating water bath for 30 - 45 minutes with intermittent shaking. Once sufficient digestion was observed, the digestate was filtered through a 500 µm nylon mesh in a biohazard safety hood. Ten millilitres of cold (4 °C) HBSS containing 0.1 % BSA was added to the digestate to inhibit the collagenase P. The pancreatic tissue contained in the digestate was then pelleted by centrifugation at 600 x g for 5 minutes at 4 °C. The pellet was resuspended in cold (4 °C) HBSS/BSA and again centrifuged (600 x g for 5 minutes at 4 °C). The pellet was then resuspended in 10 mL cold (4 °C) HBSS/BSA and a Histopaque gradient was produced in a 50 mL centrifuge tube as follows (Fig. 24): 10 mL of Histopaque 1119 was transferred to the centrifuge tube, 10 mL of the HBSS/BSA containing the pancreas digestate was layered on the Histopaque 1119 and subsequently 10 mL each of Histopaque 1083 and 1077 Histopaque was layered on top. The Histopaque gradient was centrifuged at 2000 rpm for 20 minutes at 4 °C with the brake off. The islets were then recovered from the interface between the HBSS/BSA layer and Histopaque 1077 (Fig. 24).
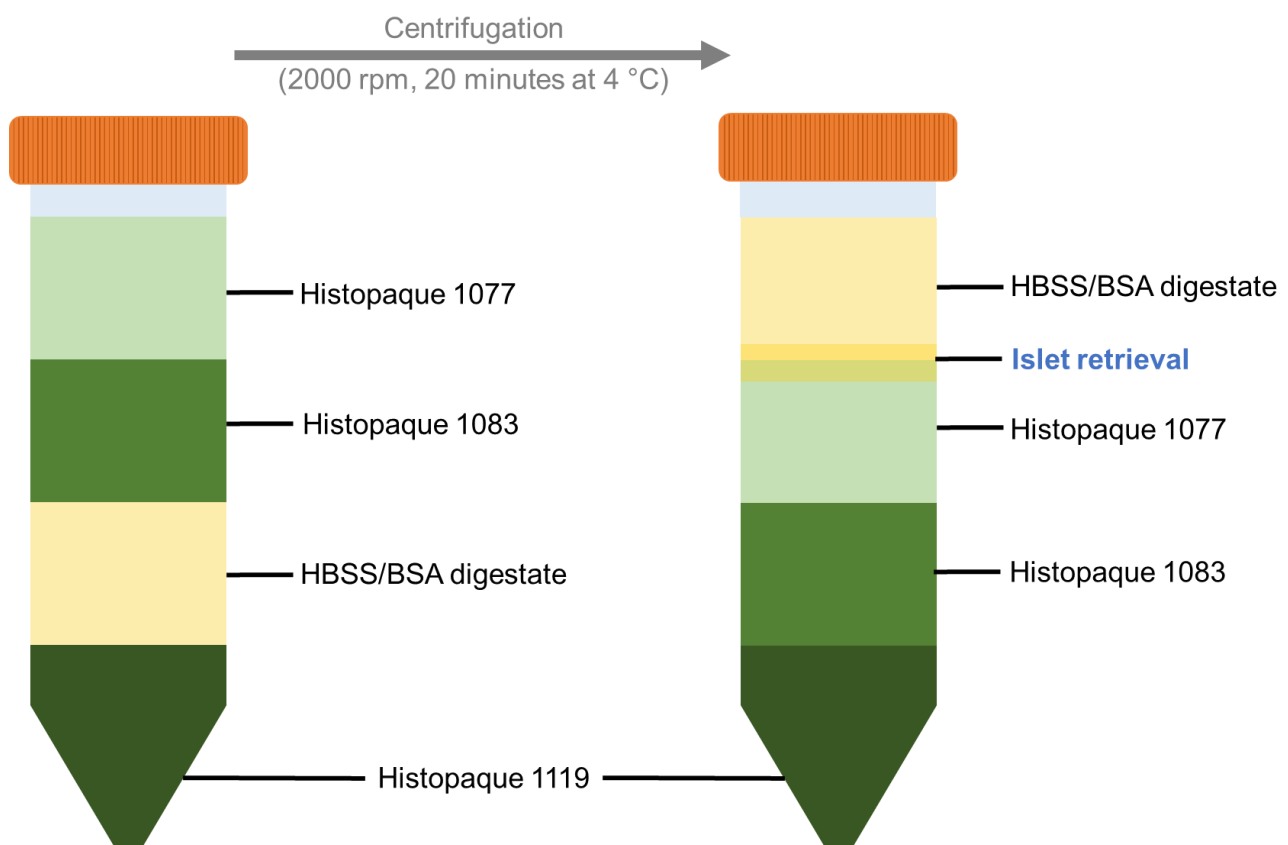
Figure 24. Histopaque density gradient separation of isolated islets.

Pancreatic digestate in HBSS/BSA was subject to Histopaque density separation in order to retrieve the islet fraction at the Histopaque 1077 and HBSS/BSA interface following centrifugation at 2000 rpm for 20 minutes at 4 °C.

The recovered islet fraction was washed with cold (4 °C) HBSS and pelleted by centrifugation (600 x g for 5 minutes at 4 °C). The pellet was resuspended in warm RPMI1640 supplemented with 10% FBS, 40 µg/mL geneticin, penicillin (100IU) and streptomycin (100 µg/mL) at 37 ºC in humidified air with 5% CO_2. Following 16 hours incubation, islets were handpicked using a 1000 µL pipette under a stereo microscope and were seeded into black walled 96 well culture plates, with 30 - 50 islets per well (depending on the yield per isolation, islets were equally divided amongst the wells). The handpicked islets were incubated in fresh RPMI1640/FBS overnight, following which islet viability, function and oxidative assays were performed as described previously (sections 1.3.3., 1.4.1., 1.5.1. and 1.5.2., respectively).

2.1.1. Islet toxicity models

The two islet toxicity models assessed in this study were based on the results observed in the RIN-5F experimentation. Since the extract was observed to be most effective in STZ and PA exposed RIN-5F cells, we sought to verify this effect *ex vivo* in pancreatic islets isolated from adult, male Wistar rats. As similarly described for the *in vitro* model, islets seeded in 96 well assay plates were exposed to either 10 mM STZ or 750 µM PA for 24 hours at 37 ºC in humidified air with 5% CO_2. Thereafter, media containing the stressor(s) was aspirated and fresh media containing either 10 µg/mL of the extract, 100 µg/mL of mangiferin or 0.01 mM NAC was added and the islets incubated for a further 24 hours at 37 ºC in humidified air with 5% CO_2.

2.2. Islet viability
2.2.1. Annexin-V and propidium iodide fluorescence in islets

In order to assess the effect of extract, mangiferin and NAC on STZ and PA exposed islets, the annexin-V and propidium iodide fluorescent staining method described in section 1.3.3. was used.

2.3. Islet β-cell function
2.3.1. Glucose stimulated insulin secretion in islets

The response of the isolated islets to glucose stimulation was used to assess the function of the islet β-cells as described for the RIN-5F cells in section 1.4.1. Protein concentration of the lysates was determined as described in section 1.3.2.1.

2.4. Islet oxidative stress

2.4.1. Diaminofluorescein-FM diacetate and dihydroethidium fluorescence in islets

Measurement of DAF and DHE fluorescence in the islets following consecutive exposure of the islets to STZ or PA, as well as the extract, mangiferin or NAC was used to determine RNS and ROS production as described in section 1.5.1.

2.4.2. Superoxide dismutase enzyme quantification in islets

The quantification of SOD enzyme activity, as described in section 1.5.2., was replicated in islets consecutively exposed to STZ or PA, as well as the extract, mangiferin or NAC.

3. *In vivo* experimental design

The efficacy of the *C. maculata* extract on the deleterious effects of STZ on pancreatic β-cells was assessed in Wistar rats (Fig. 25). In order to assess the therapeutic effect of the extract on established diabetes, adult, male Wistar rats were injected with STZ. Upon induction of diabetes (fasting plasma glucoses > 14 mmol/L) and recovery of the acute toxic effects of STZ five days thereafter, the rats were treated with either distilled water (STZ control), the extract (30 mg/kg/d and 300 mg/kg/d), metformin (125 mg/kg/d) or NAC (125 mg/kg/d) for 21 days; this group is referred to as the "treated group".

In order to assess the protective effect of the extract against STZ induced β-cell destruction, rats were pretreated with either distilled water (STZ control), the extract (30 mg/kg/d and 300 mg/kg/d), metformin (125 mg/kg/d) or NAC (125 mg/kg/d) for 15 days. At this point, the rats were injected with STZ and treatment (with either distilled water, the extract, metformin or NAC) continued for six days, totalling 21 days of treatment; this group is referred to as the "pretreated group".

A normal control group of rats, not injected with STZ, were concurrently administered distilled water for 21 days. This group served as a normal control for both the treated and pretreated groups.

On day 21, an oral glucose tolerance test (OGTT) was performed and the rats were terminated the day after (day 22). Blood and tissue (pancreas and liver) were collected post-mortem. Several parameters were assessed on blood collected, i.e. fasted glucose (section 3.3.1.), insulin (section 3.4.1.) and triglyceride (section 3.4.2.) levels; liver enzymes (section 3.4.3.); and antioxidant parameters (serum nitrites (section 3.5.1.), CAT (section 3.5.2.1.) and GSH levels (section 3.5.2.2.). To further explore the antioxidative effect of the extract, liver thiobarbituric acid reactive substances (TBARS) (section 3.5.3.) and nitrotyrosine (section 3.5.4.) was measured. Pancreata excised from the rats at termination were assessed using immunohistochemical labelling for MIB-5 (proliferation) (section 3.6.1.), as well as glucagon and insulin double-labelling (section 3.6.2.).
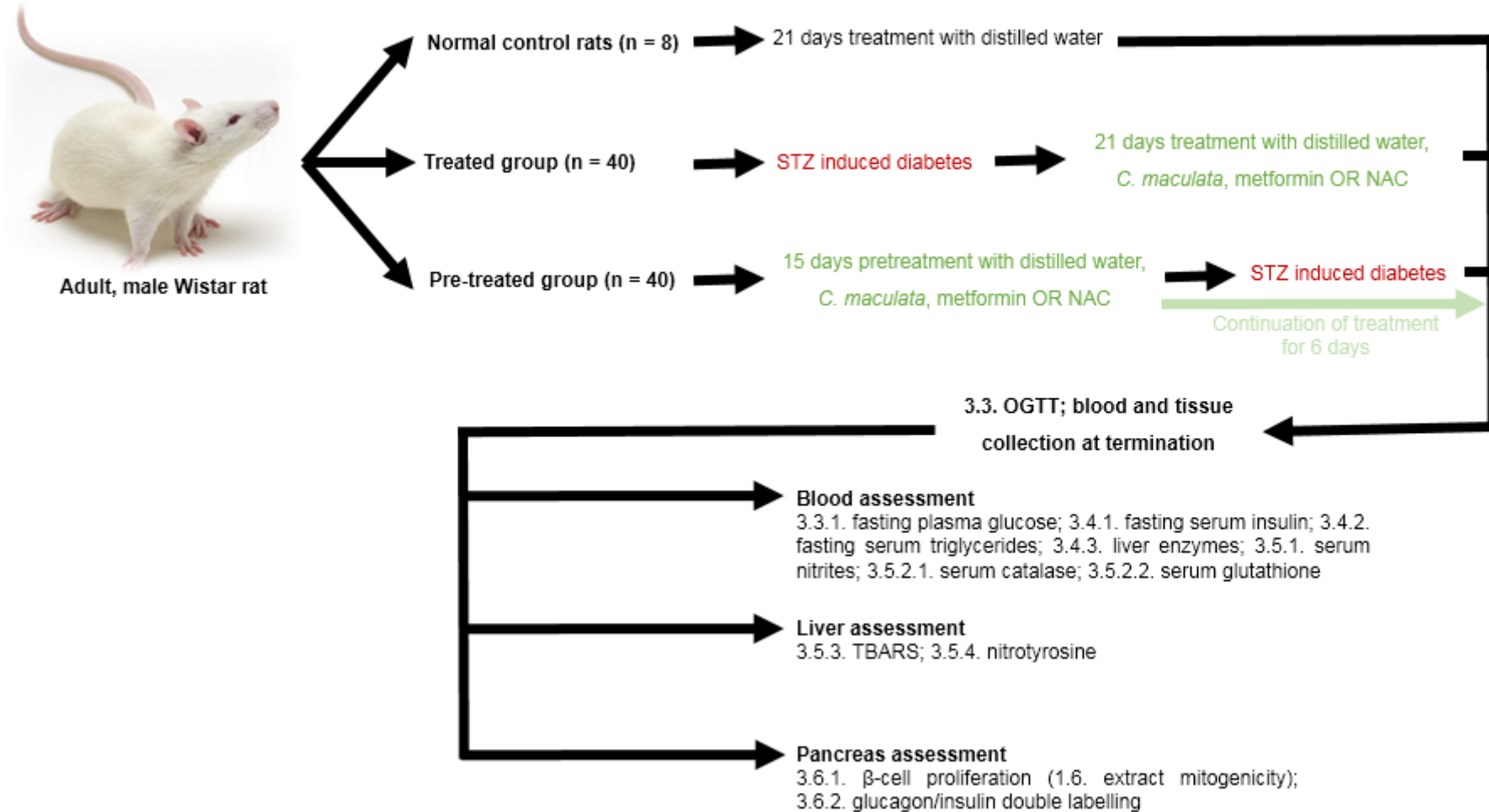
Figure 25. In vivo experimental design overview.

Adult, male Wistar rats were randomised into normal, treated and pretreated groups in order to assess the efficacy of *C. maculata* extract on the deleterious effects of STZ on pancreatic β-cells *in vivo*. (NAC – *N*-acetyl cysteine; OGTT – oral glucose tolerance test; STZ – streptozotocin; TBARS - thiobarbituric acid reactive substances).

3.1. Ethical aspects and animal observations

All animal procedures were performed in accordance with the ethical code of conduct as prescribed by the latest South African Medical Research Council "Guidelines on ethics for medical research: use of animals in research" as well as The South African National Standard for the Care and Use of Animals for Scientific Purpose (SANS 10386:2008). Ethical approval for this component of the study was obtained from the Research Ethics Committee: Animal Care and Use of Stellenbosch University (Approval no: 11GK_CHE01). Eighty eight adult, male Wistar rats of similar body weight (250 g – 300 g) were obtained from and housed at PUDAC under standard conditions (12 hour light/dark cycle at 22 ± 2 °C). The rats were randomised into groups (Table 2) and were individually caged (0.13 m^2/rat), with *ad libitum* access to fresh drinking water and a standard laboratory rodent diet (Pure Harvest rat/mouse pellets), except during stipulated periods of fasting. Routine cage side observations were performed daily as recommended by the US Food and Drug Administration, Centre for Food Safety and Applied Nutrition, Office of Food Additive Safety Redbook 2000 – Toxicological Principles for the Safety Assessment of Food Ingredients. Observations included any visible signs of changes in skin and fur condition, eyes and mucous membranes (secretions and excretions), autonomic activity (i.e. shivering, pilorection, breathing rate), changes in gait, posture, response to handling, the presence of clonic or tonic movements, stereotypic behaviour (i.e. excessive or lack of grooming, repetitive circling), severe dehydration, excessive weight loss (diabetes associated emaciation) or bizarre behaviour (i.e. self-mutilation or walking backwards). Food and water consumption was monitored throughout the study. These atypical behaviours would result in the respective animal(s) being excluded from the study. None of the animals in this study exhibited such behaviour and thus all groups were n = 8.

Table 2. Rat treatment groups (n = 8/group).

Group	Injected with STZ	Start treatment	Treatment
Normal control	N/A	Day 0	1 mL distilled water/kg/d
Treated group	Day -5	Day 0	-
STZ control			1 mL distilled water/kg/d
Metformin			125 mg/kg/d metformin
NAC			125 mg/kg/d NAC
30 mg/kg/d *C. maculata*			30 mg/kg/d *C. maculata*
300 mg/kg/d *C. maculata*			300 mg/kg/d *C. maculata*
Pre-treated group	Day 16	Day 0	-
STZ control			1 mL distilled water/kg/d
Metformin			125 mg/kg/d metformin
NAC			125 mg/kg/d NAC
30 mg/kg/d *C. maculata*			30 mg/kg/d *C. maculata*
300 mg/kg/d *C. maculata*			300 mg/kg/d *C. maculata*

3.2. Treatment and induction of diabetes

As described in table 2, rats were treated with either distilled water, metformin, NAC or extract. All treatments were administered in gelatin jelly cubes, comprising 27 g jelly powder and 3 g gelatine powder per 100 mL, as reported in a previous study (Chellan *et al.,* 2008). Each of the treatments were dissolved in 100 mL of gelatine jelly solution (metformin – 1042 mg; NAC – 2085 mg; 30 mg/kg/d *C. maculata* – 250 mg; 300 mg/kg/d *C. maculata* – 2500 mg), and the rats received 6 mL of gelatine jelly per kilogram of bodyweight twice daily, which equated to 125 mg/kg/d metformin, 125 mg/kg/d NAC, 30 mg/kg/d *C. maculata* and 300 mg/kg/d *C. maculata*. Due to the palatability of the jelly cubes, the entire treatment dose was consumed by the rats within 10 minutes of administration, which was confirmed daily. The rats received their respective treatments in two doses at approximately 8h00 and 16h00 daily.

3.2.1. Streptozotocin induced diabetes

In order to induce diabetes, 16 hour fasted rats were administered 35 mg/kg body weight STZ by intra-peritoneal injection immediately after dissolution of STZ in 0.05 M sterile filtered citric acid buffer (pH 4.5).

3.3. Oral glucose tolerance test

On Day 21 of this *in vivo* study, an oral glucose tolerance test was performed. Rats were fasted overnight for 16 hours (with access to fresh drinking water *ad libitum*) and fasting plasma glucoses were measured as described in section 3.3.1. Thereafter, rats received

their daily treatment in gelatine jelly cubes and two hours later were administered a glucose bolus of 2 g/kg as a 50 % dextrose solution by oral gavage. Plasma glucose was measured as described in section 3.3.1 at the following time points: 0, 15, 30, 60, 120 and 240 minutes.

3.3.1. Plasma glucose determination

The tails of the rats were cleaned with damp piece of tissue paper and a drop of blood (approximately 10 µL) was obtained from a tail prick. The drop of blood was directly transferred into a capillary action glucose test strip and glucose concentration was quantified by a handheld glucometer.

3.4. Blood and tissue collection at termination

On day 22, following 21 days of treatment and the OGTT, rats were anaesthetised by sodium pentobarbital intraperitoneal injection (35 mg/kg). A mid-line abdominal incision was made under anaesthesia and a total of 10 ml of blood was collected from each rat from the abdominal vena cava. Approximately 8 mL of blood collected per rat was transferred to a serum separating tube (SST) and the remaining 2 mL to a K_2 ethylenediaminetetraacetic acid (EDTA) tube for serum and plasma collection, respectively. Blood samples were placed on ice and serum and plasma were later separated by centrifugation (2000 rpm for 15 minutes at 4 °C) and stored at -20 °C in 2 mL cryogenic vials for future analysis. Pancreata and the liver were excised and dissected into two equal halves. One half of each tissue was fixed in 10 % buffered formalin for immunohistochemical analysis and the other half was snap frozen in liquid nitrogen. The snap frozen tissues were stored at -80 °C. Rats were not allowed to recover from anaesthesia and were euthanised by exsanguation and cardiac snip.

3.4.1. Fasting plasma insulin determination

Quantification of insulin in the plasma samples frozen at -20 °C was performed after bringing the samples to room temperature using an ELISA kit, as described in section 1.4.1.1.

3.4.1.1. Glucose to insulin ratio

The glucose to insulin ratio was calculated using fasted glucose and insulin values as described by McAuley *et al.* (2001), and was used to assess insulin sensitivity using arbitrary units. The following formula was used:

$$\text{Glucose to insulin ratio} = \frac{Fasting\ glucose}{Fasting\ insulin}$$

3.4.2. Serum triglyceride determination

Serum triglyceride concentrations were determined by PathCare Medical Diagnostic Laboratories (N1 City, Cape Town, South Africa), using a modified method originally described by Lofland (1964).

3.4.3. Liver function tests

In order to assess liver function, serum levels of aspartate aminotransferase (AST), alanine transaminase (ALT) and alkaline phosphatase (AP) were quantified by PathCare Medical Diagnostic Laboratories. The enzymes were quantified using methods described by the International Federation of Clinical Chemistry (1977).

3.5. Antioxidant status

3.5.1. Serum nitrite quantification

Nitrite concentrations in rat sera were measured using methods modified from Green *et al*. (1982) and Grisham *et al*. (1996). Equal amounts of serum and Griess reagent were incubated for 15 minutes in a 96 well clear walled assay plate and the absorbance was read at 540 nm on a microplate reader (BioTek, ELX800) controlled by Gen5 software.

3.5.2. Serum antioxidant enzyme quantification

Serum CAT enzyme and GSH quantification were determined using commercially available kits from BioVision®, according to the manufacturer's instruction.

3.5.2.1. Serum catalase determination

Serum samples were diluted 1:2 with kit assay sample buffer in 96 well clear walled assay plates. Equal amounts of hydrogen peroxide were added to each well to react with catalase (CAT) present in the serum, producing water and oxygen. A hydrogen peroxide standard curve was also generated. A development mix included in the kit, which consists of a chromatic development probe as well as horseradish peroxidase, was used to detect the amount of hydrogen peroxide not converted (by CAT) to water and oxygen by measuring the absorbance at 570 nm on a microplate reader (BioTek, ELX800) controlled by Gen5

software. The actual CAT enzyme activity for each sample was calculated using the following equation:

CAT activity (mU/mL) = $\dfrac{B}{30 \; x \; V}$ x sample dilution factor

Where B = decomposed amount of H_2O_2 (from standard curve) and V = sample volume.

3.5.2.2. Serum glutathione determination

Serum samples were thawed on ice and proteins were precipitated using 6 N perchloric acid. Thereafter, 6 N potassium hydroxide was added to each sample in order to neutralise the perchloric acid. The neutralised samples were then transferred to a black walled 96 well plate, along with a GSH standard curve. The samples and standard curve were incubated with the dialdehyde probe, o-phthalaldehyde. The reaction of o-phthalaldehyde with GSH thiols was measured at ex/em 340/420 nm on a fluorescent microplate reader (BioTek, FLX800) controlled by Gen5 software. The actual GSH concentration for each sample was calculated by extrapolation from the standard curve generated.

3.5.3. Hepatic thiobarbituric acid reactive substances

TBARS in frozen liver tissue was measured to assess the formation of malondialdehyde as a result of lipid peroxidation. A weighed amount of frozen liver was homogenised in a 2 mL Eppendorf tube with a steel bead at 25 Hz for 1 minute five times, with 1 minute of cooling on ice between homogenisation. The tissue lysate was centrifuged (13 000 x g for 10 minutes at 4 °C) and 150 µL of the supernatant from each sample was transferred to a clear walled 96 well assay plate. A standard curve was generated from a 500 µM stock of 1,1,3,3-tetramethoxypropane. The absorbance of the resultant reaction between 2-thiobarbituric acid, which was added to samples and standards, and malondialdehyde was measured at 532 nm on a microplate reader (BioTek, ELX800) controlled by Gen5 software. The sample TBARS concentration was extrapolated from the standard curve generated.

3.5.4. Hepatic nitrotyrosine

The remaining lysate supernatant from the TBARS assay (section 3.5.3.) was used for Western blot analysis of hepatic nitrotyrosine. Western blot analysis was performed as described in section 1.7.

3.6. Pancreatic islet staining and analysis

Pancreata fixed in 10 % buffered formalin overnight, were processed in an automated tissue processer and were embedded in paraffin wax according to standard histological procedure. Sections of approximately 5 µm were cut on a rotary microtome and were attached to aminopropyltriethoxysilane coated glass slides. Sections were dewaxed through xylene and hydrated in decreasing concentrations of ethanol into distilled water before immunohistochemical labelling as described in sections 3.6.1. and 3.6.2 for the MIB-5 antigen as well as insulin and glucagon double labelling, respectively. Stained sections of pancreata observed under the microscope were captured using Leica Qwin Professional software. For the MIB-5 labelled sections, brown MIB-5 positive β-cells were counted manually. To quantify insulin and glucagon double labelling, alternate fields were scanned and subjected to red/green/blue (RGB) colour segmentation in order to facilitate conversion to a binary image. The total area of the binary image of the insulin and glucagon double labelling was determined using the Leica software (total islet area), as were the specific areas of glucagon (brown) and insulin (red) positive islet cells. Insulin and glucagon positive cell counts were also determined.

3.6.1. Beta-cell proliferation

In order to assess proliferation of β-cells in rat pancreata, immunohistochemical labelling of the MIB-5 antibody was performed for demonstration of the Ki-67 antigen (Birner *et al.,* 2001). Endogenous peroxidases were blocked using 3 % hydrogen peroxide and non-specific binding was blocked using a 1:20 dilution of normal goat serum. Pancreas sections were then labelled with MIB-5 monoclonal antibody at a 1:50 dilution. Thereafter, a biotinylated anti-mouse secondary link anti-body was applied and positive labelling was visualised by a streptavidin complex diaminobenidizine labelling kit. Sections were counterstained in haematoxylin and thereafter mounted and coverslipped.

3.6.2. Insulin and glucagon double labelling

In order to assess islet structure, the labelling method modified from Louw *et al.* (1997) was used in this study. Briefly, the dewaxed and hydrated pancreas sections were double labelled following the blocking of endogenous peroxidases and non-specific binding as described previously. Following 30 minutes of incubation with the glucagon primary antibody, a 1:1000 dilution of biotinylated anti-rabbit IgG and was visualised using the liquid diaminobenzidine tetrachloride (DAB) Plus Substrate Chromagen System. For insulin

labelling the sections were again blocked, using normal horse serum, after which the insulin antibody was applied overnight (16 hours) at 4 °C. The Envision permanent red chromogenic substrate kit was used to visualise the binding of insulin antibody to insulin antigen in the pancreas tissue section. The number of cells with brown DAB glucagon labelling or the permanent red precipitate of the insulin labelling were counted.

4. Statistical analysis

Specific attention was given to correct sample size, appropriate controls and the avoidance of type-II errors during the experimental design phase, as per consultation with a biostatistician (Ms Ushma Galal, SA Medical Research Council). Results in the *in vitro* and *ex vivo* components of this study were expressed as the means of three independent experiments, with four intra-experimental repeats per experiment. Error bars reflect the standard error of the mean. All data were entered into Microsoft Excel spreadsheets to generate graphs and GraphPad Prism (version 5.0) was used for analysis. To determine significant differences between groups (i.e. $p < 0.05$), a one-way analysis of variance (ANOVA) test was performed, with a Tukey post hoc test. Linear regressions were used to extrapolate unknown sample values from standard curves generated. For Western blot analysis, biological fold change was additionally used to identify biologically significant changes in protein expression. Changes in biological fold were determined using a Student's t-test. For the *in vivo* component of this study, results were expressed as the mean of eight values per group, with error bars reflecting the standard errors of the respective means. Differences between rat treatment groups were determined using a one-way ANOVA and Tukey post hoc test. The areas under the curve for the OGTTs were determined using a trapezoidal method. Again, linear regressions were used to extrapolate unknown sample values from standard curves generated when assessing blood parameters measured.

Annotation:

* = $p < 0.05$; ** = $p < 0.01$; *** = $p < 0.001$ compared to the respective normal control.

† = $p < 0.05$; †† = $p < 0.01$; ††† = $p < 0.001$ compared to the respective stressor control (i.e. STZ, PA, CM or MS where appropriate).

CHAPTER 4

RESULTS

1. *In vitro* results

The efficacy of the aqueous extract of unfermented *C. maculata* as well as of its major xanthone, mangiferin, and NAC in ameliorating RIN-5F cell viability, restoring function and improving oxidative stress status was assessed *in vitro.* Following induction of cytotoxicity in RIN-5F cells, viability was assessed using the MTT and ATP assays, as well as annexin-V and propidium iodide fluorescence. Insulin secretion, cellular calcium and RIN-5F cell proliferation were parameters used to assess cell function. The anti-oxidative status of these cells was determined by measuring DAF and DHE fluorescence as well as cellular SOD activity. For all *in vitro* experimentation data are expressed as the mean of three independent experiments, with four intra-experimental repeats each, ± the standard error of the mean. The normal controls refer to cells not exposed to stressors or treatments.

1.1. Toxicity in RIN-5F cells

The induction of toxicity in RIN-5F cells was based on conditions to which β-cells are exposed in T2D; i.e. glucotoxicity, lipotoxicity, inflammation and oxidative stress conditions. The response of RIN-5F cells to increasing concentrations of these toxic stressors was assessed by measuring cell viability using the MTT assay. The normal control was set at 100 % for these toxicity data.

In the glucotoxicity investigations, compared to cells exposed to normal glucose concentrations (5.5 mM glucose), RIN-5F cells exposed to both 17 mM and 25 mM glucose for 24 hours showed reduced MTT positivity, albeit not lower than 70 % and thus not meeting the LC_{50} requirement of cytotoxicity for this study (72.16 % ± 1.00 and 79.83 % ± 2.56, respectively) (Fig. 26 A). The glucose concentrations tested had no effect on cellular ATP (Fig. 26 B). No toxic effect was elicited by the 11 or 35 mM glucose concentrations.

The effect of lipotoxicity was assessed by exposing RIN-5F cells to a range of PA concentrations. Compared to the normal control, a reduction in MTT positivity and thus cell viability was observed in cells exposed to 750 μM and 1000 μM PA for 24 hours (61.68 % ± 3.18 and 48.84 % ± 2.25, respectively) (Fig. 27).

As a known inducer of cellular ROS in β-cells, STZ was used to induce oxidative stress in the RIN-5F cells. Reduced MTT positivity of the RIN-5F cells following 24 hours exposure

to 5 mM, 10 mM, 20 mM and 40 mM STZ was observed compared to the normal control (81.44 % ± 2.69, 58.59 % ± 2.68, 36.60 % ± 1.85 and 31.32 % ± 1.23, respectively) (Fig. 28).

In order to induce an inflammatory state in the RIN-5F cells, IFN-γ, IL-1β and TNF-α pro-inflammatory cytokines were used. Although exposure of RIN-5F cells to the cytokines individually at the concentrations tested for 24 hours had no effect on MTT positivity (Fig. 29 A), in combination these cytokines (CM) reduced MTT positivity when compared to the normal control (73.42 % ± 2.00, 56.16 % ± 1.92 and 39.90 % ± 2.82, respectively) (Fig. 29 B).

A multi-factorial stress combination of PA, cytokines and STZ was also assessed. Compared to the normal control, all three MS concentrations reduced MTT positivity in RIN-5F cells (52.22 % ± 4.55, 23.69 % ± 0.44 and 0.57 % ± 0.04, respectively) (Fig. 30).

Optimised concentrations of each of the stressors (i.e. STZ, PA, CM and MS) were selected, based on the consistent reduction of RIN-5F cell viability by approximately 50 % were selected (Table 3). Interestingly, glucose (at the concentrations and under the conditions tested) was not sufficiently cytotoxic in these RIN-5F cells (MTT positivity was not sufficiently and consistently reduced by elevated glucose concentrations) and was thus excluded from the rest of the study. Lack of a toxic response as observed in the MTT assay was confirmed by the ATP assay, which demonstrated no glucose induced cytotoxicity (Fig. 26 B).

A.

B.
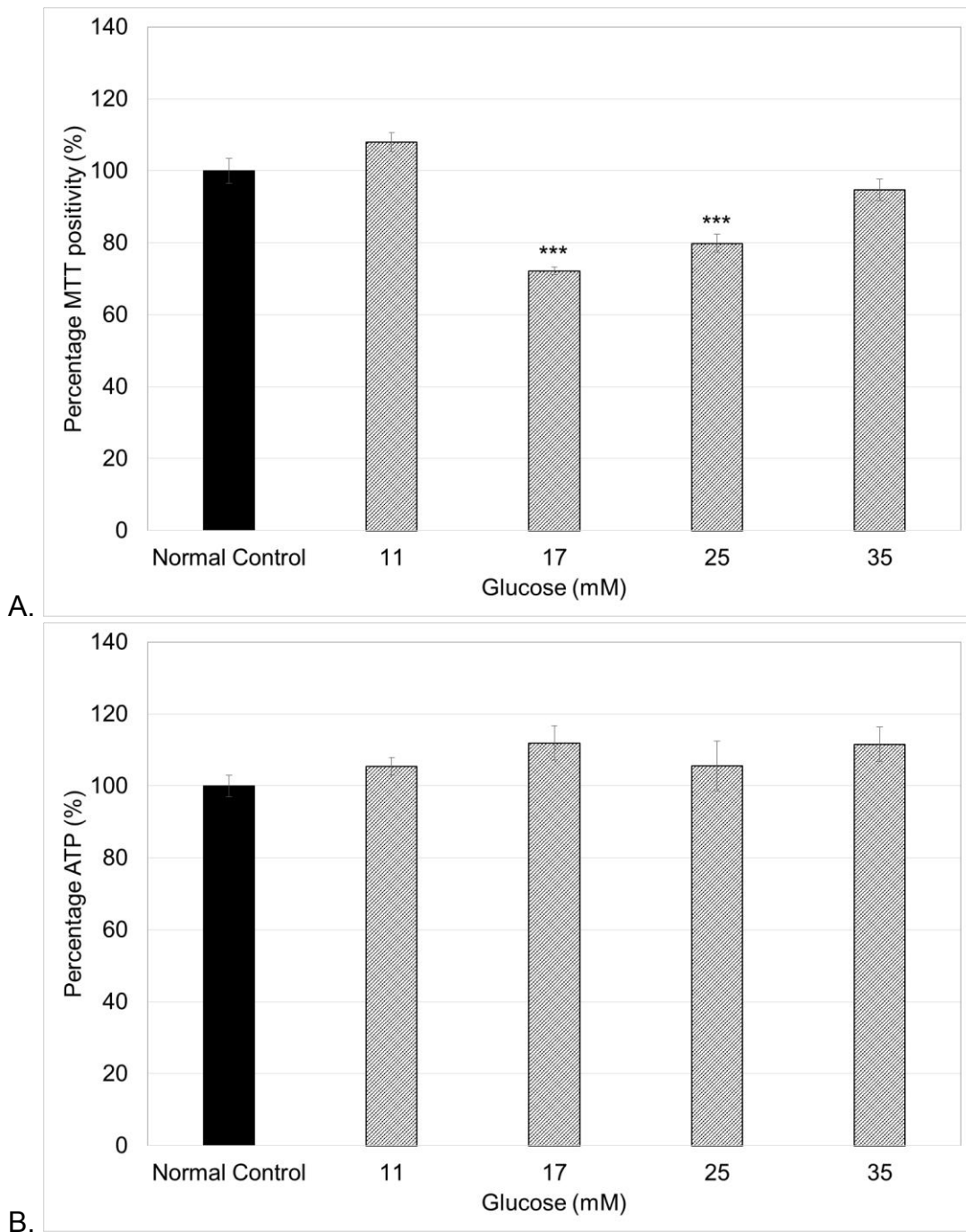
Figure 26. The effect of increasing glucose concentrations on RIN-5F cell viability after 24 hours, as measured by MTT (A) and ATP (B) assays.

RIN-5F cells were exposed to 5.5 (normal control), 11, 17, 25 and 35 mM glucose for 24 hours. Thereafter, cell viability was assessed using the MTT and ATP assays.

Where *** = $p < 0.001$ compared to the normal control.
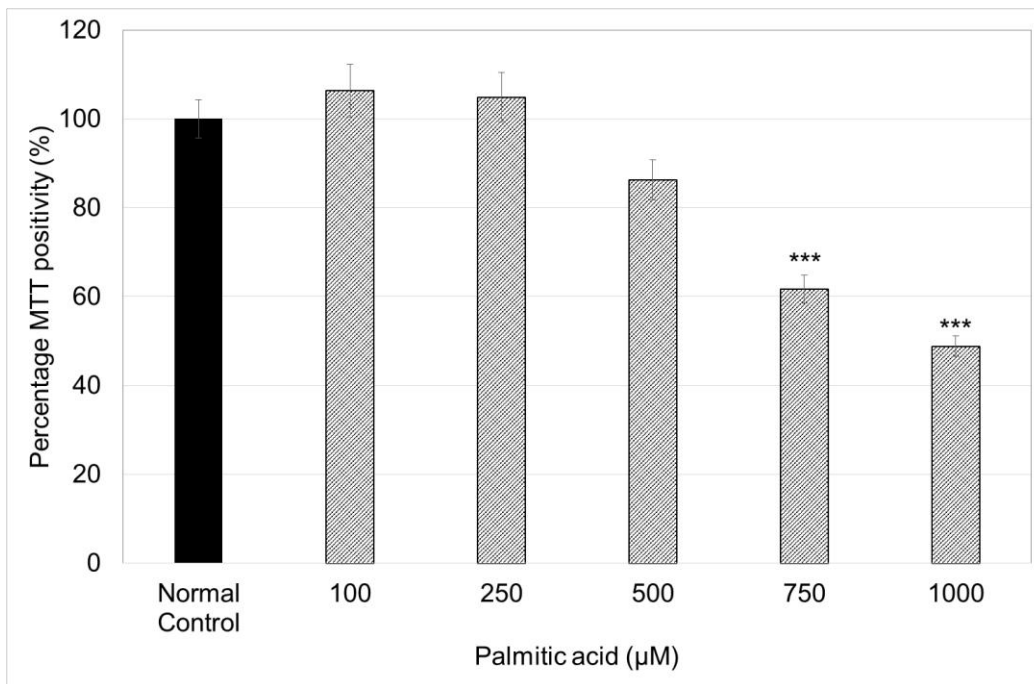
Figure 27. The effect of increasing PA concentrations on RIN-5F cell viability after 24 hours, as measured by the MTT assay.

RIN-5F cells were exposed to 0 (normal control), 100, 250, 500, 750 and 1000 µM PA for 24 hours. Thereafter, cell viability was assessed using the MTT assay.

Where *** = $p < 0.001$ compared to the normal control.
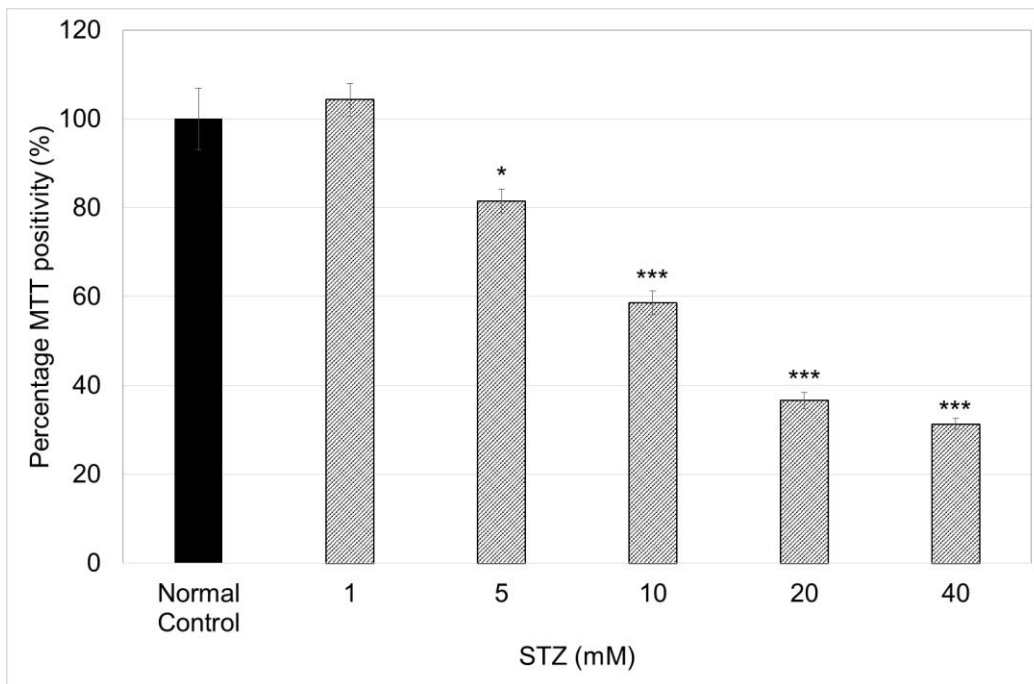
Figure 28. The effect of increasing STZ concentrations on RIN-5F cell viability after 24 hours, as measured by the MTT assay.

RIN-5F cells were exposed to 0 (normal control), 1, 5, 10, 20 and 40 mM STZ for 24 hours. Thereafter, cell viability was assessed using the MTT assay.

Where * = $p < 0.05$ and *** = $p < 0.001$ compared to the normal control.

A.

B.
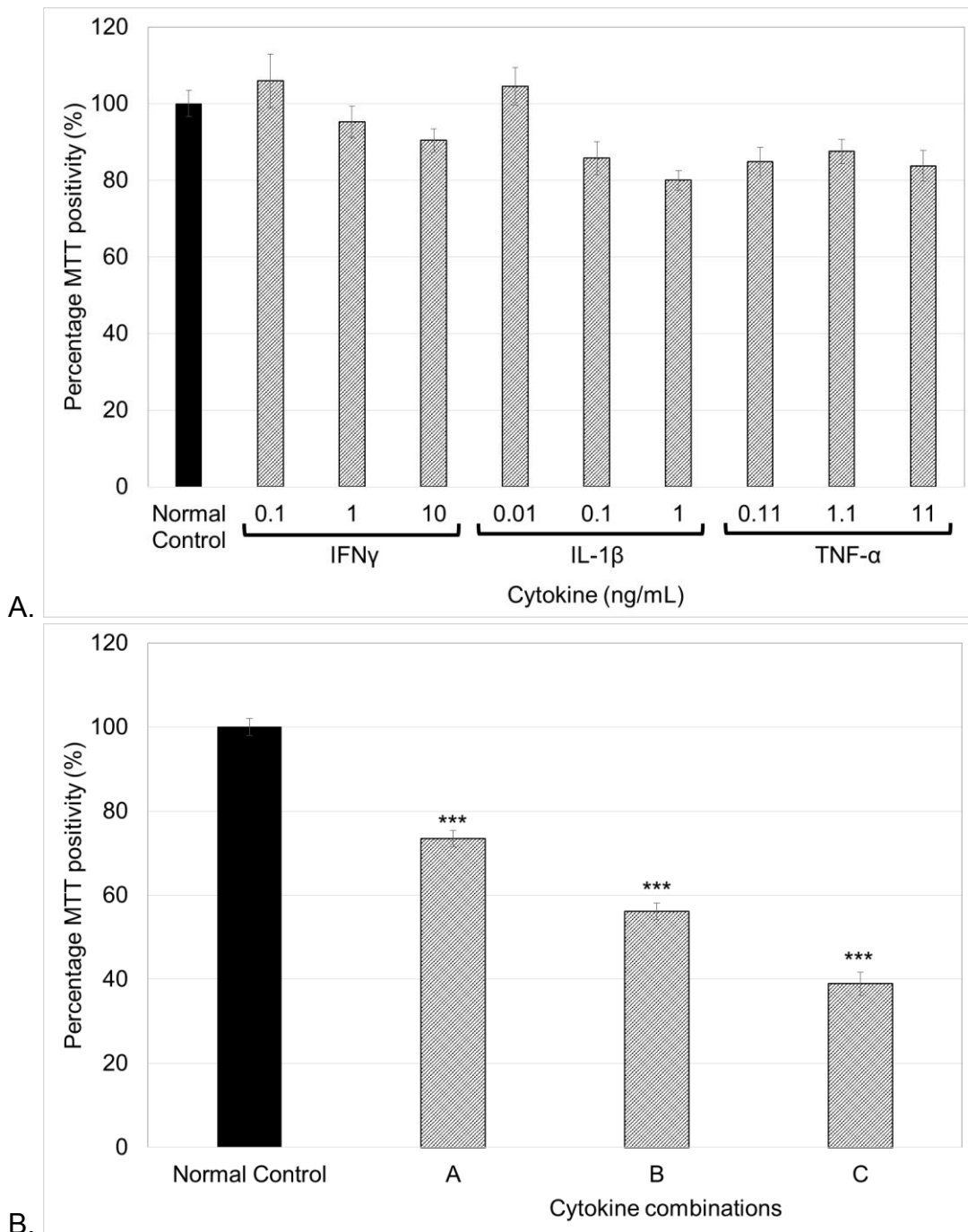
Figure 29. The effect of cytokines individually (A) and in combination (B) on RIN-5F cell viability after 24 hours exposure.

Cytokine combinations:

A - 0.1 ng/mL IFN-γ + 0.01 ng/mL IL-1β + 0.11 ng/mL TNF-α.

B - 1 ng/mL IFN-γ + 0.1 ng/mL IL-1β + 1.1 ng/mL TNF-α.

C - 10 ng/mL IFN-γ + 1 ng/mL IL-1β + 11 ng/mL TNF-α.

RIN-5F cells were exposed to IFN-γ, IL-1β and TNF-α individually and in combination for 24 hours, after which, cell viability was assessed using the MTT assay.

Where *** = $p < 0.001$ compared to the normal control.
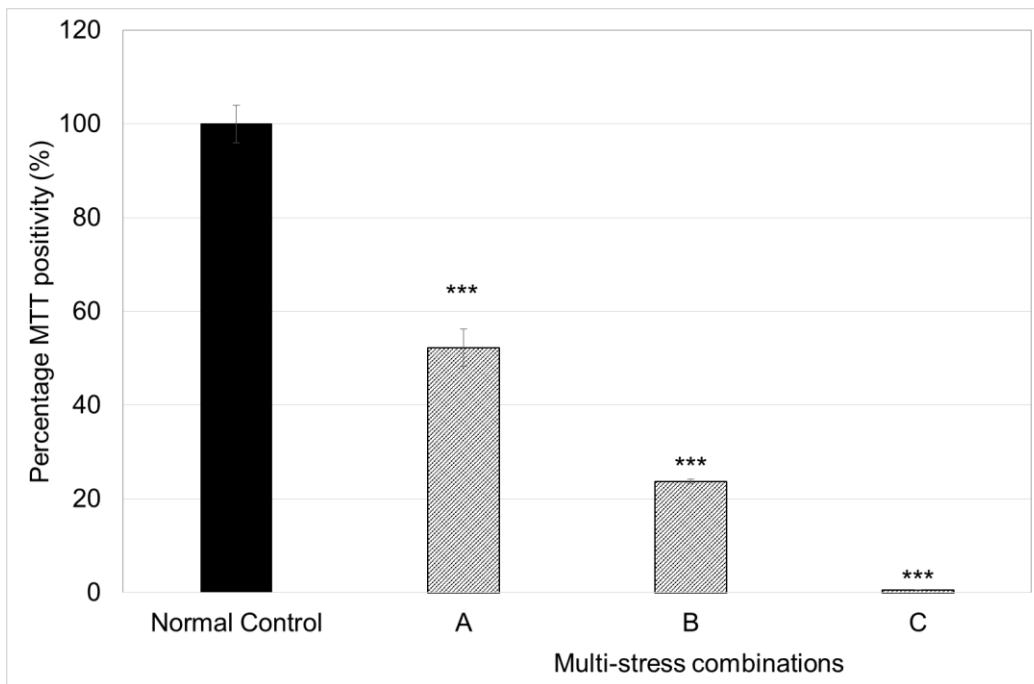
Figure 30. The effect of a combination of PA, STZ and cytokines on RIN-5F cell viability after 24 hours exposure.

Multi-stress combinations:

A – 75 µM PA + 1 mM STZ + 0.1 ng/mL IFN-γ + 0.01 ng/mL IL-1β + 0.11 ng/mL TNF-α.

B – 375 µM PA + 5 mM STZ + 0.5 ng/mL IFN-γ + 0.05 ng/mL IL-1β + 0.55 ng/mL TNF-α.

C – 750 µM PA + 10 mM STZ + 1 ng/mL IFN-γ + 0.1 ng/mL IL-1β + 1.1 ng/mL TNF-α.

RIN-5F cells were exposed to combinations of the PA, STZ and cytokines for 24 hours. Thereafter, cell viability was assessed using the MTT assay.

Where *** = $p < 0.001$ compared to the normal control.

Table 3. Optimised concentrations of β-cell stressors

Cytotoxin	Concentration
Streptozotocin	10 mM
Palmitic acid	750 µM
Cytokine mixture	1 ng/mL IFN-γ + 0.1 ng/mL IL-1β + 1.1 ng/mL TNF-α
Multi-stress	75 µM PA + 1 mM STZ + 0.1 ng/mL IFN-γ + 0.01 ng/mL IL-1β + 0.11 ng/mL TNF-α

1.2. Cell viability

Once an optimal toxic concentration was identified for each of the stressors (Table 3), the efficacy of a range of concentrations of the aqueous, unfermented *C. maculata* extract, mangiferin and NAC on RIN-5F cell viability was assessed by measuring MTT positivity, as well as by measuring cellular ATP. The normal controls refer to cells not exposed to stressors or treatments.

1.2.1. The MTT and ATP assays

In the MTT and ATP screening assays, the normal control was set at 100 %.

1.2.1.1. Screening of *Cyclopia maculata* extract

Compared to the normal control, RIN-5F cell viability was decreased following exposure to the STZ control (10 mM for 24 hours), as measured by the MTT (40.38 % ± 1.19) (Fig. 31 A) and ATP (53.05 % ± 3.32) (Fig. 31 B) assays. Subsequent exposure of STZ exposed cells to 0.01 µg/mL, 1 µg/mL, 10 µg/mL and 100 µg/mL *C. maculata* extract for 24 hours increased RIN-5F cell MTT positivity compared to the STZ control (93.62 % ± 3.26, 110.52 % ± 3.57, 107.60 % ± 4.86 and 145.25 % ± 7.74, respectively) (Fig. 31 A). The extract similarly improved cell viability compared to the STZ control as measured by the ATP assay at 0.001 µg/mL, 0.01 µg/mL, 1 µg/mL, 10 µg/mL and 100 µg/mL concentrations (113.53 % ± 7.07, 108.80 % ± 8.20, 107.12 % ± 6.37, 115.76 % ± 10.92 and 113.14 % ± 5.62, respectively) (Fig. 31 B).

RIN-5F cell viability was decreased following exposure to the PA control (750 µM for 24 hours) as measured by the MTT (45.28 % ± 1.74) (Fig. 32 A) and ATP (42.13 % ± 4.24) (Fig. 32 B) assays. PA treated cells exposed to 0.001 µg/mL, 0.01 µg/mL, 1 µg/mL, 10 µg/mL and 100 µg/mL *C. maculata* extract for 24 hours showed improved RIN-5F cell viability compared to the PA control, as measured by the MTT assay (79.18 % ± 5.56, 133.58 % ± 5.31, 151.84 % ± 5.04, 160.43 % ± 7.35 and 138.30 % ± 4.13, respectively) (Fig. 32 A) and the ATP assay (110.65 % ± 9.07, 102.00 % ± 9.65, 121.80 % ± 10.02, 128.05 % ± 9.26 and 119.64 % ± 6.29, respectively) (Fig. 32 B).

The CM control (comprising 1 ng/mL IFN-γ, 0.1 ng/mL IL-1β and 1.1 ng/mL TNF-α) reduced RIN-5F cell viability after 24 hours exposure, as measured by the MTT (39.53 % ± 1.75) (Fig.33 A) and ATP (58.49 % ± 3.90) (Fig. 33 B) assays. So too did the MS control

combination of STZ, PA and CM reduce RIN-5F cell viability as measured by the MTT (45.86 % ± 3.22) (Fig. 34 A) and ATP (53.41 % ± 1.03) (Fig. 34 B) assays. The extract did not ameliorate either CM or MS induced reductions in MTT positivity and ATP content in RIN-5F cells (Fig. 33 and 34, respectively).

This component of the study demonstrated that the extract was able to ameliorate STZ (Fig. 31) and PA (Fig. 32) induced cytotoxicity in RIN-5F cells, but not toxicity induced by CM (Fig. 33) and MS (Fig. 34).

A.

B.

Figure 31. MTT (A) and ATP (B) RIN-5F cell viability following consecutive 24 hour exposures of cells to STZ and *C. maculata* extract, respectively.

RIN-5F cells were first exposed to 10 mM STZ for 24 hours and then to increasing concentrations of the extract in fresh media for 24 hours. Cell viability was then assessed using the MTT and ATP assays.

Where ** = $p < 0.01$ and *** = $p < 0.001$ compared to the normal control; and † = $p < 0.05$ and ††† = $p < 0.001$ compared to STZ. (Data from Fig. 31 B has been published in a peer-reviewed journal; see addendum 1).

A.

B.

Figure 32. MTT (A) and ATP (B) RIN-5F cell viability following consecutive 24 hour exposures of cells to PA and *C. maculata* extract, respectively.

RIN-5F cells were first exposed to 750 µM for 24 hours and then to increasing concentrations of the extract in fresh media for 24 hours. Cell viability was then assessed using the MTT and ATP assays.

Where * = $p < 0.05$, ** = $p < 0.01$ and *** = $p < 0.001$ compared to the normal control; and † = $p < 0.05$, †† = $p < 0.01$ and ††† = $p < 0.001$ compared to PA.

A.

B.

Figure 33. MTT (A) and ATP (B) RIN-5F cell viability following consecutive 24 hour exposures of cells to CM and *C. maculata* extract, respectively.

RIN-5F cells were first exposed to 1 ng/mL IFN-γ + 0.1 ng/mL IL-1β + 1.1 ng/mL TNF-α in combination for 24 hours and then to increasing concentrations of the extract in fresh media for 24 hours. Cell viability was then assessed using the MTT and ATP assays.

Where *** = $p < 0.001$ compared to the normal control.

A.

B.
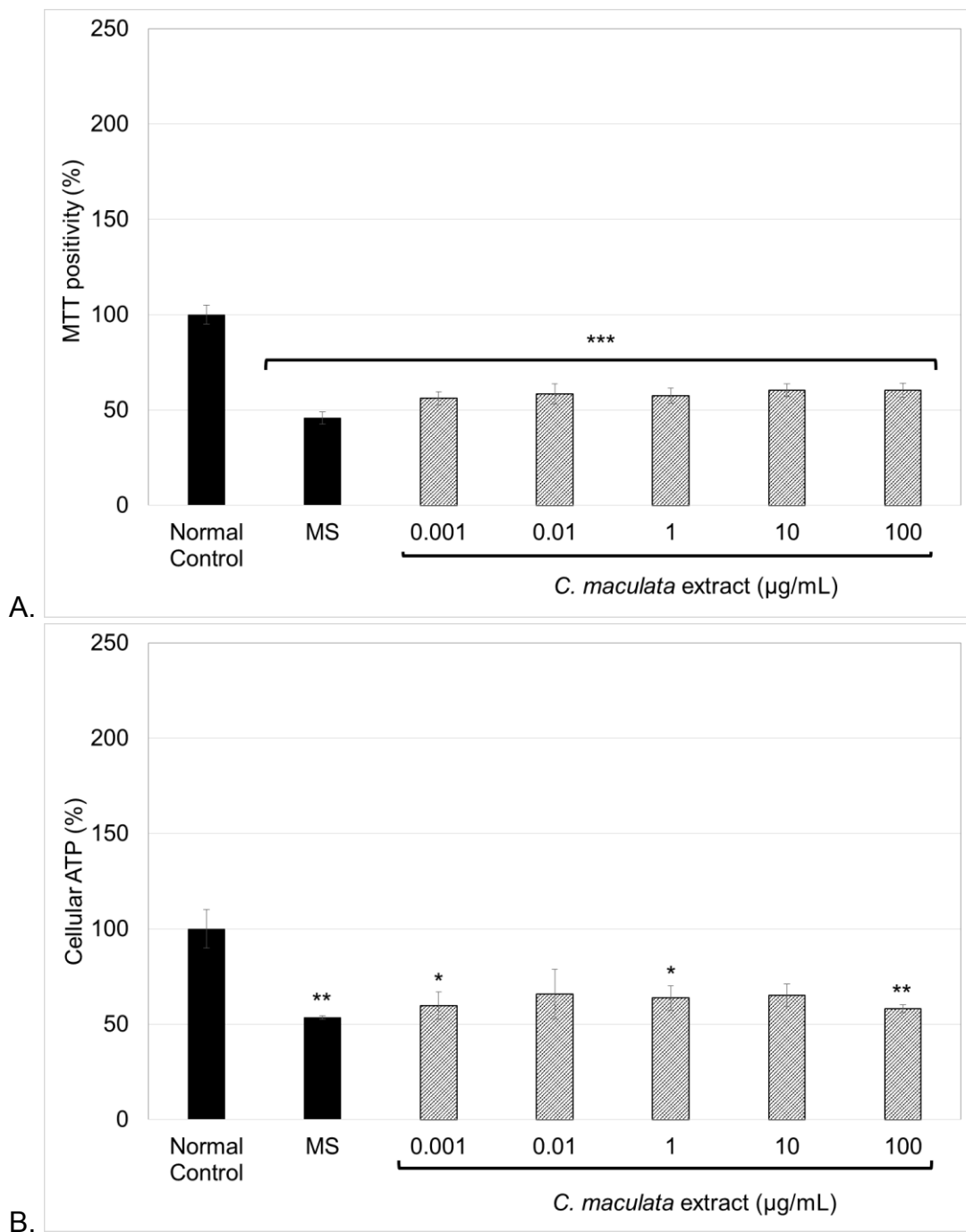
Figure 34. MTT (A) and ATP (B) RIN-5F cell viability following consecutive 24 hour exposures of cells to MS and *C. maculata* extract, respectively.

RIN-5F cells were first exposed to 75 µM PA + 1 mM STZ + 0.1 ng/mL IFN-γ + 0.01 ng/mL IL-1β + 0.11 ng/mL TNF-α in combination for 24 hours and then to increasing concentrations of the extract in fresh media for 24 hours. Cell viability was then assessed using the MTT and ATP assays.

Where * = $p < 0.05$, ** = $p < 0.01$ and *** = $p < 0.001$ compared to the normal control.

1.2.1.2. Screening of mangiferin

Compared to the normal control, RIN-5F cell viability was decreased following exposure to the STZ control, as measured by the MTT (41.49 % ± 1.01) (Fig. 35 A) and ATP (39.39 % ± 2.46) (Fig. 35 B) assays. Compared to the STZ control in the MTT assay, all concentrations of mangiferin tested (i.e. 0.001 µg/mL, 0.01 µg/mL, 1 µg/mL, 10 µg/mL and 100 µg/mL) improved cell viability, but were still reduced when compared to the normal control (72.76 % ± 1.95, 66.49 % ± 2.63, 63.92 % ± 2.01 and 65.12 % ± 1.63, respectively) (Fig. 35 A). Cellular ATP was not improved by the concentrations of mangiferin tested following exposure to STZ (Fig. 35 B).

RIN-5F cell viability was also decreased following exposure to the PA control for 24 hours, as measured by the MTT (45.95 % ± 1.49) (Fig. 36 A) and ATP (28.61 % ± 2.03) (Fig. 36 B) assays. So too was cell viability reduced by exposure to the CM control as measured by the MTT (57.20 % ± 1.60) (Fig. 37 A) and ATP (42.52 % ± 1.33) (Fig. 37 B) assays. Mangiferin had no effect on the viability of PA and CM exposed RIN-5F cells, as measured by either the MTT or ATP assays (Fig. 36 and 37).

The MS control reduced RIN-5F cell viability, as measured by the MTT (47.27 % ± 1.72) (Fig. 38 A) and ATP (57.93 % ± 3.25) (Fig. 38 B) assays. Compared to the MS control, subsequent exposure of MS treated cells to 100 µg/mL mangiferin for 24 hours improved RIN-5F cell viability as measured by the MTT assay (79.14 % ± 14.10) (Fig. 38 A). None of the concentrations of mangiferin tested ameliorated the reduction in ATP induced by MS (Fig. 38 B).

Mangiferin was mostly ineffective in ameliorating stressor induced toxicity in the RIN-5F cells in this study. Some improvement in MTT positivity was, however, observed following mangiferin treatment in cells exposed to STZ (Fig. 35 A) and MS (Fig. 38 A), with no measurable effect on cellular ATP.

A.

B.
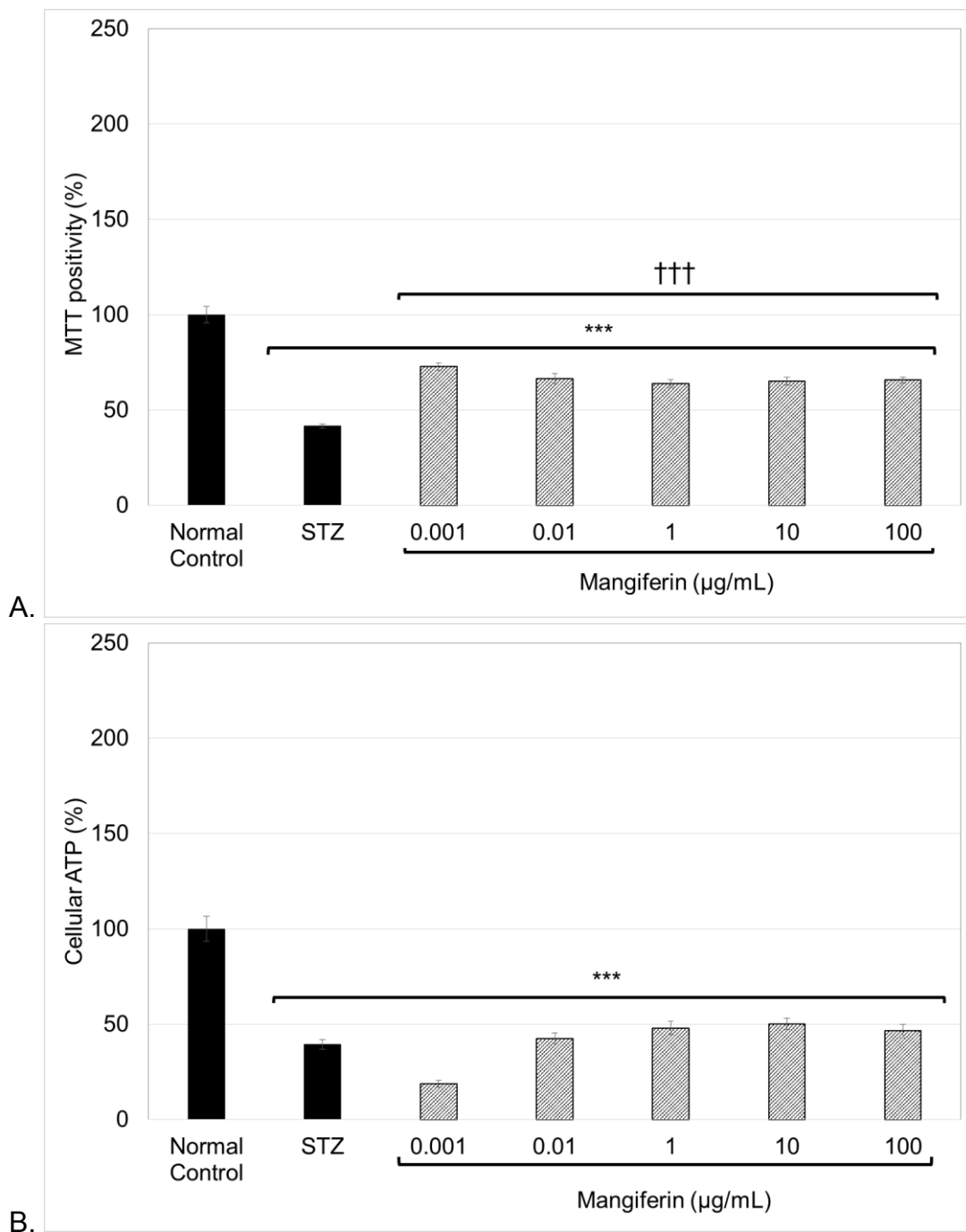
Figure 35. MTT (A) and ATP (B) RIN-5F cell viability following consecutive 24 hour exposures of cells to STZ and mangiferin, respectively.

Where *** = p < 0.001 compared to the normal control; and ††† = p < 0.001 compared to RIN-5F cells were first exposed to 10 mM STZ for 24 hours and then to increasing concentrations of mangiferin in fresh media for 24 hours. Cell viability was then assessed using the MTT and ATP assays.

STZ. (Data from Fig. 35 B has been published in a peer-reviewed journal; see addendum 1).
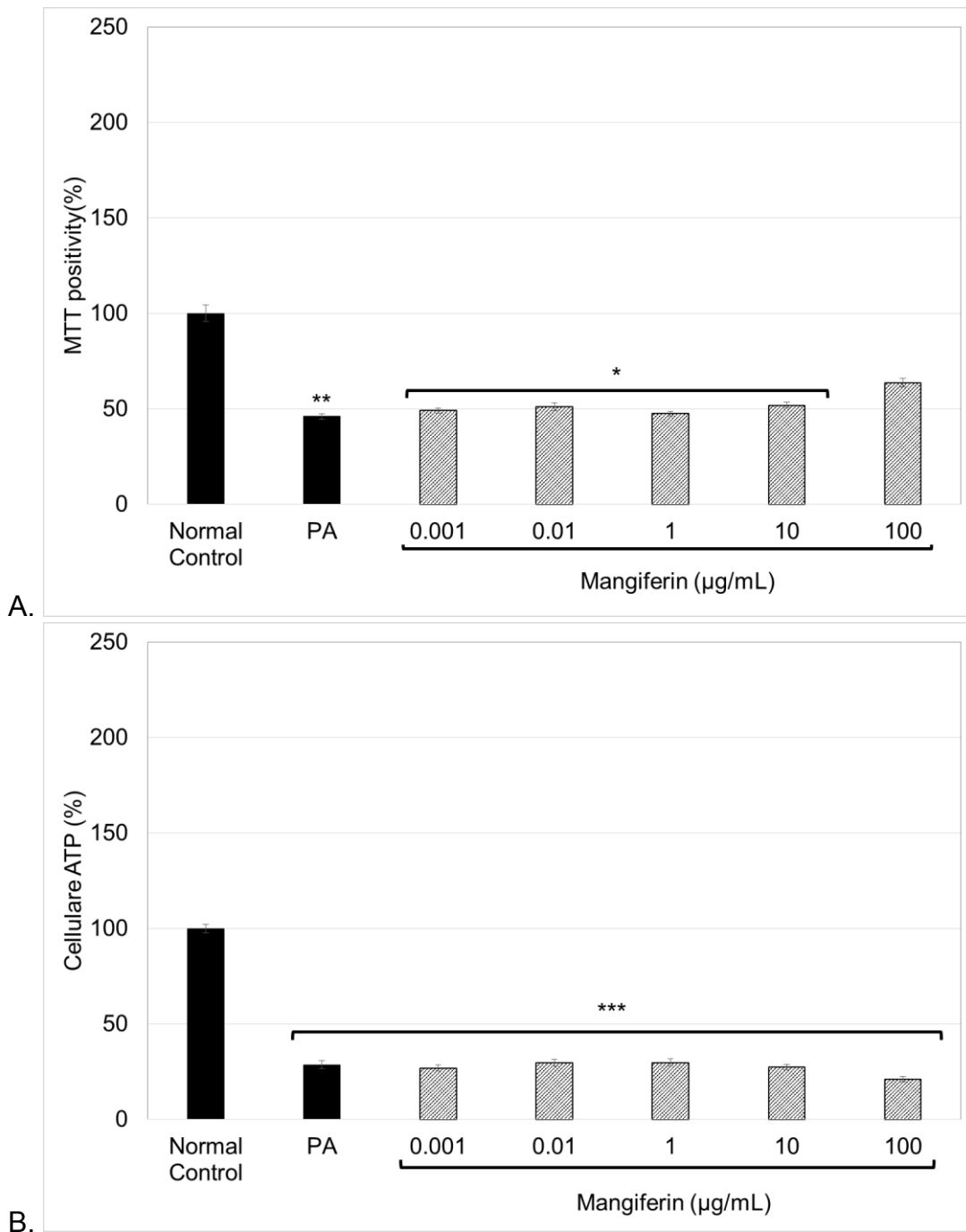
Figure 36. MTT (A) and ATP (B) RIN-5F cell viability following consecutive 24 hour exposures of cells to PA and mangiferin, respectively.

RIN-5F cells were first exposed to 750 µM for 24 hours and then to increasing concentrations of mangiferin in fresh media for 24 hours. Cell viability was then assessed using the MTT and ATP assays.

Where * = $p < 0.05$, ** = $p < 0.01$ and *** = $p < 0.001$ compared to the normal control.

A.

B.
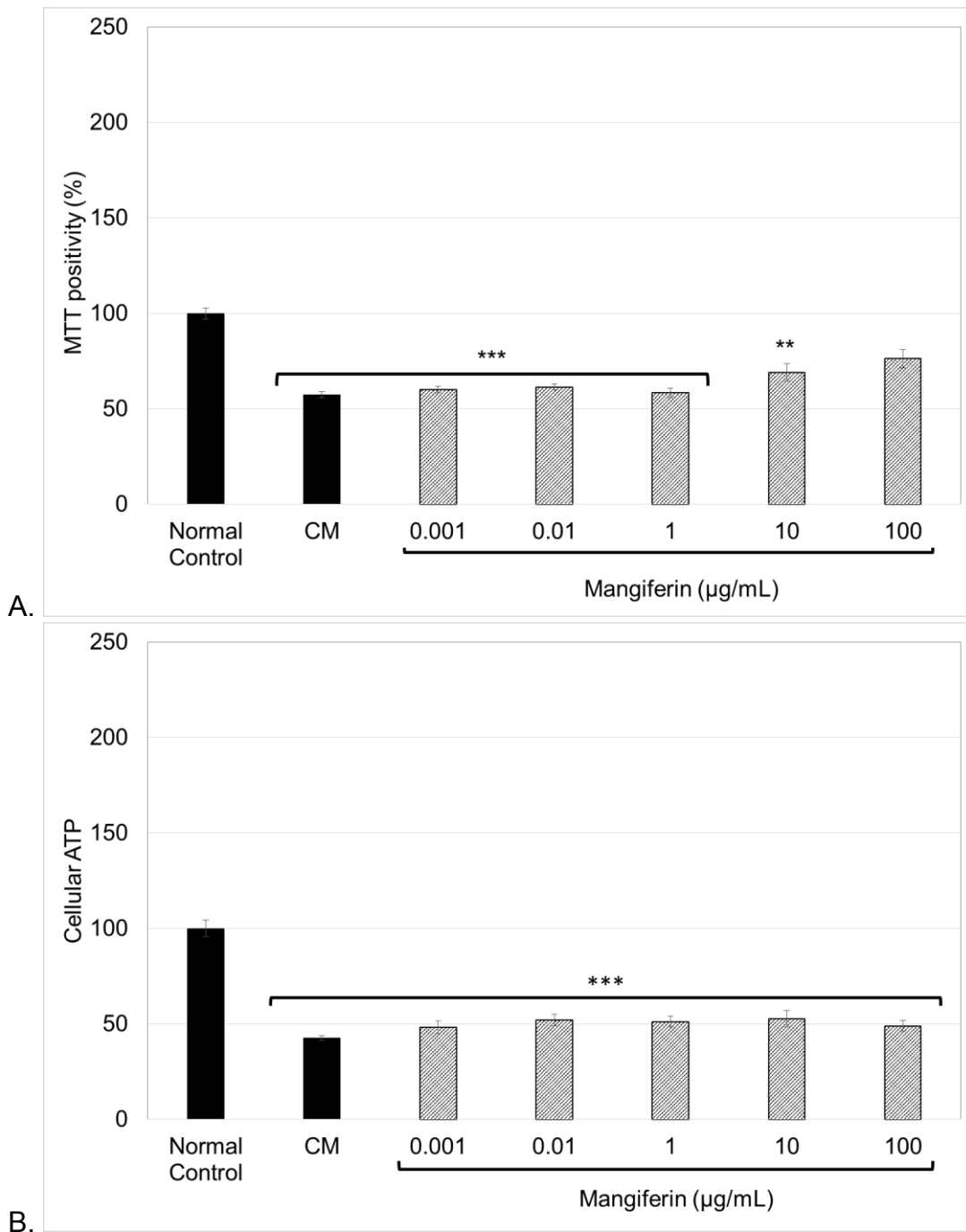
Figure 37. MTT (A) and ATP (B) RIN-5F cell viability following consecutive 24 hour exposures of cells to CM and mangiferin, respectively.

RIN-5F cells were first exposed to 1 ng/mL IFN-γ + 0.1 ng/mL IL-1β + 1.1 ng/mL TNF-α in combination for 24 hours and then to increasing concentrations of mangiferin in fresh media for 24 hours. Cell viability was then assessed using the MTT and ATP assays.

Where ** = $p < 0.01$ and *** = $p < 0.001$ compared to the normal control.

A.

B.
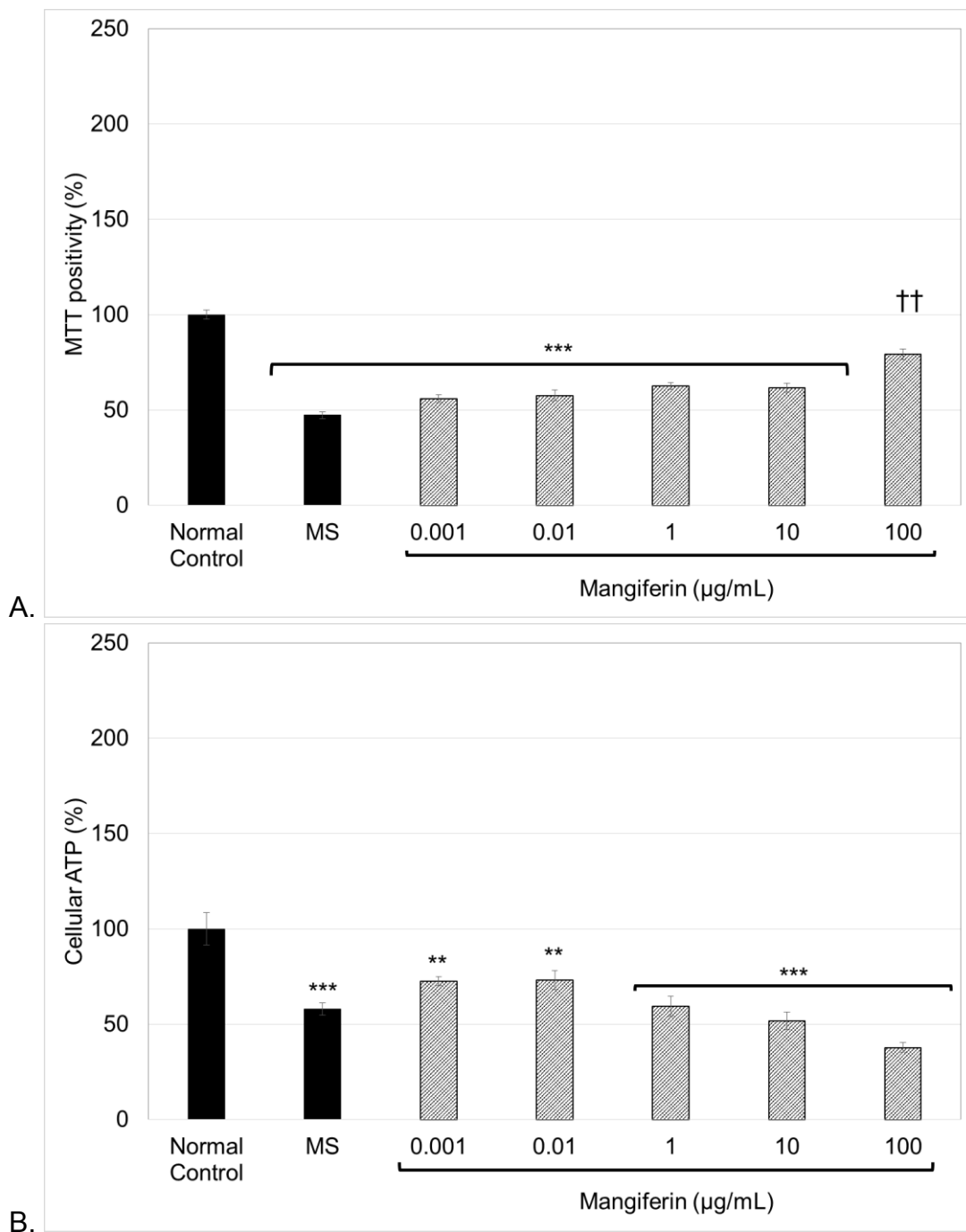
Figure 38. MTT (A) and ATP (B) RIN-5F cell viability following consecutive 24 hour exposures of cells to MS and mangiferin, respectively.

RIN-5F cells were first exposed to 75 μM PA + 1 mM STZ + 0.1 ng/mL IFN-γ + 0.01 ng/mL IL-1β + 0.11 ng/mL TNF-α in combination for 24 hours and then to increasing concentrations of mangiferin in fresh media for 24 hours. Cell viability was then assessed using the MTT and ATP assays.

Where ** = $p < 0.01$ and *** = $p < 0.001$ compared to the normal control; and †† = $p < 0.01$ compared to MS.

114

1.2.1.3. Screening of *N*-acetyl cysteine

Compared to the normal control, RIN-5F cell viability was decreased following exposure to the STZ control, as measured by the MTT (64.52 % ± 2.04) (Fig. 39 A) and ATP (49.79 % ± 4.51) (Fig. 39 B) assays. Subsequent exposure of STZ treated cells to 0.01 mM, 0.1 mM, 1 mM, 10 mM and 20 mM NAC for 24 hours improved RIN-5F cell viability as measured by the MTT assay (104.29 % ± 2.85, 138.65 % ± 3.68, 159.68 % ± 6.60, 165.16 % ± 5.20 and 141.51 % ± 5.15, respectively). NAC also improved cell viability as measured by the ATP assay at 0.01 mM, 0.1 mM and 1 mM concentrations (103.47 % ± 6.42, 103.62 % ± 6.70 and 95.77 % ± 4.94, respectively) (Fig. 39 B). Compared to the normal control, cellular ATP was still reduced in cells treated with the higher concentrations of 10 mM and 20 mM NAC (73.07 % ± 5.28 and 34.97 % ± 2.68, respectively) (Fig. 39 B).

Similarly, RIN-5F cell viability was decreased following exposure to the PA control, as measured by the MTT (41.90 % ± 3.17) (Fig. 40 A) and ATP (52.11 % ± 2.82) (Fig. 40 B) assays. Subsequent exposure of PA treated cells to 0.1 mM, 1 mM, 10 mM and 20 mM NAC for 24 hours improved RIN-5F cell viability as measured by the MTT assay (120.69 % ± 6.49, 126.94 % ± 6.78, 144.76 % ± 4.96 and 143.08 % ± 2.31, respectively) (Fig. 40 A). NAC improved cell viability as measured by the ATP assay at 0.01 mM, 0.1 mM and 1 mM concentrations compared to the PA control (115.18 % ± 7.06, 88.67 % ± 5.30 and 107.90 % ± 4.91, respectively) (Fig. 40 B), however, there was no improvement in ATP at the 10 mM and 20 mM NAC concentrations (70.41 % ± 6.34 and 34.64 % ± 2.98, respectively) (Fig. 40 B).

RIN-5F cell viability was also decreased following exposure to the CM control, as measured by the MTT (36.58 % ± 1.23) (Fig. 41 A) and ATP (63.21 % ± 3.31) (Fig. 41 B) assays. No improvement in the CM induced reduction of MTT positivity was observed following NAC exposure (Fig. 41 A). NAC improved cell viability of cells exposed to CM, as measured by the ATP assay at 0.01 mM, 0.1 mM and 1 mM concentrations (109.07 % ± 7.39, 99.97 % ± 6.37 and 94.19 % ± 5.89, respectively) (Fig. 41 B), normalising these values. The 10 mM and 20 mM concentrations of NAC had no ameliorative effect on cellular ATP in cells exposed to CM (63.09 % ± 3.41 and 40.42 % ± 2.31, respectively) (Fig. 41 B).

Compared to the normal control, RIN-5F cell viability was decreased following exposure to the MS control, as measured by the MTT (45.81 % ± 2.27) (Fig. 42 A) and ATP (65.67 % ±

4.32) (Fig. 42 B) assays. All concentrations of NAC tested failed to ameliorate the MS induced reduction in MTT positivity and cellular ATP (Fig. 42 A and B, respectively). Both the 10 mM and 20 mM NAC concentrations reduced cellular ATP compared to both the normal and MS controls (35.57 % ± 2.48 and 20.93 % ± 1.61, respectively) (Fig. 42 B).

Improved cell viability was observed in RIN-5F cells exposed to STZ (Fig. 39) and PA (Fig. 40) when exposed to NAC, with some amelioration of CM induced reduction in cellular ATP (Fig. 41 B).
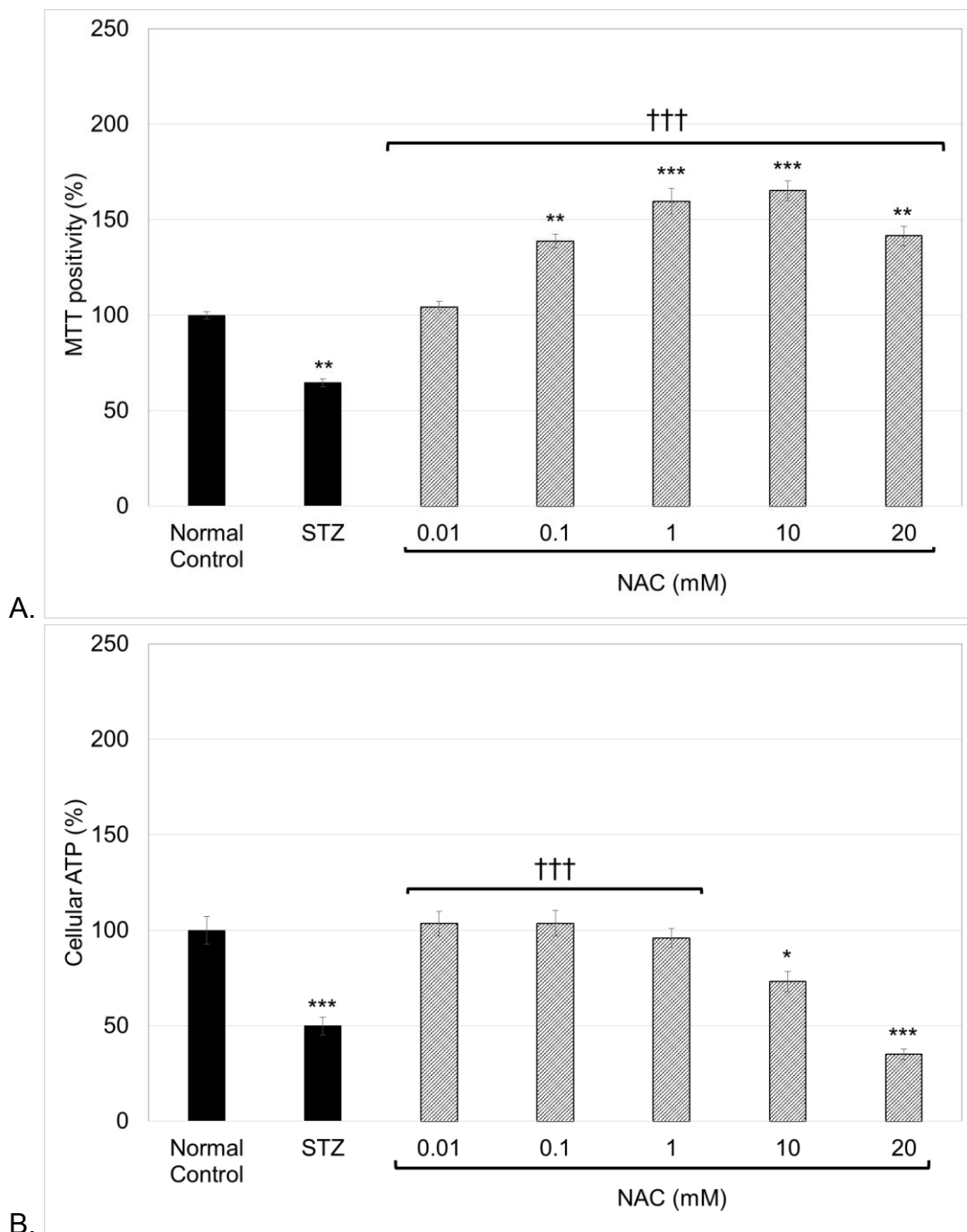
Figure 39. MTT (A) and ATP (B) RIN-5F cell viability following consecutive 24 hour exposures of cells to STZ and NAC, respectively.

RIN-5F cells were first exposed to 10 mM STZ for 24 hours and then to increasing concentrations of NAC in fresh media for 24 hours. Cell viability was then assessed using the MTT and ATP assays.

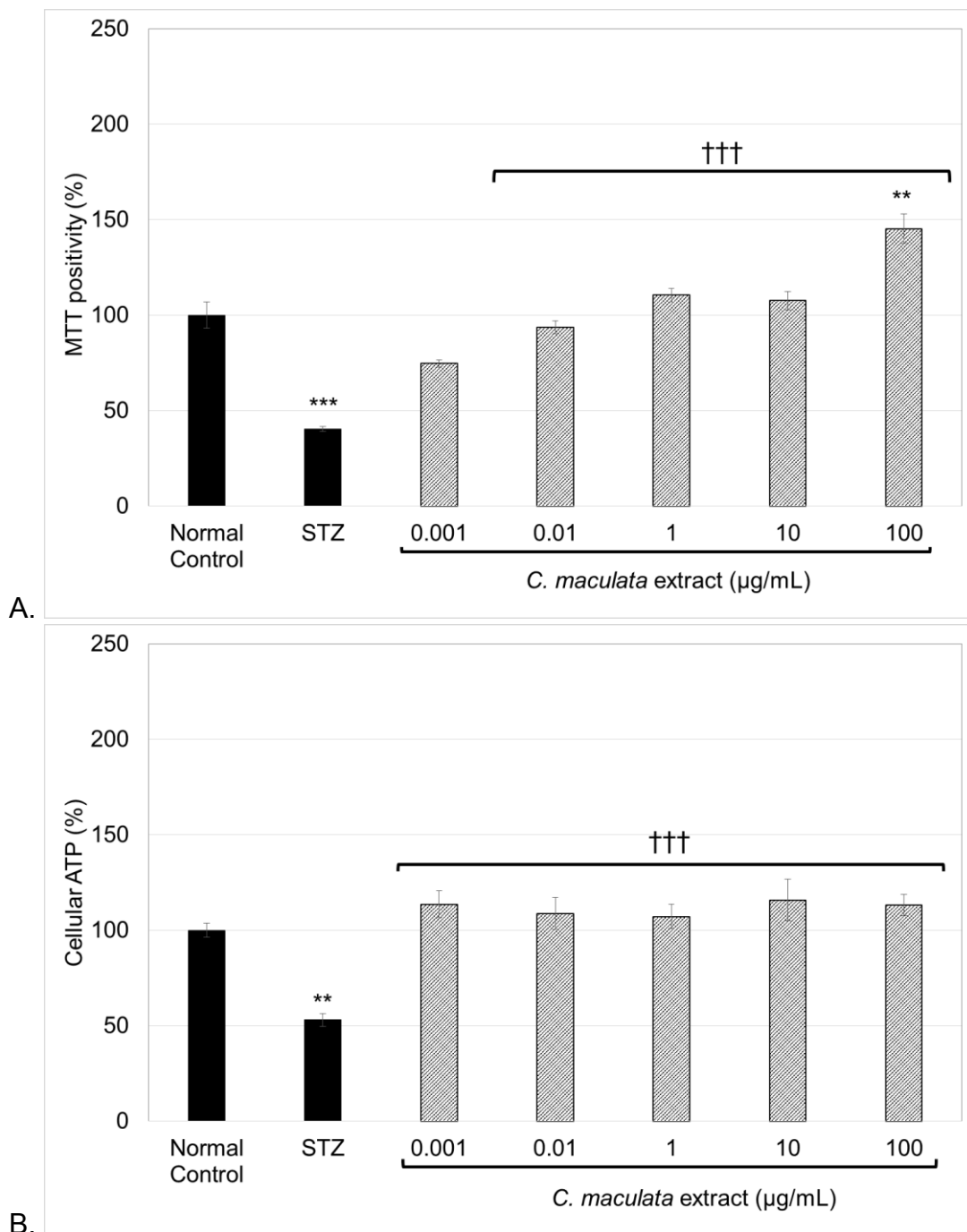Where * = $p < 0.05$, ** = $p < 0.01$ and *** = $p < 0.001$ compared to the normal control; and ††† = $p < 0.001$ compared to STZ.

117
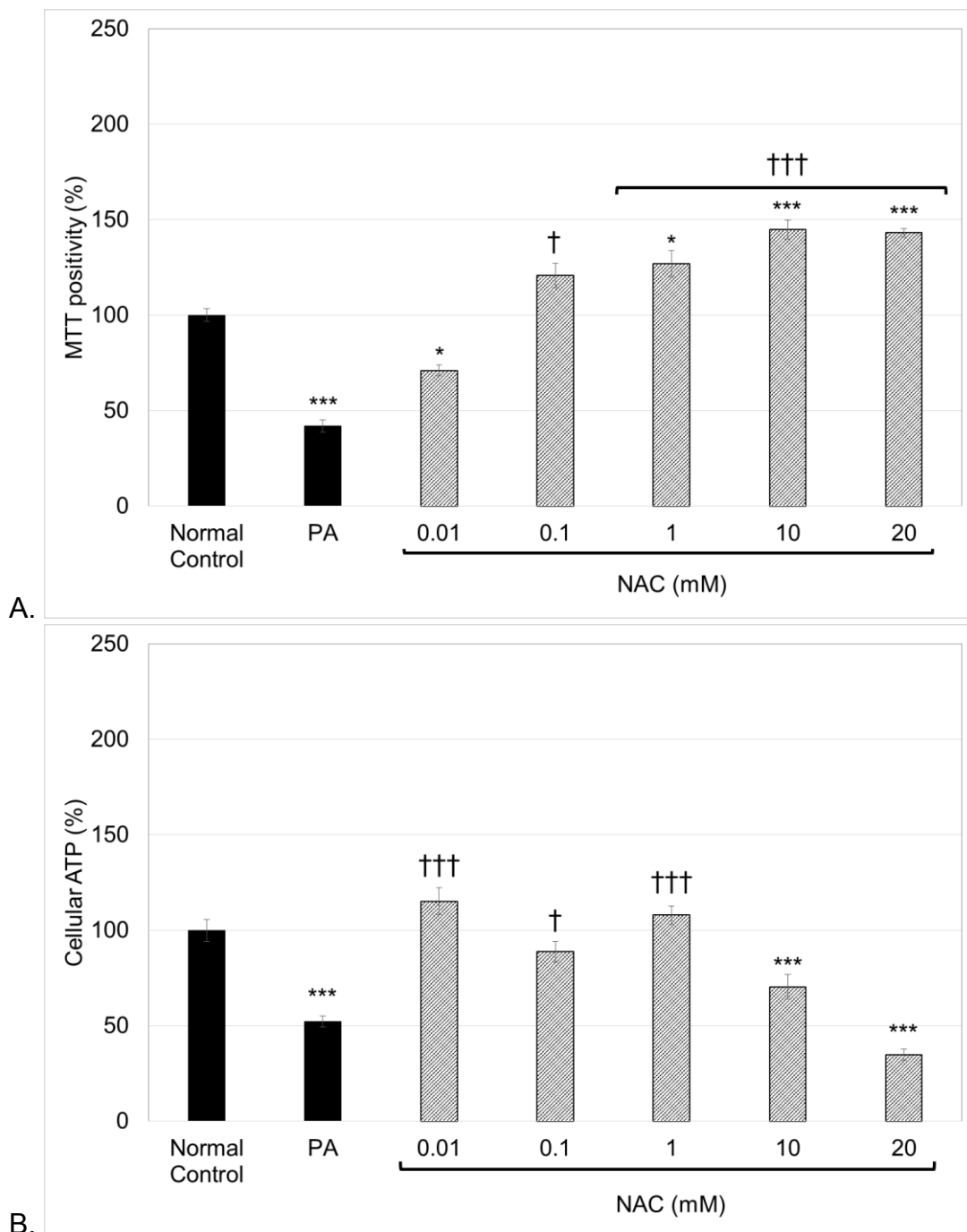
Figure 40. MTT (A) and ATP (B) RIN-5F cell viability following consecutive 24 hour exposures of cells to PA and NAC, respectively.

RIN-5F cells were first exposed to 750 µM for 24 hours and then to increasing concentrations of NAC in fresh media for 24 hours. Cell viability was then assessed using the MTT and ATP assays.

Where * = $p < 0.05$ and *** = $p < 0.001$ compared to the normal control; and † = $p < 0.05$ and ††† = $p < 0.001$ compared to PA.

A.

B.
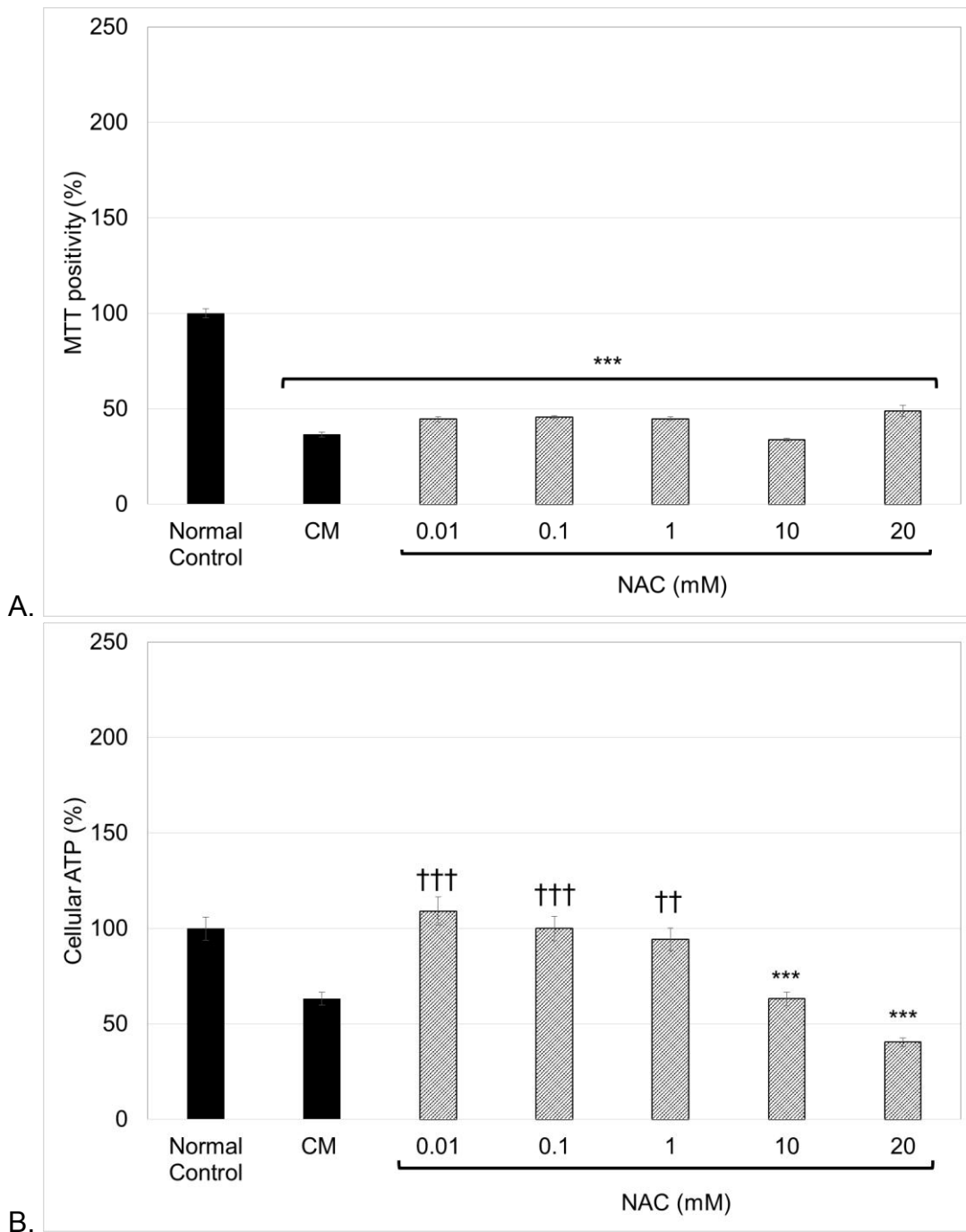
Figure 41. MTT (A) and ATP (B) RIN-5F cell viability following consecutive 24 hour exposures of cells to CM and NAC, respectively.

RIN-5F cells were first exposed to 1 ng/mL IFN-γ + 0.1 ng/mL IL-1β + 1.1 ng/mL TNF-α in combination for 24 hours and then to increasing concentrations of NAC in fresh media for 24 hours. Cell viability was then assessed using the MTT and ATP assays.

Where *** = $p < 0.001$ compared to the normal control; and †† = $p < 0.01$ and ††† = $p < 0.001$ compared to CM.

119

A.

B.
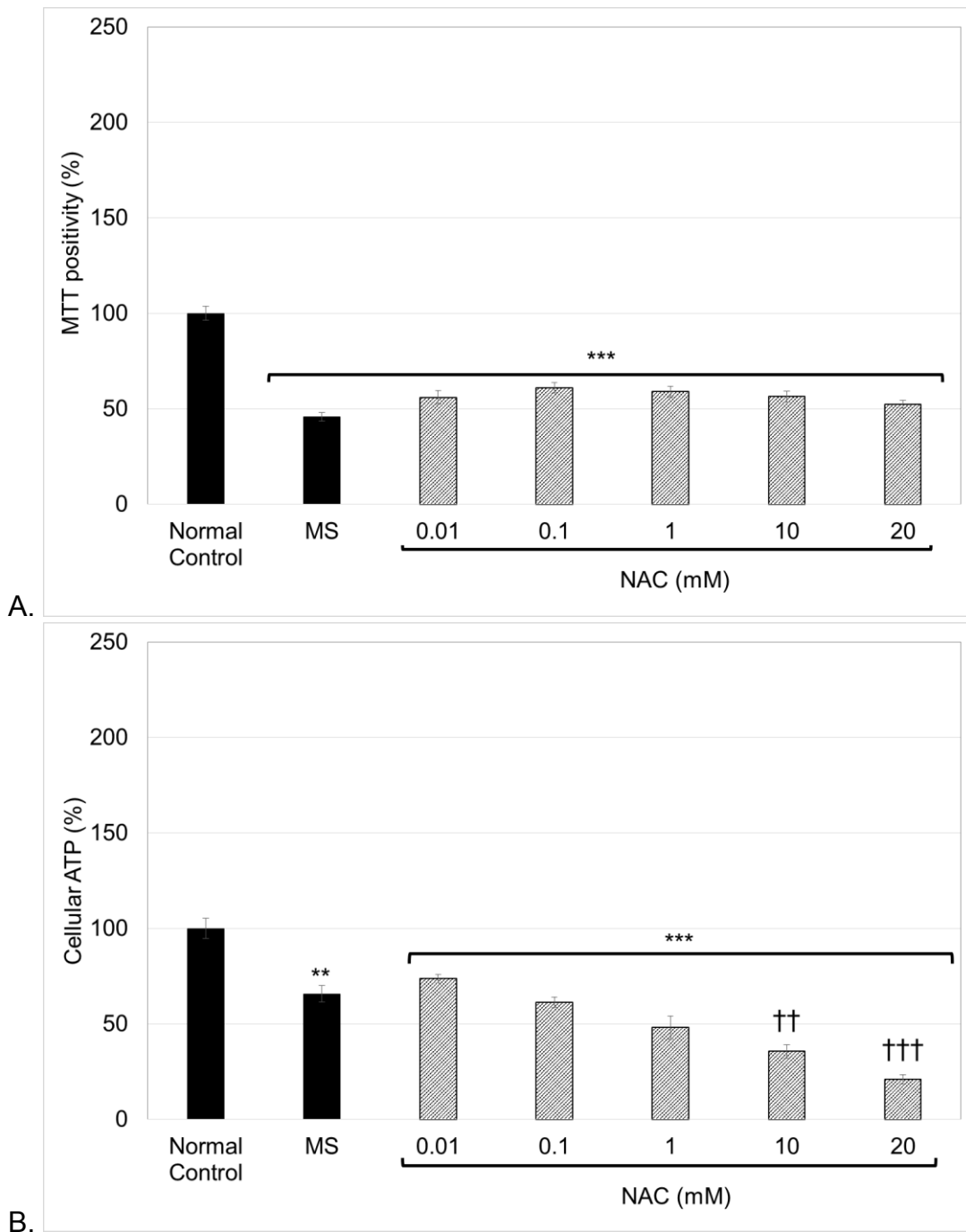
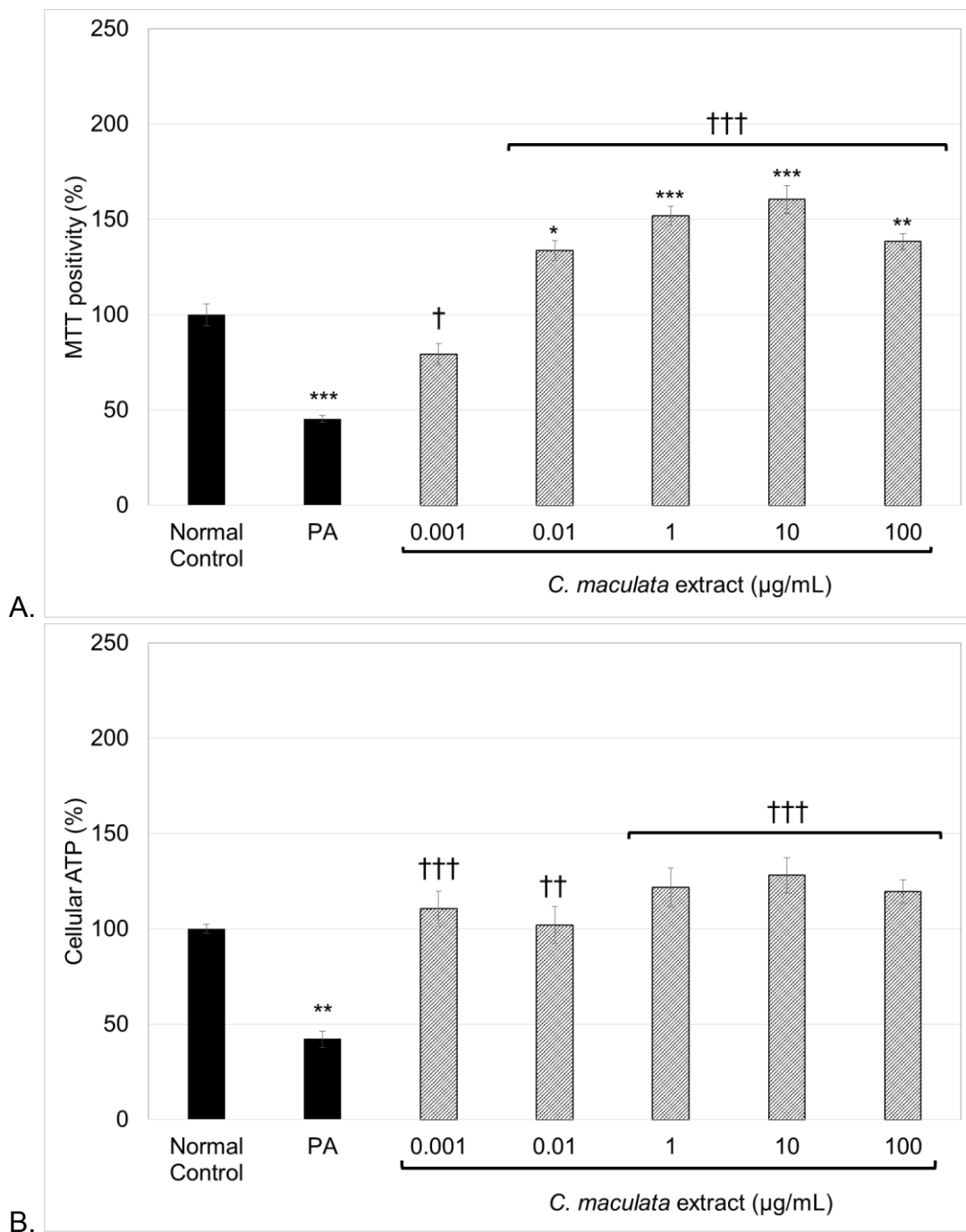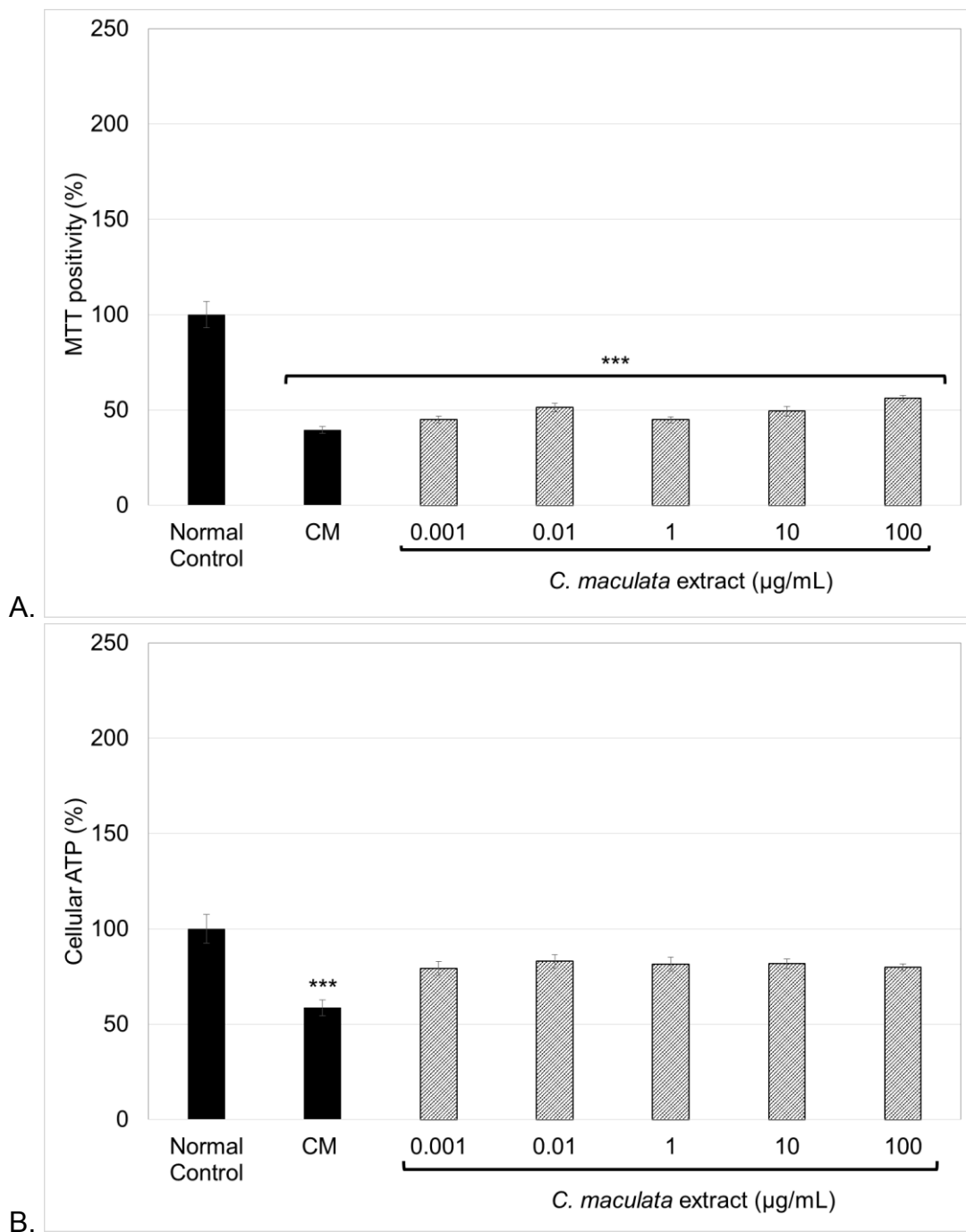**Figure 42. MTT (A) and ATP (B) RIN-5F cell viability following consecutive 24 hour exposures of cells to MS and NAC, respectively.**

RIN-5F cells were first exposed to 75 µM PA + 1 mM STZ + 0.1 ng/mL IFN-γ + 0.01 ng/mL IL-1β + 0.11 ng/mL TNF-α in combination for 24 hours and then to increasing concentrations of NAC in fresh media for 24 hours. Cell viability was then assessed using the MTT and ATP assays.

Where ** = p < 0.01 and *** = p < 0.001 compared to the normal control; and †† = p < 0.01 and ††† = p < 0.001 compared to MS.

120

1.2.2. Annexin-V and propidium iodide fluorescence

Optimised concentrations of the extract (10 µg/mL), mangiferin (100 µg/mL) and NAC (0.01 mM) were then assessed to determine their effects on RIN-5F β-cell apoptosis (annexin-V fluorescence) as well as late apoptosis and necrosis (propidium iodide fluorescence). The treatment concentrations were selected based on the lowest, most effective concentrations in the MTT and ATP screening assays (section 1.2.1.).

Compared to the normal control, both annexin-V (30.67 RFU ± 0.61 vs. 42.00 RFU ± 0.93) (Fig. 43 A) and propidium iodide (49.83 RFU ± 1.25 vs. 63.50 RFU ± 1.09) (Fig. 43 B) fluorescence were increased following exposure of RIN-5F cells to the STZ control. Exposure to *C. maculata* extract reduced annexin-V fluorescent intensity that was increased by STZ (30.83 RFU ± 1.22) (Fig. 43 A), while NAC reduced both annexin-V (31.33 RFU ± 1.26) (Fig. 43 A) and propidium iodide (59.33 RFU ± 0.49) (Fig. 43 B) increases in fluorescence. Mangiferin failed to ameliorate the STZ induced increase in annexin-V (Fig. 43 A), with the extract, mangiferin and NAC failing to reduce the STZ induced increase in propidium iodide fluorescence (Fig. 43 B).

When compared to the normal control, the PA control increased both annexin-V (30.67 RFU ± 0.61 vs. 42.00 RFU ± 1.55) (Fig. 44 A) and propidium iodide (49.83 RFU ± 1.25 vs. 56.17 RFU ± 0.70) (Fig. 44 B) fluorescence. Exposure to *C. maculata* extract reduced the PA induced annexin-V fluorescent intensity (34.67 RFU ± 1.15) (Fig. 44 A), while NAC reduced both annexin-V (34.50 RFU ± 0.96) (Fig. 44 A) and propidium iodide (41.17 RFU ± 1.99) (Fig. 44 B) increases in fluorescence. Mangiferin failed to ameliorate increased annexin-V and propidium iodide fluorescence induced by PA (Fig. 44).

Both annexin-V (30.67 RFU ± 0.61 vs. 45.33 RFU ± 0.84) (Fig. 45 A) and propidium iodide (49.83 RFU ± 1.25 vs. 54.50 RFU ± 0.76) (Fig. 45 B) fluorescence were increased compared to the normal control, following exposure of RIN-5F cells to the CM control. NAC reduced this increase in propidium iodide fluorescent intensity (47.17 RFU ± 0.48) (Fig. 45 B). Cells treated with the extract, mangiferin and NAC failed to ameliorate increased annexin-V fluorescence induced by CM (Fig. 45 A).

Compared to the normal control, both annexin-V (30.67 RFU ± 0.61 vs. 44.67 RFU ± 1.23) (Fig. 46 A) and propidium iodide (49.83 RFU ± 1.25 vs. 58.00 RFU ± 1.06) (Fig. 46 B)

121

fluorescence were increased following exposure of RIN-5F cells to the MS control. Exposure to NAC reduced this increased propidium iodide fluorescent intensity (42.50 RFU ± 1.18) (Fig. 46 B). The extract, mangiferin and NAC failed to ameliorate the increased annexin-V fluorescence induced by MS (Fig. 46 A), while the extract and mangiferin had no effect on propidium iodide fluorescence in these cells (Fig. 46 B).

The extract and NAC ameliorated STZ (Fig. 43 A) and PA induced (Fig. 44 A) apoptosis as observed in a reduction in annexin-V fluorescence, with NAC also reducing CM (Fig. 45 B) and MS induced (Fig. 46 B) increases in propidium iodide.
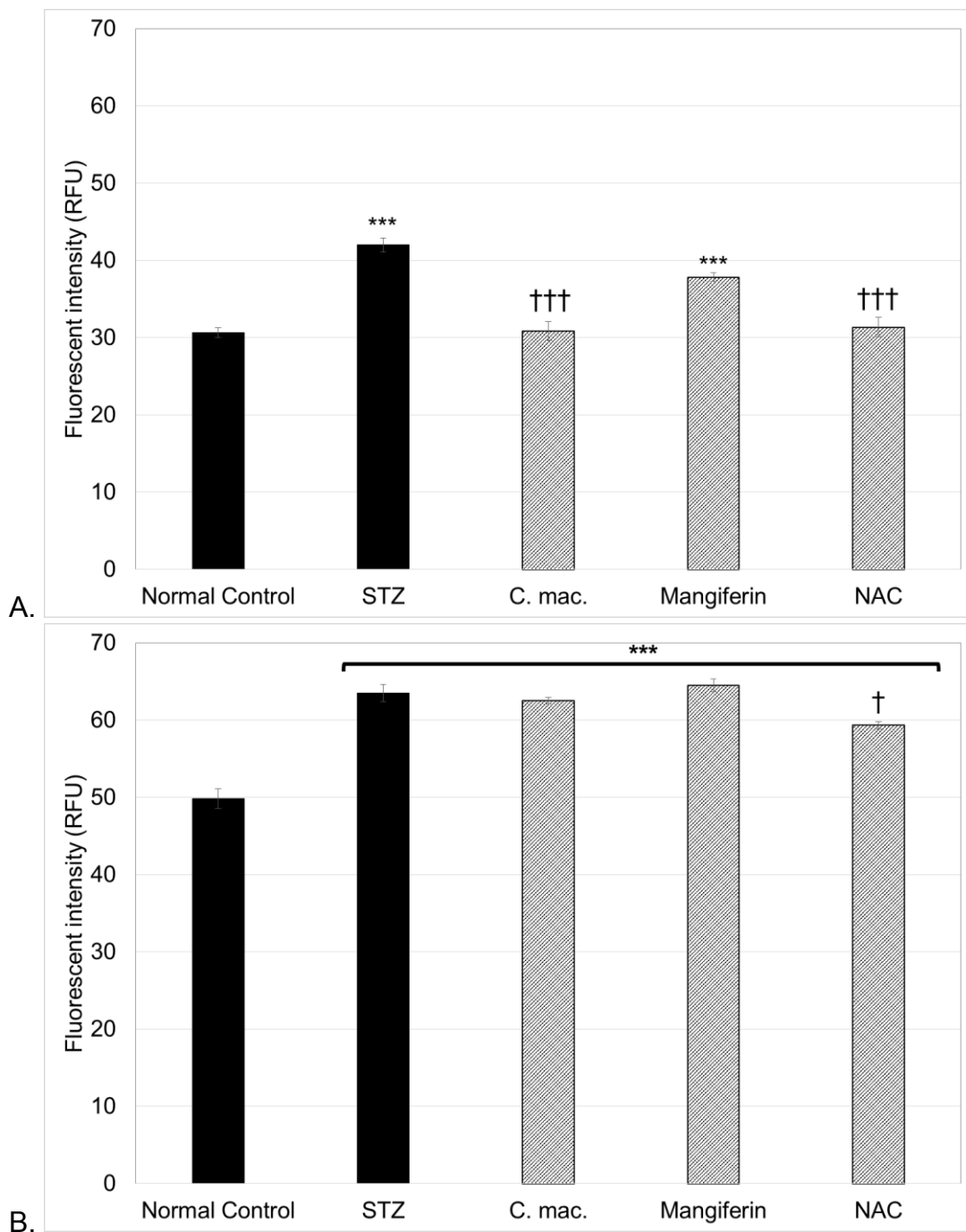
Figure 43. Annexin-V (A) and propidium iodide (B) fluorescence of RIN-5F cells exposed to STZ and subsequently treated with _C. maculata_ (C. mac.), mangiferin and NAC.

RIN-5F cells were first exposed to 10 mM STZ for 24 hours and then to 10 μg/mL extract, 100 μg/mL mangiferin and 0.01 mM NAC in fresh media for 24 hours. Cell viability was then assessed using the annexin-V and propidium iodide assay.

Where *** = $p < 0.001$ compared to the normal control; and † = $p < 0.05$ and ††† = $p < 0.001$ compared to STZ.
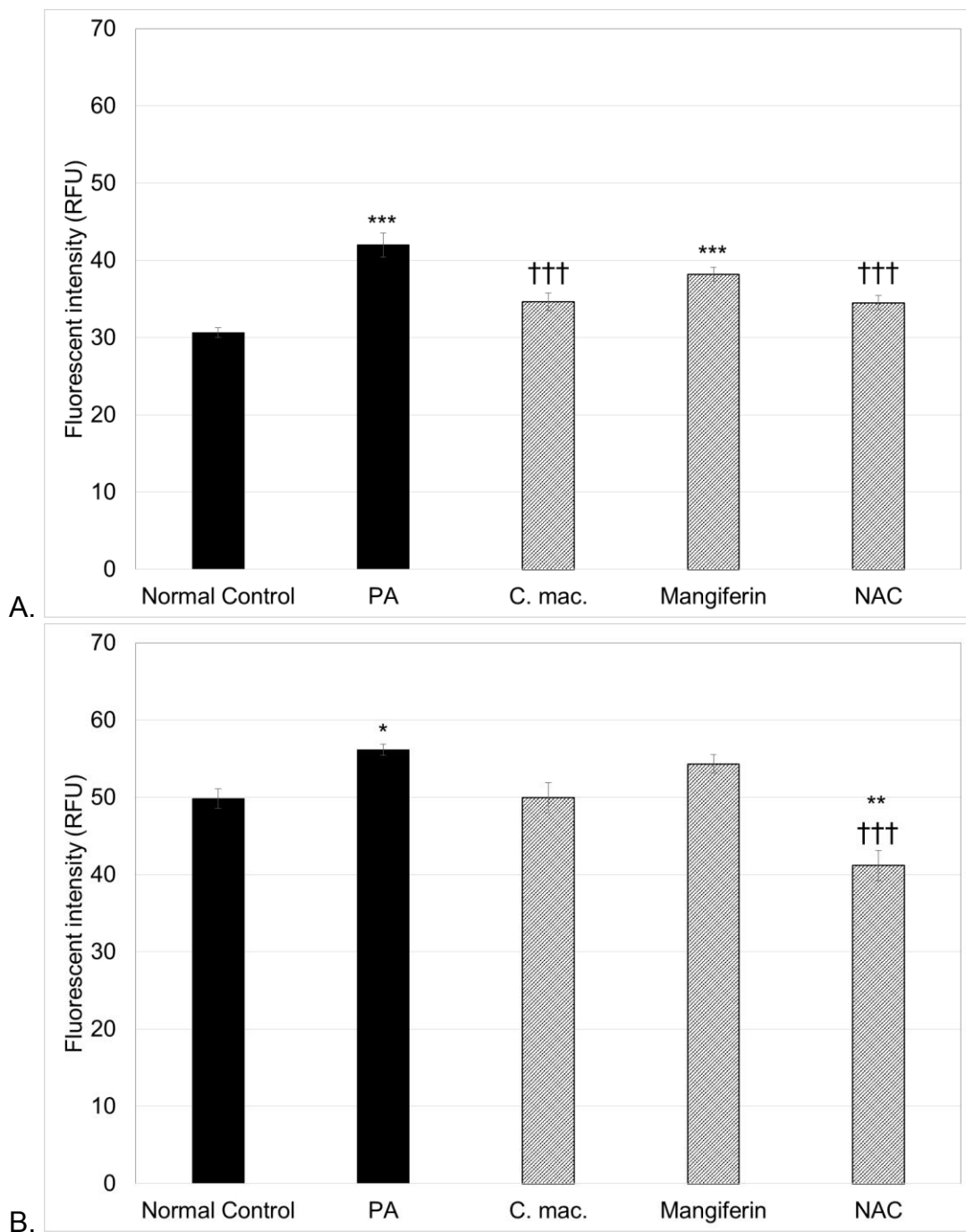
Figure 44. Annexin-V (A) and propidium iodide (B) fluorescence of RIN-5F cells exposed to PA and subsequently treated with *C. maculata* (C. mac.), mangiferin and NAC.

RIN-5F cells were first exposed to 750 µM PA for 24 hours and then to 10 µg/mL extract, 100 µg/mL mangiferin and 0.01 mM NAC in fresh media for 24 hours. Cell viability was then assessed using the annexin-V and propidium iodide assay.

Where * = $p < 0.05$, ** = $p < 0.01$ and *** = $p < 0.001$ compared to the normal control; and ††† = $p < 0.001$ compared to PA.

124

A.

B.
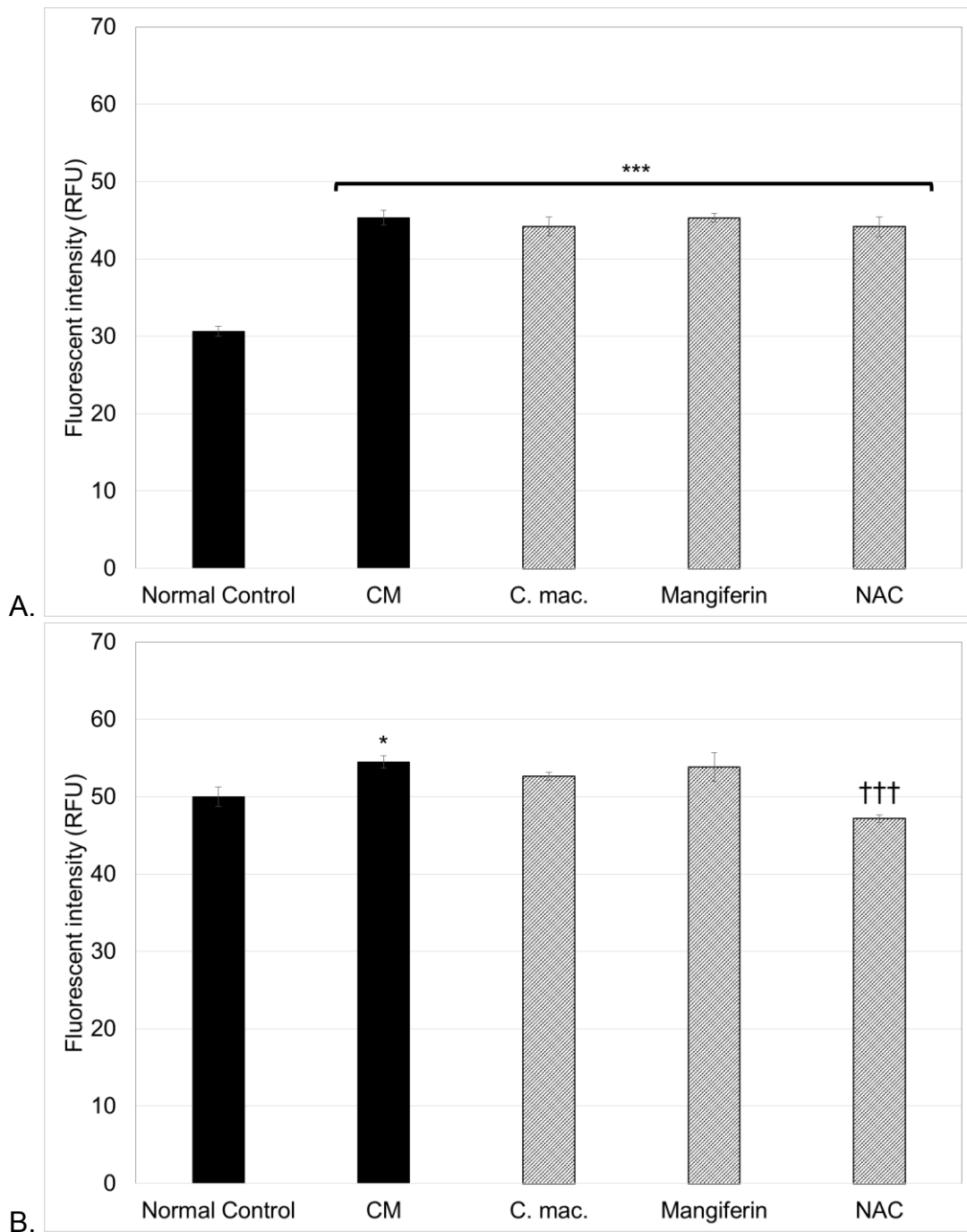
Figure 45. Annexin-V (A) and propidium iodide (B) fluorescence of RIN-5F cells exposed to CM and subsequently treated with *C. maculata* (C. mac.), mangiferin and NAC.

RIN-5F cells were first exposed to 1 ng/mL IFN-γ + 0.1 ng/mL IL-1β + 1.1 ng/mL TNF-α in combination for 24 hours and then to 10 µg/mL extract, 100 µg/mL mangiferin and 0.01 mM NAC in fresh media for 24 hours. Cell viability was then assessed using the annexin-V and propidium iodide assay.

Where * = $p < 0.05$ and *** = $p < 0.001$ compared to the normal control; and ††† = $p < 0.001$ compared to CM.

125
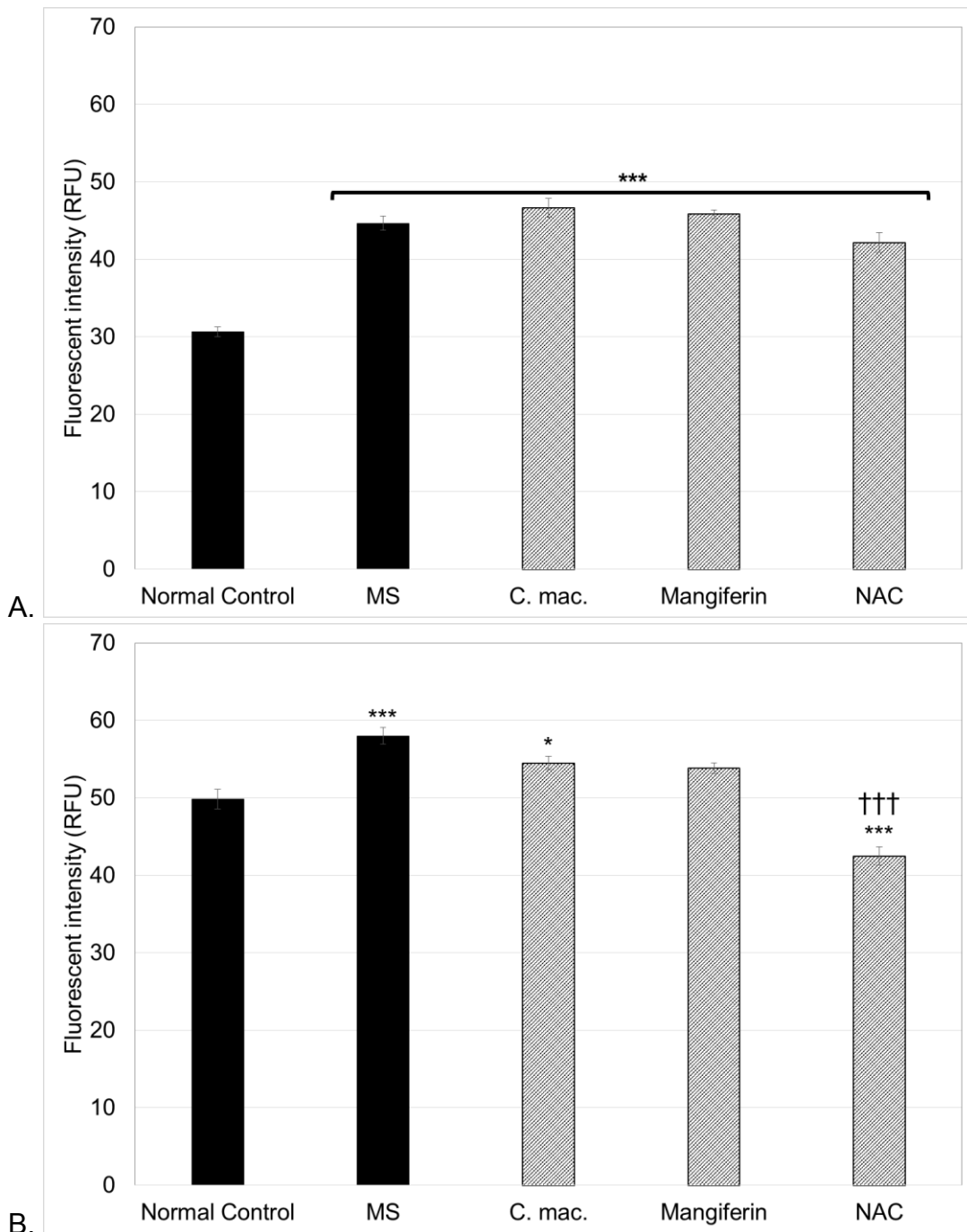
Figure 46. Annexin-V (A) and propidium iodide (B) fluorescence of RIN-5F cells exposed to MS and subsequently treated with *C. maculata* (C. mac.), mangiferin and NAC.

RIN-5F cells were first exposed to 75 µM PA + 1 mM STZ + 0.1 ng/mL IFN-γ + 0.01 ng/mL IL-1β + 0.11 ng/mL TNF-α in combination for 24 hours and then to 10 µg/mL extract, 100 µg/mL mangiferin and 0.01 mM NAC in fresh media for 24 hours. Cell viability was then assessed using the annexin-V and propidium iodide assay.

Where * = $p < 0.05$ and *** = $p < 0.001$ compared to the normal control; and ††† = $p < 0.001$ compared to MS.

126

1.2.3. Summary of the effect of treatment *in vitro* on RIN-5F cell viability

As summarised in Table 4, treatment of RIN-5F cells exposed to STZ and PA with the *C. maculata* extract, as well as NAC improved viability by increasing cellular ATP and MTT positivity and decreasing apoptosis (as seen in a reduction in annexin-V fluorescence). Only NAC showed the ability to improve CM induced toxicity in RIN-5F cells, by increasing cellular ATP and decreasing apoptosis. NAC also ameliorated late stage apoptosis and necrosis (as seen in a reduction of propidium iodide fluorescence) in RIN-5F cells exposed to CM and MS. Mangiferin showed some amelioration of STZ and MS induced cytotoxicity by increasing MTT positivity.

Table 4. *In vitro* RIN-5F cell viability summary

		C. maculata	Mangiferin	NAC
STZ	MTT	↑	↑	↑
	ATP	↑	-	↑
	Annexin-V	↓	-	↓
	PI	-	-	↓
PA	MTT	↑	-	↑
	ATP	↑	-	↑
	Annexin-V	↓	-	↓
	PI	-	-	↓
CM	MTT	-	-	-
	ATP	-	-	↑
	Annexin-V	-	-	↓
	PI	-	-	-
MS	MTT	-	↑	-
	ATP	-	-	-
	Annexin-V	-	-	-
	PI	-	-	↓

127

1.3. Cell function

The effect of optimised concentrations of *C. maculata* extract, mangiferin and NAC were also assessed in terms of RIN-5F cellular function by determining their effect on basal (5.5 mM glucose) and glucose stimulated (35 mM glucose) insulin secretion, cellular calcium and proliferation.

1.3.1. Insulin secretion assay

Exposure of RIN-5F cells to STZ (Fig. 47 A) and PA (Fig. 48 A) and treatment with *C. maculata*, mangiferin and NAC did not affect basal insulin secretion when compared to the normal control, however, insulin secretion was increased in the STZ control compared to the normal control in glucose stimulated RIN-5F cells (21.96 ng/mL ± 0.58 vs. 18.31 ng/mL ± 0.56) (Fig. 47 B). Elevated insulin secretion induced by STZ was reduced by treatment with *C. maculata* extract (17.51 ng/mL ± 0.35), while mangiferin and NAC had no effect (Fig. 47 B).

Compared to the elevated, albeit not significant, insulin concentration in cells exposed to the PA control, insulin secretion in glucose stimulated RIN-5F cells was reduced by treatment with *C. maculata* extract and mangiferin (24.78 ng/mL ± 0.30 vs. 18.55 ng/mL ± 0.57 and 18.78 ng/mL ± 0.98, respectively), but not by NAC (Fig. 48 B).

Exposure of RIN-5F cells to the CM control and treatment with *C. maculata*, mangiferin and NAC did not affect basal (Fig. 49 A) or glucose stimulated (Fig. 49 B) insulin secretion.

Exposure of RIN-5F cells to MS and subsequent treatment with mangiferin increased basal insulin secretion in RIN-5F cells compared to the normal control (10.12 ng/mL ± 0.34 vs. 8.46 ng/mL ± 0.31) (Fig. 50 A). Following a reduction in glucose stimulated insulin secretion by MS compared to the normal control (15.86 ng/mL ± 0.09 vs. 18.31 ng/mL ± 0.56) (Fig. 50 B), mangiferin increased glucose stimulated insulin secretion compared to both the normal and MS controls (20.98 ng/mL ± 0.60) (Fig. 50 B). NAC increased glucose stimulated insulin secretion compared to the MS control (18.74 ng/mL ± 0.33) (Fig. 50 B), with no effect observed for the *C. maculata* extract.

Basal insulin secretion of RIN-5F cells was not affected by the stressors used in this study. Glucose stimulated insulin secretion was, however, increased by STZ (Fig. 47 A) and to a

lesser extent, by PA (not significant) (Fig. 48 A). The extract normalised glucose stimulated insulin secretion in STZ (Fig. 47 B), PA (Fig. 48 B) and MS (Fig. 50 B) exposed cells. Mangiferin decreased the PA induced increase in glucose stimulated insulin secretion (Fig. 48 B) and, along with NAC, increased glucose stimulated insulin secretion in MS exposed cells (Fig. 50 B).

A.

B.
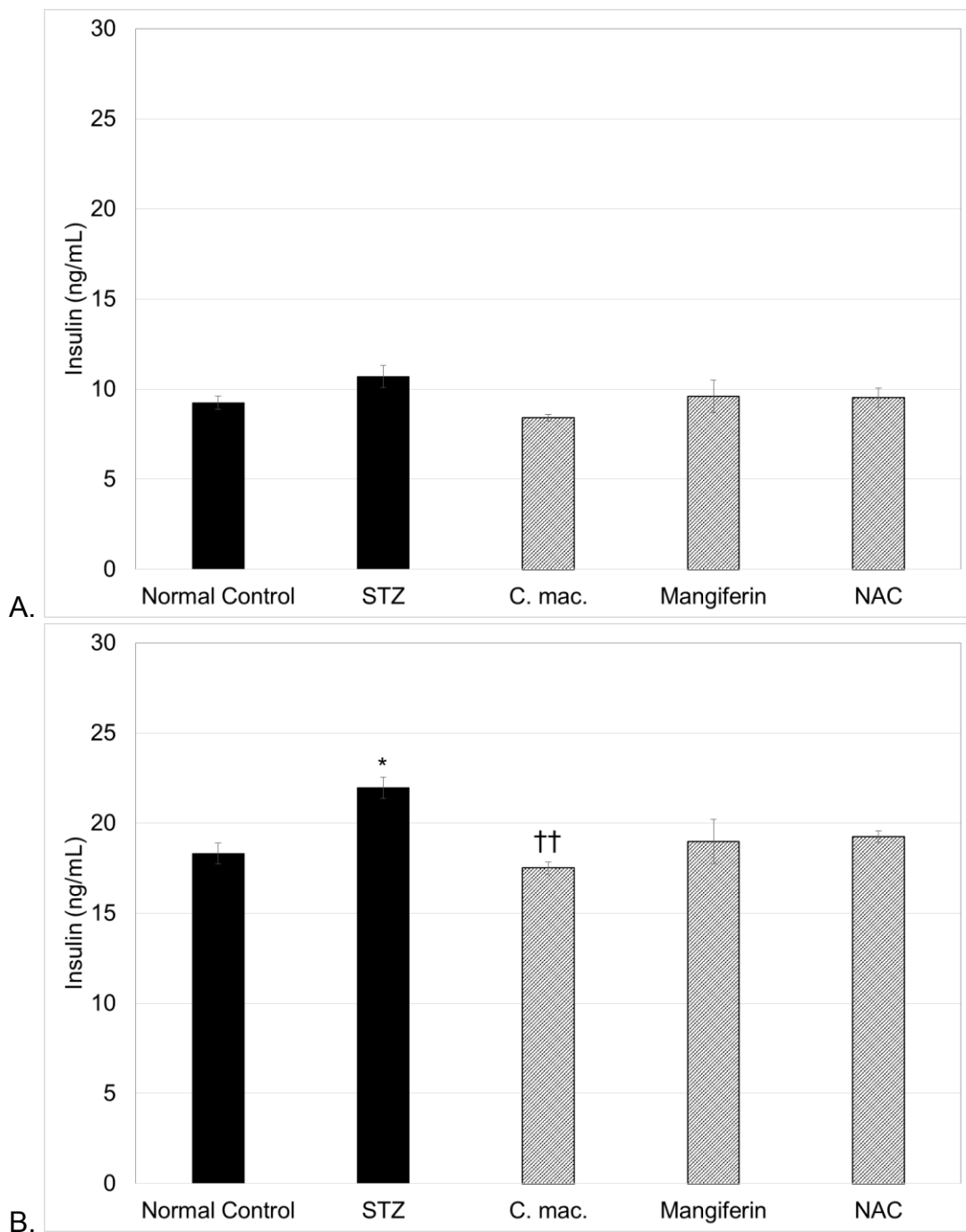
Figure 47. Basal (A) and glucose stimulated (B) insulin secretion of RIN-5F cells exposed to STZ and subsequently treated with *C. maculata* (C. mac.), mangiferin and NAC.

RIN-5F cells were first exposed to 10 mM STZ for 24 hours and then to 10 µg/mL extract, 100 µg/mL mangiferin and 0.01 mM NAC in fresh media for 24 hours. Basal and glucose stimulated insulin secretion was then determined.

Where * = $p < 0.05$ compared to the normal control; and †† = $p < 0.01$ compared to STZ.
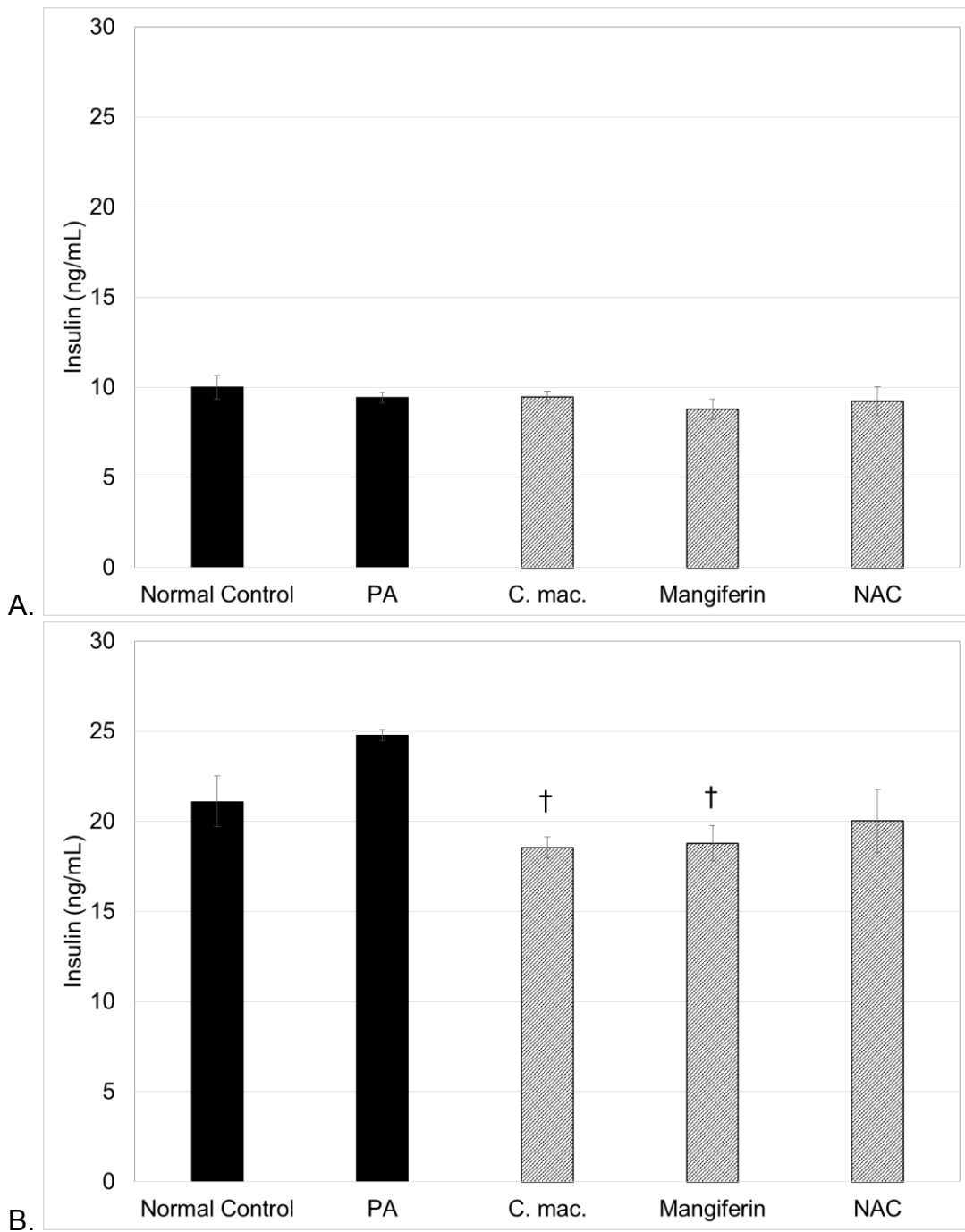
Figure 48. Basal (A) and glucose stimulated (B) insulin secretion of RIN-5F cells exposed to PA and subsequently treated with *C. maculata* (C. mac.), mangiferin and NAC.

RIN-5F cells were first exposed to 750 µM PA for 24 hours and then to 10 µg/mL extract, 100 µg/mL mangiferin and 0.01 mM NAC in fresh media for 24 hours. Basal and glucose stimulated insulin secretion was then determined.

Where † = p < 0.05 compared to PA.

A.

B.
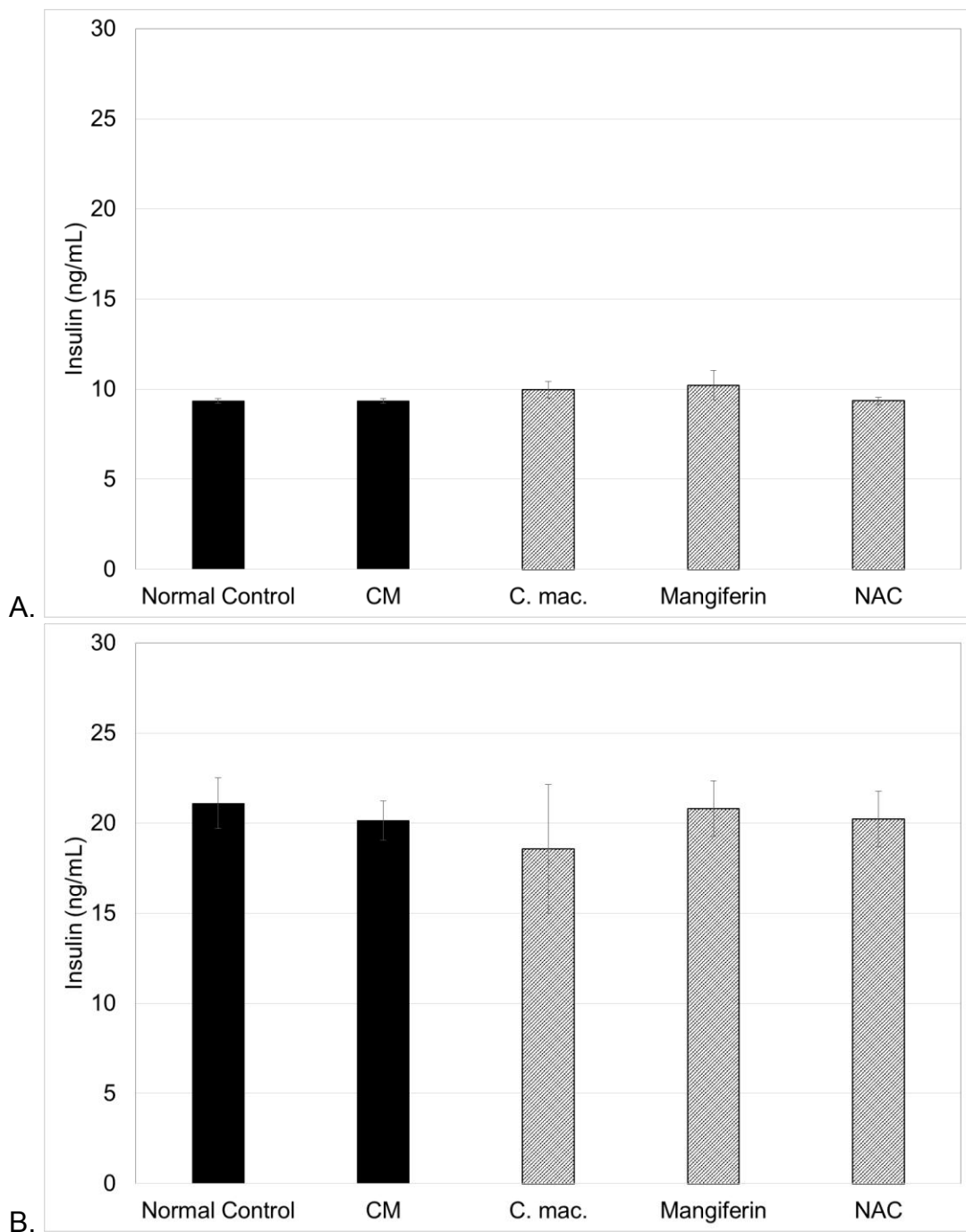
Figure 49. Basal (A) and glucose stimulated (B) insulin secretion of RIN-5F cells exposed to CM and subsequently treated with _C. maculata_ (C. mac.), mangiferin and NAC.

RIN-5F cells were first exposed to 1 ng/mL IFN-γ + 0.1 ng/mL IL-1β + 1.1 ng/mL TNF-α in combination for 24 hours and then to 10 μg/mL extract, 100 μg/mL mangiferin and 0.01 mM NAC in fresh media for 24 hours. Basal and glucose stimulated insulin secretion was then determined.
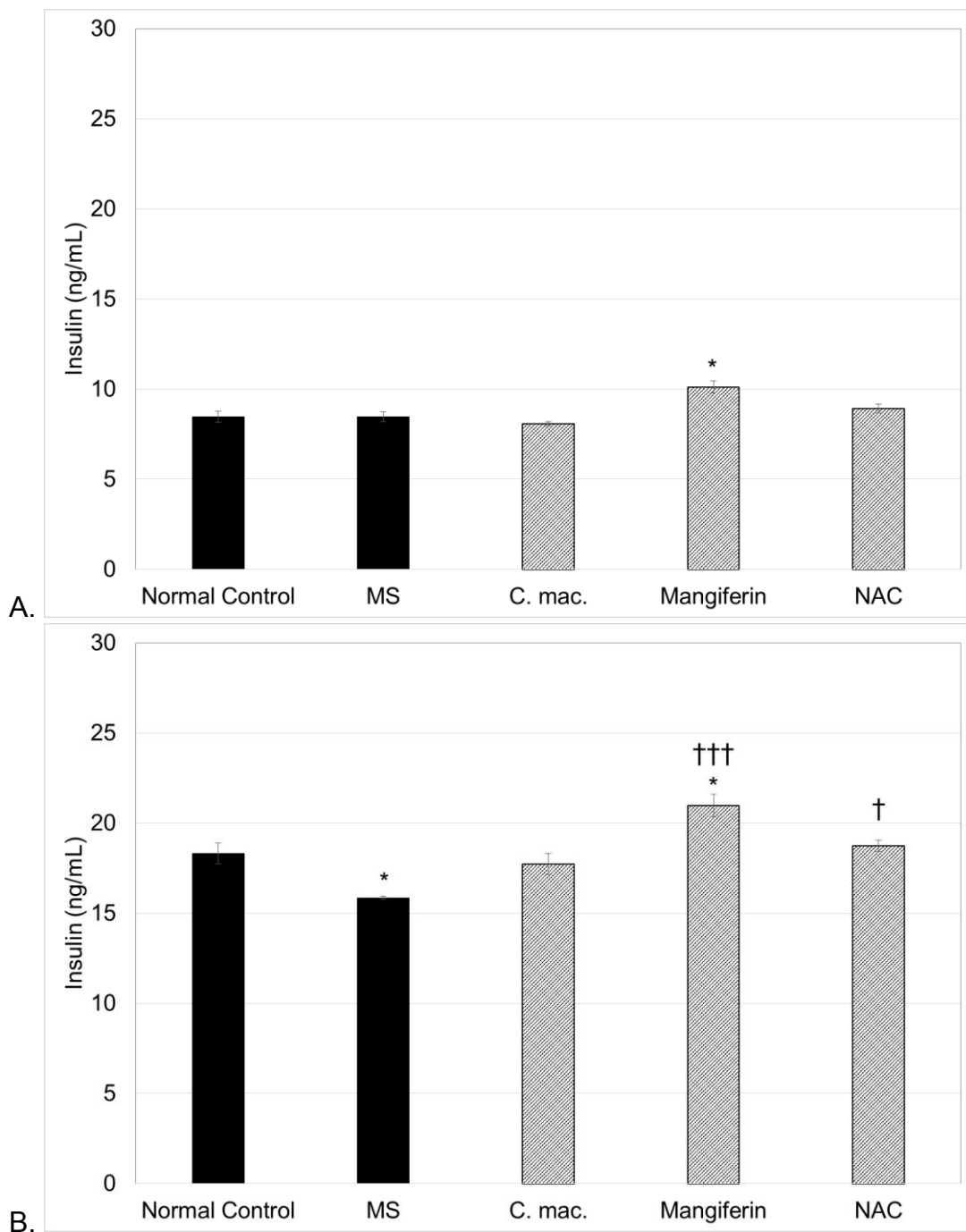
Figure 50. Basal (A) and glucose stimulated (B) insulin secretion of RIN-5F cells exposed to MS and subsequently treated with *C. maculata* (C. mac.), mangiferin and NAC.

RIN-5F cells were first exposed to 75 µM PA + 1 mM STZ + 0.1 ng/mL IFN-γ + 0.01 ng/mL IL-1β + 0.11 ng/mL TNF-α in combination for 24 hours and then to 10 µg/mL extract, 100 µg/mL mangiferin and 0.01 mM NAC in fresh media for 24 hours. Basal and glucose stimulated insulin secretion was then determined.

Where * = $p < 0.05$ compared to the normal control; and † = $p < 0.05$ and ††† = $p < 0.001$ compared to MS.

133

1.3.2. Cellular calcium fluorescent assay

Compared to the normal control, cellular calcium was reduced following exposure of RIN-5F cells to the STZ control (168.83 RFU ± 2.17 vs. 142.17 RFU ± 1.35) (Fig. 51) and the PA control (156.50 RFU ± 1.23 vs. 143.50 RFU ± 1.48) (Fig. 52). *Cyclopia maculata* extract increased the reduced cellular calcium content (161.67 RFU ± 5.15), while mangiferin failed to ameliorate the STZ induced reduction in cellular calcium (Fig. 51). The extract increased cellular calcium content when compared to the PA control (166.67 RFU ± 1.48) while mangiferin and NAC failed to ameliorate the PA induced reduction in cellular calcium (Fig. 52).

Exposure of RIN-5F cells to the CM control reduced cellular calcium content (154.00 RFU ± 1.93 vs. 129.67 RFU ± 5.77) (Fig. 53), while NAC increased cellular calcium content (151.67 RFU ± 3.68), with the extract and mangiferin treatment failing to ameliorate the CM induced reduction in calcium content (Fig. 53).

Compared to the normal control, RIN-5F cells exposed to the MS control had reduced cellular calcium (165.50 RFU ± 0.99 vs. 153.67 RFU ± 1.56) (Fig. 54). The extract, mangiferin and NAC failed to ameliorate the reduction in calcium induced by MS (Fig. 54).

The *C. maculata* extract and NAC ameliorated both STZ (Fig. 51) and PA (Fig. 52) induced reduction in cellular calcium, with NAC increasing cellular calcium in CM exposed cells (Fig. 53).
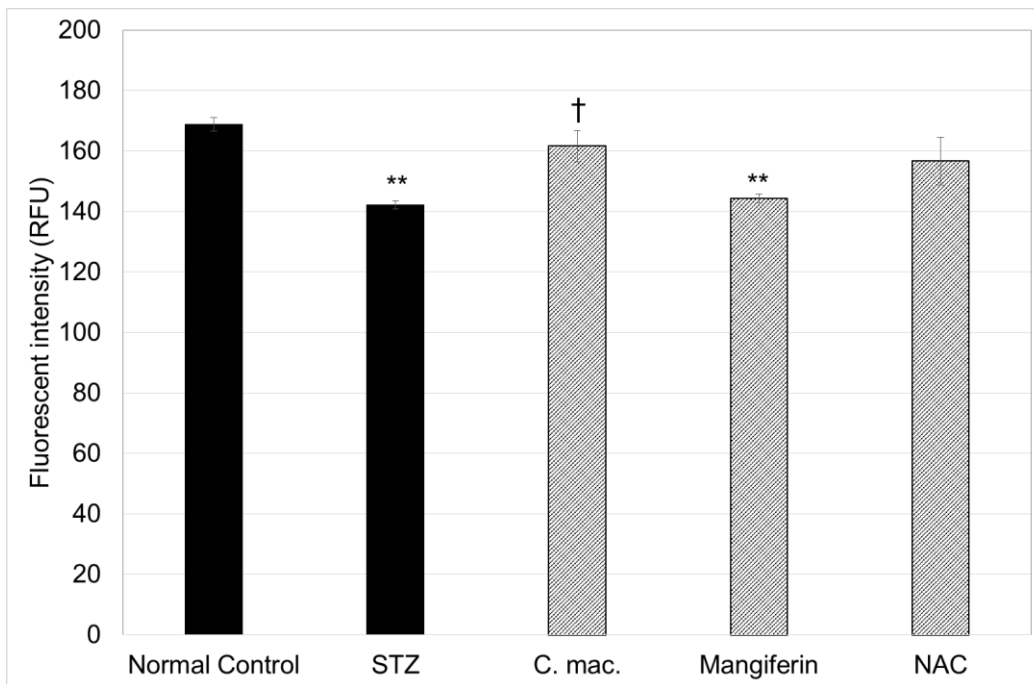
Figure 51. Cellular calcium content of RIN-5F cells exposed to STZ and subsequently treated with *C. maculata* (C. mac.), mangiferin and NAC.

RIN-5F cells were first exposed to 10 mM STZ for 24 hours and then to 10 µg/mL extract, 100 µg/mL mangiferin and 0.01 mM NAC in fresh media for 24 hours. Thereafter, cellular calcium was quantified.

Where ** = $p < 0.01$ compared to the normal control; and † = $p < 0.05$ compared to STZ.
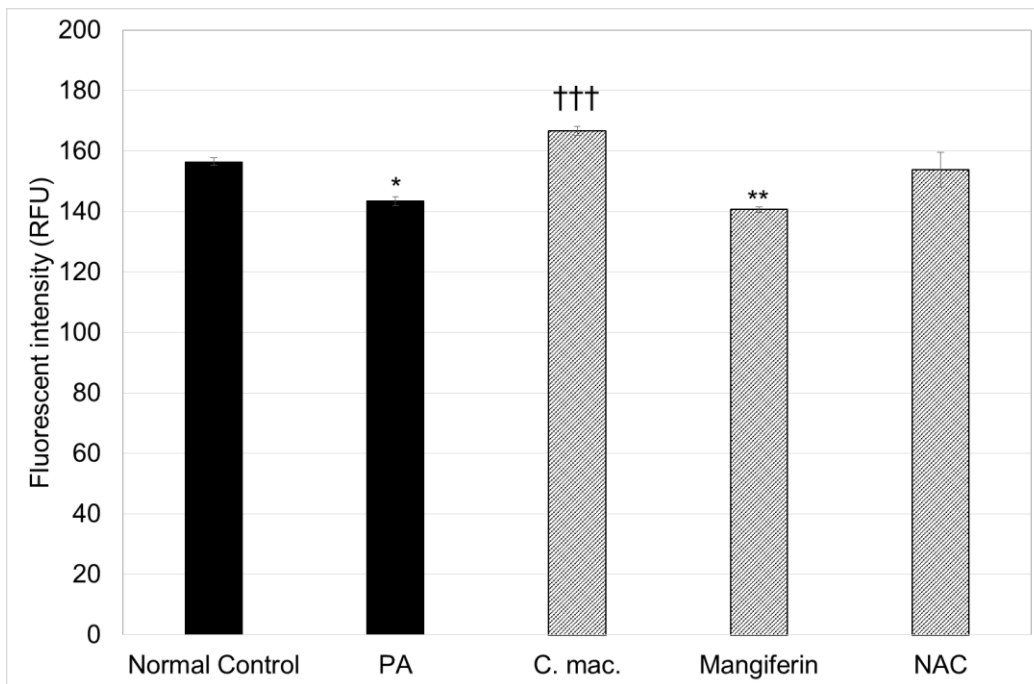
Figure 52. Cellular calcium content of RIN-5F cells exposed to PA and subsequently treated with *C. maculata* (C. mac.), mangiferin and NAC.

RIN-5F cells were first exposed to 750 µM PA for 24 hours and then to 10 µg/mL extract, 100 µg/mL mangiferin and 0.01 mM NAC in fresh media for 24 hours. Thereafter, cellular calcium was quantified.

Where * = $p < 0.05$ and ** = $p < 0.01$ compared to the normal control; and ††† = $p < 0.001$ compared to PA.
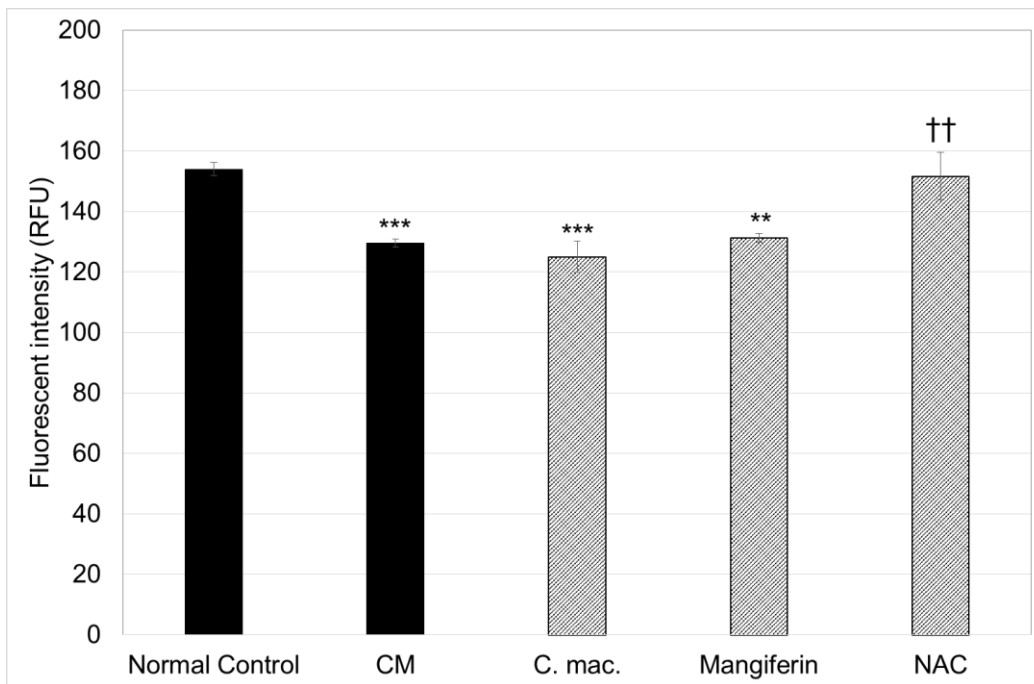
Figure 53. Cellular calcium content of RIN-5F cells exposed to CM and subsequently treated with *C. maculata* (C. mac.), mangiferin and NAC.

RIN-5F cells were first exposed to 1 ng/mL IFN-γ + 0.1 ng/mL IL-1β + 1.1 ng/mL TNF-α in combination for 24 hours and then to 10 µg/mL extract, 100 µg/mL mangiferin and 0.01 mM NAC in fresh media for 24 hours. Thereafter, cellular calcium was quantified.

Where ** = $p < 0.01$ and *** = $p < 0.001$ compared to the normal control; and †† = $p < 0.01$ compared to CM.
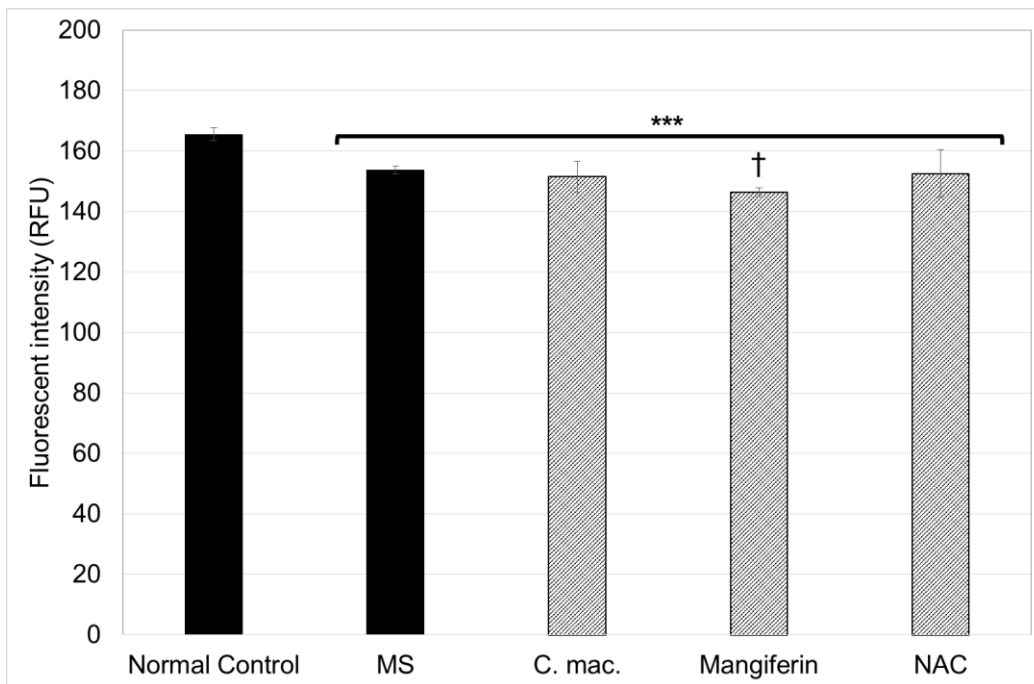
Figure 54. Cellular calcium content of RIN-5F cells exposed to MS and subsequently treated with *C. maculata* (C. mac.), mangiferin and NAC.

RIN-5F cells were first exposed to 75 µM PA + 1 mM STZ + 0.1 ng/mL IFN-γ + 0.01 ng/mL IL-1β + 0.11 ng/mL TNF-α in combination for 24 hours and then to 10 µg/mL extract, 100 µg/mL mangiferin and 0.01 mM NAC in fresh media for 24 hours. Thereafter, cellular calcium was quantified.

Where *** = $p < 0.001$ compared to the normal control; and † = $p < 0.05$ compared to MS.

1.3.3. Cell proliferation assay

The STZ control induced a reduction in cell proliferation compared to the normal control (292.03 fmol ± 8.12 vs. 470.35 fmol ± 25.03) (Fig. 55). Compared to the STZ control after 24 hours, both *C. maculata* extract and NAC increased cell proliferation, as measured by the incorporation of tritiated thymidine into RIN-5F cells (394.61 fmol ± 9.15 and 463.59 fmol ± 20.92, respectively) (Fig. 55).

Compared to the normal control, a decrease in tritiated thymidine incorporation into RIN-5F cells after 24 hours exposure to the PA control was observed (305.78 fmol ± 18.50 vs. 165.79 fmol ± 4.94) (Fig. 56). *Cyclopia maculata* extract, mangiferin and NAC increased the reduction in cell proliferation (283.76 fmol ± 13.63, 336.66 fmol ± 27.43 and 336.79 fmol ± 163.56, respectively) (Fig. 56).

Following a decrease in tritiated thymidine incorporation into RIN-5F cells after 24 hours exposure to the CM control compared to the normal control (102.05 fmol ± 7.42 vs. 176.94 fmol ± 7.89), *C. maculata* extract, mangiferin and NAC increased the cell proliferation (198.08 fmol ± 14.45, 191.33 fmol ± 3.74 and 168.89 fmol ± 6.67, respectively) (Fig. 57).

Both *C. maculata* extract and NAC increased RIN-5F cell proliferation compared to the MS control (353.02 fmol ± 26.53 and 447.63 fmol ± 16.56 vs. 214.62 fmol ± 5.39, respectively) that was initially reduced from the normal control (353.82 fmol ± 8.11) by 24 hours exposure to MS (Fig. 58).

The extract and NAC ameliorated the reduction of cell proliferation induced by STZ (Fig. 55), PA (Fig. 56), CM (Fig. 57) and MS (Fig. 58). Mangiferin was effective at improving cell proliferation in PA and CM exposed RIN-5F cells only.
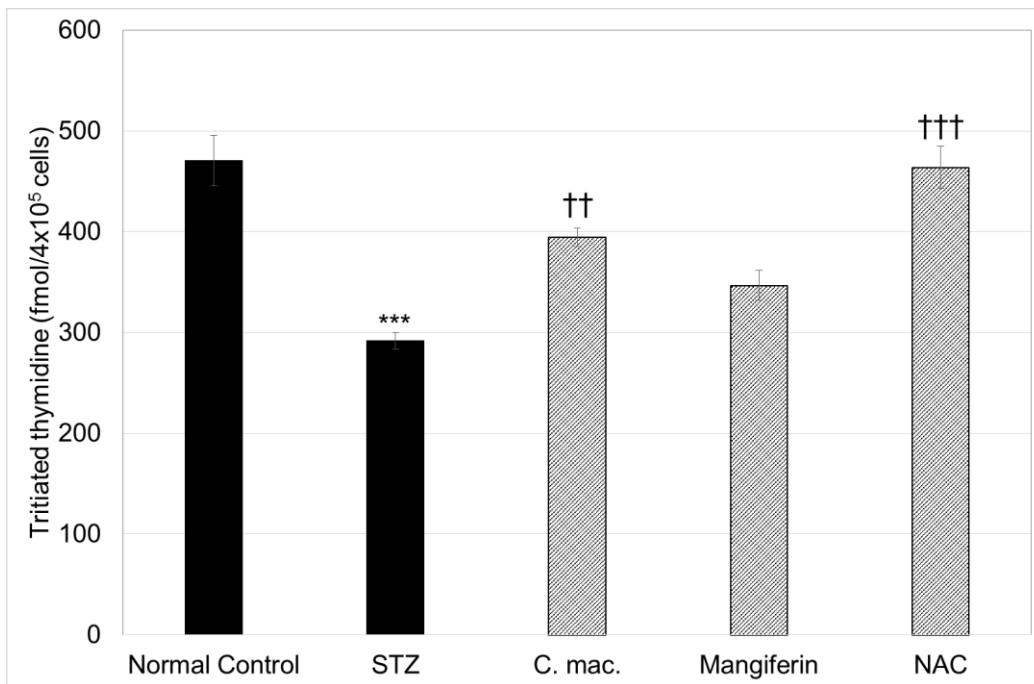
Figure 55. The effect of *C. maculata* extract (C. mac.), NAC and mangiferin on cell proliferation following STZ-induced cytotoxicity.

RIN-5F cell proliferation was measured following exposure first to 10 mM STZ for 24 hours and then to 10 µg/mL extract, 100 µg/mL mangiferin and 0.01 mM NAC in fresh media for 24 hours.

Where *** = $p < 0.001$ compared to the normal control; and †† = $p < 0.01$ and ††† = $p < 0.001$ compared to STZ.
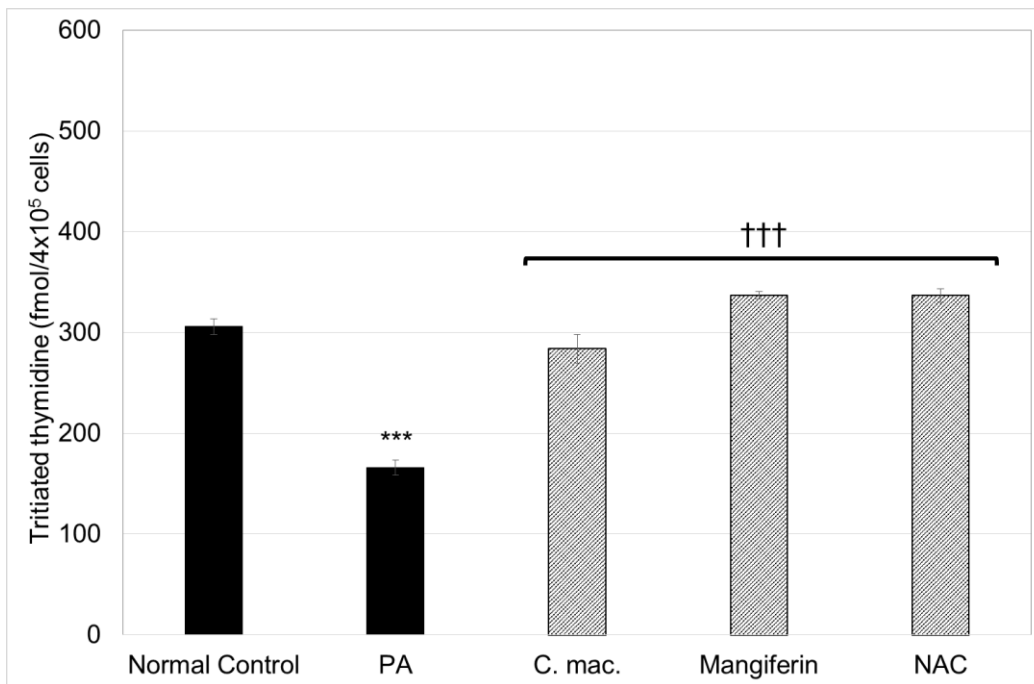
Figure 56. The effect of *C. maculata* extract (C. mac.), NAC and mangiferin on cell proliferation following PA-induced cytotoxicity.

RIN-5F cell proliferation was measured following exposure first to 750 µM PA for 24 hours and then to 10 µg/mL extract, 100 µg/mL mangiferin and 0.01 mM NAC in fresh media for 24 hours.

Where *** = $p < 0.001$ compared to the normal control; and ††† = $p < 0.001$ compared to PA.
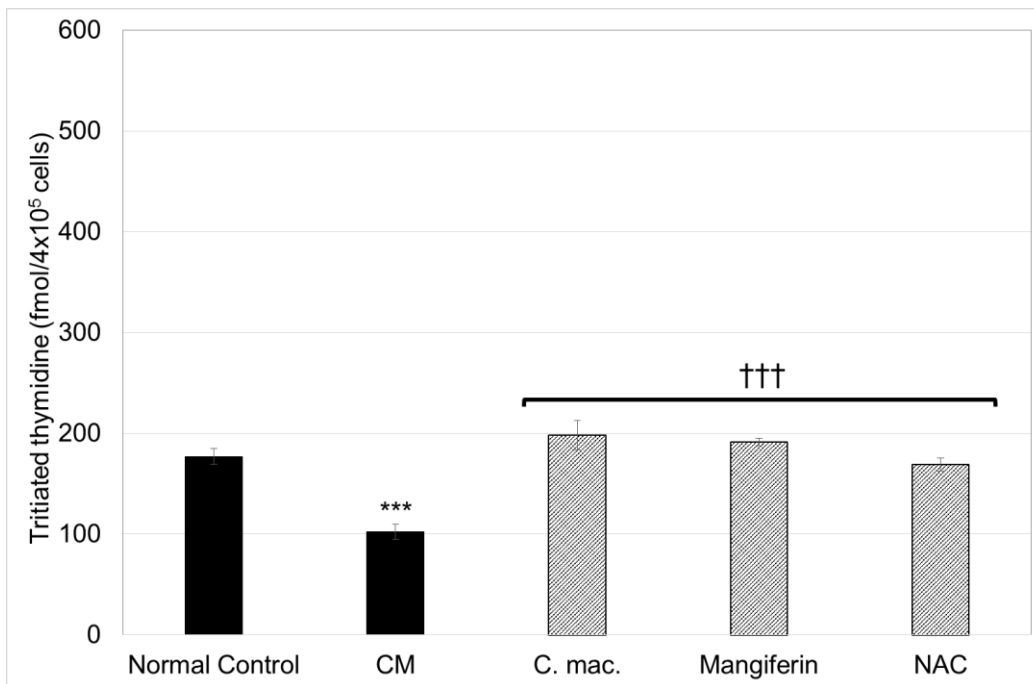
Figure 57. The effect of *C. maculata* extract (C. mac.), NAC and mangiferin on cell proliferation following CM-induced cytotoxicity.

RIN-5F cell proliferation was measured following exposure first to 1 ng/mL IFN-γ + 0.1 ng/mL IL-1β + 1.1 ng/mL TNF-α in combination for 24 hours and then to 10 µg/mL extract, 100 µg/mL mangiferin and 0.01 mM NAC in fresh media for 24 hours.

Where *** = $p < 0.001$ compared to the normal control; and ††† = $p < 0.001$ compared to CM.
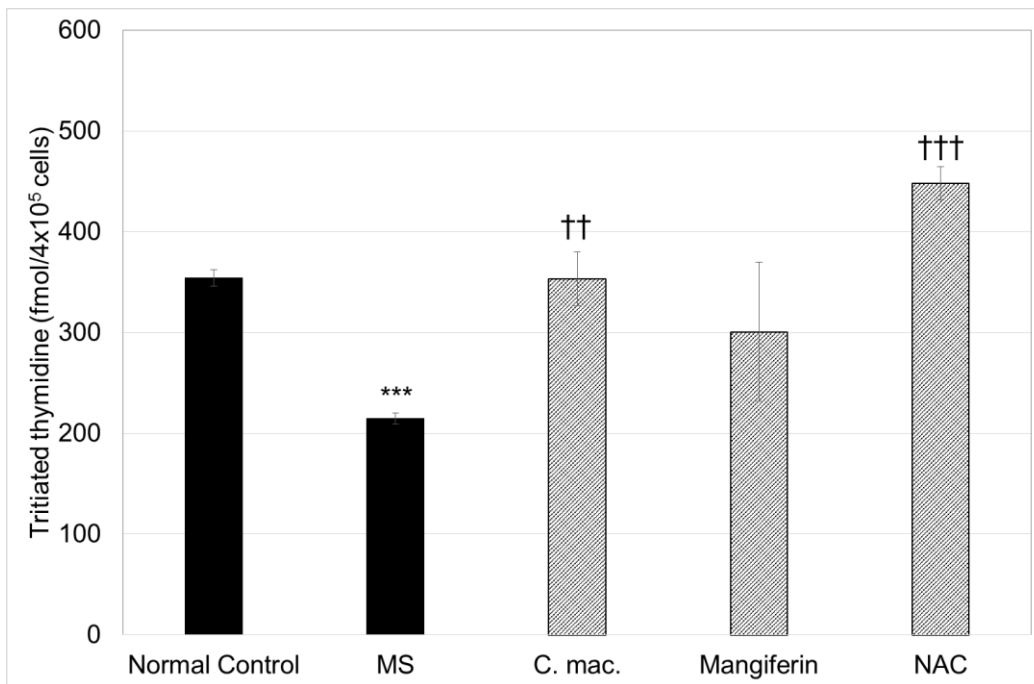
Figure 58. The effect of *C. maculata* extract (C. mac.), NAC and mangiferin on cell proliferation following MS-induced cytotoxicity.

RIN-5F cell proliferation was measured following exposure first to 75 µM PA + 1 mM STZ + 0.1 ng/mL IFN-γ + 0.01 ng/mL IL-1β + 0.11 ng/mL TNF-α in combination for 24 hours and then to 10 µg/mL extract, 100 µg/mL mangiferin and 0.01 mM NAC in fresh media for 24 hours.

Where *** = $p < 0.001$ compared to the normal control; and †† = $p < 0.01$ and ††† = $p < 0.001$ compared to MS.

1.3.4. Summary of the effect of treatment *in vitro* on RIN-5F cell function

As summarised in Table 5, the extract and NAC significantly improved RIN-5F cell function under all four cytotoxic conditions. Mangiferin improved cell function, in terms of cell proliferation, in RIN-5F cells exposed to PA and CM only.

Table 5. *In vitro* RIN-5F cell function summary.

		C. maculata	Mangiferin	NAC
STZ	Insulin secretion	↓	-	-
	Calcium	↑	-	↑
	Proliferation	↑	-	↑
PA	Insulin secretion	↓	↓	-
	Calcium	↑	-	↑
	Proliferation	↑	↑	↑
CM	Insulin secretion	-	-	-
	Calcium	-	-	↑
	Proliferation	↑	↑	↑
MS	Insulin secretion	↑	↑	↑
	Calcium	-	-	-
	Proliferation	↑	-	↑

1.4. Oxidative stress status

In order to elucidate the antioxidative effects of the extract, mangiferin and NAC in β-cells, the effects on cellular RNS (DAF fluorescence) and ROS (DHE fluorescence) were measured. Furthermore, the concentrations of naturally occurring cellular antioxidant enzymes were to be determined. The detection kits used for CAT and GSH levels in RIN-5F cells were unable to detect low amounts of these enzymes, thus only data for the SOD enzyme are presented.

1.4.1. Diaminofluorescein-FM and dihydroethidium fluorescence

Known to induce oxidative stress, DMNQ was used to validate the fluorescent detection method used in this study. Compared to the respective normal controls, DMNQ increased DAF (21.83 RFU ± 1.60 vs. 36.17 RFU ± 2.48) and DHE (20.00 RFU ± 0.68 vs. 22.33 RFU ± 0.21) fluorescence in RIN-5F cells over one hour (Fig. 59).

The STZ control increased both DAF (31.00 RFU ± 1.67 vs. 23.17 RFU ± 1.11) (Fig. 60 A) and DHE (34.33 RFU ± 0.42 vs. 23.50 RFU ± 0.24) (Fig. 60 B) fluorescence compared to the normal control. The extract reduced both DAF (24.17 RFU ± 0.79) (Fig. 60 A) and DHE (25.50 RFU ± 0.34) (Fig. 60 B) increases in fluorescence, whereas NAC was observed to reduce DAF fluorescence only (23.83 RFU ± 0.60) (Fig. 60 B). Mangiferin had no measurable effect on either DAF or DHE fluorescence (Fig. 60).

Compared to the normal control, the PA control increased both DAF (23.17 RFU ± 1.11 vs. 28.17 RFU ± 0.91) (Fig. 61 A) and DHE (23.50 RFU ± 0.24 vs. 27.33 RFU ± 0.49) (Fig. 61 B) fluorescence. The *C. maculata* extract and NAC reduced the increased DHE fluorescence (22.17 RFU ± 0.48 and 22.33 RFU ± 0.42, respectively) (Fig. 61 B). Mangiferin and NAC failed to ameliorate the PA induced increase in DAF fluorescence (Fig. 61 A).

An increase in both DAF (23.17 RFU ± 1.11 vs. 38.67 RFU ± 0.71) (Fig. 62 A) and DHE (23.50 RFU ± 0.24 vs. 36.67 RFU ± 0.61) (Fig. 62 B) fluorescence compared to the normal control was observed in cell exposed to the CM control. The extract, mangiferin and NAC failed to reduce these increases (Fig. 62).

Compared to the normal control, the MS control increased both DAF (23.17 RFU ± 1.11 vs. 39.67 RFU ± 0.42) (Fig. 63 A) and DHE (23.50 RFU ± 0.24 vs. 37.33 RFU ± 0.49) (Fig. 63

B) fluorescence. NAC reduced the increase in DHE fluorescence (34.33 RFU ± 0.42) (Fig. 63 B) but failed to reduce DAF fluorescence (Fig. 63 A). Both the extract and mangiferin had no effect (Fig. 63).

The *C. maculata* extract ameliorated increased DAF and DHE fluorescence in STZ (Fig. 60) and PA (Fig. 61) exposed RIN-5F cells. NAC ameliorated both DAF and DHE increases in fluorescence in STZ exposed cells (Fig. 60), as well as increases in DHE induced by PA (Fig. 61) and MS (Fig. 63). Mangiferin had no measurable effect on either DAF or DHE fluorescence (Fig. 60-63).
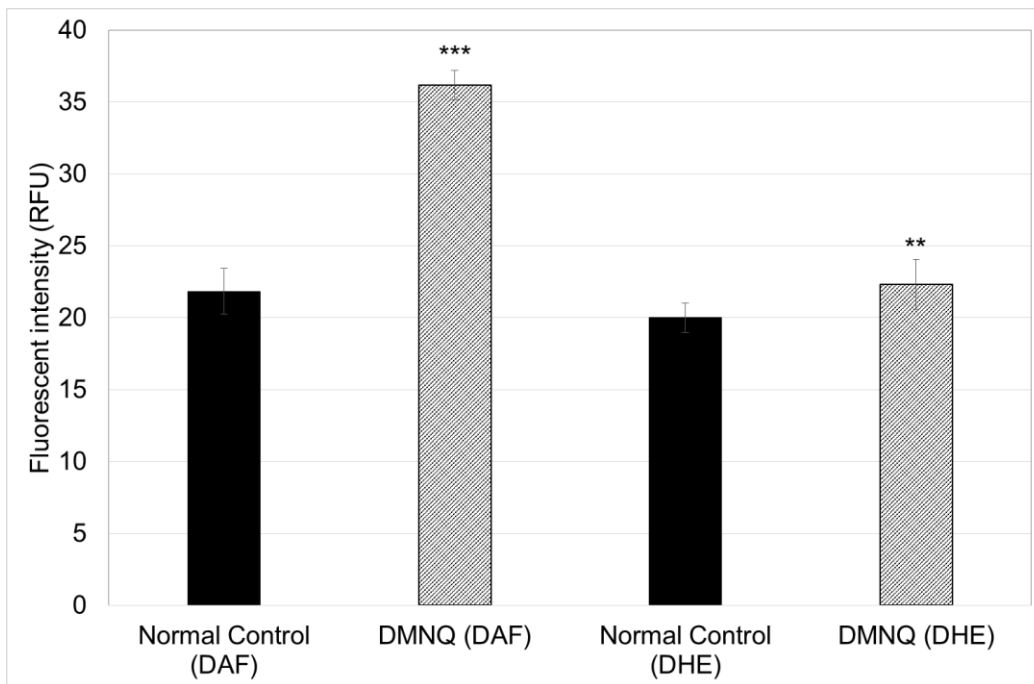
Figure 59. The effect of DMNQ on DAF and DHE fluorescent intensity in RIN-5F cells over one hour.

DAF and DHE fluorescence was measured following 120 minute exposure to 100 µM DMNQ. Where ** = $p < 0.01$ and *** = $p < 0.001$ compared to the respective normal control.
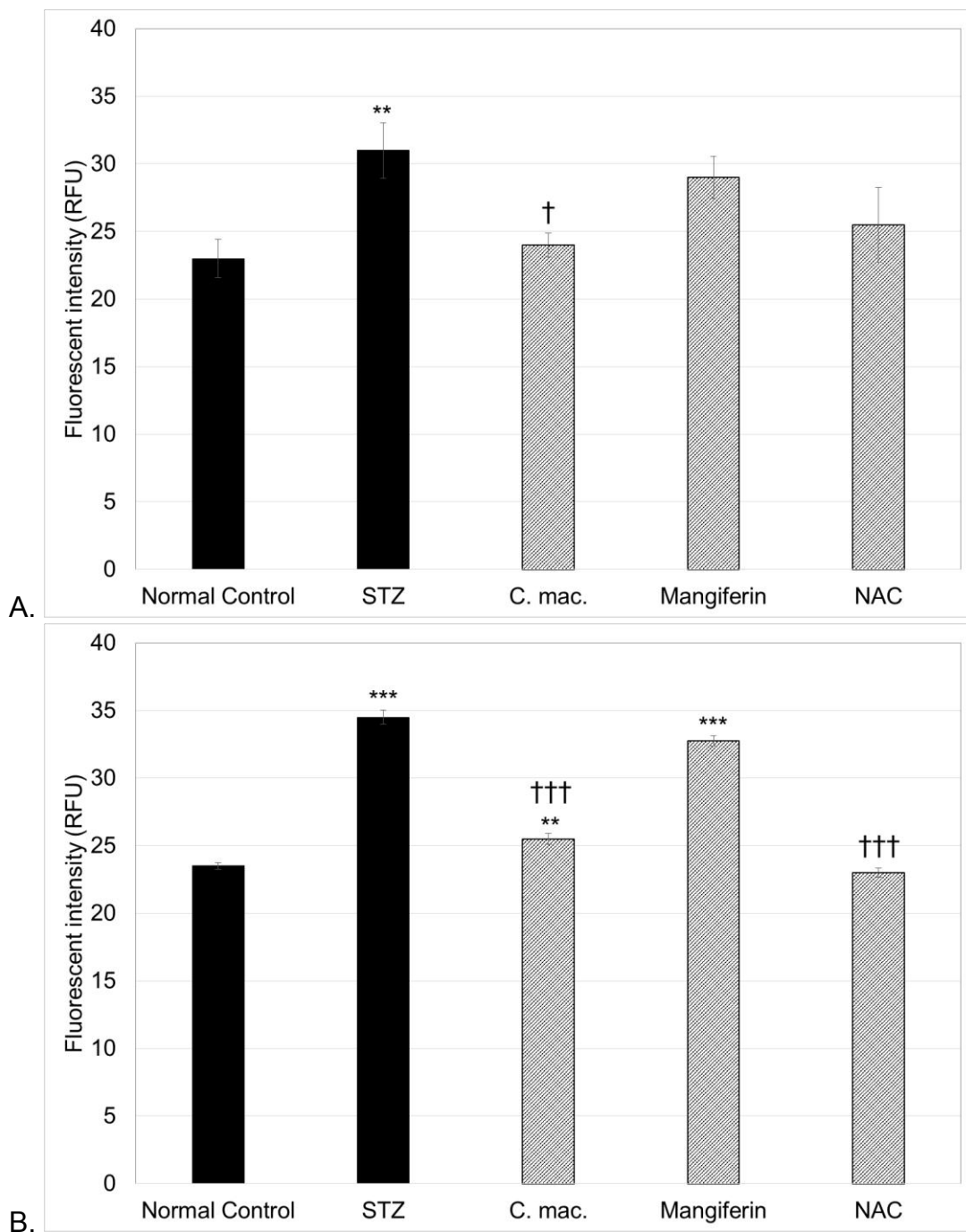
Figure 60. The effect of *C. maculata* extract (C. mac.), mangiferin and NAC on DAF (A) and DHE (B) fluorescence in RIN-5F cells exposed to STZ for 24 hours.

RIN-5F cells were first exposed to 10 mM STZ for 24 hours and then to 10 µg/mL extract, 100 µg/mL mangiferin and 0.01 mM NAC in fresh media for 24 hours. DAF and DHE fluorescence was then determined.

Where ** = $p < 0.01$ and *** = $p < 0.001$ compared to the normal control; and † = $p < 0.05$ and ††† = $p < 0.001$ compared to STZ.
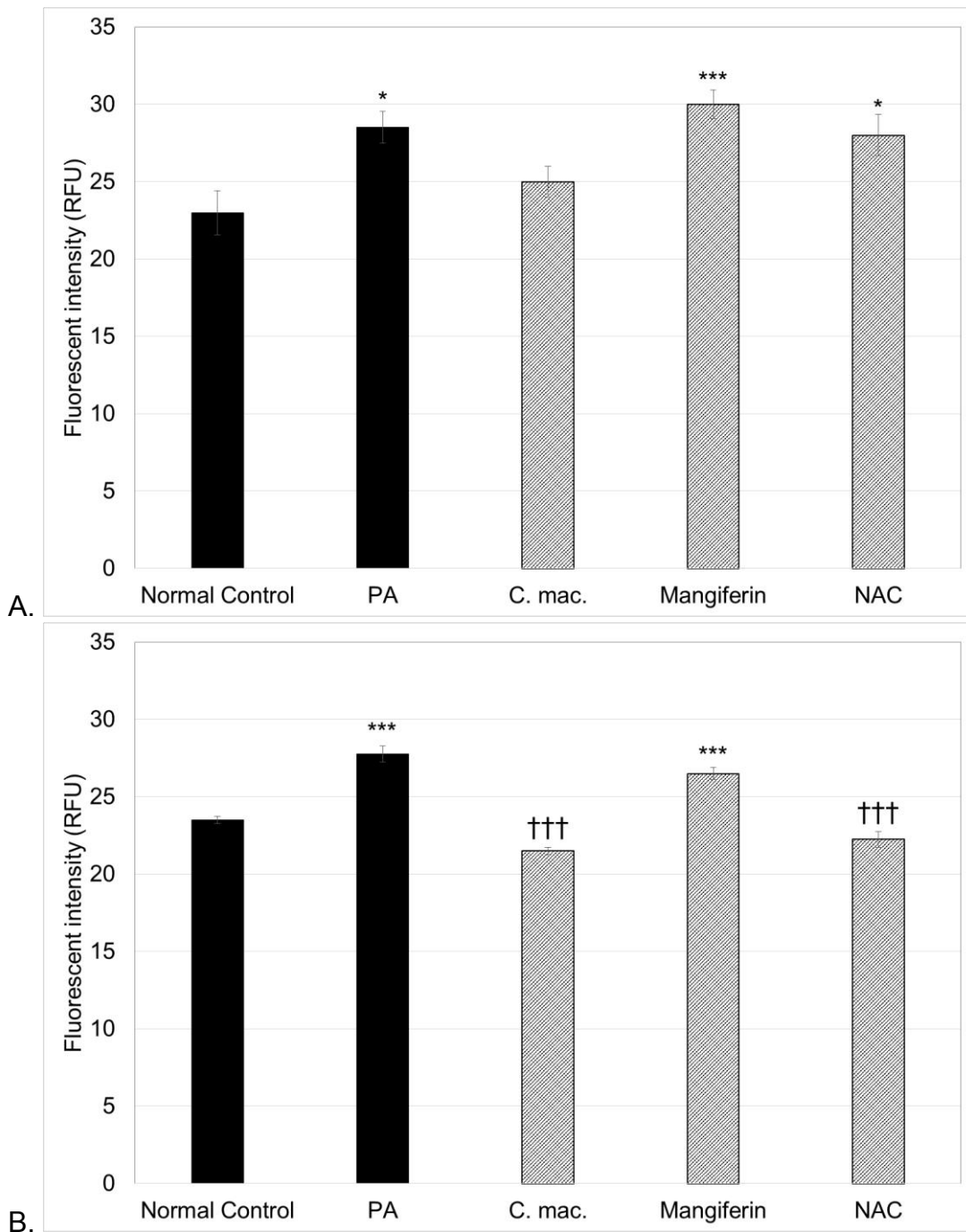
Figure 61. The effect of *C. maculata* extract (C. mac.), mangiferin and NAC on DAF (A) and DHE (B) fluorescence in RIN-5F cells exposed to PA for 24 hours.

RIN-5F cells were first exposed to 750 μM PA for 24 hours and then to 10 μg/mL extract, 100 μg/mL mangiferin and 0.01 mM NAC in fresh media for 24 hours. DAF and DHE fluorescence was then determined.

Where * = $p < 0.05$ and *** = $p < 0.001$ compared to the normal control; and ††† = $p < 0.001$ compared to PA.
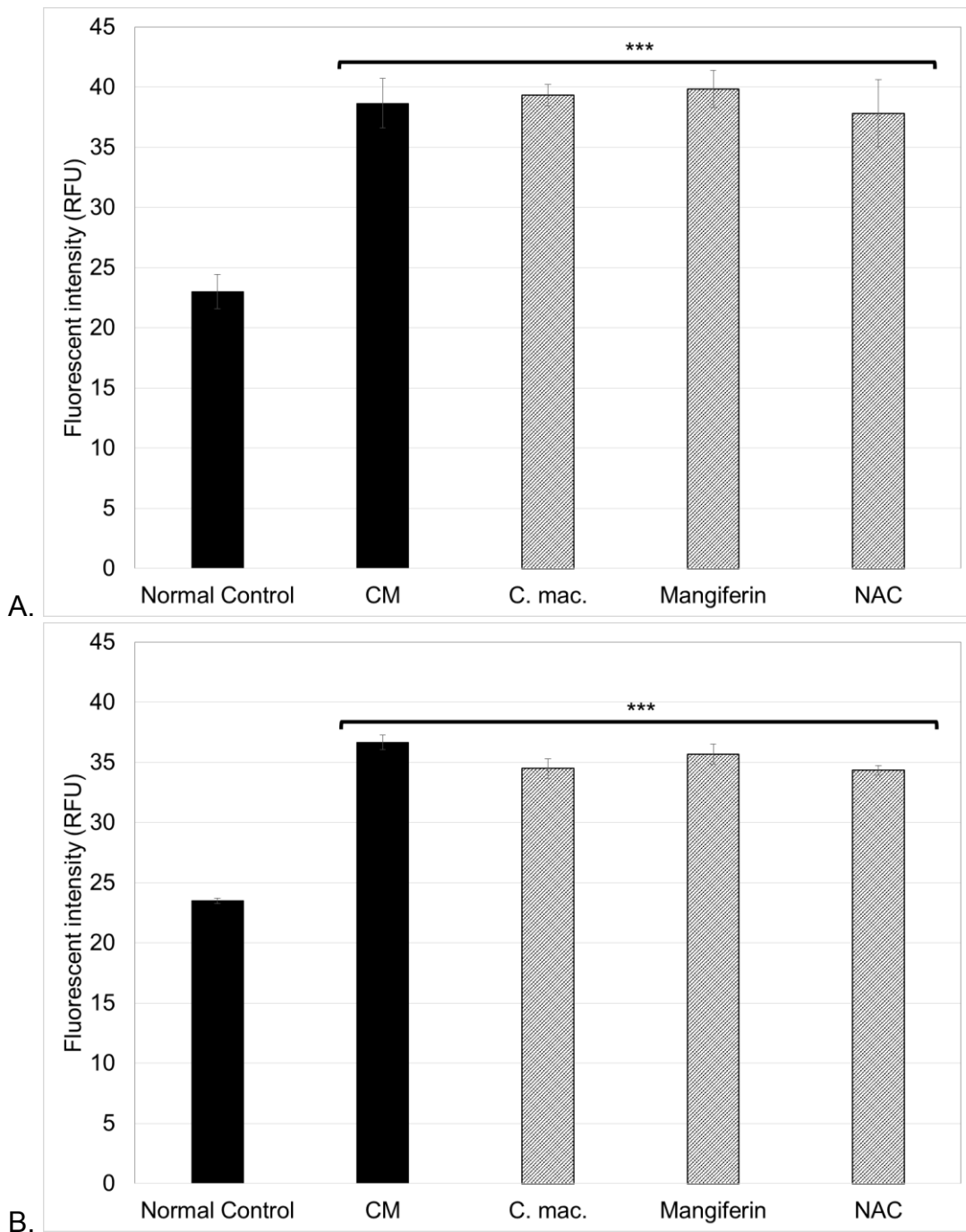
Figure 62. The effect of *C. maculata* extract (C. mac.), mangiferin and NAC on DAF (A) and DHE (B) fluorescence in RIN-5F cells exposed to CM for 24 hours.

RIN-5F cells were first exposed to 1 ng/mL IFN-γ + 0.1 ng/mL IL-1β + 1.1 ng/mL TNF-α in combination for 24 hours and then to 10 µg/mL extract, 100 µg/mL mangiferin and 0.01 mM NAC in fresh media for 24 hours. DAF and DHE fluorescence was then determined. Where *** = $p < 0.001$ compared to the normal control.
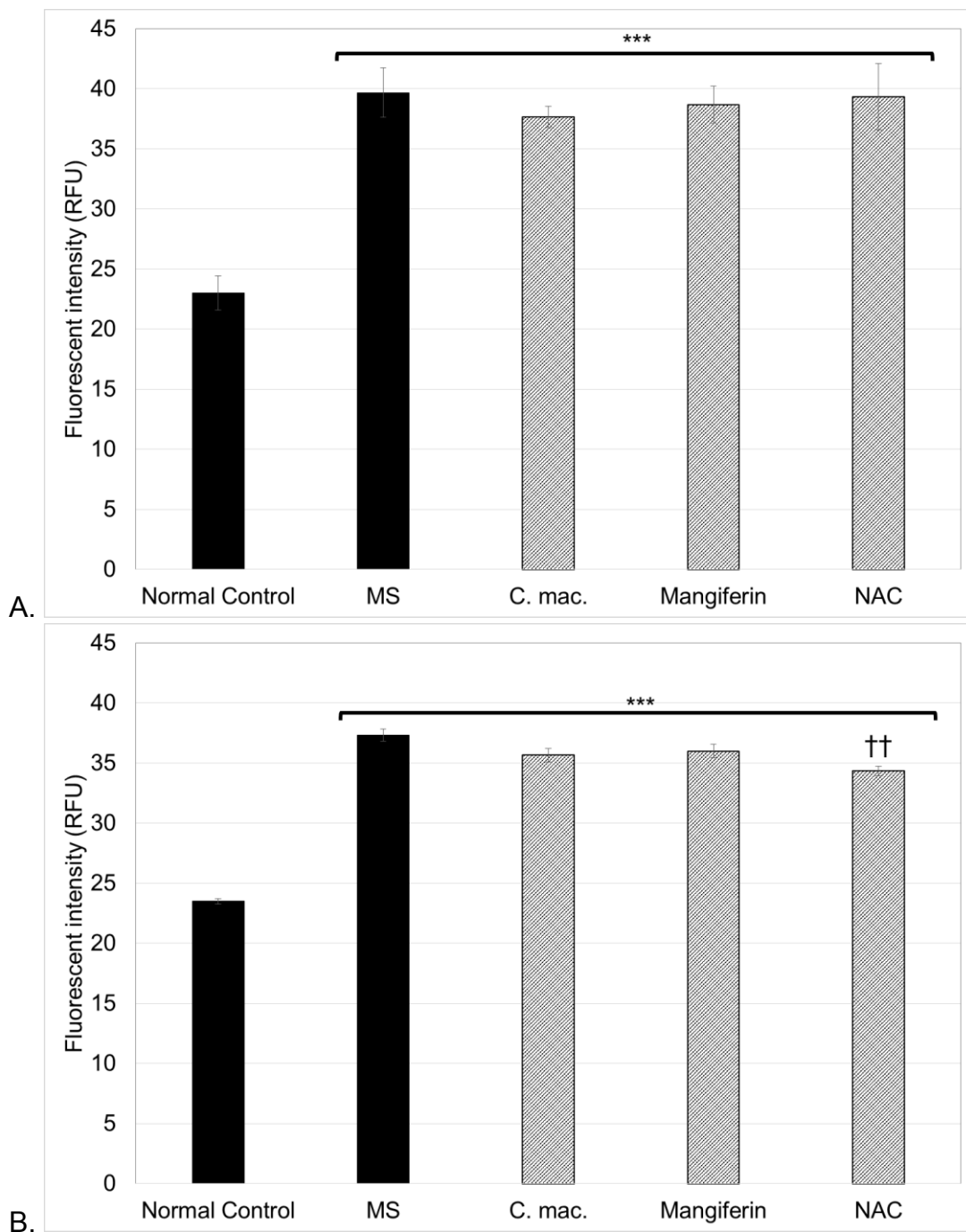
Figure 63. The effect of *C. maculata* extract (C. mac.), mangiferin and NAC on DAF (A) and DHE (B) fluorescence in RIN-5F cells exposed to MS for 24 hours.

RIN-5F cells were first exposed to 75 µM PA + 1 mM STZ + 0.1 ng/mL IFN-γ + 0.01 ng/mL IL-1β + 0.11 ng/mL TNF-α in combination for 24 hours and then to 10 µg/mL extract, 100 µg/mL mangiferin and 0.01 mM NAC in fresh media for 24 hours. DAF and DHE fluorescence was then determined.

Where *** = $p < 0.001$ compared to the normal control; and †† = $p < 0.01$ compared to MS.

1.4.2. Superoxide dismutase enzyme activity

Superoxide dismutase activity was assessed as the percentage inhibition of superoxide radicals. Compared to the normal control, SOD activity was reduced following exposure to the STZ (20.46 % ± 0.29 vs. 9.26 % ± 2.19) (Fig. 64) and PA (20.46 % ± 0.29 vs. 7.65 % ± 3.07) (Fig. 65) controls. Both *C. maculata* extract and mangiferin increased the reduced SOD activity (16.45 % ± 0.90 and 17.74 % ± 0.55, respectively) (Fig. 64), while NAC was not observed to be effective. The extract, mangiferin and NAC failed to ameliorate the PA induced reduction of SOD activity (Fig. 65).

Compared to the normal control, the CM (20.46 % ± 0.29 vs. 12.58 % ± 0.97) and MS controls (20.46 % ± 0.29 vs. 2.00 % ± 0.41) reduced SOD activity (Fig. 66), which was not ameliorated by the extract or NAC. Mangiferin increased SOD activity in the RIN-5F cells compared to the MS control (8.32 % ± 1.88), albeit still significantly lower than the normal control (Fig. 67).

The extract and mangiferin ameliorated the STZ induced reduction in SOD activity (Fig. 64), with mangiferin showing some improvement in MS exposed cells (Fig. 67).
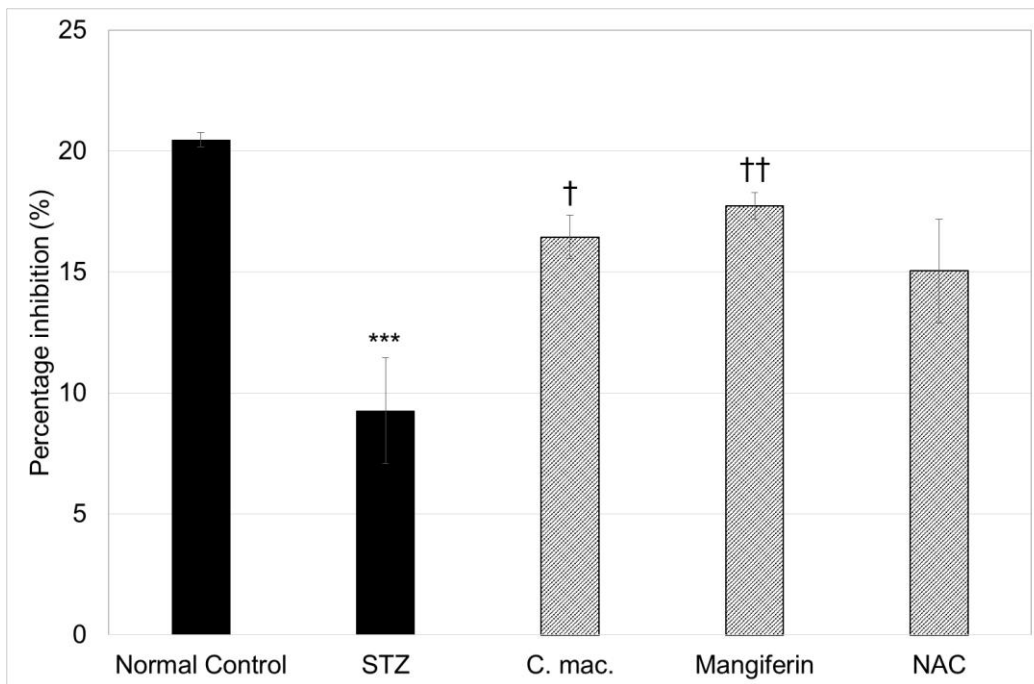
Figure 64. The effect of *C. maculata* extract (C. mac.), mangiferin and NAC on SOD activity in RIN-5F cells exposed to STZ for 24 hours.

SOD enzyme activity was measured in RIN-5F cells first exposed to 10 mM STZ for 24 hours and then to 10 µg/mL extract, 100 µg/mL mangiferin and 0.01 mM NAC in fresh media for 24 hours.

Where *** = $p < 0.001$ compared to the normal control; and † = $p < 0.05$ and †† = $p < 0.01$ compared to STZ.
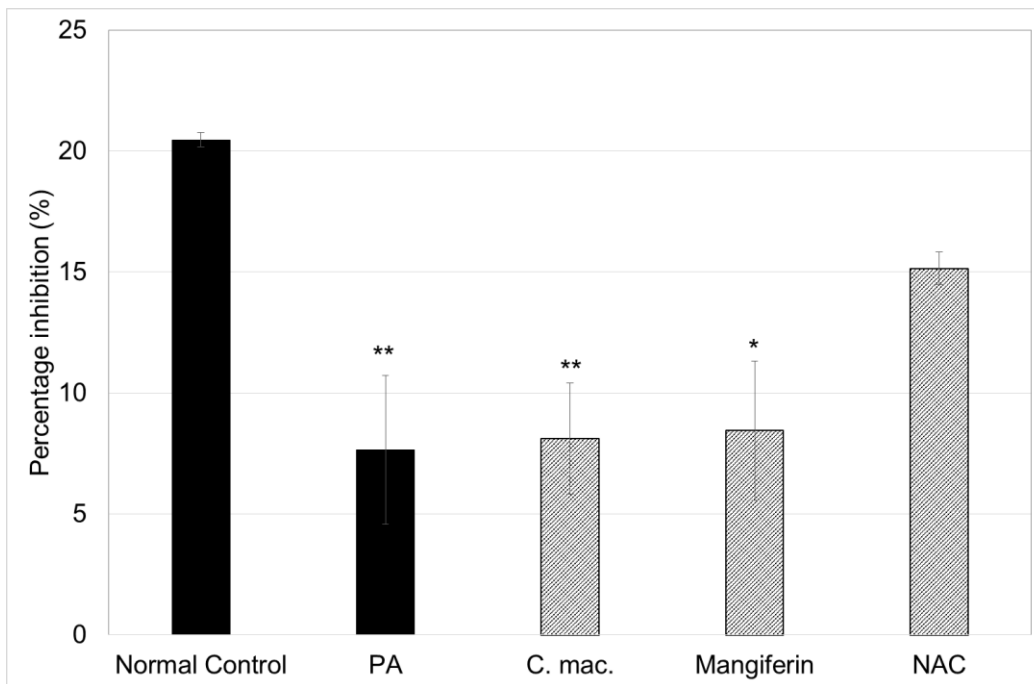
Figure 65. The effect of *C. maculata* extract (C. mac.), mangiferin and NAC on SOD activity in RIN-5F cells exposed to PA for 24 hours.

SOD enzyme activity was measured in RIN-5F cells first exposed to 750 µM PA for 24 hours and then to 10 µg/mL extract, 100 µg/mL mangiferin and 0.01 mM NAC in fresh media for 24 hours.

Where * = $p < 0.05$ and ** = $p < 0.01$ compared to the normal control.
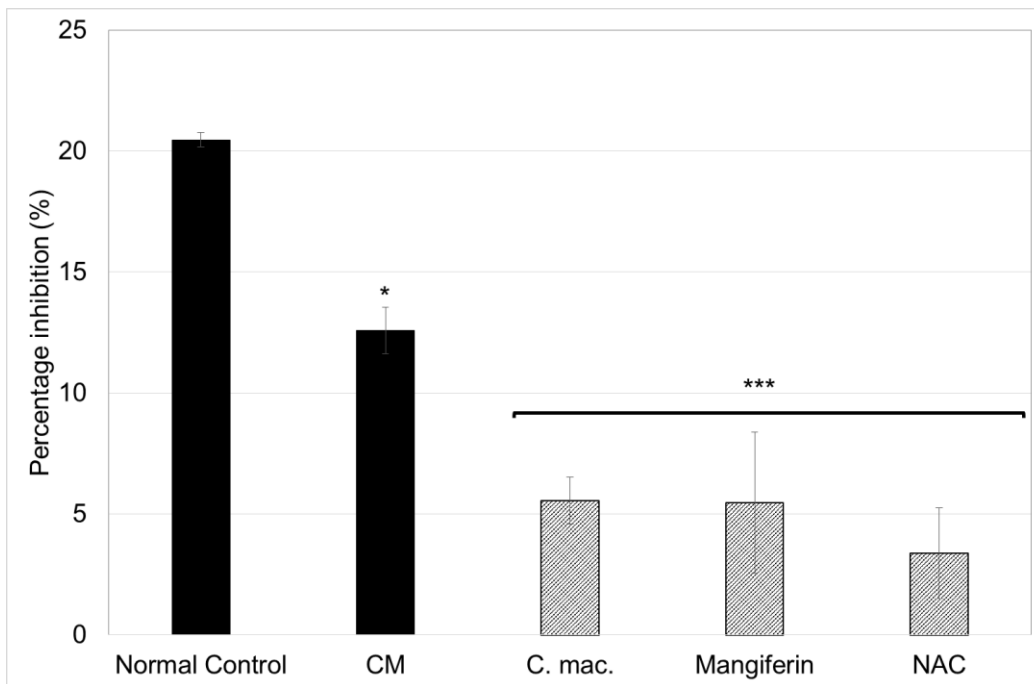
Figure 66. The effect of *C. maculata* extract (C. mac.), mangiferin and NAC on SOD activity in RIN-5F cells exposed to CM for 24 hours.

SOD enzyme activity was measured in RIN-5F cells first exposed to 1 ng/mL IFN-γ + 0.1 ng/mL IL-1β + 1.1 ng/mL TNF-α in combination for 24 hours and then to 10 µg/mL extract, 100 µg/mL mangiferin and 0.01 mM NAC in fresh media for 24 hours.

Where * = p < 0.05 and *** = p < 0.001 compared to the normal control.
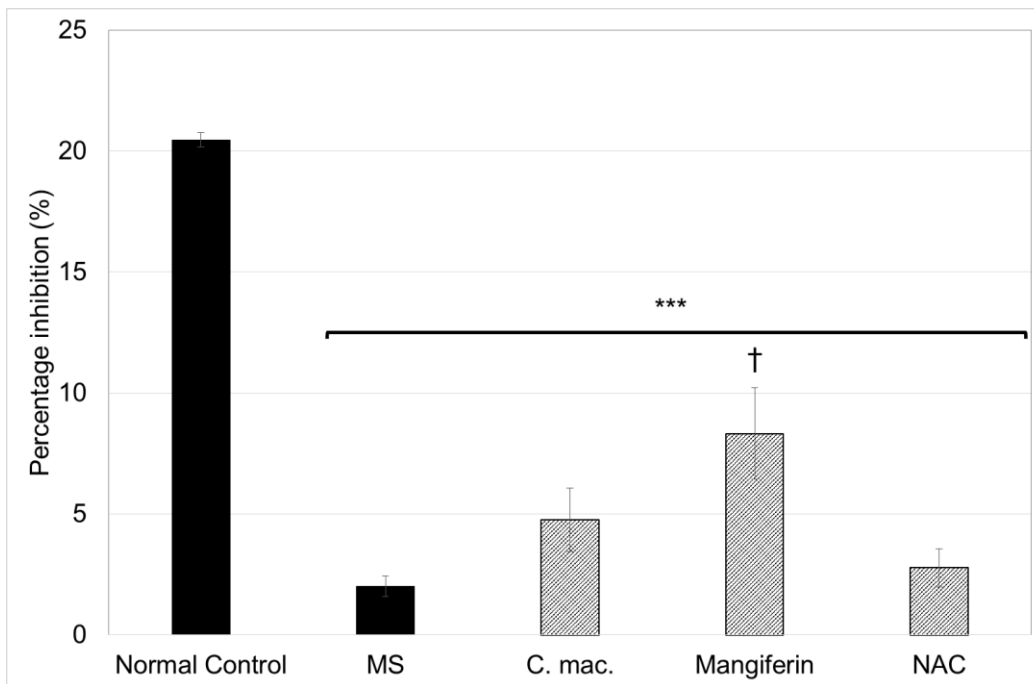
Figure 67. The effect of *C. maculata* extract (C. mac.), mangiferin and NAC on SOD activity in RIN-5F cells exposed to MS for 24 hours.

SOD enzyme activity was measured in RIN-5F cells first exposed to 75 μM PA + 1 mM STZ + 0.1 ng/mL IFN-γ + 0.01 ng/mL IL-1β + 0.11 ng/mL TNF-α in combination for 24 hours and then to 10 μg/mL extract, 100 μg/mL mangiferin and 0.01 mM NAC in fresh media for 24 hours.

Where *** = $p < 0.001$ compared to the normal control; and † = $p < 0.05$ compared to MS.

1.4.3. Summary of the effect of treatment *in vitro* on RIN-5F cell oxidative stress

As summarised in Table 6, the *C. maculata* extract improved all oxidative stress parameters tested in RIN-5F cells exposed to STZ; i.e. reduced RNS (DAF fluorescence) and ROS (DHE fluorescence), as well as increased SOD activity. Mangiferin also increased SOD activity in cells exposed to STZ, with NAC decreasing STZ associated ROS. Both the extract and NAC reduced PA induced ROS. Mangiferin increased SOD activity in MS exposed RIN-5F cells, with NAC reducing MS associated ROS.

Table 6. Summary of *in vitro* oxidative stress status.

		C. maculata	Mangiferin	NAC
STZ	DAF	↓	-	↓
	DHE	↓	-	↓
	SOD	↑	↑	-
PA	DAF	↓	-	-
	DHE	↓	-	↓
	SOD	-	-	-
CM	DAF	-	-	-
	DHE	-	-	-
	SOD	-	-	-
MS	DAF	-	-	-
	DHE	-	-	↓
	SOD	-	↑	-

1.5. Extract mitogenicity

To eliminate the potential mitogenic effect of the *C. maculata* extract on β-cells, its effect on RIN-5F cell proliferation was determined using tritiated thymidine incorporation and crystal violet assays. The response of these cells to known inducers of β-cell proliferation, i.e. high glucose concentration (25 mM) and the GLP-1 agonist, liraglutide, was first assessed in order to validate use of this assay. Compared to the normal control, high glucose (25 mM), as a positive control, increased tritiated thymidine incorporation into RIN-5F cells (813.85 fmol ± 66.55 vs. 1184.51 fmol ± 59.16), as did liraglutide, as a positive control, at concentrations of 1 nM, 10 nM and 1000 nM (813.85 fmol ± 66.55 vs.1142.91 fmol ± 16.30, 1170.31 fmol ± 27.99 and 1397.46 fmol ± 78.39, respectively) (Fig. 68).

At the concentrations tested, *C. maculata* extract was not seen to be mitogenic in RIN-5F cells, since proliferation was not increased compared to the normal control as measured by either crystal violet (Fig. 69 A) or tritiated thymidine (Fig. 69 B) incorporation. Compared to the normal control, the 100 μg/mL concentration in fact reduced RIN-5F cell proliferation in the crystal violet assay (100.00 % ± 2.27 vs. 72.64 % ± 1.31) (Fig. 69 A) as well as the tritiated thymidine assay (271.36 fmol ± 10.86 vs. 190.51 fmol ± 1.97) (Fig. 69 B).

158
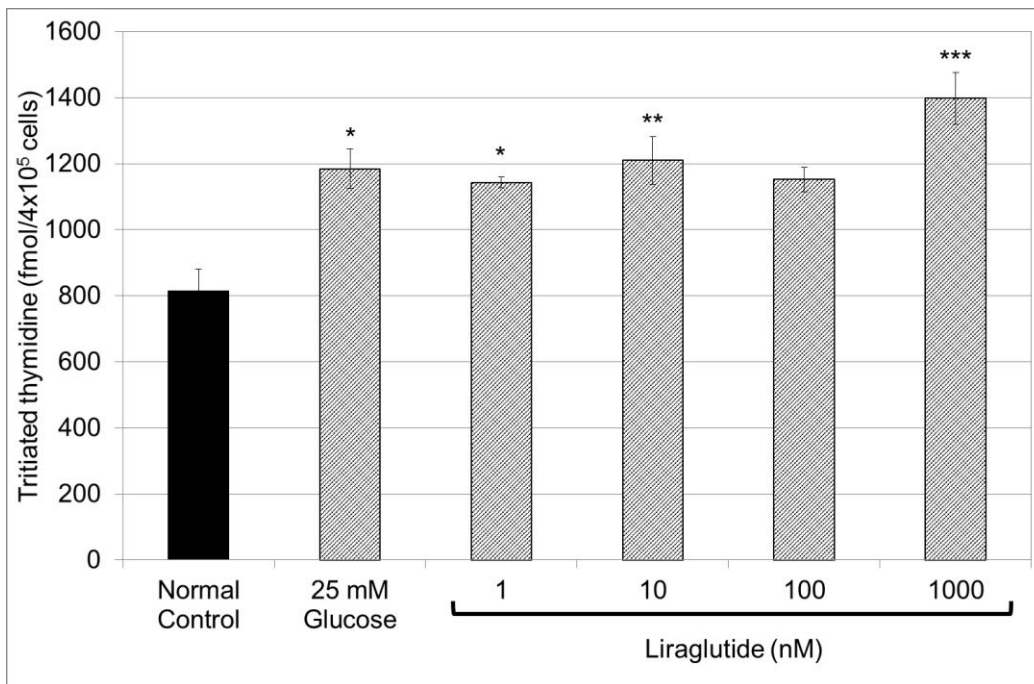
Figure 68. The effect of liraglutide and glucose stimulation on RIN-5F cell proliferation after 24 hours.

RIN-5F cells were exposed to 25 mM glucose and increasing concentrations of liraglutide for 24 hours, after which, cell proliferation was assessed using the tritiated thymidine assay. Where * = $p < 0.05$, ** = $p < 0.01$ and *** = $p < 0.001$ compared to the normal control.
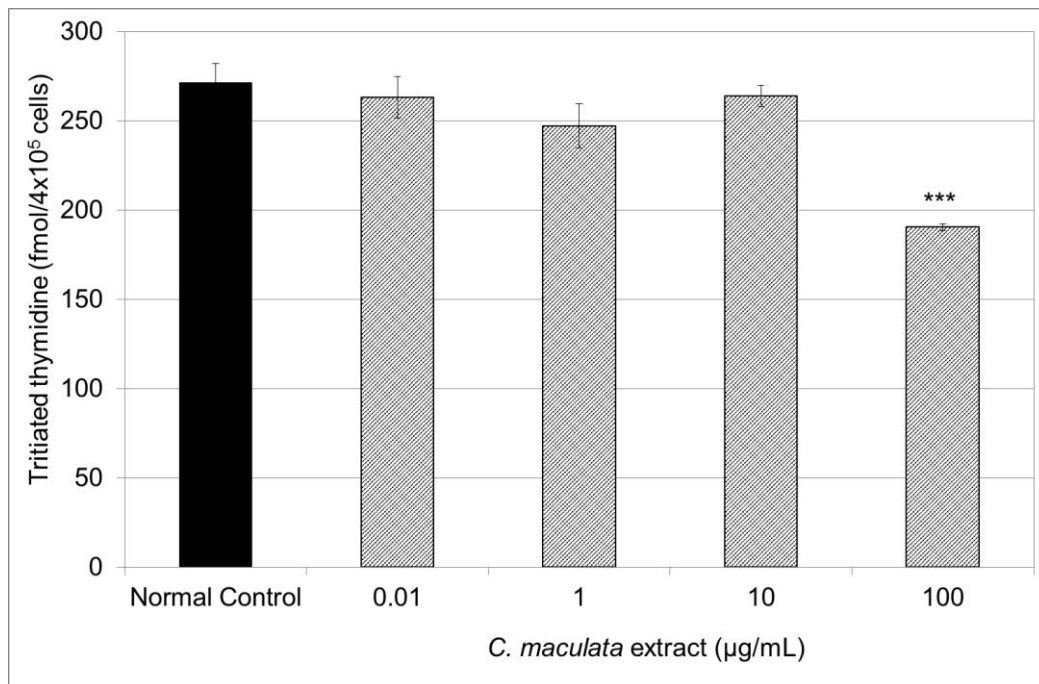
A.
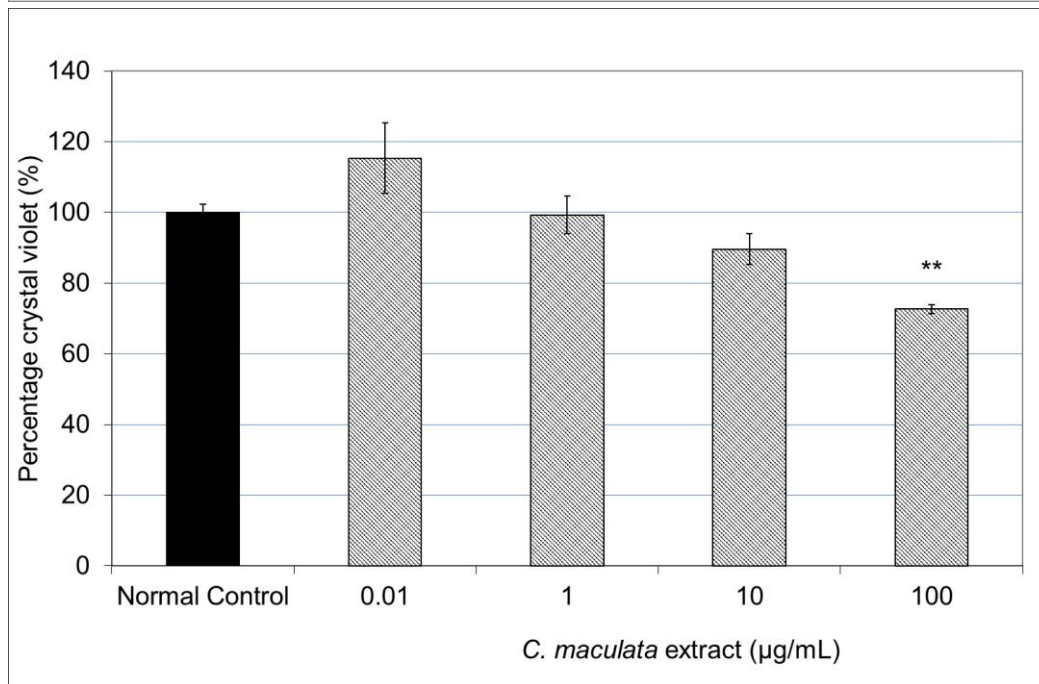
B.

Figure 69. The effect of C. maculata extract on RIN-5F cell proliferation after 24 hours as determined by tritiated thymidine incorporation (A) and crystal violet (B).

RIN-5F cell proliferation was assessed following exposure to increasing concentrations of extract using tritiated thymidine incorporation and crystal violet assays.

Where ** = $p < 0.01$ and *** = $p < 0.001$ compared to the normal control. (Data from Fig. 69 has been published in a peer-reviewed journal; see addendum 1).

1.6. Western blot analysis

Proteins involved in β-cell function and apoptosis were assessed using Western blot analysis in RIN-5F cells treated with the extract, mangiferin and NAC. Data are expressed as fold change compared to the normal control and normalised to the β-tubulin housekeeping protein. The *C. maculata* extract, mangiferin and NAC had no measurable effect on BCL-2 (Fig. 70), NF-κB (Fig. 71) or caspase-3 (Fig. 72) protein expression in RIN-5F cells first exposed to either STZ or PA for 24 hours. The *C. maculata* extract, mangiferin and NAC had no measurable effect on cleaved caspase-3 protein expression in RIN-5F cells first exposed to PA for 24 hours (Fig. 73 B). However, treatment of STZ exposed cells with NAC increased cleaved caspase-3 protein expression in RIN-5F cells compared to the STZ control (1.77 ± 0.36 vs. 0.35 ± 0.03) (Fig. 73 A).

RIN-5F cells exposed to the STZ control showed reduced PDX-1 protein expression compared to the normal control (1.00 ± 0.11 vs. 0.17 ± 0.02) with treatment with *C. maculata* extract, mangiferin and NAC failing to increase the expression (Fig. 74 A). Exposure of RIN-5F cells to PA increased PDX-1 expression, albeit not significantly. The *C. maculata* extract, mangiferin and NAC had no effect on the PA induced increase in PDX-1 expression (Fig. 74 B). The *C. maculata* extract, mangiferin and NAC had no measurable effect on GLUT-2 protein expression in RIN-5F cells first exposed to STZ for 24 hours (Fig. 75 A) however, NAC increased GLUT-2 expression in cells first exposed to PA compared to both the normal (2.69 ± 0.31 vs. 1.00 ± 0.21) and PA (2.69 ± 0.31 vs. 1.35 ± 0.18) controls (Fig. 75 B).

161
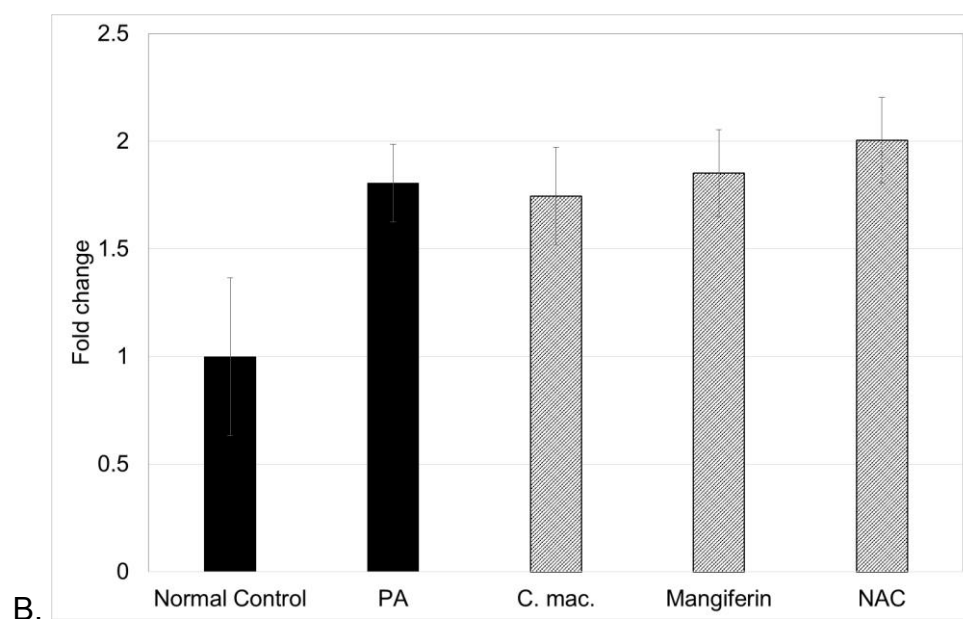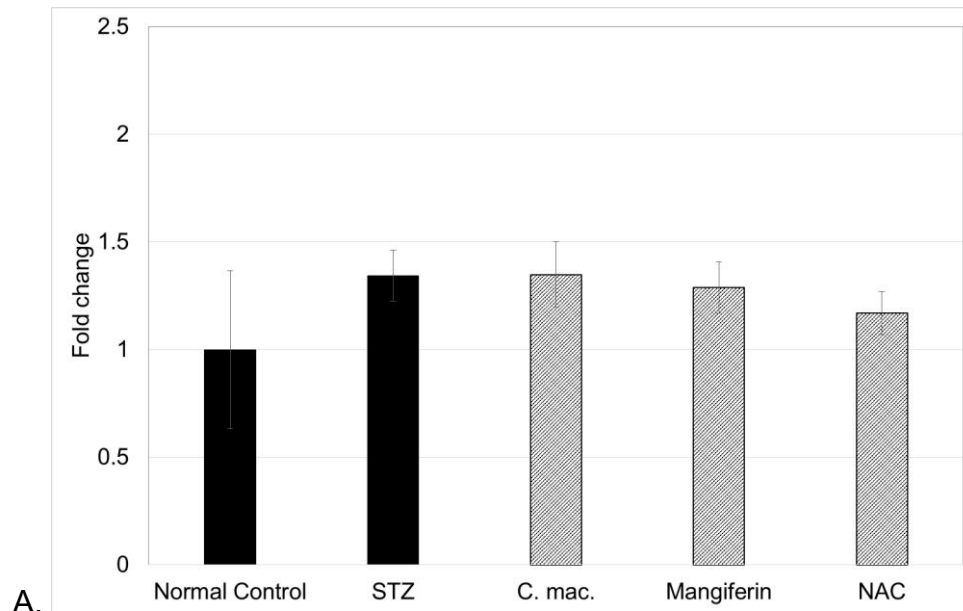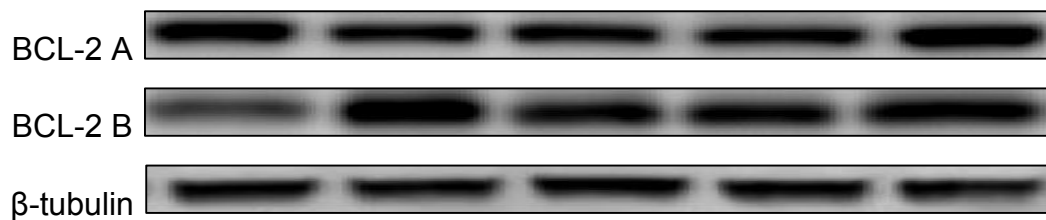
Figure 70. The effect of *C. maculata* extract (C. mac.), mangiferin and NAC on BCL-2 protein expression in RIN-5F cells exposed to STZ (A) and (PA) for 24 hours.

BCL-2 protein expression was assessed by Western blot analysis in RIN-5F cells first exposed to 10 mM STZ or 750 μM PA for 24 hours and then to 10 μg/mL extract, 100 μg/mL mangiferin and 0.01 mM NAC in fresh media for 24 hours. The representative results are shown in the Western blot images above.
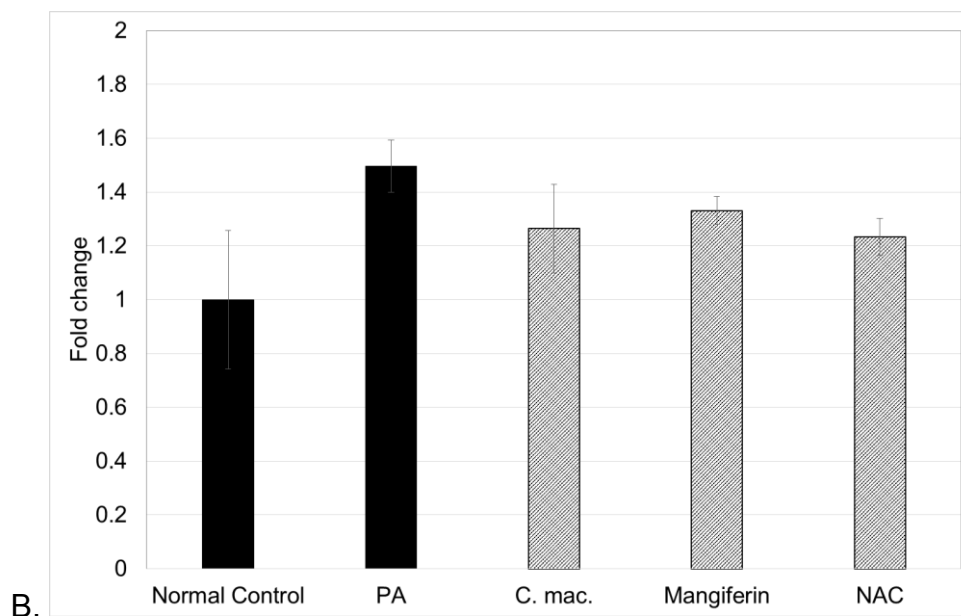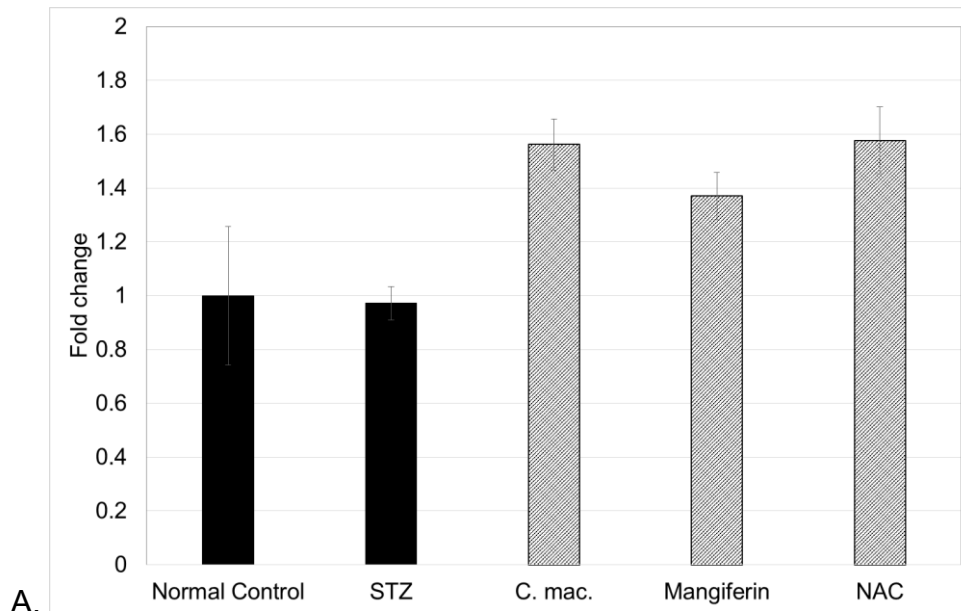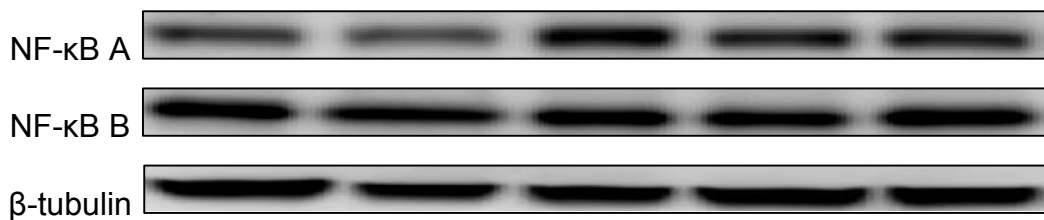
Figure 71. The effect of *C. maculata* extract (C. mac.), mangiferin and NAC on NF-κB protein expression in RIN-5F cells exposed to STZ (A) or PA (B) for 24 hours.

NF-κB protein expression was assessed by Western blot analysis in RIN-5F cells first exposed to 10 mM STZ or 750 µM PA for 24 hours and then to 10 µg/mL extract, 100 µg/mL mangiferin and 0.01 mM NAC in fresh media for 24 hours. The representative results are shown in the Western blot images above.

Caspase-3 A

Caspase-3 B

β-tubulin

A.

B.
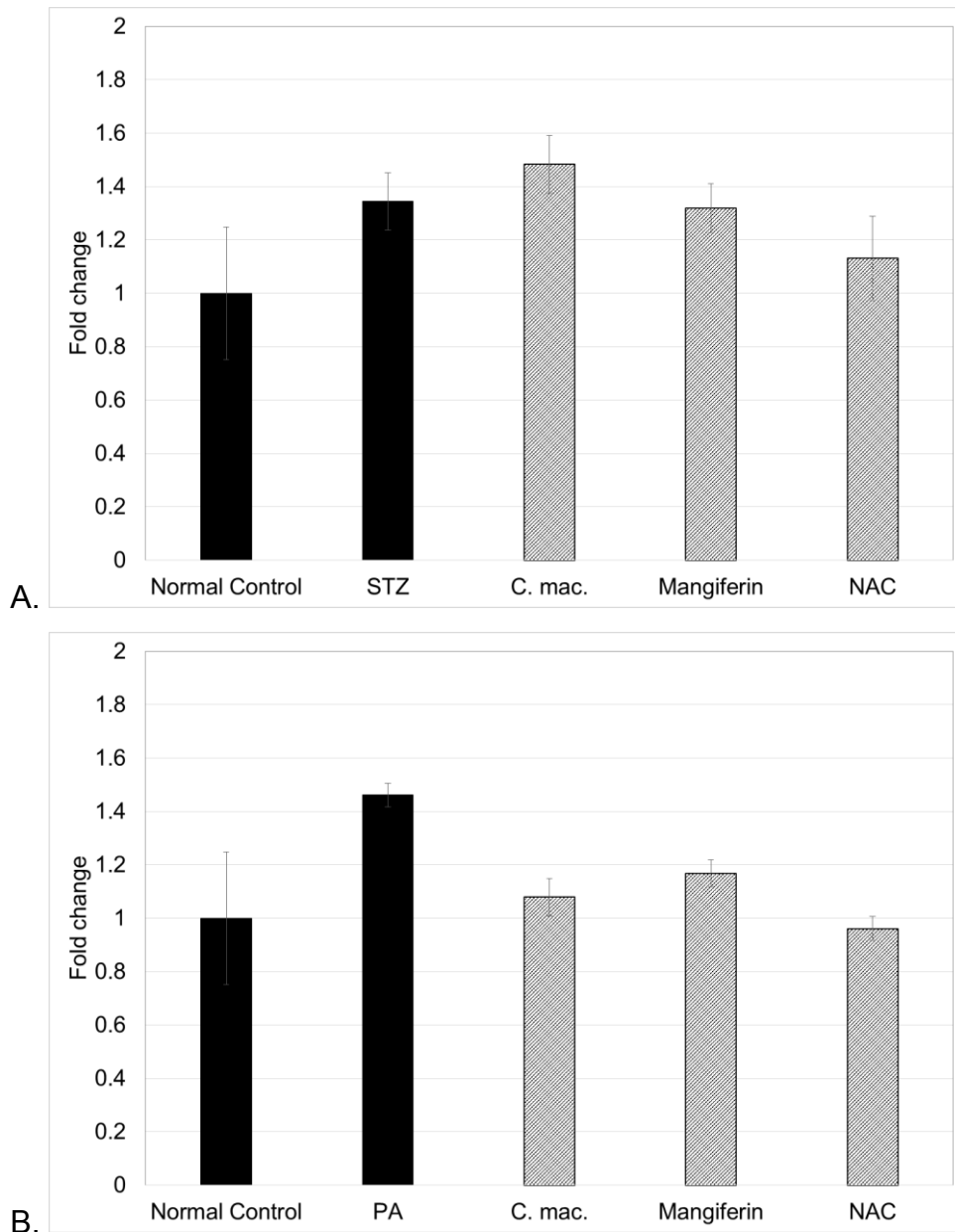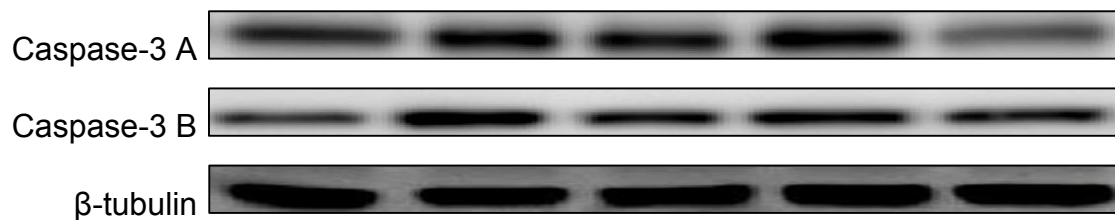
Figure 72. The effect of *C. maculata* extract (C. mac.), mangiferin and NAC on caspase-3 protein expression in RIN-5F cells exposed to STZ (A) or PA (B) for 24 hours.

Caspase-3 protein expression was assessed by Western blot analysis in RIN-5F cells first exposed to 10 mM STZ or 750 µM PA for 24 hours and then to 10 µg/mL extract, 100 µg/mL mangiferin and 0.01 mM NAC in fresh media for 24 hours. The representative results are shown in the Western blot images above.

164
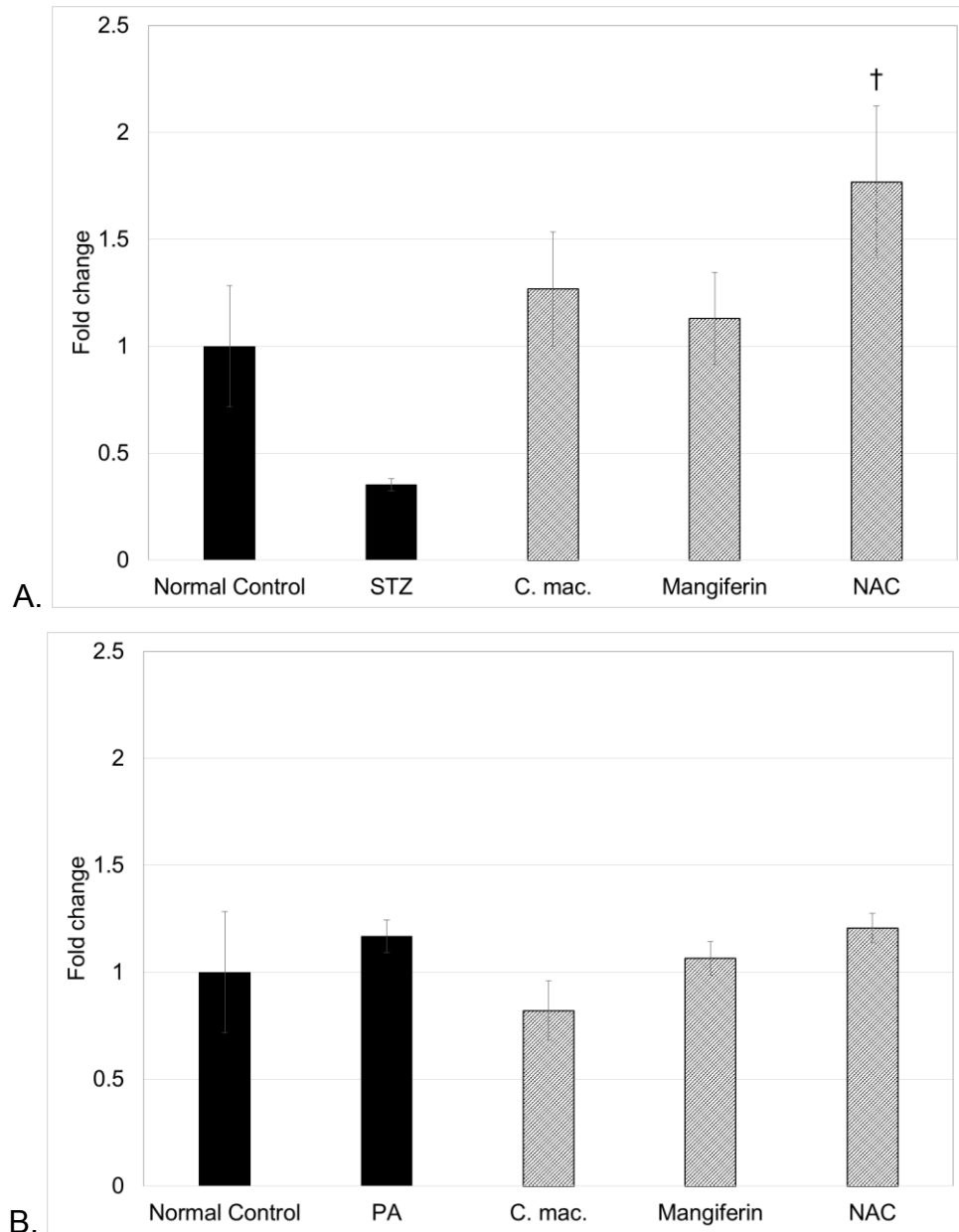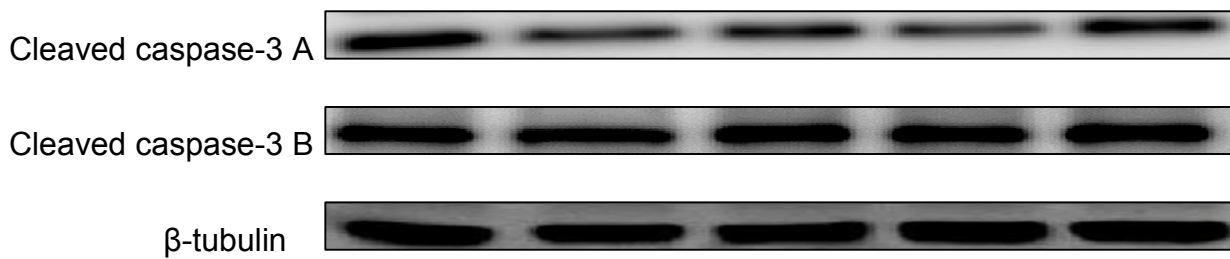
Figure 73. The effect of *C. maculata* extract (C. mac.), mangiferin and NAC on cleaved caspase-3 expression in RIN-5F cells exposed to STZ (A) or PA (B) for 24 hours.

Cleaved caspase-3 protein expression was assessed by Western blot analysis in RIN-5F cells first exposed to 10 mM STZ or 750 µM PA for 24 hours and then to 10 µg/mL extract, 100 µg/mL mangiferin and 0.01 mM NAC in fresh media for 24 hours. The representative results are shown in the Western blot images above. Where † = $p < 0.05$ compared to PA.

PDX-1 A

PDX-1 B

β-tubulin
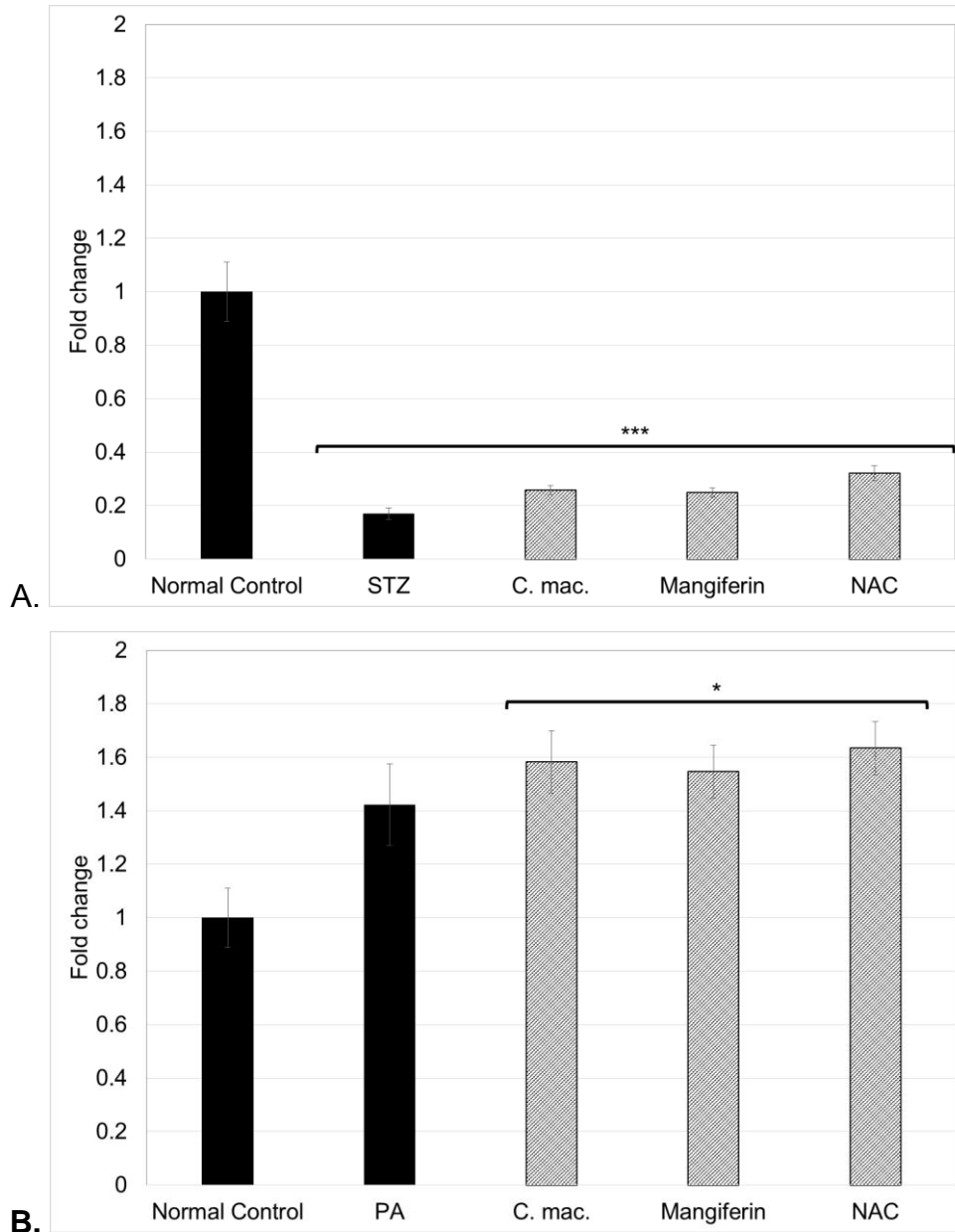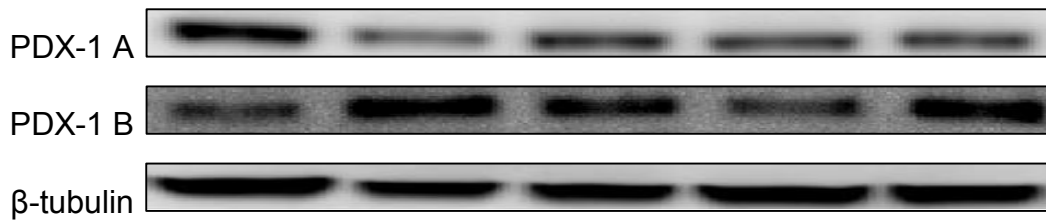
Figure 74. The effect of *C. maculata* extract (C. mac.), mangiferin and NAC on PDX-1 protein expression in RIN-5F cells exposed to STZ (A) and PA (B) for 24 hours.

PDX-1 protein expression was assessed by Western blot analysis in RIN-5F cells first exposed to 10 mM STZ or 750 µM PA for 24 hours and then to 10 µg/mL extract, 100 µg/mL mangiferin and 0.01 mM NAC in fresh media for 24 hours. The representative results are shown in the Western blot images above. Where * = $p < 0.05$ and *** = $p < 0.001$ compared to the normal control.
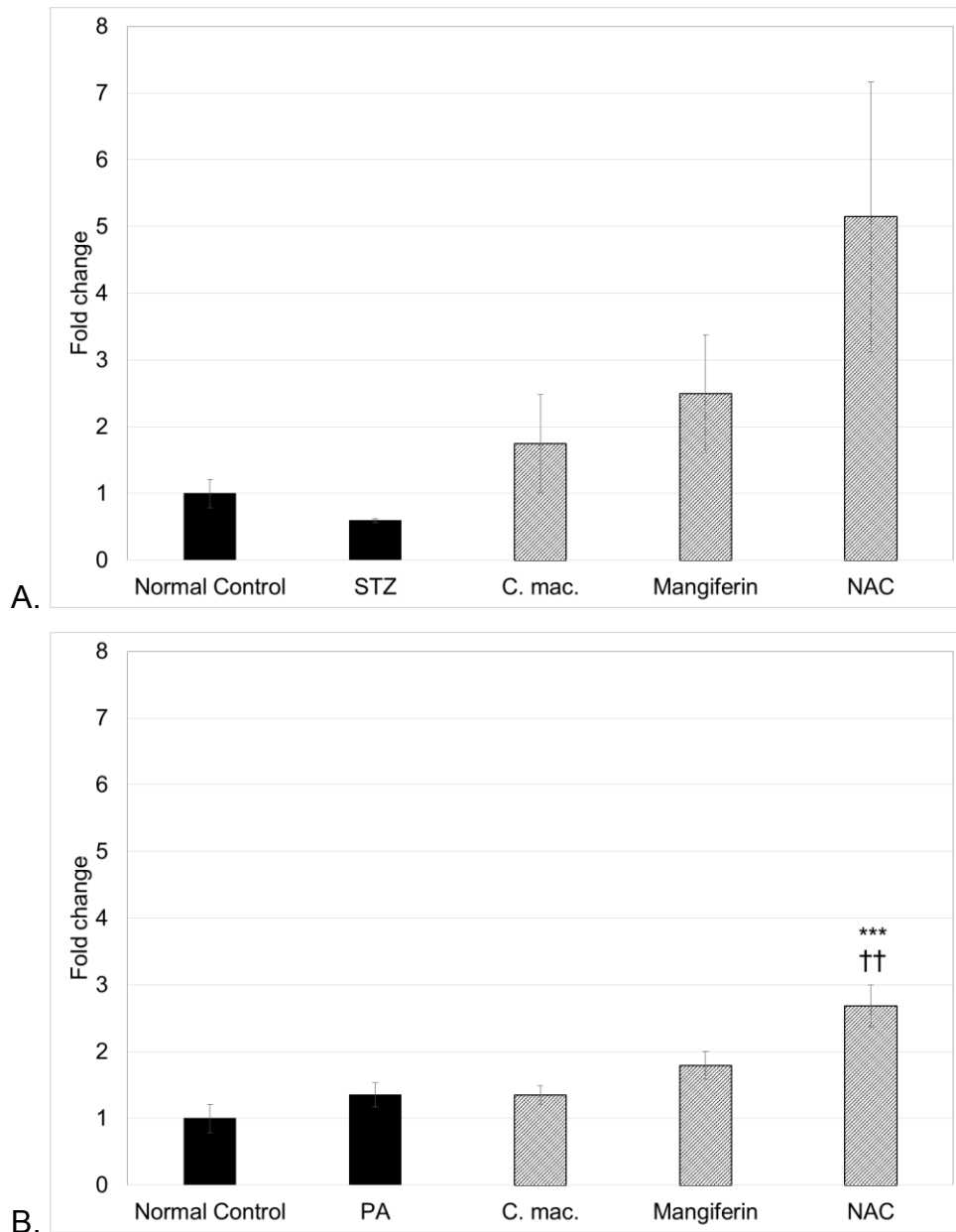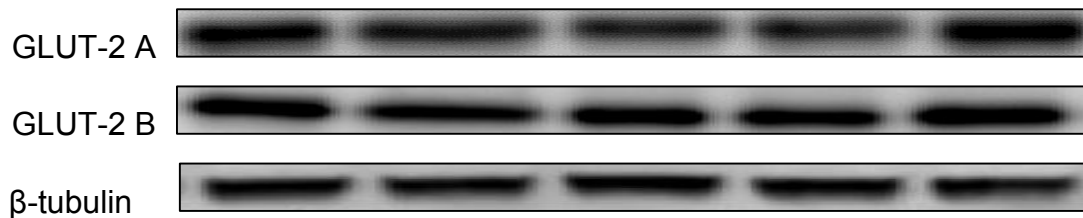
Figure 75. The effect of *C. maculata* extract (C. mac.), mangiferin and NAC on GLUT-2 protein expression in RIN-5F cells exposed to STZ (A) and PA (B) for 24 hours.

GLUT-2 protein expression was assessed by Western blot analysis in RIN-5F cells first exposed to 10 mM STZ or 750 μM PA for 24 hours and then to 10 μg/mL extract, 100 μg/mL mangiferin and 0.01 mM NAC in fresh media for 24 hours. The representative results are shown in the Western blot images above. Where *** = $p < 0.001$ compared to the normal control; and †† = $p < 0.01$ compared to PA.

2. *Ex vivo* results

The effects of the *C. maculata* extract, mangiferin and NAC observed in RIN-5F cells exposed to STZ and PA were then verified *ex vivo* in pancreatic islets isolated from adult Wistar rats. Islet cell viability was assessed using the annexin-V and propidium iodide fluorescent assay and cell function was assessed by measuring basal and glucose stimulated insulin secretion. The effect of the extract, mangiferin and NAC on islet oxidative status was determined by measuring DAF and DHE fluorescence, as well as SOD enzyme activity. For all *ex vivo* experimentation, data are expressed as the mean of three independent experiments, each with four replicates ± the standard errors of the mean. The normal controls refer to islets not exposed to stressors or treatments.

2.1. Cell viability – Annexin-V and propidium iodide fluorescence

Compared to the normal control, exposure of pancreatic islets isolated from adult Wistar rats to the STZ control for 24 hours increased propidium iodide fluorescence (42.25 RFU ± 0.20 vs. 48.00 RFU ± 0.33) (Fig. 76 B). The extract, mangiferin and NAC failed to ameliorate the STZ induced increase in propidium iodide fluorescence (Fig. 76 B). In this study, STZ did not affect annexin-V fluorescence in isolated islets (Fig. 76 A).

Exposure of isolated islets to the PA control for 24 hours increased both annexin-V (50.50 RFU ± 0.96 vs. 36.75 RFU ± 0.48) (Fig. 77 A) and propidium iodide (52.25 RFU ± 1.31 vs. 42.25 RFU ± 0.20) (Fig. 77 B) fluorescence compared to the normal control. Both *C. maculata* extract and NAC reduced the increased annexin-V fluorescence (42.50 RFU ± 1.50 and 42.00 RFU ± 0.58, respectively) (Fig. 77 A). Mangiferin failed to improve the PA induced increase in annexin-V and propidium iodide fluorescence (Fig. 77). The extract and NAC also failed to ameliorate the increase in propidium iodide induced by PA (Fig. 77 B).

The extract, mangiferin and NAC failed to ameliorate the increase in propidium iodide fluorescence induced by STZ (Fig. 76 B) and PA (Fig. 77 B), however, extract and NAC reduced increased annexin-V fluorescence induced by PA (Fig. 77 A).
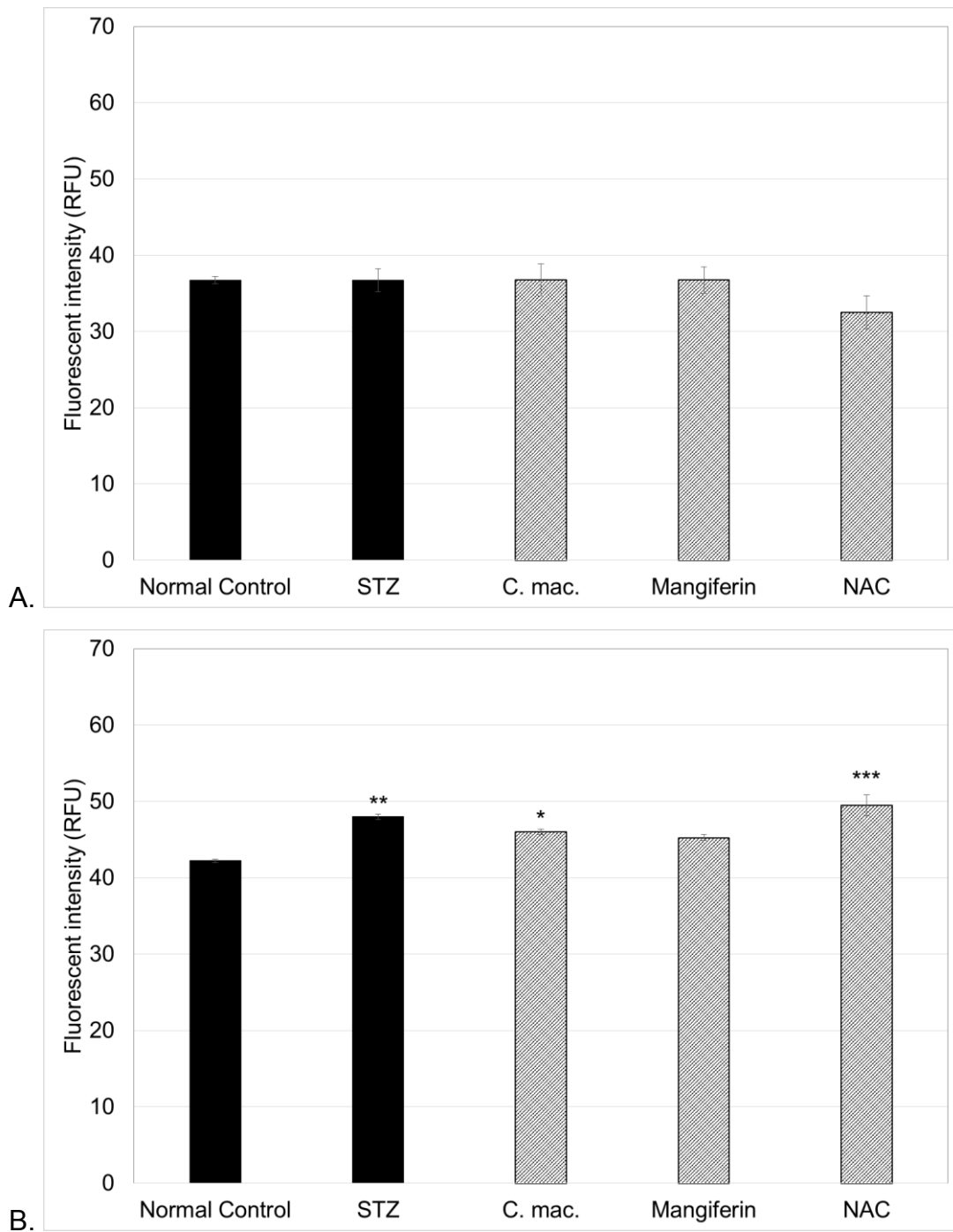
Figure 76. Annexin-V (A) and propidium iodide (B) fluorescence of pancreatic islets exposed to STZ and treated with *C. maculata* (C. mac.), mangiferin and NAC.

Isolated islets were first exposed to 10 mM STZ for 24 hours and then to 10 µg/mL extract, 100 µg/mL mangiferin and 0.01 mM NAC in fresh media for 24 hours. Cell viability was then assessed using the annexin-V and propidium iodide assay.

Where * = $p < 0.05$, ** = $p < 0.01$ and *** = $p < 0.001$ compared to the normal control.
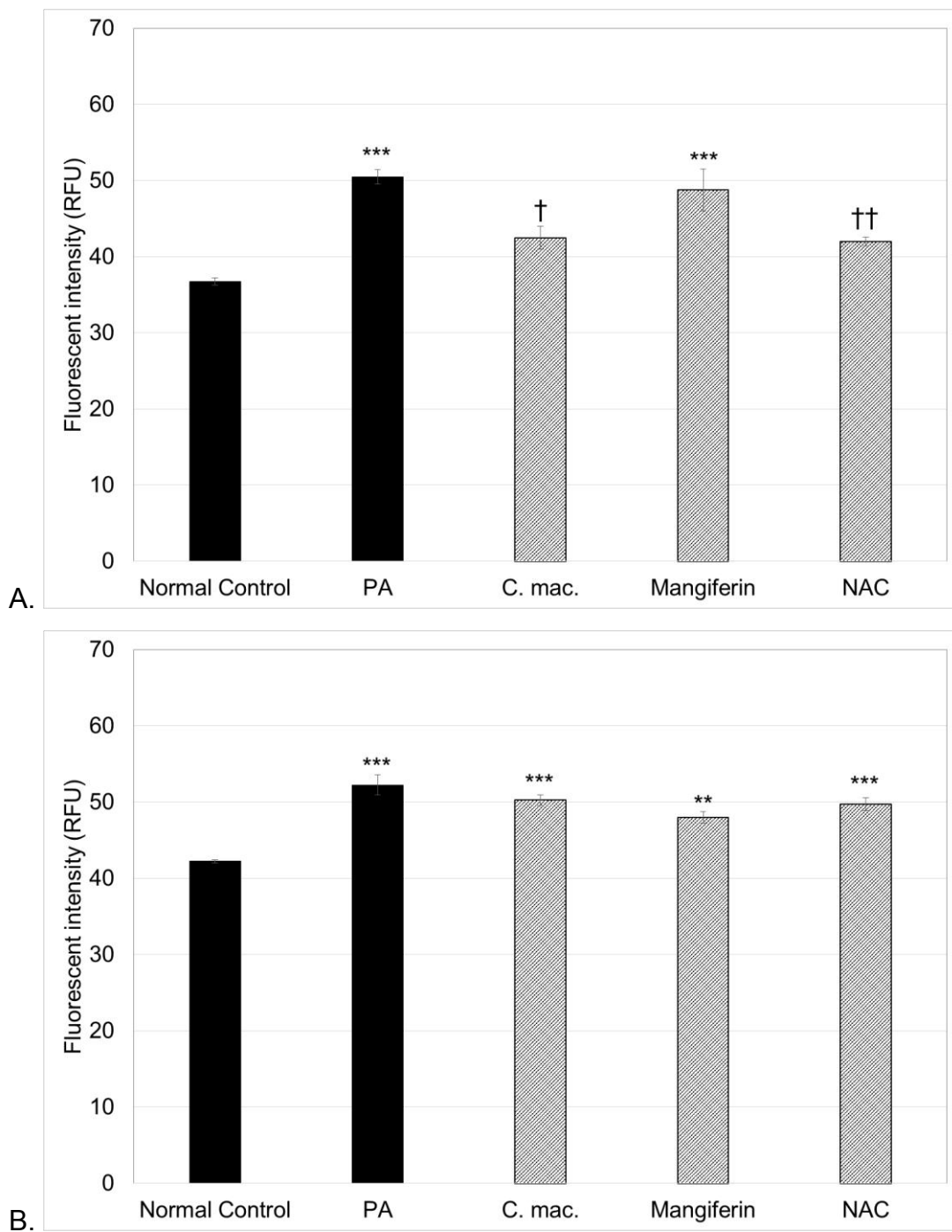
Figure 77. Annexin-V (A) and propidium iodide (B) fluorescence of pancreatic islets exposed to PA and treated with *C. maculata* (C. mac.), mangiferin and NAC.

Isolated islets were first exposed to 750 µM PA for 24 hours and then to 10 µg/mL extract, 100 µg/mL mangiferin and 0.01 mM NAC in fresh media for 24 hours. Cell viability was then assessed using the annexin-V and propidium iodide assay.

Where ** = $p < 0.01$ and *** = $p < 0.001$ compared to the normal control; and † = $p < 0.05$ and †† = $p < 0.01$ compared to PA.

2.2. Cell function – Insulin secretion

No changes in basal insulin secretion was observed in islets exposed to STZ (Fig. 78 A). Compared to the normal control, the STZ control increased glucose stimulated insulin secretion (5.96 ng/mL ± 0.40 vs. 9.36 ng/mL ± 0.21) (Fig. 78 B). The extract and mangiferin reduced the STZ induced increase in glucose stimulated insulin secretion (5.53 ng/mL ± 0.68 and 5.97 ng/mL ± 0.59, respectively), while NAC had no effect (Fig. 78 B).

Exposure to the PA control increased both basal (6.66 ng/mL ± 0.62 vs. 3.57 ng/mL ± 0.11) (Fig. 79 A) and glucose stimulated (9.94 ng/mL ± 0.46 vs. 5.96 ng/mL ± 0.40) (Fig. 79 B) insulin secretion from isolated islets compared to the normal control. The extract decreased glucose stimulated insulin secretion compared to the PA control (6.23 ng/mL ± 0.30) (Fig. 79 B).

The extract and mangiferin normalised glucose stimulated insulin secretion in STZ exposed islets (Fig. 78 B), while only the extract reduced the increase in glucose stimulated insulin secretion induced by PA (Fig. 79 B).

A.

B.
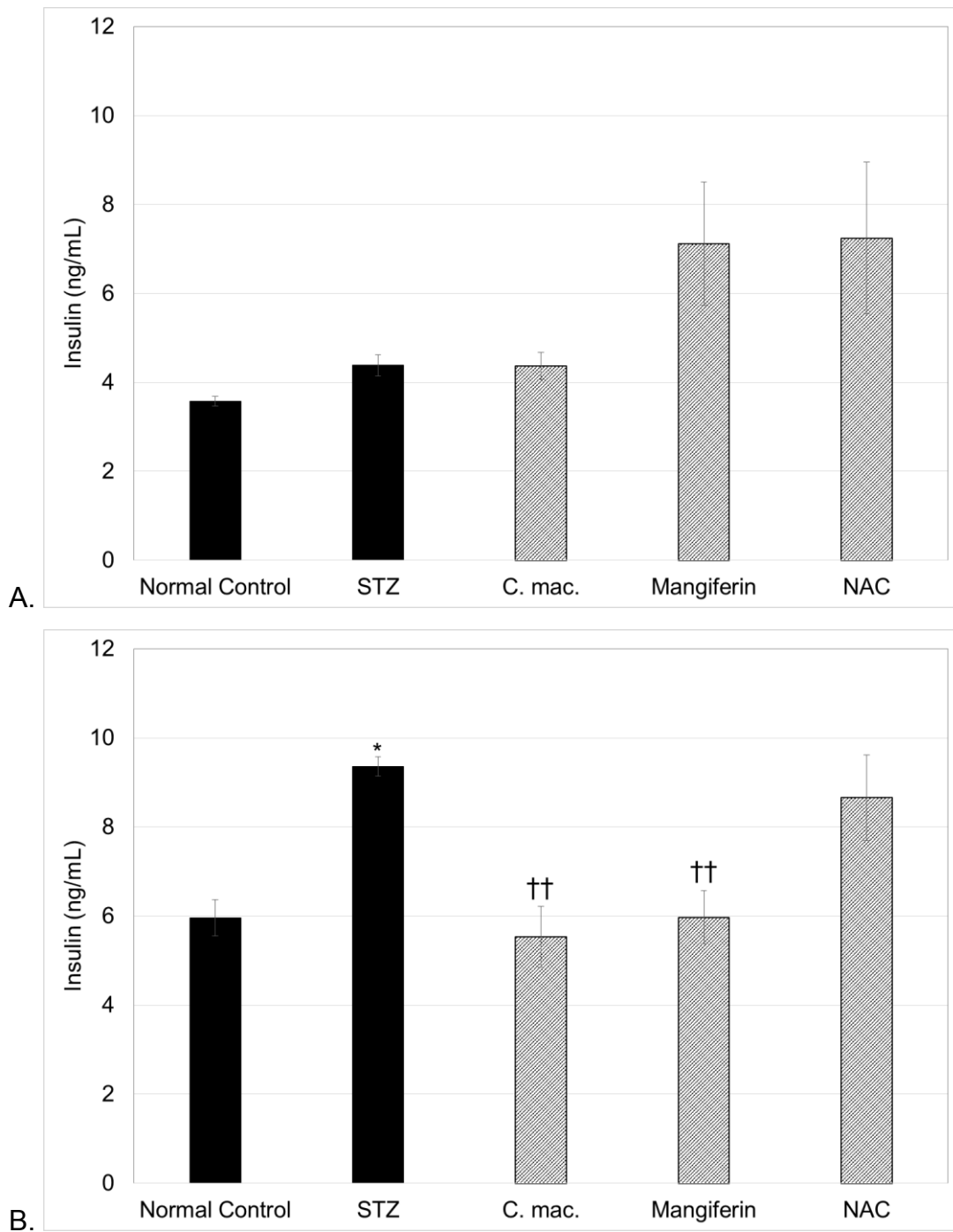
Figure 78. Basal (A) and glucose stimulated (B) insulin secretion of isolated islets exposed to STZ and treated with *C. maculata* (C. mac.), mangiferin and NAC.

Isolated islets were first exposed to 10 mM STZ for 24 hours and then to 10 µg/mL extract, 100 µg/mL mangiferin and 0.01 mM NAC in fresh media for 24 hours. Basal and glucose stimulated insulin secretion was then determined.

Where * = $p < 0.05$ compared to the normal control; and †† = $p < 0.01$ compared to STZ.
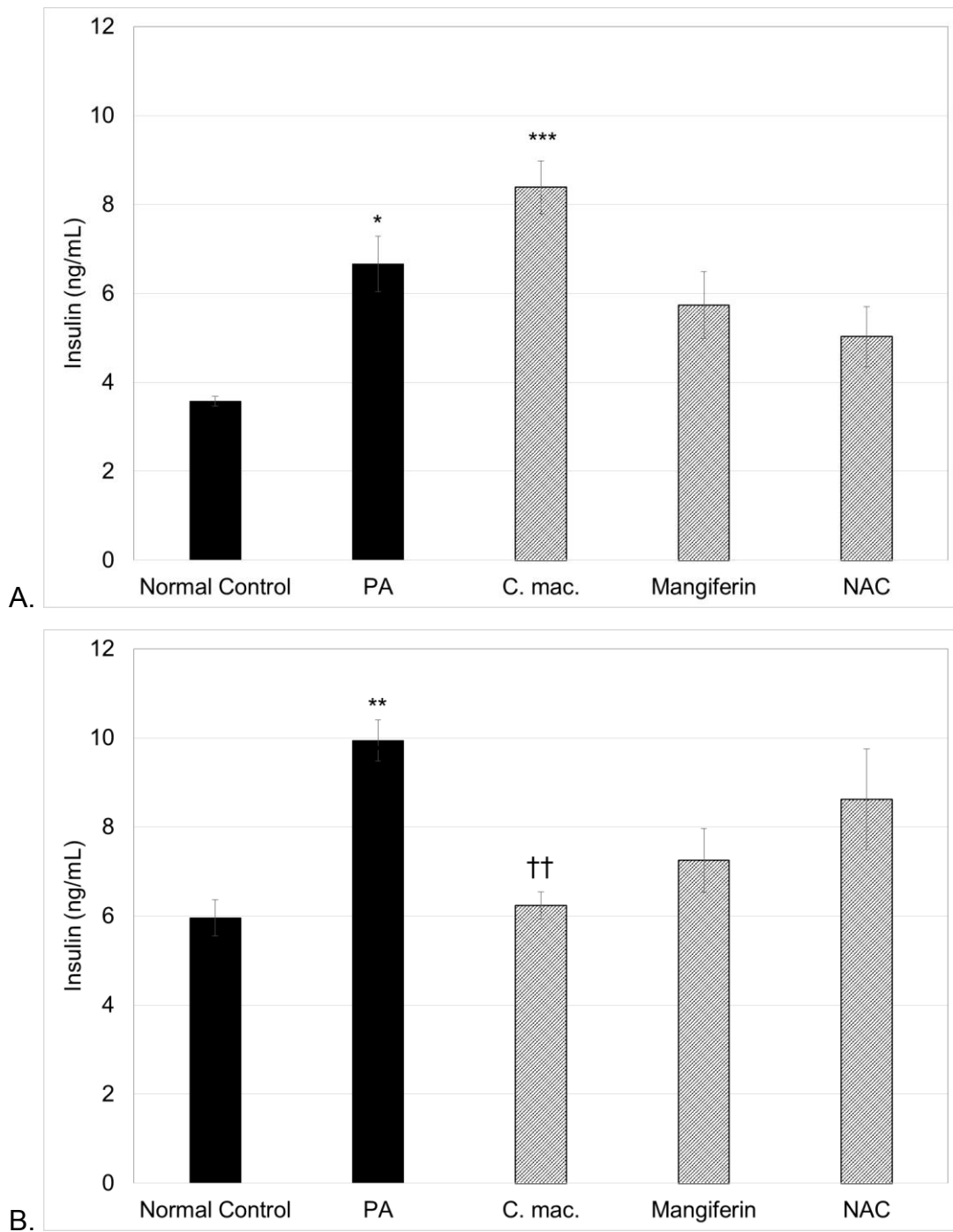
Figure 79. Basal (A) and glucose stimulated (B) insulin secretion of isolated islets exposed to STZ and treated with *C. maculata* (C. mac.), mangiferin and NAC.

Isolated islets were first exposed to 750 µM PA for 24 hours and then to 10 µg/mL extract, 100 µg/mL mangiferin and 0.01 mM NAC in fresh media for 24 hours. Basal and glucose stimulated insulin secretion was then determined.

Where * = $p < 0.05$, ** = $p < 0.01$ and *** = $p < 0.001$ compared to the normal control; and †† = $p < 0.01$ compared to PA.

2.3. Oxidative stress status

2.3.1. Diaminofluorescein-FM and dihydroethidium fluorescence

Compared to the normal control, exposure of isolated islets to the STZ control increased both DAF (508.25 RFU ± 3.84 vs. 569.00 RFU ± 7.87) (Fig. 80 A) and DHE fluorescence (122.00 RFU ± 0.58 vs. 134.75 RFU ± 0.70) (Fig. 80 B). Both *C. maculata* extract and NAC treatment reduced the increased DAF fluorescence (449.50 RFU ± 18.19 and 507.13 RFU ± 7.37, respectively) (Fig. 80 A), as well as DHE fluorescence (108.00 RFU ± 2.03 and 120.88 RFU ± 1.59, respectively) to levels below even that of the normal control (Fig. 80 B). Mangiferin did not ameliorate STZ induced increases in DAF nor DHE fluorescence (Fig. 80).

An increase in both DAF (456.00 RFU ± 7.84 vs. 502.50 RFU ± 7.41) (Fig. 81 A) and DHE (115.25 RFU ± 0.91 vs. 126.75 RFU ± 0.51) (Fig. 81 B) fluorescence compared to the normal control was observed following exposure of isolated islets to the PA control. All three treatments, namely *C. maculata* extract, mangiferin and NAC, reduced the increased DAF fluorescence (442.75 RFU ± 1.65, 475.00 RFU ± 5.43 and 458.88 RFU ± 3.29, respectively) (Fig. 81 A), as well as DHE fluorescence (110.50 RFU ± 1.03, 107.50 RFU ± 2.70 and 109.00 RFU ± 1.44, respectively) (Fig. 81 B).

The extract and NAC ameliorated STZ induced oxidative stress in rat islets as observed in reductions in both DAF (Fig. 80 A) and DHE (Fig. 80 B) fluorescence. All three treatments ameliorated PA induced oxidative stress in isolated islets (Fig. 81).

A.

B.
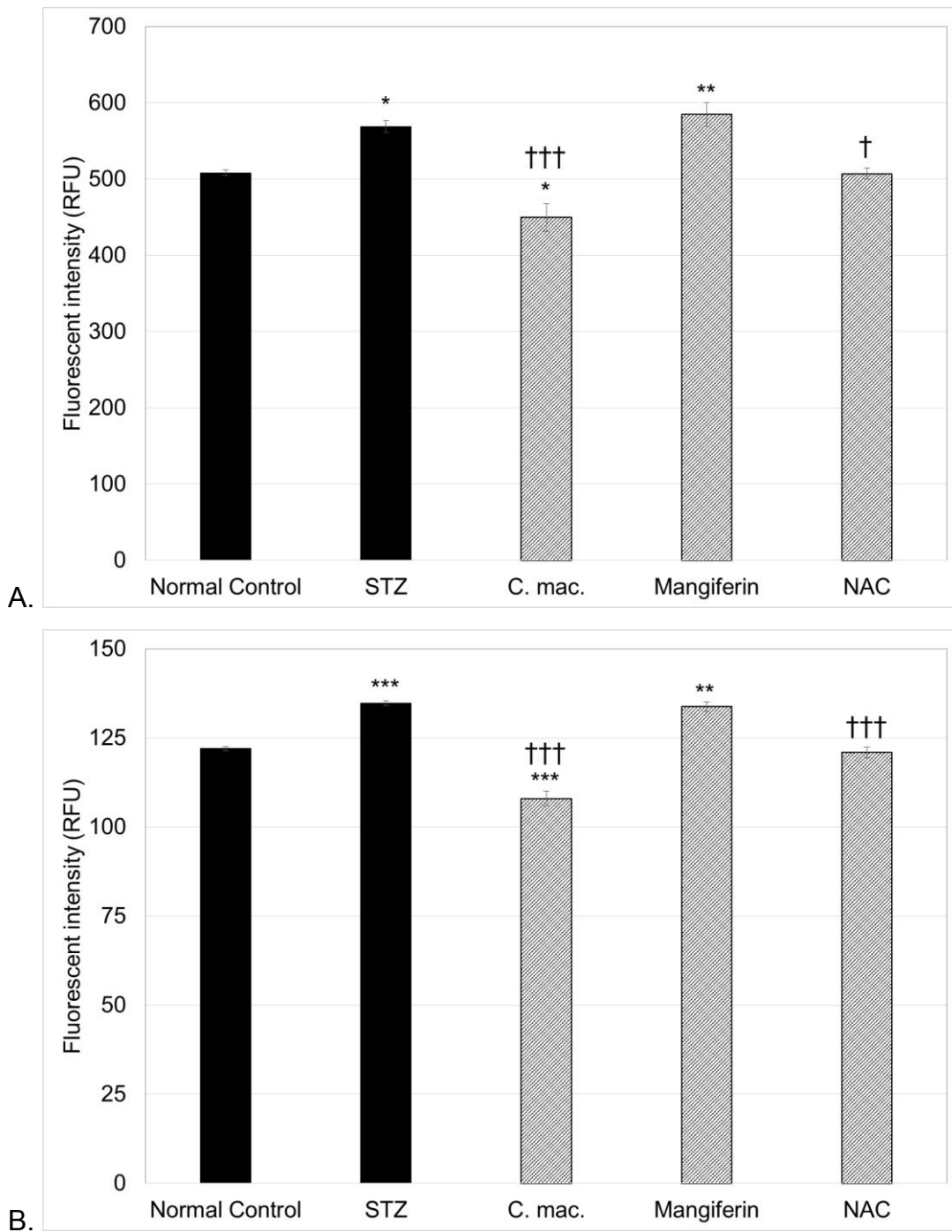
Figure 80. DAF (A) and DHE (B) fluorescence of pancreatic islets exposed to STZ and treated with *C. maculata* (C. mac.), mangiferin and NAC.

Isolated islets were first exposed to 10 mM STZ for 24 hours and then to 10 μg/mL extract, 100 μg/mL mangiferin and 0.01 mM NAC in fresh media for 24 hours. DAF and DHE fluorescence was then measured.

Where * = $p < 0.05$, ** = $p < 0.01$ and *** = $p < 0.001$ compared to the normal control; and † = $p < 0.05$ and ††† = $p < 0.001$ compared to STZ.
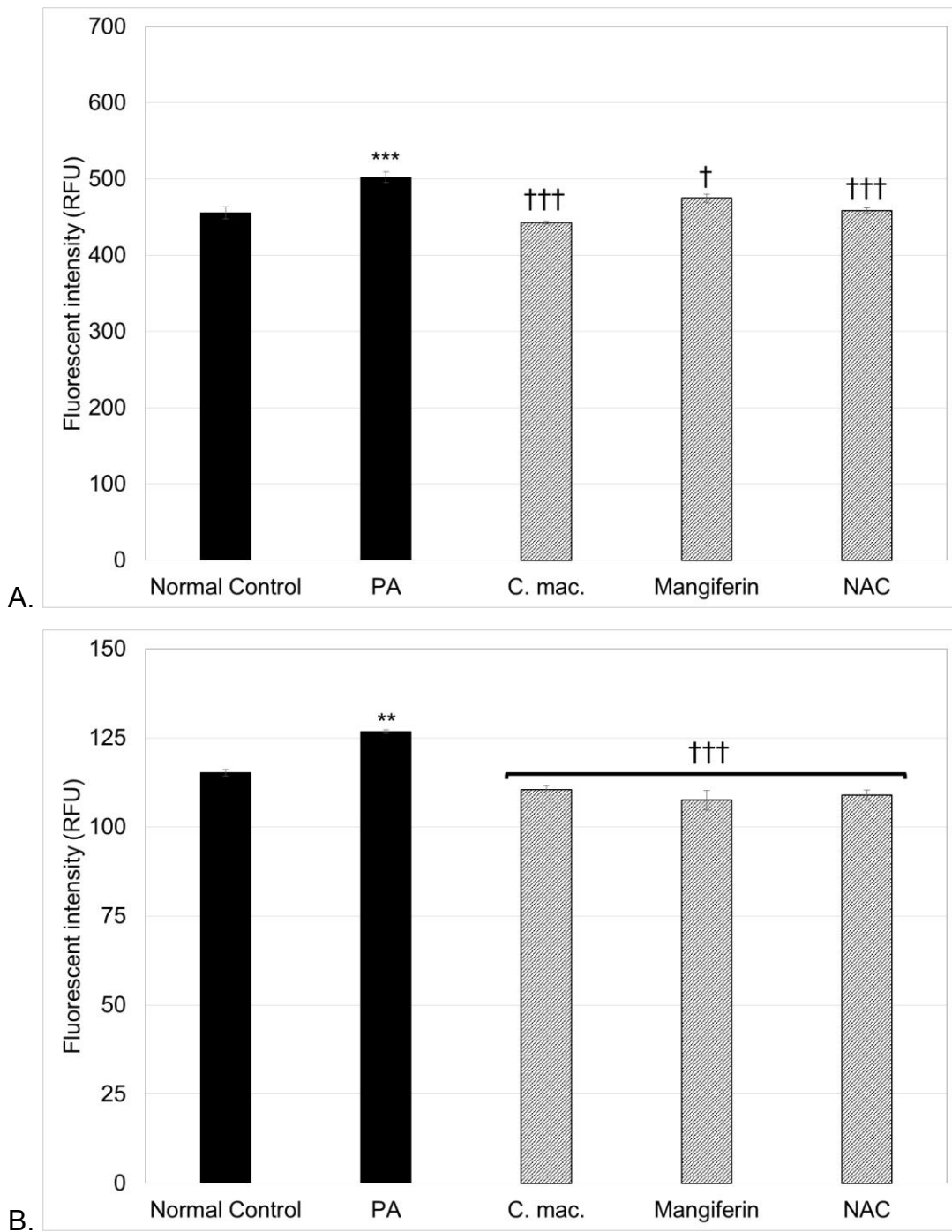
Figure 81. DAF (A) and DHE (B) fluorescence of pancreatic islets exposed to PA and treated with *C. maculata* (C. mac.), mangiferin and NAC.

Isolated islets were first exposed to 750 µM PA for 24 hours and then to 10 µg/mL extract, 100 µg/mL mangiferin and 0.01 mM NAC in fresh media for 24 hours. DAF and DHE fluorescence was then measured.

Where ** = $p < 0.01$ and *** = $p < 0.001$ compared to the normal control; and † = $p < 0.05$ and ††† = $p < 0.001$ compared to PA.

2.3.2. Superoxide dismutase enzyme activity

Exposure of isolated pancreatic islets to the STZ control reduced SOD activity compared to the normal control (2.59 % ± 0.20 vs. 0.90 % ± 0.10) (Fig. 82). Treatment with mangiferin and NAC increased SOD activity compared to the STZ control, as well as to that of the normal control (13.35 % ± 1.04 and 7.10 % ± 1.75, respectively) (Fig. 82).

The PA control reduced SOD activity compared to the normal control (1.0 % ± 0.27 vs. 2.59 % ± 0.20) (Fig. 83). Treatment with mangiferin and NAC increased SOD activity compared to the PA control, as well as to that of the normal control (15.61 % ± 1.06 and 9.13 % ± 2.40, respectively) (Fig. 83).

Mangiferin and NAC increased SOD activity that was reduced by both STZ (Fig. 82) and PA in isolated islets (Fig. 83).
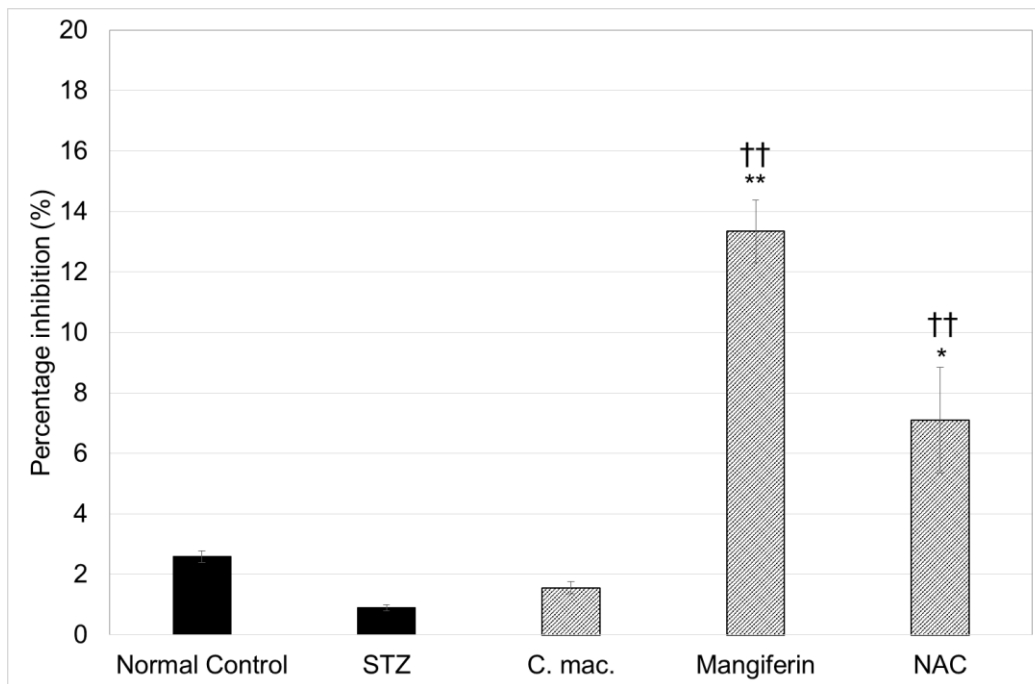
Figure 82. The effect of _C. maculata_ extract (C. mac.), mangiferin and NAC on SOD activity in isolated islets exposed to STZ for 24 hours.

Isolated islets were first exposed to 10 mM STZ for 24 hours and then to 10 µg/mL extract, 100 µg/mL mangiferin and 0.01 mM NAC in fresh media for 24 hours. Thereafter, SOD enzyme activity was determined.

Where * = $p < 0.05$ and ** = $p < 0.01$ compared to the normal control; and †† = $p < 0.01$ compared to STZ.
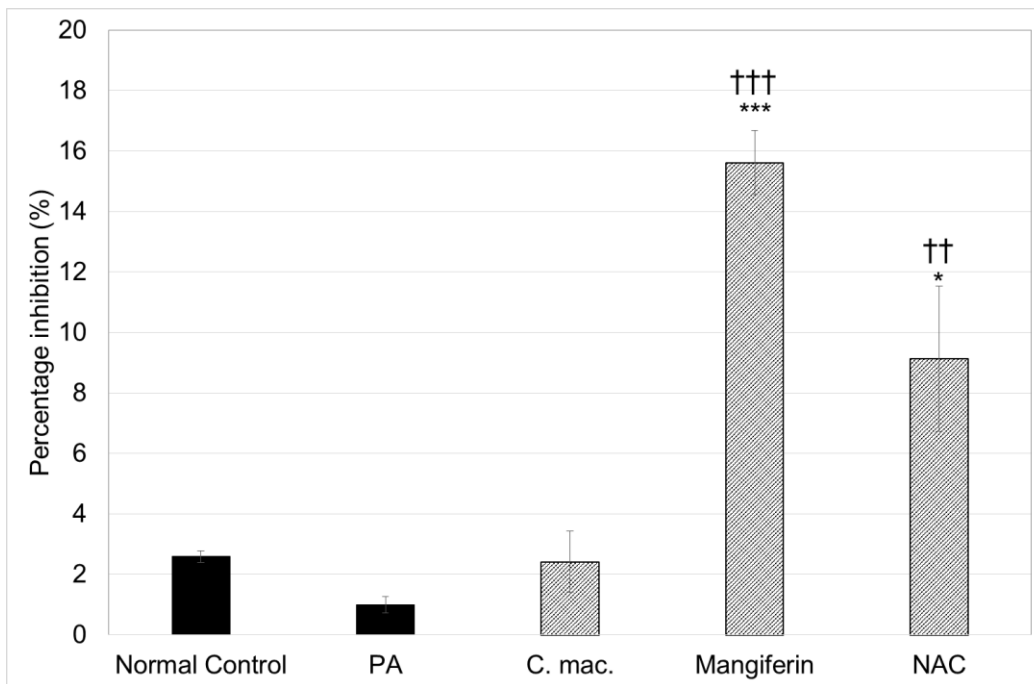
Figure 83. The effect of *C. maculata* extract (C. mac.), mangiferin and NAC on SOD activity in isolated islets exposed to PA for 24 hours.

Isolated islets were first exposed to 750 µM PA for 24 hours and then to 10 µg/mL extract, 100 µg/mL mangiferin and 0.01 mM NAC in fresh media for 24 hours. Thereafter, SOD enzyme activity was determined.

Where * = $p < 0.05$ and *** = $p < 0.001$ compared to the normal control; and †† = $p < 0.01$ and ††† = $p < 0.001$ compared to PA.

179

2.4. Summary of treatment effects in isolated pancreatic islets

None of the treatments, at the concentrations tested, had an effect on viability of isolated pancreatic islets exposed to STZ, in terms of annexin-V and propidium iodide fluorescence (Table 7 A). The extract and NAC, however, did reduce RNS and ROS induced by STZ, with NAC and mangiferin increasing SOD activity in these islets (Table 7 A). Elevated insulin secretion induced by STZ was reduced by treatment with mangiferin and the extract (Table 7 A).

In PA exposed islets, the extract and NAC appeared to decrease early stage apoptosis as measured by annexin-V fluorescence, and reduce both RNS and ROS. The PA induced elevation of insulin secretion was reduced in extract treated islets and an increase in SOD activity in NAC treated islets was observed (Table 7 B). Mangiferin improved the oxidative stress status of the PA exposed islets, with decreased RNS and ROS, as well as increased SOD activity (Table 7 B).

Table 7. Summary of the effects of *C. maculata*, mangiferin and NAC on STZ (A) and PA (B) exposed pancreatic islets.

A.

		C. maculata	Mangiferin	NAC
Cell viability	Annexin-V	-	-	-
	Propidium iodide	-	-	-
Oxidative stress	DAF	↓	-	↓
	DHE	↓	-	↓
	SOD	-	↑	↑
Cell function	Insulin secretion	↓	↓	-

B.

		C. maculata	Mangiferin	NAC
Cell viability	Annexin-V	↓	-	↓
	Propidium iodide	-	-	-
Oxidative stress	DAF	↓	↓	↓
	DHE	↓	↓	↓
	SOD	-	↑	↑
Cell function	Insulin secretion	↓	-	-

3. *In vivo* results

The efficacy of the *C. maculata* extract and NAC was assessed in STZ induced diabetic Wistar rats. The hypoglycaemic drug, metformin, was used as a treatment control. The efficacy of the extract and NAC were assessed both as therapeutic as well as preventative agents in T2D. As potential therapeutic agents, the extract and NAC (as well as metformin) were administered to rats five days after injection with STZ (the respective control rats were injected with STZ simultaneously and treated with water vehicle); this group of rats is referred to hereafter as the treated group (N = 6). As potential preventative agents, extract, NAC and metformin were administered to rats for 15 days prior to STZ injection and for five days post injection (with their respective STZ control rats injected with STZ simultaneously) and are referred to as the pretreated group (N = 8). Extract, NAC and metformin were administered to treated and pretreated rats for a total of 21 days.

3.1. Metabolic parameters

Metabolic parameters assessed in this component of the study were glucose tolerance, fasting serum insulin and serum triglycerides following 21 days of treatment. Compared to the normal control, in the treated group, the diabetic STZ control rats, and diabetic rats treated with metformin, NAC, as well as 30 and 300 mg/kg/d extract after STZ injection had elevated fasting plasma glucoses (5.76 mmol/L ± 0.20 vs. 16.92 mmol/L ± 3.00, 21.68 mmol/L ± 3.18, 23.58 mmol/L ± 2.19, 20.74 mmol/L ± 2.70 and 19.99 mmol/L ± 2.37, respectively) (Fig. 85 A). OGTT areas under the curve (AUCs) of these rats treated with metformin, NAC, 30 mg/kg/d extract and 300 mg/kg/d extract after STZ injection were not improved compared to the STZ control rats (Fig. 86 A), nor were the fasting serum insulin levels (Fig. 87 A).

The STZ control rats in the pretreated group also had elevated fasting plasma glucose levels compared to the normal control rats (16.21 mmol/L ± 1.93 vs. 5.76 mmol/L ± 0.20) (Fig. 85 B). In this pretreated group, rats pretreated with metformin and 300 mg/kg/d of extract showed reduced fasting plasma glucose compared to the STZ control rats (6.29 mmol/L ± 0.66 and 6.7 mmol/L ± 1.17 vs. 16.21 mmol/L ± 1.93, respectively) (Fig. 85 B). Compared to the normal control rats, an increase in the AUC of OGTTs of STZ control rats in the pretreated group was observed (1461.25 ± 12.70 vs. 5264.38 ± 396.14) (Fig. 86 B), which was reduced by pretreatment with metformin and both concentrations of *C. maculata* extract (i.e. 30 and 300 mg/kg/d) (2677.25 ± 483.80, 3114.13 ± 752.23 and 2824.38 ± 536.00,

181

respectively) (Fig. 86 B). Pretreatment of rats with metformin and NAC failed to significantly ameliorate the STZ induced reduction in fasting serum insulin (Fig. 87 B). When compared with the normal rats, injection with STZ increased the G:I ratio of STZ control rats in the pretreated group (1.49 ± 0.56 vs. 12.69 ± 2.34) (Fig. 88). Pretreatment with metformin and the 300 mg/kg/d concentration of *C. maculata* extract reduced the STZ induced increase in G:I ratio (3.27 ± 0.77 and 2.89 ± 0.67, respectively) (Fig. 88 B). Fasting serum triglycerides were increased in the STZ control rats in the pretreated group, when compared to the normal control rats (1.48 mmol/L ± 0.48 vs. 0.30 mmol/L ± 0.03) (Fig. 89 B). Pretreatment with the 300 mg/kg/d concentration of *C. maculata* extract reduced this increase in serum triglycerides (0.40 mmol/L ± 0.04 vs. 1.48 mmol/L ± 0.48) (Fig. 89 B).

No effect on serum levels of AP, AST or ALT were observed in this study (Table 9 A and B, addendum 4).

Overall, pretreatment of rats with the extract improved glucose tolerance, as seen in reduced fasting plasma glucose levels (Fig. 85 B), OGTT AUCs (Fig. 86 B) and G:I ratios (Fig. 88 B) (all of which were comparable with metformin). An improvement in fasting serum triglycerides was also observed in rats pretreated with *C. maculata* extract (Fig. 89 B), with some amelioration, albeit not significant, of fasting serum insulin levels compared to the STZ control (Fig. 87 B).
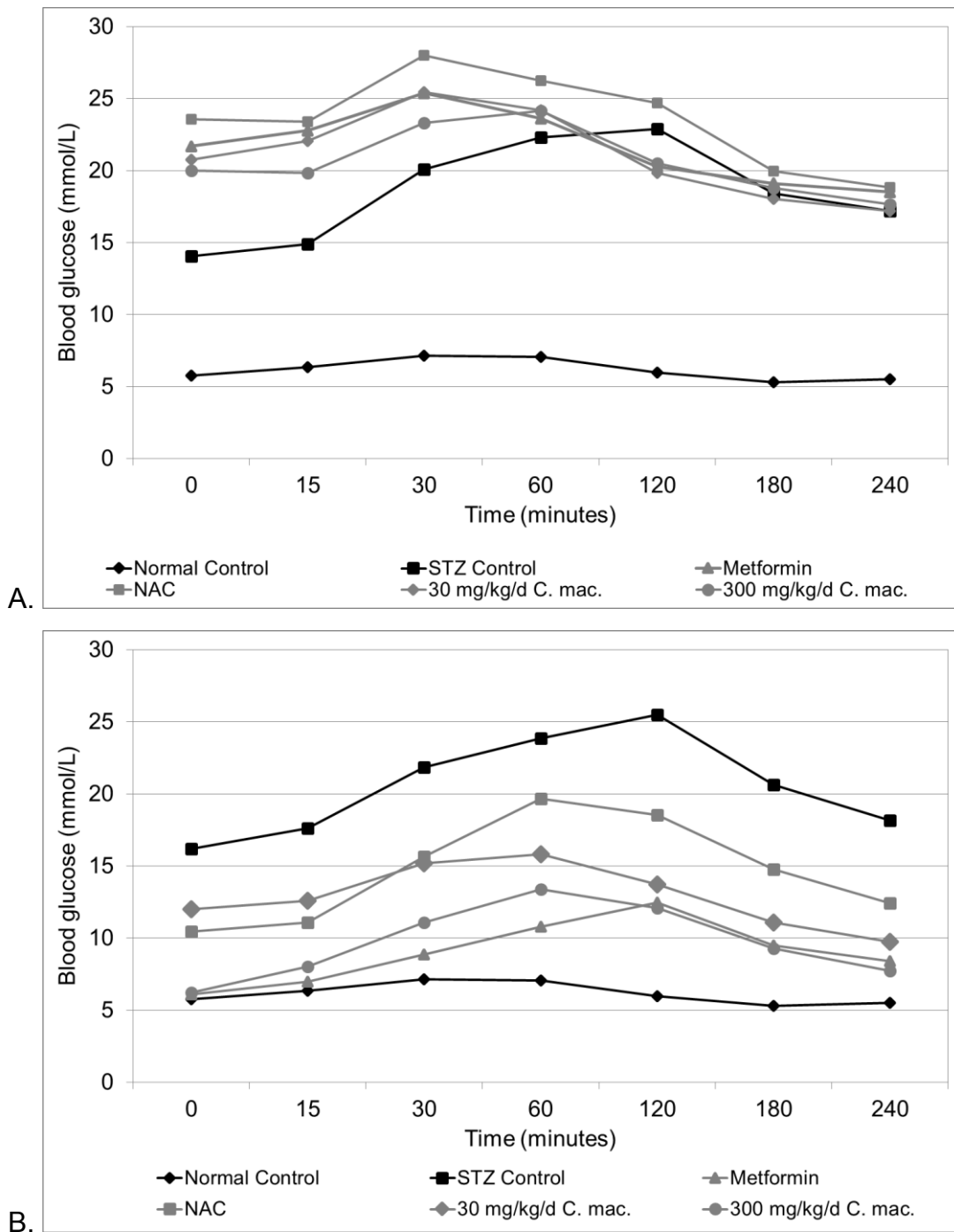
Figure 84. OGTTs of rats injected with STZ and treated (A) and rats pretreated (B) with metformin, NAC and *C. maculata* extract (C. mac.) and then injected with STZ.

Following a total of 21 days treatment and a 16 hour overnight fast, STZ induced diabetic Wistar rats were subjected to an OGTT over four hours.

A.

B.
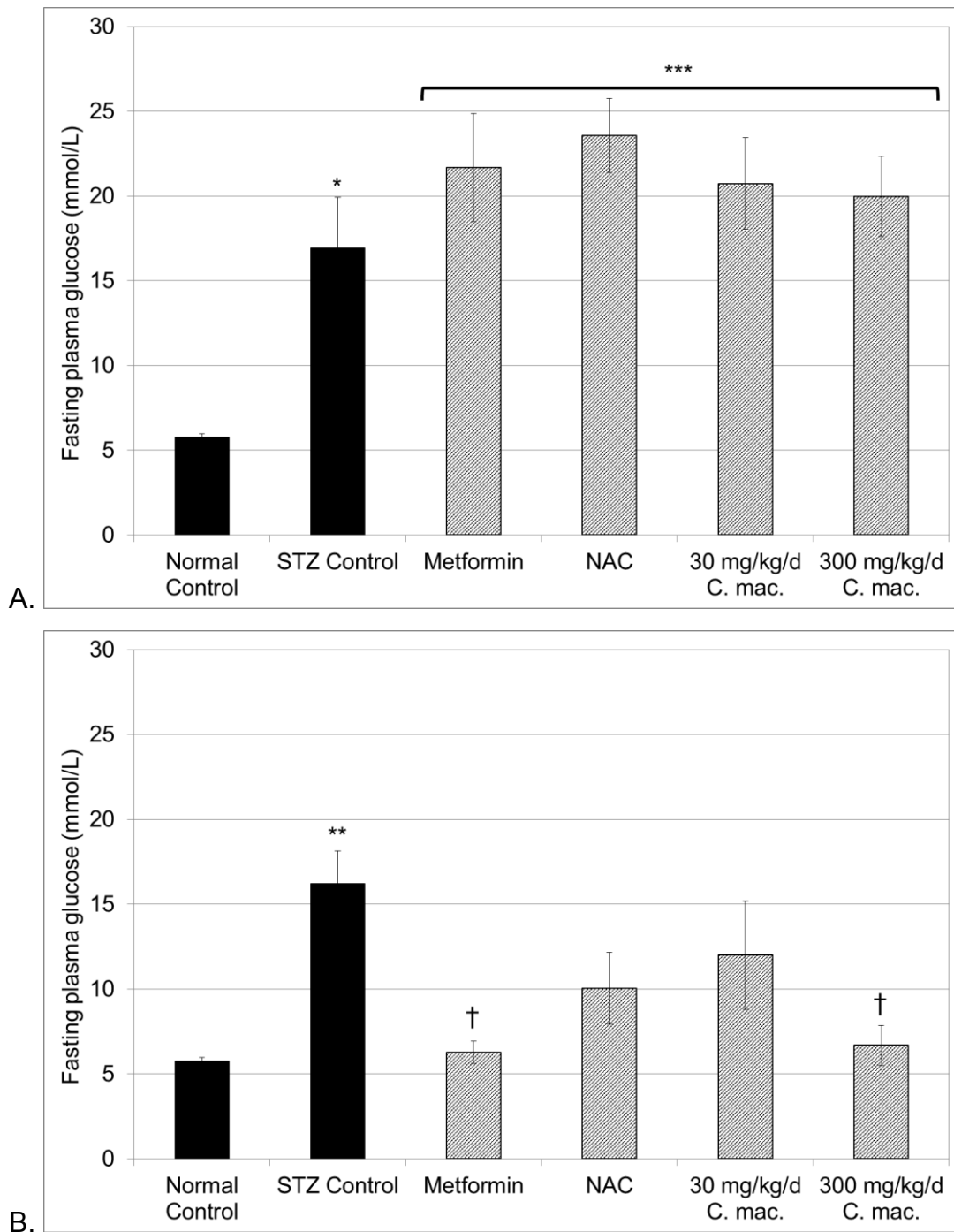
Figure 85. Fasting plasma glucoses of OGTTs of rats injected with STZ and treated (A) and rats pretreated (B) with metformin, NAC and C. maculata extract (C. mac.) and then injected with STZ.

Fasting plasma glucose of rats was determined at 0 minutes of the OGTT, prior to glucose administration.

Where * = $p < 0.05$, ** = $p < 0.01$ and *** = $p < 0.001$ compared to the normal control; and † = $p < 0.05$ compared to the STZ control. (Data from Fig. 85 B has been published in a peer-reviewed journal; see addendum 1).

184

A.

B.
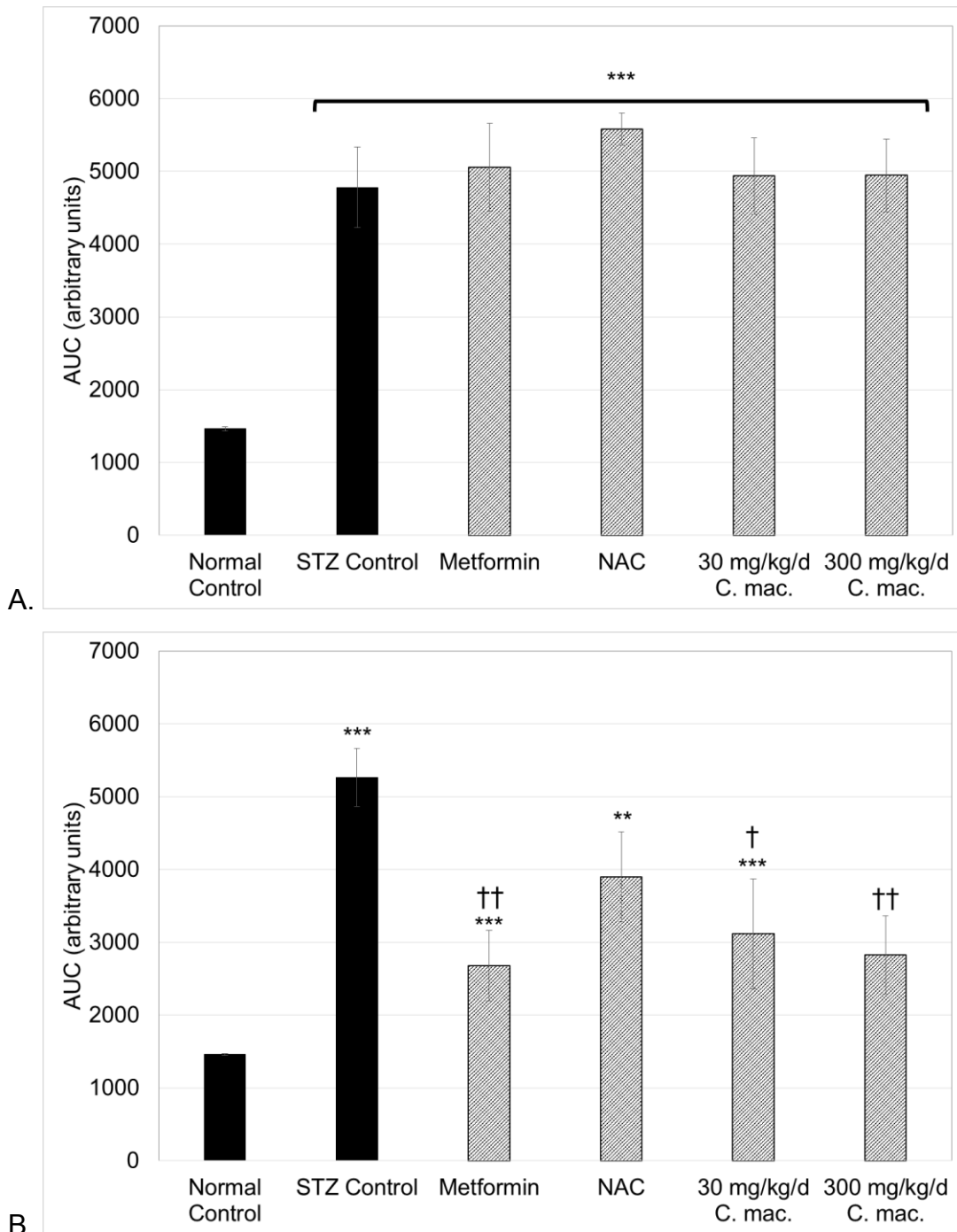
Figure 86. AUC of OGTTs of rats injected with STZ and treated (A) and rats pretreated (B) with metformin, NAC and *C. maculata* extract (C. mac.) and then injected with STZ. AUC of the glucose levels over four hours in the OGTT were calculated.

Where ** = $p < 0.01$ and *** = $p < 0.001$ compared to the normal control; and † = $p < 0.05$ and †† = $p < 0.01$ compared to the STZ control. (Data from Fig. 86 B has been published in a peer-reviewed journal; see addendum 1).

185

A.

B.
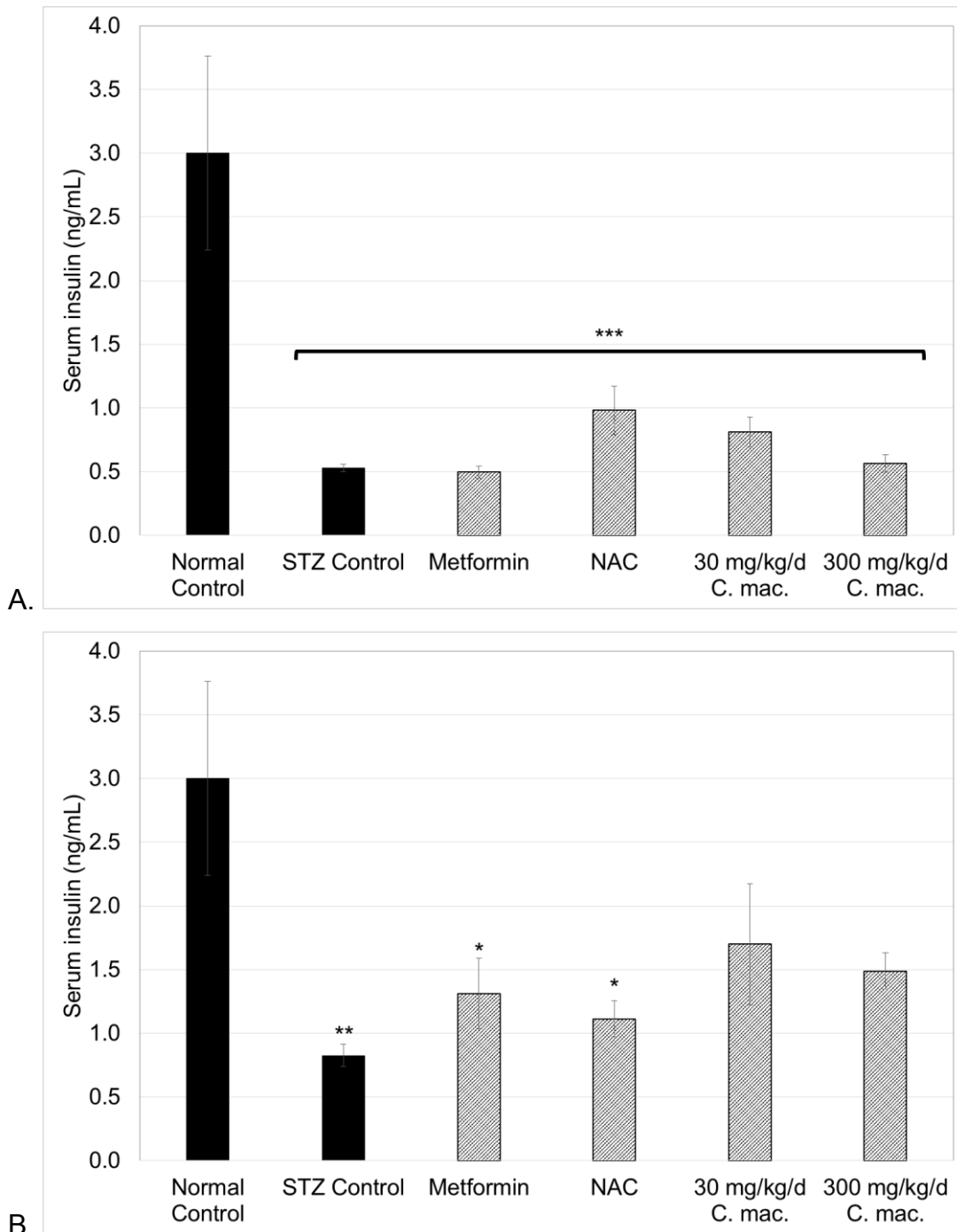
Figure 87. Fasting serum insulin concentration of rats injected with STZ and treated (A) and rats pretreated (B) with metformin, NAC and C. maculata extract (C. mac.) and then injected with STZ.

Fasted serum insulin levels were determined from blood collected at termination, following a 16 hour overnight fast.

Where * = $p < 0.05$, ** = $p < 0.01$ and *** = $p < 0.001$ compared to the normal control. (Data from Fig. 87 B has been published in a peer-reviewed journal; see addendum 1).

186
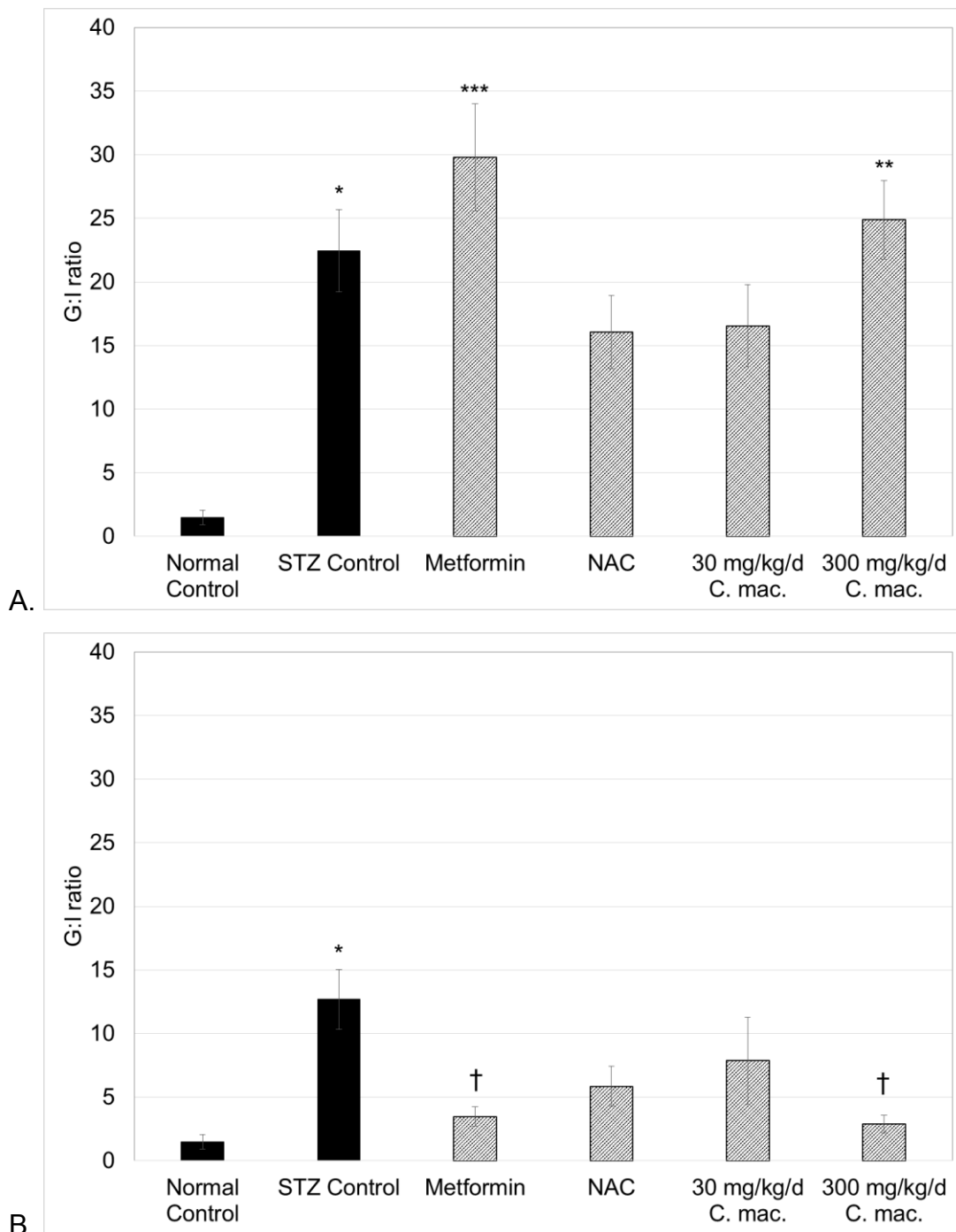
Figure 88. G:I of rats injected with STZ and treated (A) and rats pretreated (B) with metformin, NAC and *C. maculata* extract (C. mac.) and then injected with STZ.

The glucose to insulin ratio was calculated using fasted glucose and insulin values.

Where * = $p < 0.05$, ** = $p < 0.01$ and *** = $p < 0.001$ compared to the normal control; and † = $p < 0.05$ compared to the STZ control. (Data from Fig. 88 B has been published in a peer-reviewed journal; see addendum 1).

A.

B.
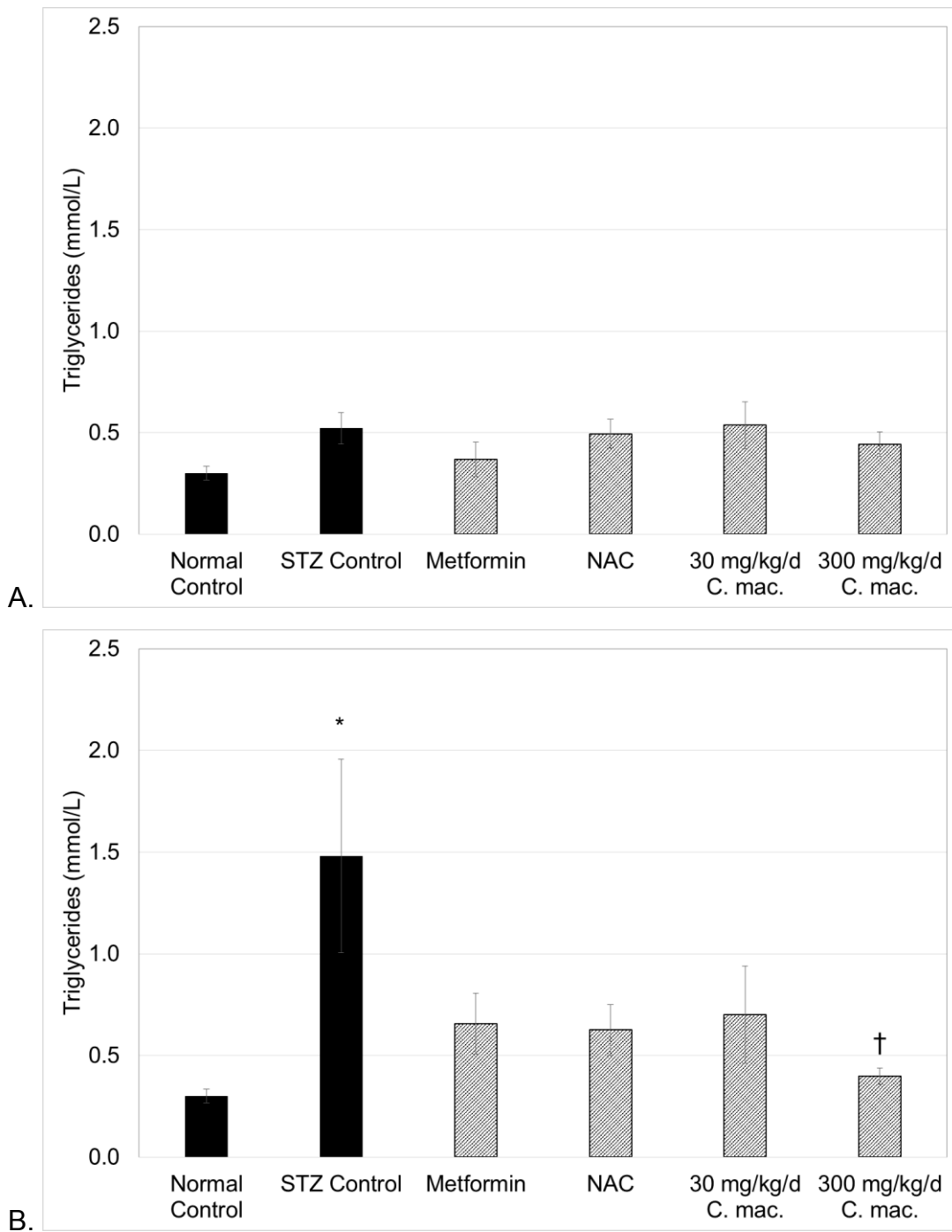
Figure 89. Fasting serum triglycerides of rats injected with STZ and treated (A) and rats pretreated (B) with metformin, NAC and C. maculata (C. mac.) extract and then injected with STZ.

Fasted serum triglyceride levels were determined from blood collected at termination, following a 16 hour overnight fast.

Where * = $p < 0.05$ compared to the normal control; and † = $p < 0.05$ compared to the STZ control. (Data from Fig. 89 B has been published in a peer-reviewed journal; see addendum 1).

188

3.2. Antioxidative effects

The potential antioxidative effects of the extract were assessed by the following methods, serum nitrite and antioxidant enzyme levels, as well as hepatic TBARS levels and nitrotyrosine expression. Compared to the normal control rats, injection with STZ increased fasting serum nitrites of control rats in the pretreated group (0.40 μM ± 0.03 vs. 0.56 μM ± 0.08) (Fig. 90 B). Pretreatment with metformin and the 30 mg/kg/d and 300 mg/kg/d concentrations of *C. maculata* extract reduced the STZ induced increase in serum nitrites (0.43 μM ± 0.01, 0.42 μM ± 0.01 and 0.42 μM ± 0.02, respectively) (Fig. 90 B). Since an effect on serum nitrites was only observed in rats pretreated with extract, NAC and metformin, the remaining antioxidant assays were only performed on this group. No effect was observed on hepatic TBARS levels (Fig. 91), serum levels of CAT (Fig. 92) or GSH (Fig. 93), nor on hepatic nitrotyrosine expression (Fig. 94) in rats pretreated with extract, NAC and metformin.
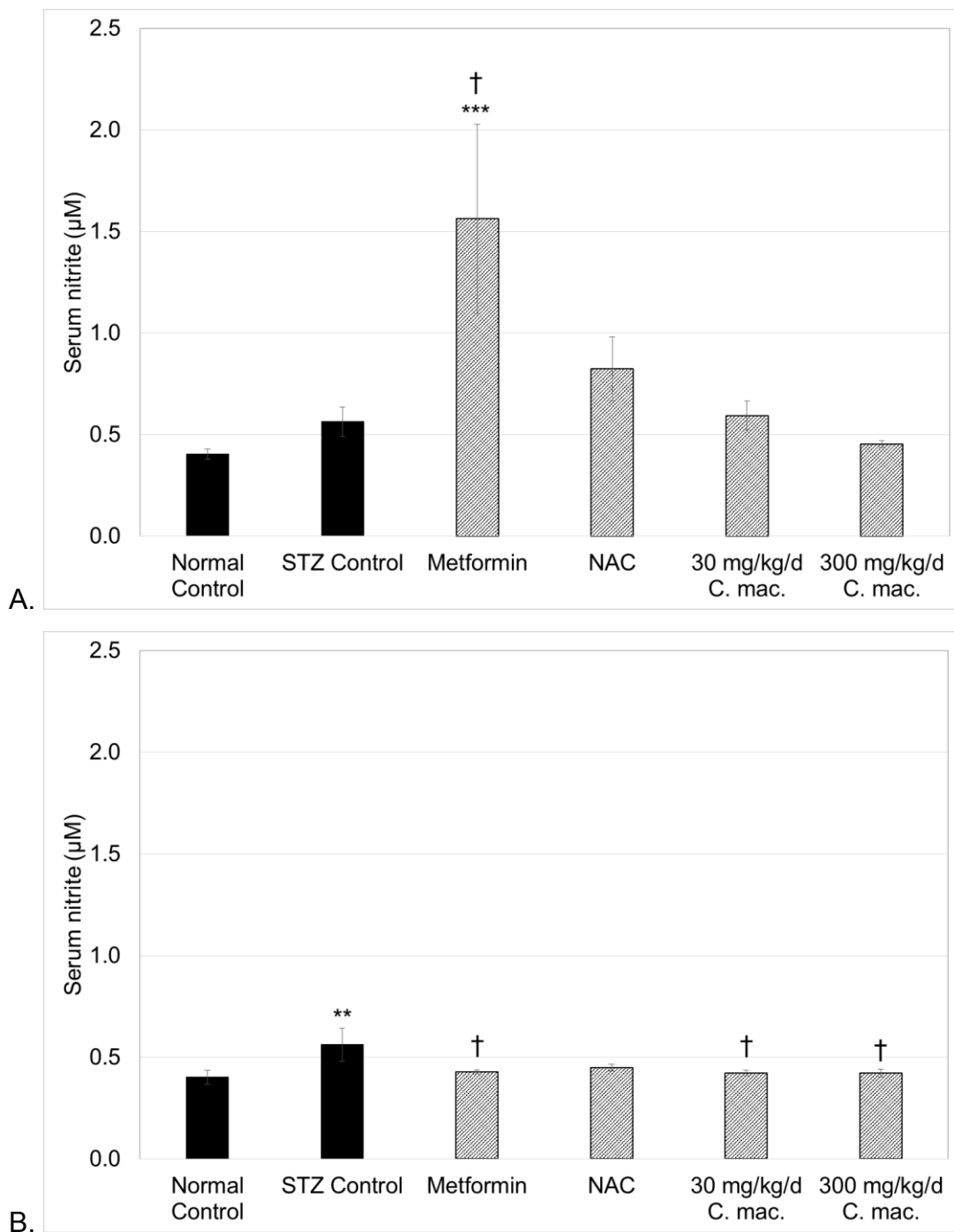
Figure 90. Fasting serum nitrites of rats injected with STZ and treated (A) and rats pretreated (B) with metformin, NAC and C. maculata extract (C. mac.) and then injected with STZ.

Fasted serum nitrite levels were determined from blood collected at termination, following a 16 hour overnight fast.

Where ** = $p < 0.01$ and *** = $p < 0.001$ compared to the normal control; and † = $p < 0.05$ compared to the STZ control. (Data from Fig. 90 B has been published as supplementary data in a peer-reviewed journal; see addendum 1).

190
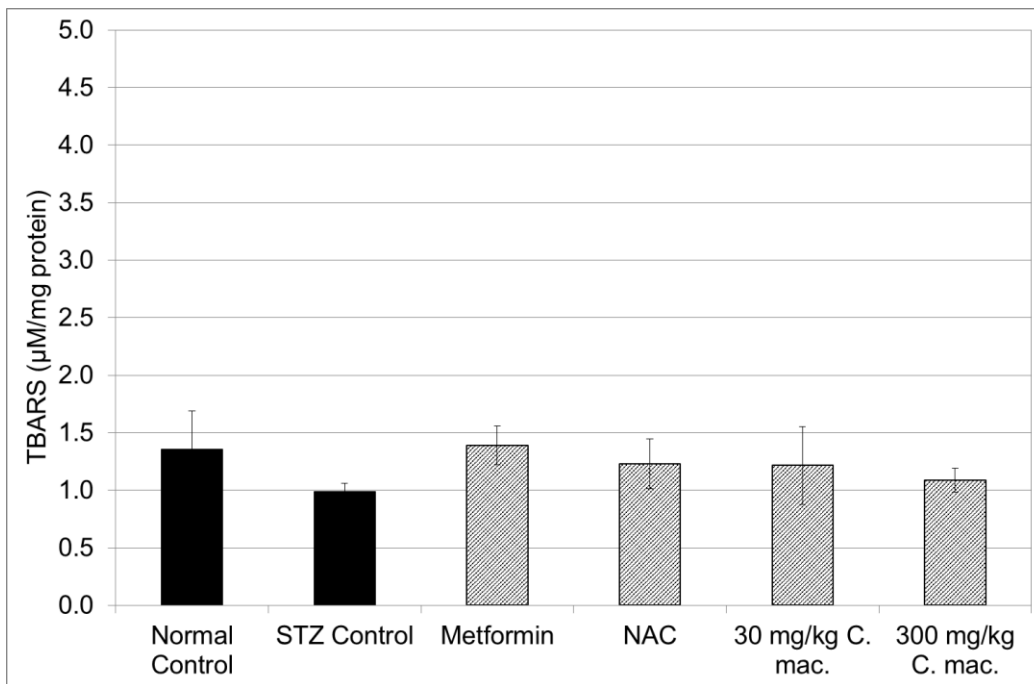
Figure 91. Hepatic TBARS of rats pretreated with metformin, NAC and *C. maculata* extract (C. mac.) and then injected with STZ.

TBARS in rat liver collected at termination was determined in homogenised tissue from pretreated rats only.
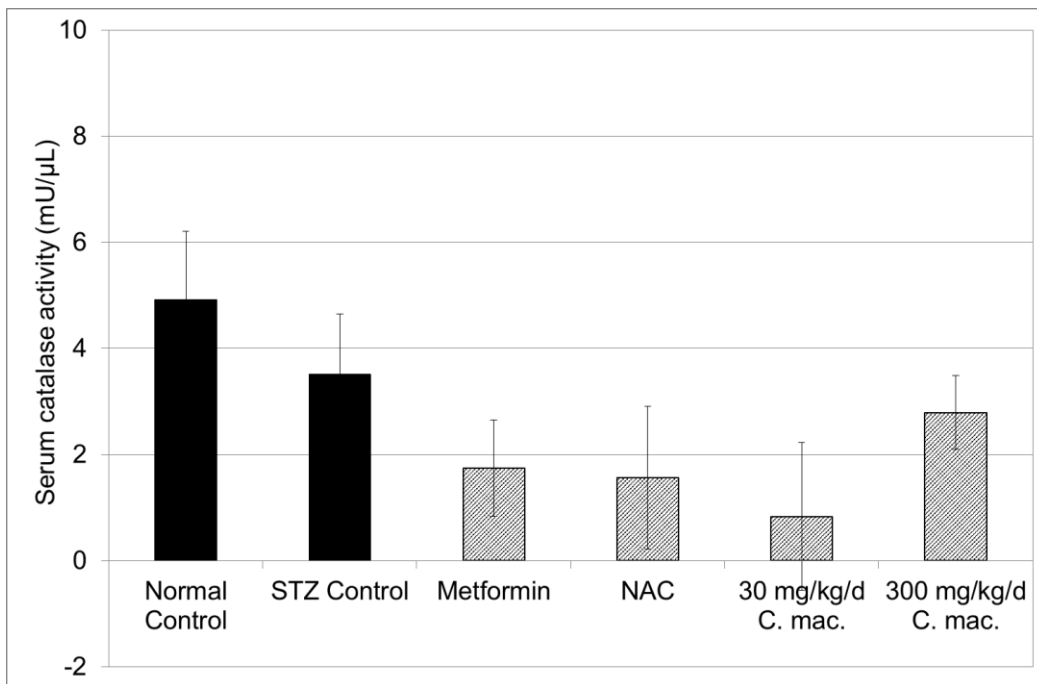
Figure 92. Serum CAT of rats pretreated with metformin, NAC and *C. maculata* extract (C. mac.) and then injected with STZ.

Serum CAT levels were determined from blood collected at termination in pretreated rats only, following a 16 hour overnight fast.
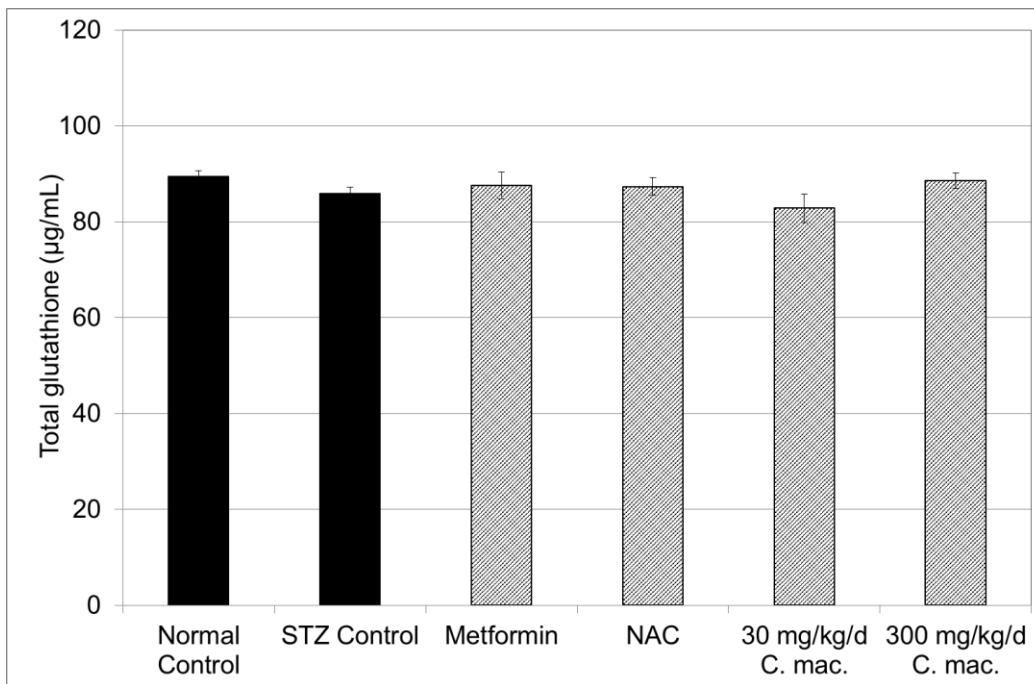
Figure 93. Serum total GSH of rats pretreated with metformin, NAC and *C. maculata* extract (C. mac.) and then injected with STZ.

Serum GSH levels were determined from blood collected at termination in pretreated rats only, following a 16 hour overnight fast.
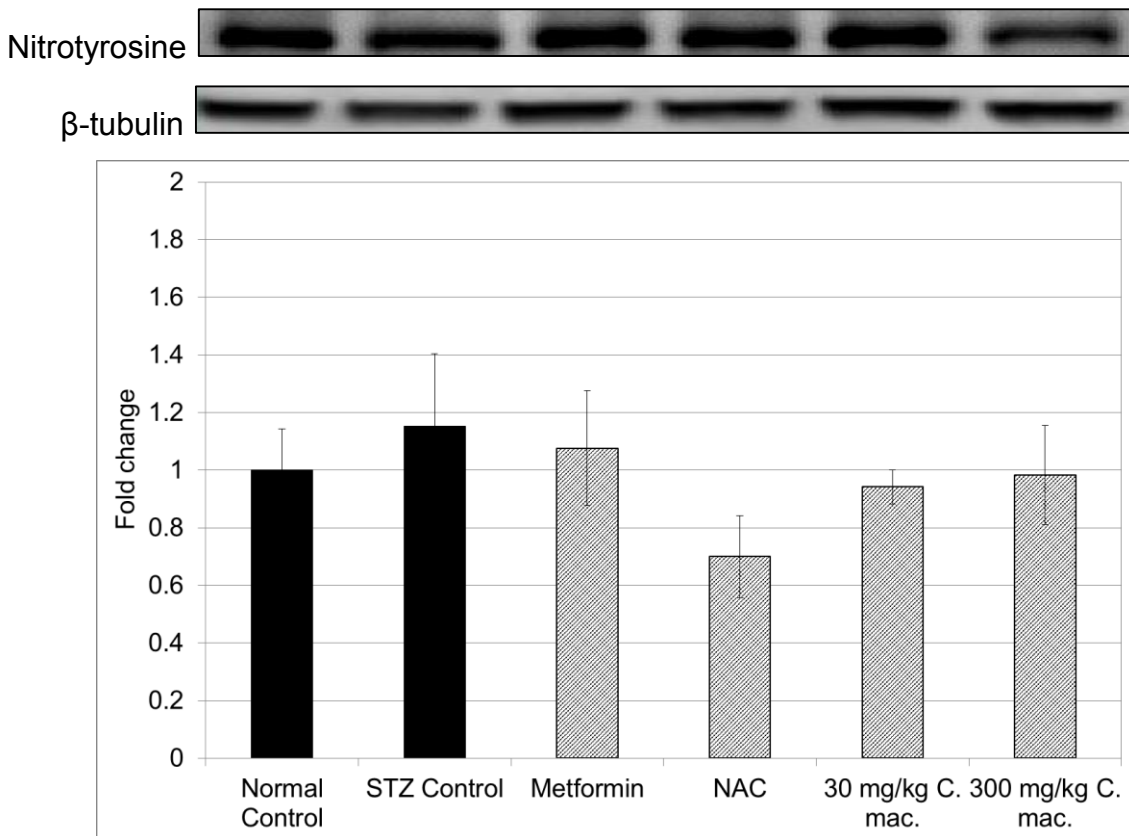
Figure 94. Hepatic nitrotyrosine expression of rats pretreated with metformin, NAC and *C. maculata* extract (C. mac.) and then injected with STZ.

Nitrotyrosine expression termination, in pretreated rats only, was assessed in liver homogenate (from liver tissue collected at termination).

194

3.3. Pancreatic islet morphometry

Since pretreatment with the extract, NAC and metformin improved glucose tolerance in STZ induced diabetic Wistar rats, their effect/s on the pancreatic islets of these rats was assessed by immunohistochemical labelling of islets for insulin, glucagon and MIB-5. Morphometric analysis of the immunohistochemical labelling provided insight into islet area, cell numbers, as well as cell proliferation. Compared to the normal control rats, a decrease in pancreatic β-cell area to total islet area in the STZ control rats was observed (81.30 ± 1.65 vs. 36.34 ± 5.01) (Fig. 95 A), with a concomitant increase in α-cell area to total islet area (0.08 ± 0.01 vs. 0.19 ± 0.01) (Fig. 95 B). Compared to the STZ control rats, both 30 and 300 mg/kg/d *C. maculata* extract pretreatment increased β-cell area to total islet area (59.38 ± 7.17 and 59.15 ± 3.56, respectively) (Fig. 95 A), as well as decreased α-cell area to total islet area (0.12 ± 0.02 and 0.12 ± 0.01, respectively) (Fig. 95 B). Metformin pretreatment also increased β-cell area to total islet area compared to the STZ control (59.22 ± 5.08) (Fig. 95 A), however, NAC failed to increase the β-cell area to total islet area (Fig. 95 A). The STZ control group also showed a reduction in ratio of the total number of β-cells to total number of α-cells, which was somewhat ameliorated (albeit not significantly) by the pretreatments, particularly by the two concentrations of extract tested (Fig. 96). The images in Fig. 97 demonstrate changes in pancreatic architecture from normal control rats (Fig. 97 A), in STZ control (B), metformin (Fig. 97 C), NAC (Fig. 97 D), 30 mg/kg/d extract (Fig. 97 E) and 300 mg/kg/d extract (Fig. 97 F) pretreated rats. No changes were observed in the ratio of total islet to total pancreatic tissue area (Table 10 A, addendum 4), as well as the ratio of β-cell area to the total number of β-cells (Table 10 B, addendum 4).

The 300 mg/kg/d *C. maculata* extract pretreated group showed an increased number of MIB-5 positive β-cells to total β-cells compared to both the normal and STZ control rats (3.64 ± 0.42 vs. 1.78 ± 0.40 and 1.63 ± 0.43, respectively) (Fig. 98). The representative images in Fig. 99 are of pancreata from normal control (Fig. 99 A) and 300 mg/kg/d extract pretreated (Fig. 99 B) rats.

Pretreatment with the *C. maculata* extract showed improved β- to α-cell area in pancreatic islets, which was distorted by STZ (Fig. 95), which may, in part, be due to increased β-cell proliferation (Fig. 97).
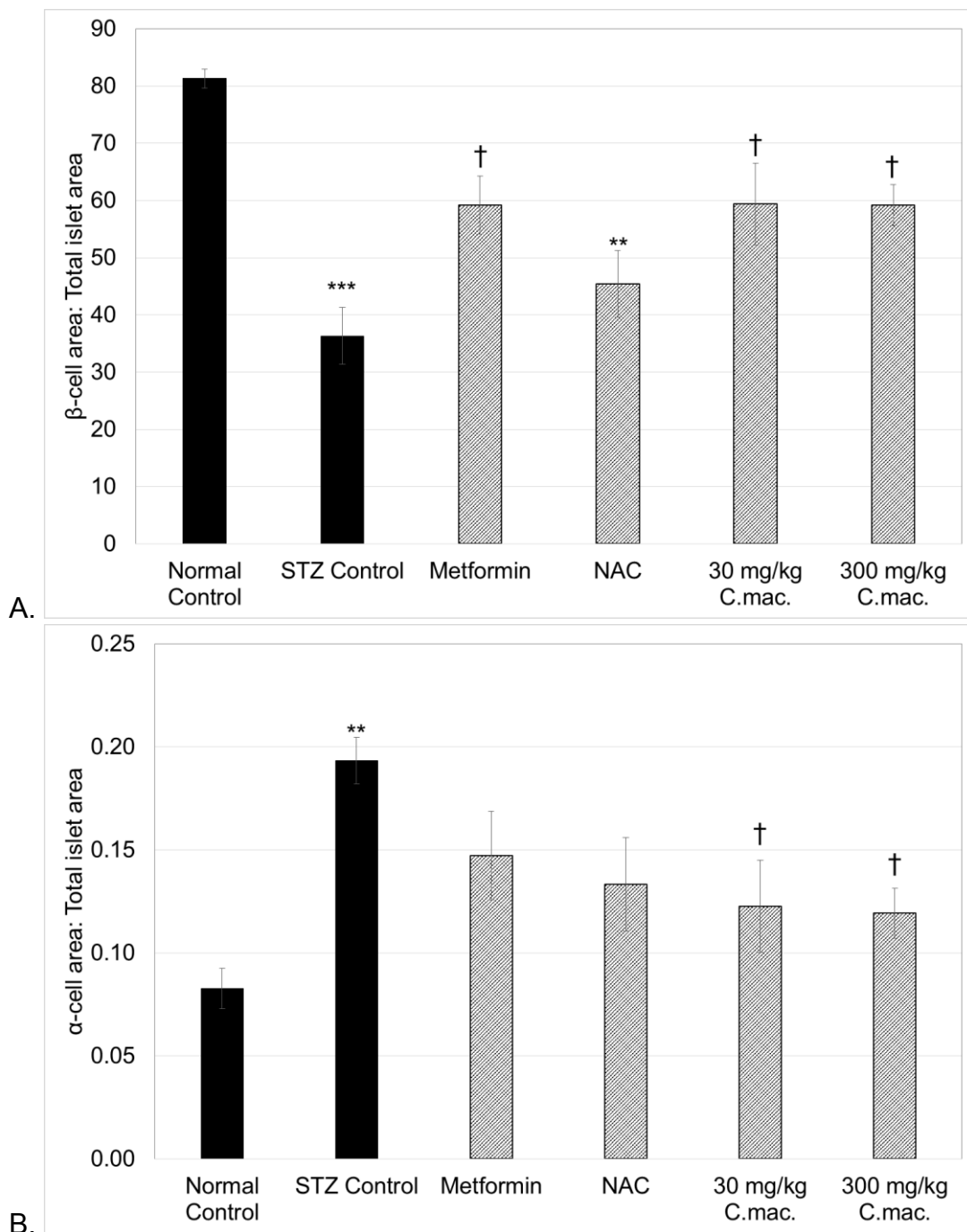
Figure 95. Pancreatic β-cell (A) and α-cell (B) area to total islet area of rats pretreated with metformin, NAC and *C. maculata* extract (C. mac.) and then injected with STZ.

Pancreata collected at termination were fixed and processed histologically for immunohistochemical detection of insulin (β-cells) and glucagon (α-cells) positive cells. The α- and β-cell areas were measured and a ratio thereof was calculated.

Where ** = $p < 0.01$ and *** = $p < 0.001$ compared to the normal control; and † = $p < 0.05$ compared to the STZ control. (Data from Fig. 95 A has been published in a peer-reviewed journal; see addendum 1).

196
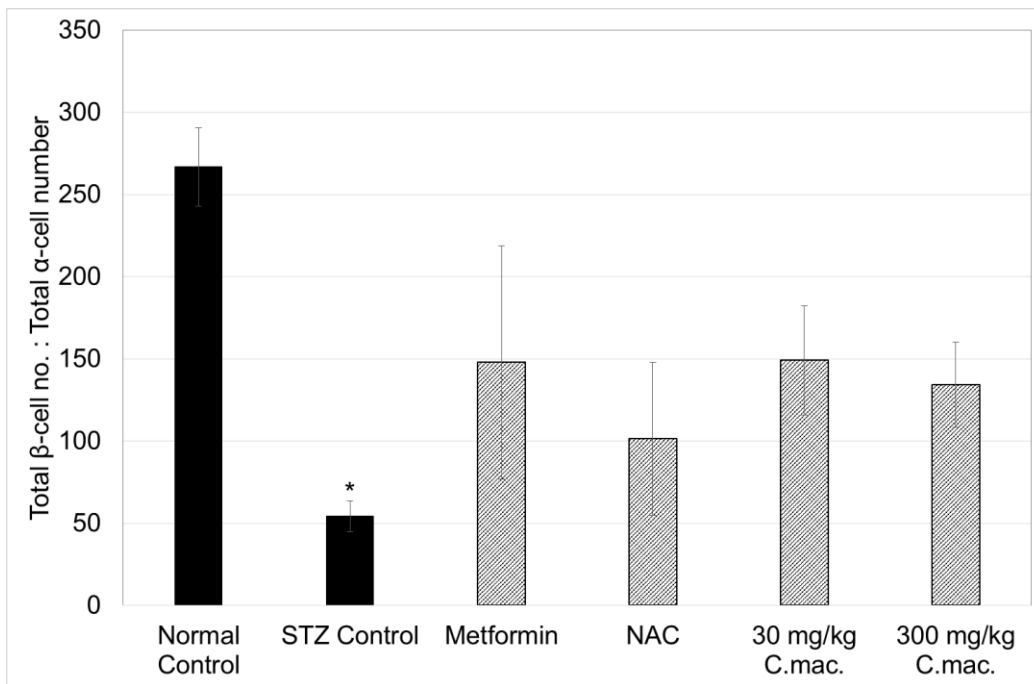
Figure 96. Total number of β-cells to total number of α-cells of rats pretreated with metformin, NAC and *C. maculata* extract (C. mac.) and then injected with STZ.

The total number of insulin positive β-cells following immunohistochemical labelling of insulin and glucagon in fixed rat pancreata were counted.

Where * = $p < 0.05$ compared to the normal control.
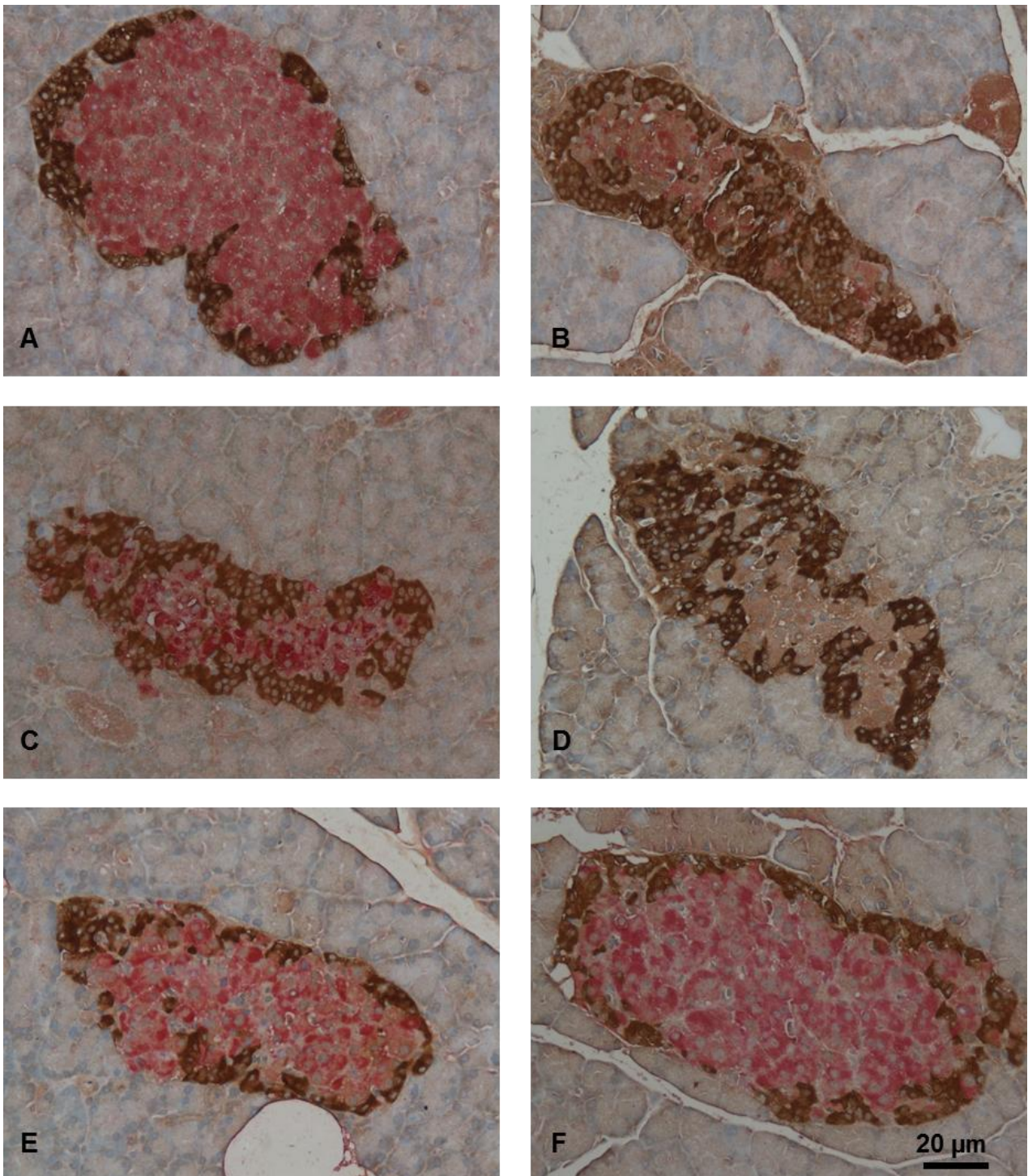
Figure 97. Representative images of insulin and glucagon immunohistochemical labelling of rat islets.

Representative images of islets in normal control rats (**A**), STZ control rats (**B**), metformin pretreated (**C**), NAC pretreated (**D**), 30 mg/kg/d extract pretreated (**E**) and 300 mg/kg/d extract pretreated (**F**) rats at 200 x magnification. Red/pink labelling demonstrates insulin positive β-cells and brown labelling glucagon positive α-cells.
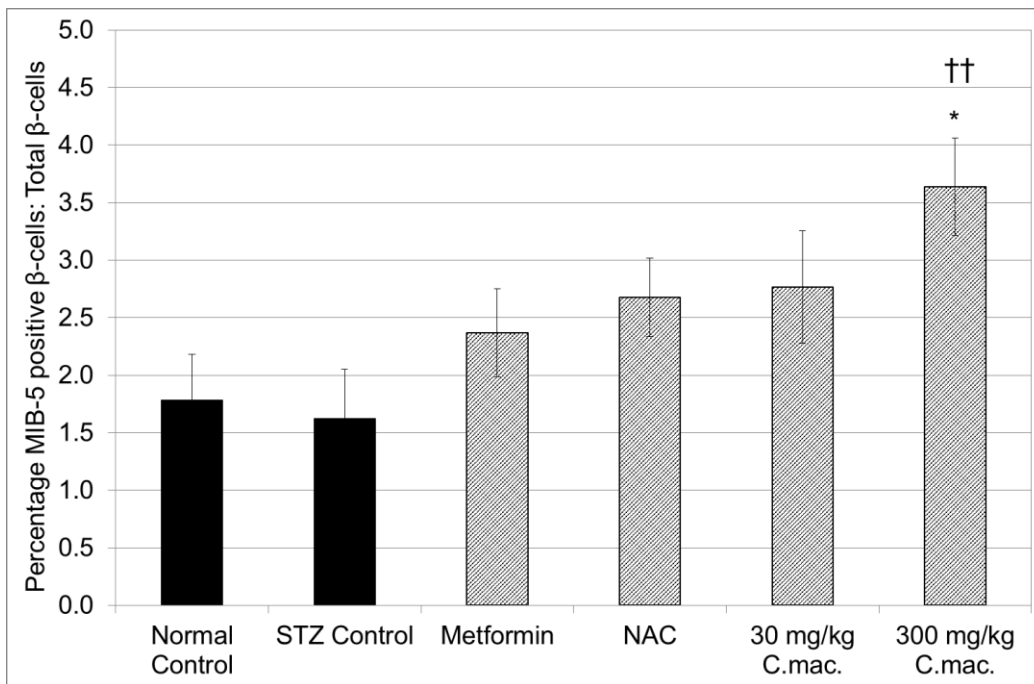
Figure 98. Percentage MIB-5 positive β-cells in pancreatic islets of rats pretreated with metformin, NAC and *C. maculata* extract (C. mac.) and then injected with STZ.

Pancreata collected at termination were fixed and processed histologically for immunohistochemical detection of MIB-5 positive β-cells.

Where * = p < 0.05 compared to the normal control; and †† = p < 0.01 compared to the STZ control. (Data from Fig. 98 has been published in a peer-reviewed journal; see addendum 1).
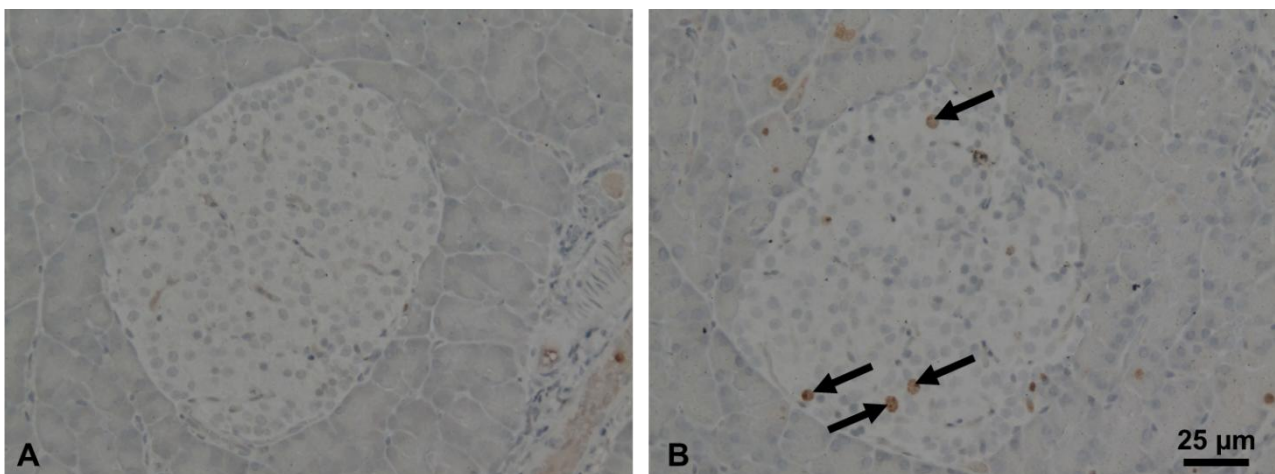
Figure 99. Representative images if islets from MIB-5 immunohistochemical labelling of rat pancreata.

Representative images of islets from normal control (**A**) and 300 mg/kg/d extract pretreated (**B**) rats at 200 x magnification. The arrows demonstrate intra-islet proliferating (MIB-5 positive) β-cells.

199

4. Summary of the effects of the treatments used in this study

As summarised in Table 8 below, the *C. maculata* extract used in this study improved β-cell viability, function and oxidative stress in STZ and PA toxicity models both *in vitro* (in RIN-5F cells) and *ex vivo* (in isolated pancreatic islets from Wistar rats). Mangiferin showed some improvement in RIN-5F cell function by increasing cell proliferation, as well as marginally improving RIN-5F oxidative status by increasing SOD activity. Mangiferin also improved STZ induced dysfunction in insulin secretion in isolated islets and reduced PA induced oxidative stress. In RIN-5F cells only, NAC improved cell viability and function, however, a reduction in oxidative stress both *in vitro* and *ex vivo* by NAC was also observed. In Wistar rats, pretreatment with the extract was as effective as, if not better than, metformin in improving glucose tolerance and pancreatic islet parameters associated with β-cell function. Pretreatment with the extract also showed hypotriglyceridaemic effects in these STZ induced diabetic rats.

Table 8. Summary of the effects of *C. maculata* extract, mangiferin, NAC and metformin *in vitro, ex vivo* and *in vivo* (where applicable).

		C. maculata	Mangiferin	NAC	Metformin
In vitro	Cell viability*	↑↑	-	↑↑	N/A
	Cell function	↑↑	↑	↑↑	N/A
	Oxidative stress	↓↓	↓	↓↓	N/A
Ex vivo*	Cell viability	↑	-	↑	N/A
	Cell function	↑↑	↑	-	N/A
	Oxidative stress	↓↓	↓	↓↓	N/A
In vivo	Glucose tolerance	↑	N/A	-	↑
	Triglyceridaemia	↓	N/A	-	-
	Islet parameters	↑↑	N/A	-	↑

* In PA and STZ exposed β-cells only.

CHAPTER 5

DISCUSSION

The pancreatic β-cell has been shown to be exceedingly vulnerable in T2D patients, both in terms of cell function as well as viability (Meier and Bonadonna, 2013). Pancreatic β-cell dysfunction has been shown to be initiated in the very early stages of T2D, with patients eventually requiring oral anti-diabetic medication and even insulin therapy (Turner, 1998; Meier and Bonadonna, 2013). Decreased β-cell mass associated with the progression of T2D has been reported to be as a result of an imbalance in loss of β-cells, by cell death mechanisms including apoptosis and necrosis, and renewal of β-cells, by either proliferation of existing β-cells or neogenesis (Butler *et al.*, 2003; Bonner-Weir and O'Brien, 2008 and Meier and Bonadonna, 2013). Glucotoxicity, lipotoxicity and inflammation are all associated with an increase in oxidative stress, mitochondrial dysfunction and ER stress, and have been found to be causative features in β-cell dysfunction in T2D (Stumvoll *et al.*, 2005; Maedler, 2008 and Biden *et al.,* 2014). Elevated levels of oxidative stress are characteristic of T2D patients (Johansen *et al.*, 2005; Houstis *et al.*, 2006), which is particularly detrimental to the β-cells, due to their naturally low amounts of cellular antioxidants (Sakuraba *et al.,* 2002; Tanaka *et al.,* 2002; Abdollahi *et al.*, 2004).

Introducing a β-cell protective agent, in combination with current anti-diabetic therapies, may reduce long term complications associated with T2D, as well as slow disease progression, particularly in terms of β-cell mass preservation. Much attention has been given to the potential role of plant-derived extracts and polyphenols in treating diseases such as T2D, predominantly due to their antioxidative and anti-inflammatory properties which contribute to their broad spectrum therapeutic potential (Hanhineva *et al.*, 2010; Ding *et al.*, 2013). South African herbal teas, in particular rooibos and honeybush (*Cyclopia* spp.), are renowned for their antioxidant properties, associated with their phenolic constituents (Joubert *et al.*, 2008) and recently, their anti-diabetic effects (Kawano *et al.,* 2009; Muller *et al.*, 2011; Muller *et al.*, 2012). Thus, for this study, an unfermented, aqueous extract of polyphenol-rich *C. maculata* was considered as a potential agent/therapeutic to protect β-cells in T2D. Aqueous extract was selected as this type of extract is produced by extract manufacturers for use in food and beverages or supplements.

5.1. Toxicity in RIN-5F cells

In order to assess the therapeutic potential of this extract, and its major polyphenol, mangiferin, in β-cells, *in vitro* toxicity models were designed to mimic conditions characteristic of T2D in RIN-5F cells; i.e. the induction of glucotoxicity, lipotoxicity and

inflammation, as well as oxidative stress. The MTT assay was used to assess cell viability following exposure to the aforementioned conditions.

5.1.1. Glucotoxicity in RIN-5F cells

The MTT data showed minimally reduced cell viability induced by 17 mM and 25 mM glucose, with no effect on MTT positivity induced by 35 mM glucose (Fig. 26 A). Since the reductions in MTT positivity were less than 30 %, we also measured cellular ATP to determine if high glucose concentrations were in fact cytotoxic and found no changes (Fig. 26 B). Despite glucotoxicity being a contributing factor in β-cell dysfunction and death, RIN-5F cells in this study showed no changes in cell viability in terms of cellular ATP when exposed to elevated glucose concentrations (up to 35 mM) for 24 hours (Fig. 26 B). It is plausible that these RIN-5F cells have a high tolerance to chronically elevated glucose due to desensitisation (Purrello *et al.,* 1996). Historically, RIN-5F cells, as well as their original clone RIN-m5F, have been reported to exhibit altered glucose metabolism (despite being able to secrete insulin in response to glucose) when compared to isolated islets (Gylfe *et al.,* 1983; Nielsen *et al.*, 1985). It was proposed that glucose induces a net uptake of calcium ions into the RIN cells, in addition to the passive inflow of calcium following glucose stimulation. This means that the additional uptake of calcium is independent of membrane depolarization (Gylfe *et al.,* 1983). The link between the depolarization independent net uptake of calcium in RIN cells and the relative ineffectiveness of hyperglycaemia to induce cytotoxicity under the conditions tested in these cells has yet to be elucidated. It has been shown that increased mitochondrial stimulation by elevated glucose levels alters β-cell calcium flux and decreases insulin secretion (Tordjman *et al.,* 2002). The ensuing reduction in insulin secretion is indicative of mild β-cell dysfunction, and it occurs despite the normal generation of ATP (Maechler *et al.,* 1998). Therefore, moderate cellular dysfunction may be present after 24 hours of glucotoxic conditions in our RIN-5F cells, however, we were unable to detect this since the cytotoxic effects of glucotoxicity in this study were measured in terms of mitochondrial function (MTT positivity and cellular ATP).

Recent studies in RIN-5F cells by Son *et al.* (2012 and 2014) in which the toxic effects of chronic hyperglycemia were investigated, showed that exogenously added AGEs, which are normally formed by glucose directly reacting with free amine groups on proteins and lipids, successfully elicited oxidative stress in these cells. Contrary to our study, Hu *et al.* (2014) demonstrated a low level of glucotoxicity in RIN-5F cells when exposed to 33 mM glucose

over 48 hours, as measured by cell dysfunction. Since we were not able to adequately demonstrate glucotoxic effects in the RIN-5F cells over 24 hours, the use of high glucose as a model to induce cytotoxicity was excluded from the rest of the study.

Lipotoxicity (induced by PA) and toxicity caused by STZ, cytokine and MS were successfully induced, resulting in approximately 50 % cell death following 24 hours exposure to 750 μM PA (Fig. 27), 10 mM STZ (Fig. 28) and a cytokine combination of 1 ng/mL IFN-γ, 0.1 ng/mL IL-1β and 1.1 ng/mL TNF-α (Fig. 29 B), as well as the MS combination of 375 μM PA, 5 mM STZ, 0.5 ng/mL IFN-γ, 0.05 ng/mL IL-1β and 0.55 ng/mL TNF-α (Fig. 30), respectively.

5.1.2. Lipotoxicity in RIN-5F cells

Similar findings for PA induced β-cell toxicity were reported by several researchers for RIN-5F cells (Beeharry *et al.,* 2004), as well as MIN6 (Meidute Abaraviciene *et al.,* 2008; Sargsyan *et al.,* 2008) and INS1E (Sargsyan *et al.,* 2008) β-cell lines. The mechanism(s) of PA induced β-cell toxicity are mediated by lipid metabolites, such as acetyl CoA and ceramide, and result in apoptosis via NF-κB independent pathways (Maedler *et al.,* 2001; Kharroubi *et al.,* 2004).

5.1.3. Streptozotocin toxicity in RIN-5F cells

More than 70 % cell death was observed in INS1 cells exposed to 10 mM STZ for 30 minutes (Pospisilik *et al.,* 2003) and MIN6 cells exposed to 5 mM STZ for 8 hours (Gao *et al.,* 2000), demonstrating increased susceptibility in the INS1 and MIN6 cells to STZ induced cytoxicity compared to the RIN-5F cells used in this study. Approximate LC_{50} levels were achieved at 24 hours of RIN-5F cell exposure to 10 mM STZ. A study by Kweon *et al.* (2011) found the optimal toxic concentration of STZ in RIN-5F cells to be half that of ours (i.e. 5 mM) over double the incubation time (i.e. 48 hours). The discrepancy between the concentrations used in this study could be related to the stability of STZ, particularly at neutral concentrations, such as in culture media. Although similar culture medium was used (RPMI1640 supplemented with 10 % FBS) in the aforementioned and the present study, antibiotics were not included for assay purposes in the present study. This, and other environmental culture conditions, could account for the difference in optimal toxic concentrations used in each study.

5.1.4. Cytokine toxicity in RIN-5F cells

Similar to the present study, a cytokine combination as described above was used by others to induce RIN-5F cell dysfunction and oxidative stress (Tabatabaie *et al.*, 2000), as well as induce mitochondrial membrane depolarization in RIN-m5F cells (Barbu *et al.,* 2002). The cytokine combination used in the present study has been shown to initiate β-cell death by several mechanisms, thus bypassing normally adequate cell defence mechanisms; both IL-1β and TNF-α directly induce NF-κB activation, with IL-1β also secondarily activating NF-κB via ERK 1/2, and IFN-γ stimulates the JAK/STAT-1 pathway (Vincenz *et al.,* 2011; Vetere *et al.* 2014). The combination of these cytokines also stimulate both ROS and RNS (nitric oxide specifically) production in RIN-m5F cells, associated with a nitric oxide dependent loss of mitochondrial membrane potential and resultant cell death by apoptosis and necrosis (Barbu *et al.,* 2002). Increased NF-κB induced inducible nitric oxide synthase activity is responsible for the cytokine induced increase in production of nitric oxide (Kharroubi *et al.,* 2004). Interestingly, the cytokines on their own did not affect RIN-5F cell viability at the concentrations tested in this study (Fig. 29 A). As reported by Wang *et al.* (2010), TNF-α and IFN-γ were also unable to induce β-cell apoptosis on their own.

5.1.5. Multiple stress toxicity in RIN-5F cells

According to current literature at our disposal, no studies have been performed on RIN-5F cells, specifically, which assess the effect of a multiple stressor combination which includes STZ, lipotoxicity (PA) and inflammation (TNF-α/IL-1β/IFN-γ cytokine combination). Such a stressor combination activates multiple, distinct pathways involved in β-cell dysfunction and death that are characteristic of T2D.

In the present study, the use of a combination of stressors (MS), as well as the individual stressors themselves (PA, STZ, CM) to induce toxicity in RIN-5F cells presents an adaptive cell model that represents the conditions in which pancreatic β-cells are found in T2D. The model affords the opportunity to test the effectivity of potential therapeutic agents, including plant extracts, plant polyphenols and other compounds, that may protect β-cells. In this model we are able to assess the ameliorative effect of potential therapeutic agents as well as elucidate their specific protective effect against each of the stressors used in this study. This would provide some insight into the potential mechanism of action of the therapeutic agents in β-cell protection.

5.2. The effect of *C. maculata* extract, mangiferin and NAC on RIN-5F cell and pancreatic islet viability

In order to select an optimal, effective concentration of the *C. maculata* extract, mangiferin and NAC treatments, RIN-5F cell viability was assessed using the MTT and ATP assays following 24 hours exposure to each of the optimised toxic stressors (i.e. PA, STZ, CM and MS) and subsequent exposure to a range of concentrations of extract, mangiferin and NAC. Direct interactions between the treatments (i.e. extract, mangiferin and NAC) and the stressors were eliminated by incubating the cells first with the respective stressors and then incubating with each of the treatments (without stressors present). We were able to demonstrate that even after removal of the stressor(s) 24 hours prior to the assay, cell viability and function remained reduced, indicating that the deleterious effects of the stressors persisted during and after the subsequent treatment period.

The effect on annexin-V and propidium iodide fluorescence of the optimised concentrations of the treatments were then assessed in RIN-5F cells, as well as pancreatic islets isolated from Wistar rats. Decreased cellular ATP and MTT positivity are indicative of reduced mitochondrial function (Brand and Nicholls, 2011) and thus a measure of β-cell viability. Increased annexin-V and propidium iodide fluorescence was used to measure cell death; i.e. apoptosis and necrosis, respectively (Oh *et al.,* 2011). The treatment of RIN-5F cells with *C. maculata* extract and NAC was effective in improving the viability of these cells exposed to STZ (Fig. 41) and PA (Fig. 42) by increasing cellular ATP and MTT positivity, and reducing cellular apoptosis (as seen in a reduction in annexin-V fluorescence) (Fig. 43 A and Fig. 44 A, respectively). The improvement in cellular ATP may potentially be associated with mitochondrial biogenesis and stabilisation of mitochondrial membrane potential, since both STZ and PA are negatively associated with these parameters (Jeng *et al.* 2009).

Since the efficacy of the extract was most pronounced in STZ and PA exposed cells, we attempted to validate this effect in isolated pancreatic islets. In PA exposed islets, the extract and NAC also appeared to decrease early stage apoptosis in terms of annexin-V fluorescence (Fig. 77 A), which validates the effect observed in RIN-5F cells; no effect was, however, observed in STZ exposed islets (Fig. 76 A). The lack of effect of STZ on early apoptosis in isolated islets is an unexpected finding and difficult to explain, but may infer that cell death is predominantly by necrosis. The variance between *in vitro* and *ex vivo*

results in STZ exposed RIN-5F cells and islets, respectively, could also be explained by the fact that β-cells in an islet structure react differently to stimuli compared to conventional, flat cultured insulinoma β-cells. The paracrine effect of other islet cells, such as endothelial cells and α-cells, as well as β-cell to β-cell interactions may be responsible for the different responses (Kelly *et al.,* 2010; Chowdhury *et al.,* 2013). Furthermore, it has been demonstrated that β-cell death in mouse islets occurred via mechanisms that did not involve characteristic changes associated with apoptosis, referred to as necroptosis (Yang and Johnson, 2013). One of the anomalies was that mouse islet β-cells underwent partial apoptosis with no incorporation of annexin-V, whereas MIN6 β-cells underwent classic apoptosis in response to hyperglycaemia, a pro-inflammatory cytokine mix (25 ng/mL TNF-α, 10 ng/mL IL-1β and 10 ng/mL IFN-γ) and an inducer of ER stress (thapsigargin) (Yang and Johnson, 2013). Thus the β-cells in islets isolated from Wistar rats in the present study may also display this altered method of partial apoptotic cell death when exposed to STZ.

The extract, NAC and mangiferin failed to ameliorate the increase in propidium iodide fluorescence induced by STZ (Fig. 76 B) and PA (Fig. 77 B) in isolated islets, indicating that the protective effect is observed in earlier, rather than later stages of apoptosis or necrosis. This infers that cells terminally damaged during exposure to STZ and PA (i.e. propidium iodide positive cells) could not be rescued by subsequent treatment. NAC also showed the ability to improve CM induced toxicity in RIN-5F cells, by increasing cellular ATP (Fig. 41 B). NAC ameliorated late stage apoptosis and necrosis (as measured by propidium iodide fluorescence) in RIN-5F cells exposed to STZ (Fig. 43 B), PA (Fig. 44 B), CM (Fig. 45 B) and MS (Fig. 46 B). These data are consistent with previously reported effects of NAC in β-cells (Kaneto *et al.,* 1999; Hou *et al.,* 2008; Jin *et al.,* 2013). Mangiferin showed some amelioration of STZ (Fig. 35 A) and MS (Fig. 38 A) induced cytotoxicity by increasing MTT positivity. Overall, NAC treatment of the RIN-5F cells, at concentrations ranging from 0.01 mM – 1 mM, showed the largest improvement in cell viability under all cytotoxic conditions except MS (Fig. 39 - 41 and 43 - 45); at the higher concentrations of 10 mM and 20 mM, the efficacy was lost, possibly due to the ability of thiolic compounds (such as NAC) to act as pro-oxidants at high concentrations (Sagrista *et al.,* 2002). The extract improved STZ (Fig. 31 and 43) and PA (Fig. 32 and 44) induced cytotoxicity. The hypolipidaemic effect of the extract, as well as the ability of the extract to blunt the deleterious effects of STZ in rodents will be discussed later (section 5.7.1.). The reduced efficacy of the extract against the effects of inflammation (induced by CM) on RIN-5F cell viability is likely to be the reason that the

extract was also observed to be ineffective against MS induced toxicity. Furthermore, the extent of multifactorial cellular damage induced by MS (even though STZ, PA and CM were diluted ten times in this combination) in the RIN-5F cells may be too severe for amelioration by the extract alone. However, the ability of the extract to reduce any one of these stressors in this MS combination could decrease the potency of the assault on β-cells.

5.3. The effect of *C. maculata* extract, mangiferin and NAC on RIN-5F cell and pancreatic islet function

Cell function in RIN-5F cells was assessed by measuring glucose stimulated insulin secretion, cellular calcium and cell proliferation; in isolated islets, glucose stimulated insulin secretion was used to assess β-cell function. The extract and NAC significantly improved RIN-5F cell function under all four cytotoxic conditions, with mangiferin improving cell function in terms of cell proliferation, only in cells exposed to PA and CM. Similar results were observed in isolated islets, with the extract and mangiferin normalising glucose stimulated insulin secretion in STZ exposed islets (Fig. 78 B), while only the extract reduced the increase in glucose stimulated insulin secretion induced by PA (Fig. 79 B). Interestingly, basal insulin secretion of RIN-5F cells was not affected by the stressors used in this study. This concurs with previous data suggesting that β-cell dysfunction is only truly evident when the cell is challenged, as in this case, by glucose stimulation; this has been described as the second stage of β-cell dysfunction in T2D (Weir and Bonner-Weir, 2004). However, PA was able to increase basal insulin secretion in isolated islets and none of the three treatments were able to ameliorate this increase (Fig. 79 A). Glucose stimulated insulin secretion was increased by STZ (Fig. 47 A) and to a lesser extent, by PA (not significant) (Fig. 48 A) in RIN-5F cells; a similar effect was also observed in the isolated pancreatic islets (Fig. 78 B and 79 B, respectively). The mechanism(s) by which STZ (Fig. 47 B) increases glucose stimulated insulin secretion is unknown, but we postulate that STZ induced alterations in glucose response in the RIN-5F cells may be responsible for the unexpected STZ induced increase in glucose stimulated insulin secretion. It has been demonstrated that STZ alters β-cell responsiveness to glucose; where, initial acute hyperglycaemia and concomitant hypoinsulinaemia two hours post STZ injection in rats is followed by transiently increased levels of circulating insulin (hyperinsulinaemia) and hypoglycaemia (West *et al.,* 1996). The reduction in glucose stimulated insulin secretion induced by the extract in STZ exposed RIN-5F cells and islets could therefore be related to extract induced improvement in cell viability and protection against STZ induced alteration in glucose response (Fig. 47 B and Fig. 78

B). PA is a known stimulus of insulin secretion (Warnotte *et al.,* 1994). The increased insulin secretion in response to direct exposure to exogenous PA may have promoted β-cell adaptations that resulted in increased insulin synthesis and secretion capabilities of these cells, since fatty acids are known to have a large capacity to augment glucose stimulated insulin secretion (Nolan *et al.,* 2006). Such "priming" of the PA exposed cells could cause increased insulin secretion in response to glucose stimulation as a result of increased insulin synthesis (and secretion) capacity. The ability of the extract to normalise the elevated glucose stimulated insulin secretion induced by PA in both RIN-5F cells (Fig. 48 B) and isolated islets (Fig. 79 B) may act as a protective mechanism by promoting β-cell rest by means of a reduction in insulin hypersecretion, similar to the effect of bromocriptine in β-cells (De Leeuw van Weenen *et al.,* 2010). Mangiferin similarly decreased the PA induced increase in glucose stimulated insulin secretion (Fig. 48 B) and, along with NAC, increased glucose stimulated insulin secretion in MS exposed RIN-5F cells (Fig. 50 B). The improvement in glucose stimulated insulin secretion induced by mangiferin was independent of calcium influx since this parameter was in fact reduced in these cells (Fig. 54), and may be due to direct stimulatory effects of cyclic adenosine monophosphate (cAMP) (Ammala *et al.,* 1993). The improved insulin secretion mediated by cAMP may be associated with a stabilising effect on insulin messenger ribonucleic acid (mRNA), as described by Welsh *et al.* (1985), induced by mangiferin in RIN-5F cells and isolated islets.

The *C. maculata* extract ameliorated both the STZ (Fig. 51) and PA (Fig. 52) induced reduction in cellular calcium, with NAC increasing cellular calcium in CM exposed cells (Fig. 53). Normalisation of cellular calcium is crucial to normal functioning of the ER within β-cells, as well as overall β-cell function, particularly in terms of insulin secretion and cell proliferation, often with accompanied regulation of the ERK1/2 pathway (Lipson *et al.,* 2006; Maedler, 2008; Rorsman *et al.,* 2012; Biden *et al.,* 2014). We also cannot exclude that reactive species generated in the β-cells caused degradation of the fluorescent calcium ion probe used in this assay (Sarvazyan and Martinez-Zaguilan*,* 1998).

The extract and NAC ameliorated the reduction of cell proliferation in RIN-5F cells induced by STZ (Fig. 55), PA (Fig. 56), CM (Fig. 57) and MS (Fig. 58), thereby indicating improved β-cell survival, since proliferation has been shown to be directly inhibited in dysfunctional β-cells (Sharma and Alonso, 2014). A concomitant increase in cellular calcium was observed in cells treated with the extract following exposure to STZ (Fig. 51) and PA (Fig. 52), which

may be a contributing factor to the increased proliferation seen in these cells, which could have implications for β-cell regeneration in the T2D pancreas (Herchuelz *et al.,* 2012). Mangiferin only increased PA (Fig. 56) and CM (Fig. 57) induced reductions in proliferation. This protective function, of the extract in particular, in terms of increased proliferation was also observed in the *in vivo* component of this study where increased β-cell proliferation was observed in islets of STZ induced diabetic Wistar rats pretreated with 300 mg/kg/d of the extract (Fig. 98). A concomitant increase in the β-cell area in the islets of extract pretreated rats was also observed, and was comparable to the effect elicited by the reference drug metformin (Fig. 95 A).

Similar improvements in islet structure were observed in STZ induced diabetic rats following treatment with 40 mg/kg/d of mangiferin for 30 days (Sellamuthu *et al.,* 2013). The changes in islet architecture in our study may indicate a progression towards characteristics of a less diseased state, since decreased β-cell mass is a distinguishing factor in T2D patients (Butler *et al.*, 2003; Bonner-Weir and O'Brien, 2008 and Meier and Bonadonna, 2013).

5.4. The effect of *C. maculata* extract, mangiferin and NAC on RIN-5F cell and pancreatic islet oxidative stress

In order to fully understand the effect of the stressors and treatments on total free radicals in this study, we measured both RNS and ROS production, using DAF and DHE fluorescent probes, respectively. We were able to demonstrate that changes in RNS and ROS fluorescence as induced by DMNQ, a known inducer of ROS (Fig. 59), were measurable in the RIN-5F cells. Although RNS is cytotoxic at elevated levels, physiological levels of RNS (i.e. constitutive nitric oxide synthase generated nitric oxide) play an important role in activation of glycolysis, the tricarboxylic acid (TCA) cycle, oxidative phosphorylation to produce ATP, as well as the regulation of insulin release in β-cells (Smukler *et al.,* 2002; Newsholme *et al.,* 2012). It is elevated nitric oxide levels, as a result of inducible nitric oxide synthase, that contributes to cellular oxidative stress and is harmful to cells, including β-cells (Kacheva *et al.,* 2011). In the present study, we were unable to differentiate between constitutive and inducible nitric oxide synthase generated nitric oxide and thus confirmed induction of oxidative stress by also measuring cellular ROS. We found that the stressors used in this study elevated both DAF and DHE, which, as discussed above, resulted in reduced cell viability and function.

The *C. maculata* extract was able to ameliorate both increased DAF and DHE fluorescence in STZ (Fig. 60) and PA (Fig. 61) exposed RIN-5F cells, albeit that the reduction induced by the extract in PA exposed cells was not significant. While NAC ameliorated both increased DAF and DHE fluorescence in STZ exposed cells only (Fig. 60), as well as increased DHE fluorescence induced by PA (Fig. 61) and MS (Fig. 63). Similarly, the extract and NAC ameliorated STZ induced oxidative stress in isolated rat islets as seen in reductions in both DAF (Fig. 80 A) and DHE (Fig. 80 B) fluorescence. As observed in the RIN-5F cells, the extract and NAC ameliorated PA induced increases in DAF (Fig. 81 A) and DHE (Fig. 81 B) fluorescence in the islets. In the PA exposed islets, mangiferin also reduced both DAF (Fig. 81 A) and DHE (Fig. 81 B) fluorescence.

Knowing that β-cells have naturally low levels of antioxidants (Sakuraba *et al.,* 2002; Tanaka *et al.,* 2002; Abdollahi *et al.*, 2004), we were not surprised when we were unable to detect CAT and GSH in the RIN-5F and islet cell lysates. However, total SOD enzyme activity was detected and was in fact altered by the treatments used in this study. The extract, mangiferin and NAC ameliorated the STZ induced reduction in SOD activity in RIN-5F cells (Fig. 64). Similarly, mangiferin and NAC increased SOD activity that was reduced by both STZ (Fig. 82) and PA (Fig. 83) in isolated islets. In the RIN-5F cells, NAC showed some improvement in SOD activity in PA exposed cells (Fig. 65) and mangiferin in MS exposed cells (Fig. 67). Improved SOD enzyme activity could be beneficial to β-cells by reducing the amount of free ROS in the cell (Robertson *et al.,* 2003). However, we have yet to determine the fate of increased hydrogen peroxide produced as a result of SOD conversion of ROS; this is important since, in the presence of heavy metals, hydrogen peroxide forms the highly toxic hydroxyl radical ($^{\cdot}$OH) (Hunt *et al.,* 1988; Newsholme *et al.,* 2012). Overall, we found that the extract and NAC had ameliorative antioxidative activity in the RIN-5F cells and isolated islets.

5.5. The effect of *C. maculata* extract, mangiferin and NAC on protein expression in RIN-5F cells

Although not deemed statistically significant, using a one-way ANOVA, differential expression of proteins can be biologically meaningful if fold change (compared to the normal control) is greater than 1.5 (McCarthy and Smyth, 2009). Both the extract and NAC increased NF-κB expression in RIN-5F cells exposed to STZ by 1.56 fold and 1.58 fold, respectively (Fig. 71 A). The increase may be an adaptive protective mechanism since

relatively small increases in NF-κB may regulate the expression of genes that play important roles in cellular stress responses, cell growth and cell survival (Karin and Lin, 2002). NAC treated cells showed increased cleaved caspase-3 expression in STZ exposed RIN-5F cells (1.77 fold) (Fig. 73 A) and GLUT-2 expression in both STZ (5.15 fold) (Fig. 75 A) and PA (2.70 fold) (Fig. 75 B) exposed cells. The increase in cleaved caspase-3 may indicate that the mechanism of cell death favoured is apoptosis, which is strongly favoured in β-cells rather than the highly inflammatory necrotic process (Augstein *et al.,* 1998). The pro-oncogenic protein BCL-2, known to suppress the intrinsic apoptotic pathway, was unchanged in RIN-5F cells in this study (Fig. 70), indicating that cell protection by the extract or NAC is not regulated by inhibition of apoptosis via the BCL-2 pathway, since BCL-2 expression was not reduced by PA nor STZ. It has been previously demonstrated that STZ has no effect on BCL-2 expression in isolated rat islets (Mellado-Gil and Aguilar-Diosdado, 2004). The increase in GLUT-2 expression induced by NAC may indicate a level of functional restoration of the RIN-5F cells since this constitutive β-cell protein is important in glucose sensing (Schuit, 1997). The decrease in PDX-1 expression in RIN-5F cells exposed to STZ was not ameliorated by any of the three treatments (Fig. 74 A) indicating that STZ induced dysfunction remained present in the RIN-5F cells.

5.6. The variance in efficacy of *C. maculata* extract and mangiferin

Our *in vitro* and *ex vivo* findings suggest that the extract, not exclusively dependent on mangiferin activity, had ameliorative effects on β-cell viability and function with a concomitant reduction in oxidative stress. Mangiferin was not as effective as the whole extract; a similar effect was observed in HepG2 liver cells exposed to tert-butyl hydroperoxide or amiodarone to induce oxidative stress, where *Mangifera indica L.* stem bark aqueous extract induced greater hepatoprotective effects compared to the equivalent mangiferin content concentration on its own (i.e. 20 µg/mL mangiferin) (Tolosa *et al.,* 2013). This was also observed for other polyphenolic extracts and compounds, such as the ameliorative effect of *Olea europea L.* (olive) leaf and fruit extract in INS-1 β-cells, which was also observed to be greater than that of its predominant phenolic compound, oleuropein (Cumaoglu *et al.,* 2011). A study by Muller *et al.* (2012) demonstrated that an aspalathin-enriched extract of unfermented Rooibos, containing 18.44 % aspalathin, was more effective than pure aspalathin at increasing glucose uptake in C2C12 myotubules. The beneficial effects of the *C. maculata* extract may therefore be as a result of synergistic and/or additive effects between the major polyphenolic constituent, mangiferin, and other polyphenols or

constituents (such as polysaccharides; the content of which was not determined) found in the extract. Hesperidin, present at 0.80 % in the extract, has previously been demonstrated to improve glycaemic control in diabetic mice (Jung *et al.,* 2004; Mahmoud *et al.,* 2012), with norathyriol (an aglycone of mangiferin) treatment improving glucose homeostasis and insulin sensitivity in obese C57BL/6J *ob/ob* mice (Ding *et al.,* 2014). Isomangiferin, present at 2.08 % in the extract, has been shown to have a higher peroxyl radical scavenging activity than mangiferin (Malherbe *et al.,* 2014) and may thus significantly contribute to the antioxidant properties of the extract. The role of other minor polyphenolic compounds may also play a significant role that could be as effective as or even more effective than mangiferin due to higher bioavailability. Work on rosmarinic acid has demonstrated that extracts with a high content of different compounds, such as luteolin and apigenin, increases the bioavailability of rosmarinic acid (Fale *et al.,* 2013). Luteolin has also been shown to be present in the extract used in the present study (Schulze, 2013). The complexity of polyphenolic interactions in extracts was further demonstrated when fractionation of an enriched hibiscus extract was shown to be less effective at suppressing adipogenesis than the whole extract (Herranz-Lopez *et al.,* 2012). Similarly, Qin *et al.* (2012) suggested that the correct proportion of specific natural products at sub-potent drug levels could enhance intracellular bioavailability and activity to clinically relevant levels.

5.7. The effect of *C. maculata* extract, metformin and NAC in diabetic Wistar rats

In order to test if the beneficial effects of the extract demonstrated *in vitro* and *ex vivo* have merit, we investigated the *in vivo* effect of the extract in STZ induced diabetic rats following a two-fold approach; i.e. (i) by treating STZ induced diabetic rats, as well as by (ii) pretreating rats prior to STZ induced diabetes. As a potential therapeutic agent in the amelioration of a pre-existing diseased state, the extract and NAC (as well as the reference drug, metformin) were administered to rats five days after injection with STZ; this group of rats is referred to as the treated group and is similar to the approach used *in vitro*. As potential agents that will either prevent or reduce the deleterious effects of STZ in these Wistar rats, extract, NAC and metformin were administered to rats for 15 days prior to STZ injection and for five days post injection and are referred to as the pretreated group.

5.7.1. The effect of *C. maculata* extract, metformin and NAC on metabolic parameters in diabetic Wistar rats

Treating STZ induced diabetic rats with the extract, as well as NAC and metformin, five days after STZ injection did not ameliorate the toxic effects of STZ on glucose metabolism (Fig. 84 A – 89 A). However, pretreatment of the rats with extract resulted in improved glucose tolerance, as observed in reduced AUC of the OGTT (Fig. 86 B) and fasting glucose levels (Fig. 85 B), as well as having a hypotriglyceridaemic effect (Fig. 89 B). The reduction in serum triglycerides by the extract may infer some benefit to hepatic function in these rats (Mahmoud *et al.,* 2012), which may potentially reduce the effects of long-term complications associated with hyperglycaemia and hypertriglyceridaemia, such as cardiovascular disease. Liver function tests on all rats (see addendum 4) revealed no measurable liver toxicity. A study using mangiferin, which is the predominant polyphenol in our extract, demonstrated hypolipidaemic and hypoglycaemic effects in STZ-induced diabetic rats (Muruganandan *et al.*, 2005), which may be as a result of suppression of pancreatic lipase activity by mangiferin (Yoshikawa *et al.,* 2002; Guo *et al.,* 2011). Furthermore, the hypolipidaemic effects of hesperidin, another phenolic constituent of the extract, have also been described in rodent models of T2D (Mahmoud *et al.,* 2012), which may in part be due to the ability of hesperidin to decrease pancreatic lipase activity (Kawaguchi *et al.,* 1997). Hesperidin has also been shown to have direct hepatic effects in C57BL/KsJ-*db/db* mice by increasing hepatic glycolysis and lowering HGP (Jung *et al.,* 2004). The high mangiferin content, as well as the presence of other bio-active and antioxidative compounds in our extract (Dudhia *et al.,* 2013; Malherbe *et al.,* 2014) may be responsible for the amelioration of STZ induced toxicity in the Wistar rats. Although mangiferin on its own was not as effective as the extract in improving cell viability and function in RIN-5F cells and isolated islets, as discussed previously in section 5.6., a synergistic effect between the polyphenols found in our extract should be considered, whereby modulation of hepatic and intestinal enzymes and transporters occurs to improve oral bioavailability (Efferth and Koch, 2011; Yang *et al.,* 2014).

Despite not seeing significant changes in fasting serum insulin values, we found that pretreatment with extract improved insulin sensitivity as determined by the glucose to insulin ratios of the rats (Fig. 88 B), comparable with that of metformin. The glucose to insulin ratio is a more applicable measure of insulin sensitivity than the homeostatic model of assessment of insulin resistance (HOMA-IR) in this study since STZ induced changes are

214

not readily demonstrated by the latter (McAuley *et al.,* 2001). An interesting observation in the fasting serum insulin levels of pretreated rats was that the values of extract pretreated rats were increased by more than double compared to STZ control (Fig. 87 B). Although the increase in fasting serum insulin induced by extract pretreatment was not significant, the more than two-fold increase in circulating insulin could infer substantial improvement in glucose metabolism. Several postulations regarding the mechanism of action of the extract could be derived from the *in vivo* data, in addition to the observed increased fasting insulin, enhancement of insulin action, stimulation of glucose uptake independent of insulin, or reduction of blood glucose in an insulin mimetic manner; thereby suggesting both pancreatic and extra-pancreatic extract effects.

5.7.2. The effect of *C. maculata* extract, metformin and NAC on oxidative stress in diabetic Wistar rats

Interestingly, the *in vitro* and *ex vivo* antioxidative effect was not observed in the overall oxidative status of Wistar rats pretreated with the extract. In fact, no measurable changes were observed in serum levels of CAT (Fig. 92) and GSH (Fig. 93), liver lipid peroxidation (Fig. 91) and liver nitrotyrosine (Fig. 94). We cannot, however, exclude that the extract could have had a pronounced antioxidant effect closer to the induction of diabetes by STZ and that the parameters measured had returned to homeostatic levels by the time blood was collected; this effect may be further substantiated by serum nitrite data of diabetic rats treated post STZ injection being unchanged, even in the STZ control group 28 days after injection. A small reduction in serum nitrites in rats pretreated with extract compared to the increased levels in the STZ control rats was observed, but, given that no other measurable changes were observed in antioxidative measures in this component of the study, it is possible that the changes in serum nitrites are not physiologically significant (Sun *et al.,* 2003). The elevated serum nitrites in the STZ control rats in the latter pretreated group (Fig. 90 B) may have been measurable since these rats were injected with STZ only five days before blood collection. Furthermore, several endogenous and exogenous compounds can interfere with the Griess assay used to measure nitrites in this study, including compounds such as ascorbate, reduced thiols and heparin (Cortas and Wakid, 1990; Ishibashi *et al.,* 2000). We consider the finding of high levels of serum nitrites in rats treated with metformin after STZ injection as aberrant, since this effect was not observed in the pretreated group.

5.7.3. The effect of *C. maculata* extract, metformin and NAC on pancreatic islet morphometry in diabetic Wistar rats

As previously mentioned, an increase in β-cell area and proliferation was induced by the extract (Fig. 98), indicating that pretreatment with the extract offered some protection to the β-cells against the cytotoxicity of STZ. The increased proliferation of β-cells in extract pretreated rats may be an indirect adaptive response due to improved physiological status in these animals (i.e. improved hyperglycaemia, hypertriglyceridaemia and reduced oxidative stress). Since increased β-cell proliferation in the extract pretreated rats was such a significant and unexpected finding, we assessed the incorporation of tritiated thymidine, as well as crystal violet (Fig. 69) into RIN-5F cells exposed to a range of extract concentrations, in order to eliminate the potential mitogenic effect of the extract on β-cells. Crystal violet incorporation was measured in addition to tritiated thymidine incorporation, since we could not exclude the possibility that the extract could affect the intracellular pool of thymidine, inferring that we would not only be measuring thymidine incorporated into DNA, and thus not truly measuring proliferation. We first demonstrated that these RIN-5F cells respond to stimulation of proliferation by exposing them to 25 mM glucose, as well as increasing concentrations of the GLP-1 analogue liraglutide (Fig. 68). These combined data revealed no detectable increase in proliferation induced by the extract and thus no measurable mitogenic effect. A direct extract induced mitogenic effect is even more unlikely, since mangiferin has been shown to inhibit MAPKs both *in vitro* and *in vivo* (Pal *et al.,* 2013). In fact, the highest concentration of extract tested (i.e. 100 µg/mL) showed a reduction in RIN-5F proliferation as measured by both crystal violet and tritiated thymidine incorporation (Fig. 69). The role of the extract in ameliorating inflammation induced by hyperglycaemia has yet to be elucidated, and may in fact play a significant role since mangiferin is seen to reduce TNF-α induced activation of NF-κB in human histiocytic lymphoma cells, as well as inhibit NF-κB and downstream pro-inflammatory cytokines in macrophages (Leiro *et al.,* 2004; Sarkar *et al.,* 2004).

5.8. Potential mechanism(s) of β-cell protection by *C. maculata* extract

We propose that the *C. maculata* extract used in this study ameliorates the deleterious effects of T2D on pancreatic β-cells by reducing oxidative stress, improving mitochondrial and ER function, as well as by improving exogenous factors deleteriously affecting the β-cells (i.e. hyperglycaemia, hypertriglyceridaemia and potentially systemic inflammation)

(Fig. 100). These effects were independent of PDX-1 regulation, with reductions in β-cell apoptosis independent of BCL-2 and caspase-3. Potential systemic anti-inflammatory properties of the extract in rodents may be associated with the high mangiferin content, as previously mentioned (Leiro *et al.,* 2004; Sarkar *et al.,* 2004).

Evidence of reduced oxidative stress in RIN-5F cells and isolated islets included reductions in both ROS and RNS. We found that SOD activity was increased and may thus be responsible for the reduction in ROS observed. Other mechanisms may also ameliorate oxidative stress in β-cells, including improved mitochondrial function (as evident in extract induced increases in cellular ATP and MTT positivity), decreased ER stress, as well as a potential direct radical scavenging effect of the extract. A previous study on the effect(s) of andrographolide, the primary component of *Andrographis paniculata*, in alloxan induced diabetic BALB/c mice and RIN-m cells showed the free radical scavenging effect of the plant derived compound to have β-cell protective effects (Zhang *et al.,* 2009). The study also showed that reduction of NF-κB activation, induced by inflammation, caused a reduction in ROS. In our study we not only observed reduced cell death, in terms of both apoptosis and necrosis, but some β-cell regeneration was evident in terms of increased cell proliferation, both *in vitro* and *in vivo*. The isoflavone, genistein, was shown to enhance both INS1 and human islet β-cell proliferation, as well as β-cell proliferation in the pancreata of STZ induced diabetic mice (Fu *et al.,* 2010). Genistein was thought to modulate this effect via cAMP and protein kinase-A signalling. Furthermore, one of the main green tea catechins, EGCG, has been shown to reduce β-cell apoptosis by decreasing DNA and oxidative damage, and directly scavenging hypoxia induced ROS in rat islets (Hara *et al.,* 2007).

A combination of decreased oxidative stress, improved mitochondrial and cell function, and increased functional β-cell mass as a result of treatment with the *C. maculata* extract used in this study provides some evidence for direct protective effects of the extract on T2D damaged pancreatic β-cells. In addition, pretreatment with the extract blunts and/or ameliorates extra-pancreatic metabolic aberrations, as well as β-cell specific deleterious effects of STZ in Wistar rats.

One of the shortcomings of current T2D treatment is that anti-diabetic medication is only prescribed once hyperglycemia appears. Leading trends in T2D promote proactive treatment of early stages of dysfunctional glucose metabolism, before actual β-cell

217

destruction occurs (Seufert *et al.*, 2004). Such a therapeutic approach is supported by the *in vivo* component of our study, whereby the *C. maculata* extract assessed demonstrated the ability to protect β-cells prior to the induction of diabetes by STZ in Wistar rats. However, the extract, on its own, was ineffective at restoring β-cell function following destruction of β-cells induced by STZ. It may be possible that this extract, prepared from unfermented *C. maculata*, in combination with current hypoglycaemic drugs, will enhance T2D therapy by protecting the functional β-cell mass.
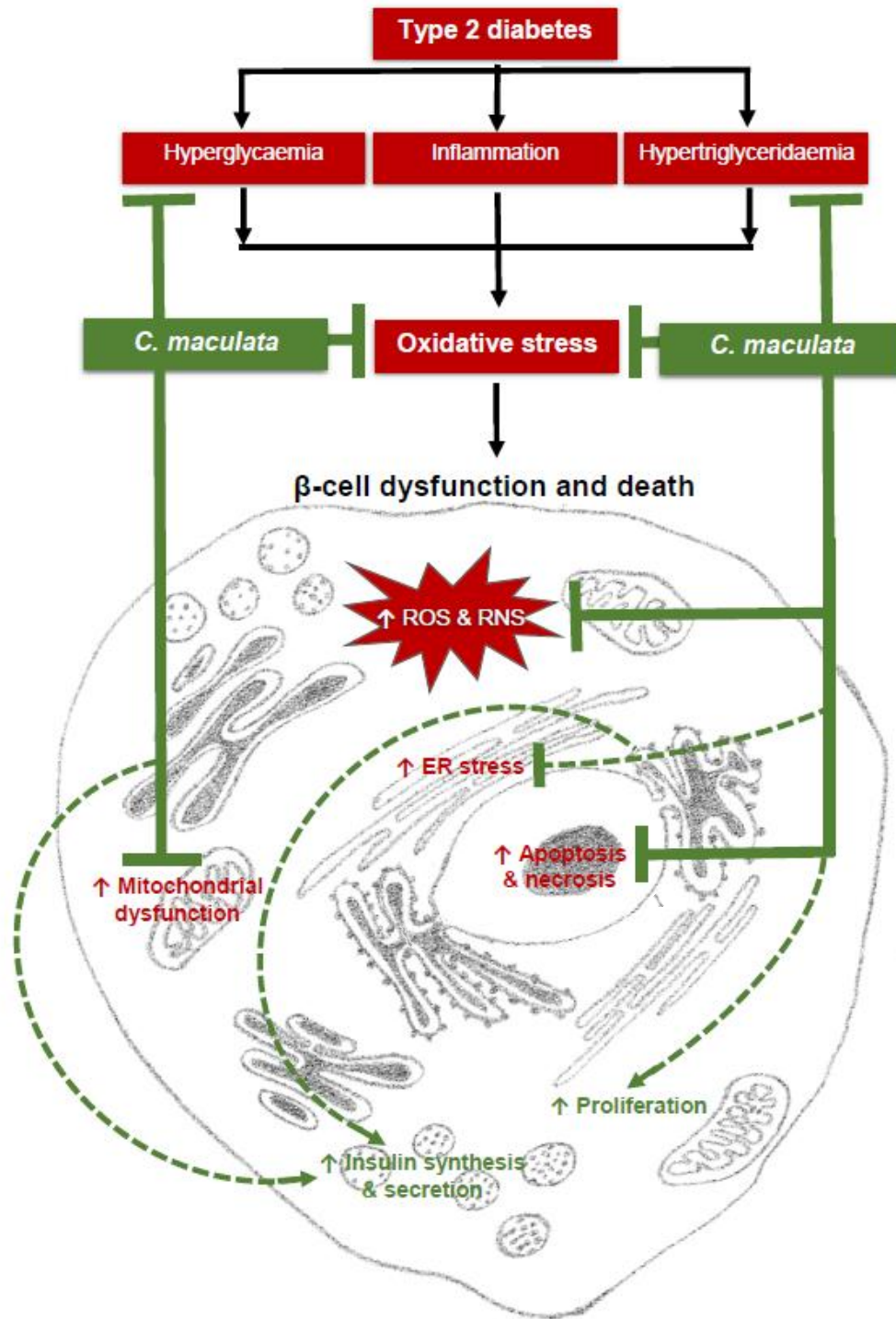
Figure 100. Potential mechanism(s) of β-cell protection by unfermented, aqueous *C. maculata* extract.

Cyclopia maculata extract ameliorates the deleterious effects of T2D on pancreatic β-cells by improving STZ induced hyperglycaemia, hypertriglyceridaemia and potentially resultant systemic inflammation, as well as by reducing oxidative stress and improving β-cell mitochondrial and ER function. The resultant effect is improved β-cell function and reduced β-cell death. Type 2 diabetes associated hypertriglyceridaemia, inflammation and oxidative stress were mimicked *in vitro* in this study using PA, CM and STZ (ER – endoplasmic reticulum; RNS – reactive nitrogen species; ROS – reactive oxygen species).

CHAPTER 6

CONCLUSIONS

Several conclusions arise from this study, with the most prominent and promising being that the aqueous extract of unfermented *C. maculata* does in fact offer protection to pancreatic β-cells exposed to conditions characteristic of T2D. In particular, the extract was observed to protect RIN-5F cells and isolated rat pancreatic islets from the deleterious effects of STZ and lipotoxicity, induced by PA, by reducing oxidative stress and improving mitochondrial function. Concomitantly, β-cell function was improved in the RIN-5F cells and islets.

The extract was observed to be substantially more effective than its most abundant polyphenol, mangiferin, while showing similar effectivity to NAC *in vitro* and *ex vivo.*

In vivo, pretreatment of STZ induced diabetic Wistar rats with the extract improved glucose metabolism similar to that of metformin, with a reduction in hypertriglyceridaemia. Improvements in pancreatic islet morphology were also observed in the pretreated Wistar rats, with increased β-cell proliferation and a concomitant increase in the β-cell to total islet area. However, treating already diabetic Wistar rats had no restorative effects on pancreatic β-cells.

In RIN-5F cells, β-cell proliferation was also enhanced by the extract in a non-mitogenic manner. This finding is important since depletion of β-cell mass, as a result of reduced β-cell replenishment following increased apoptosis, is characteristic of T2D. Not only was proliferation increased both *in vitro* and *in vivo*, but the ability of the extract to reduce apoptosis was also observed in the RIN-5F cells and isolated islets.

In combination with current T2D therapies, a formulation of the aqueous extract of unfermented *C. maculata* may slow disease progression and reduce long term complications associated with T2D by protecting pancreatic β-cells.

Shortcomings and future work arising from this study

The inability to induce glucotoxicity in the RIN-5F cells was a shortcoming of this study that requires further investigation, particularly since the role of glucolipotoxicity is so prominent in T2D. The predefined conditions of cytotoxicity in the RIN-5F cells in this study (i.e. LC_{50}, as determined by reduction of mitochondrial function and ATP production) limited the assessment of glucotoxicity as an effective stressor in these cells. Future studies into the glucotoxic effects in RIN-5F cells will require additional measurements of cell viability and function in order to determine an effective glucotoxic concentration; the use of the MTT and ATP assays have their limitations, since these cells are able to maintain mitochondrial function despite defective insulin synthesis and secretion induced by glucotoxic conditions (Maechler *et al.,* 1998).

The role of IRS-2 overexpression in reducing the toxic effect of elevated glucose has been previously reported (Maedler *et al.,* 2007) and should be assessed in the RIN-5F cells used in this study, either by immunohistochemical labelling or Western blot analysis. A longer incubation period should also be considered, since a previous study reported that 48 hours of glucotoxicity induced β-cell dysfunction in RIN-5F cells (Hu *et al.,* 2014). The use of exogenously added AGEs to induce glucotoxicity could also be considered, since they are derived from the direct reaction of glucose with free amine groups on proteins and lipids.

In this study apoptosis and necrosis were measured using the annexin-V and propidium iodide assay in order to determine changes in β-cell viability in RIN-5F cells and isolated islets. In order to extract further information regarding changes in apoptosis and necrosis, flow cytometric analysis of single cell suspensions could be used to measure the co-expression of annexin-V and propidium iodide cell populations, thereby further distinguishing the apoptotic stages. To further elucidate the effect on apoptosis in this study, particularly in light of no measurable changes in BCL-2 protein expression, other proteins involved in intrinsic and extrinsic apoptotic pathways should be investigated. These include Fas, BAX, BCL-XL, p53 and cytochrome C.

The source of the increased RNS production observed *in vitro* and *ex vivo* requires further investigation since we were unable to determine if the increased levels of nitric oxide was as a result of increased stimulation of inducible or constitutive nitric oxide synthase. The use

of specific inducible nitric oxide synthase inhibitors (e.g. lentiviral vector gene silencing or the 1400W molecule) (Hynes *et al.,* 2011; Quintana-Lopez *et al.,* 2013) or Western blot analysis of inducible nitric oxide synthase protein expression should thus be considered.

In order to further assess the antioxidative effect(s) of the extract, the fate of hydrogen peroxide produced as a result of elevated SOD activity should be investigated. In this study, the commercial kits used to detect GSH and CAT (which are responsible for decomposing hydrogen peroxide) in RIN-5F cells and isolated islets were unable to detect the substantially low levels of the respective antioxidant molecules. More sensitive detection kits could be considered and Western blot detection of the protein expression or changes in mRNA expression ought to be assessed.

Another limitation in this study was the lack of measurable changes in antioxidant parameters measured in the Wistar rats. The measurement of serum antioxidant parameters should be constantly monitored over time from STZ induction of diabetes (and not just at the end of the treatment period) in order to determine the precise antioxidative effect, if any, of the extract *in vivo.*

The *in vivo* anti-inflammatory effect(s) of the extract require further elucidation, particularly since mangiferin has been reported to have anti-inflammatory effects in diabetic models (Leiro *et al.,* 2004; Sarkar *et al.,* 2004). Inflammatory markers in stored serum and tissue (liver and pancreas) could be determined.

The interesting finding in this study, that both STZ and lipotoxicity induced increases in glucose stimulated insulin secretion, warrants further investigation into the regulation of insulin secretion by both the stressors (STZ and PA), as well as the effect of the extract. Current literature is severely limited in reporting on this aspect of insulin secretion, with mechanisms of stress induced increases in insulin secretion being near absent. Determining total insulin synthesised (not just secreted) by the β-cells, by also quantifying intracellular insulin *per se*, should be considered in future studies.

Since we propose that a formulation of the *C. maculata* extract may be beneficial as an adjunctive therapy in T2D, further investigation is needed to validate the effects of co-therapeutics, both with current antidiabetic drugs (e.g. metformin, TZDs or liraglutide), as

well as different combination effects of the polyphenolic constituents of the extract (e.g. hesperidin in combination with mangiferin).

"There will come a time when you believe everything is finished; that will be the beginning."

Louis L'Amour

REFERENCES

Abdollahi M, Ranjbar A, Shadnia S, Shekoufeh N and Rezaie A. Pesticide and oxidative stress: a review. *Med Sci Monit.* 2004; 10: 141-147.

Akiyama S, Katsumata S-I, Suzuki K, Ishimi Y, Wu J and Uehara M. Dietary hesperidin exerts hypoglycemic and hypolipidemic effects in streptozotocin-induced marginal type 1 diabetic rats. *J Clin Biochem Nutr.* 2010; 46(1): 87–92.

Alberti KGMM and Zimmet PZ. Diabetes: a look to the future. *Lancet Diabetes Endocrin.* 2014; 2(1): e1-e2.

Ammala C, Ashcroft FM and Rorsman P. Calcium-independent potentiation of insulin release by cyclic AMP in single β-cells. *Nature* 1993; 363(6427): 356-358.

Andreu GP, Delgado R, Velho JA, Curti C and Vercesi AE. Iron complexing activity of mangiferin, a naturally occurring glucosylxanthone, inhibits mitochondrial lipid peroxidation induced by Fe2+-citrate. *Eur J Pharmacol.* 2005; 513(1-2): 47-55.

Anitha S and Rose AML. Comparative evaluation of antihyperglycaemic effect of various parts of *Salacia chinensis L. J Med Sci (Pakistan)* 2013; 13: 493-496.

Arora S. Molecular mechanisms of insulin resistance in type 2 diabetes mellitus. *World J Diabetes* 2010; 1(3): 68-75.

Augstein P, Elefanty AG, Allison J and Harrison LC. Apoptosis and β-cell destruction in pancreatic islets of NOD mice with spontaneous and cyclophosphamide-accelerated diabetes. *Diabetologia* 1998; 41: 1381-1388.

Aziz A and Wheatcroft S. Insulin resistance in type 2 diabetes and obesity: implications for endothelial dysfunction. *Expert Rev Cardiovasc Ther.* 2011; 9(4): 403-407.

Bahadoran Z, Mirmiran P and Azizi F. Dietary polyphenols as potential nutraceuticals in management of diabetes: a review. *J Diabetes Metab Disord.* 2013; 12(1): 12-43.

Barbu A, Welsh N and Saldeen J. Cytokine-induced apoptosis and necrosis are preceded by disruption of the mitochondrial membrane potential (Δψm) in pancreatic RINm5F cells: prevention by Bcl-2. *Mol Cell Endocrinol.* 2002; 190(1–2): 75–82.

Bastard JP, Maachi M, Lagathu C, Kim MJ, Caron M, Vidal H, Capeau J and Feve B. Recent advances in the relationship between obesity, inflammation and insulin resistance. *Eur Cytokine Netw.* 2006; 17: 4-12.

Beeharry N, Chambers JA and Green IC. Fatty acid protection from palmitic acid-induced apoptosis is lost following PI3-kinase inhibition. *Apoptosis* 2004; 9(5): 599-607.

Benoit SC, Air EL, Coolen LM, Strauss R, Jackman A, Clegg DJ, Seeley RJ and Woods SC. The catabolic action of insulin in the brain is mediated by melanocortins. *J Neurosci.* 2002; 22: 9048–9052.

Bertram MY, Jaswal AV, Van Wyk VP, Levitt NS and Hofman KJ. The non-fatal disease burden caused by type 2 diabetes in South Africa, 2009. *Glob Health Action* 2013; 6(19244): 206-212.

Biden TJ, Boslem E, Chu KY and Sue N. Lipotoxic endoplasmic reticulum stress, β-cell failure, and type 2 diabetes mellitus. *Trends Endocrinol Metab.* 2014; Epub ahead of print. Doi: 10.1016/j.tem.2014.02.003.

Bonner-Weir S and O'Brien TD. Islets in type 2 diabetes: In honor of Dr. Robert C. Turner. *Diabetes* 2008; 57(11): 2899-2904.

Bosi E, Lucotti P, Setola E, Monti L and Piatti PM. Incretin-based therapies in type 2 diabetes: A review of clinical results. *Diab Res Clin Res.* 2008; 82: 102-107.

Boslem E, Weir JM, MacIntosh G, Sue N, Cantley J, Meikle PJ and Biden TJ. Alteration of endoplasmic reticulum lipid rafts contributes to lipotoxicity in pancreatic b-cells. *J Biol Chem.* 2013; 288: 26569–26582.

Baynes JW. Role of oxidative stress in development of complication in diabetes. *Diabetes* 1991; 40: 405-411.

Bradford MM. Rapid and sensitive method for the quantitation of microgram quantities of protein utilizing the principle of protein-dye binding. *Anal Biochem.* 1976; 72: 248-254.

Brand MD and Nicholls DG. Assessing mitochondrial dysfunction in cells. *Biochem J.* 2011; 435(2): 297–312.

Brash AR. Lipoxygenases: Occurrence, functions, catalysis and acquisition of substrate. *J Biol Chem.* 1999; 274: 23679-23682.

Brissova M, Fowler MJ, Nicholson WE, Chu A, Hirshberg B, Harlan DM and Powers AC. Assessment of human pancreatic islet architecture and composition by laser scanning confocal microscopy. *J Histoch Cytochem.* 2005; 53(9): 1087–1097.

Buchanan TA, Xiang AH, Peters RK, Kjos SL, Marroquin A, Goico J, Ochoa C, Tan S, Berkowitz K, Hodis HN and Azen SP. Preservation of pancreatic β-cell function and prevention of type 2 diabetes by pharmacological treatment of insulin resistance in high-risk Hispanic women. *Diabetes* 2002; 51: 2796–2803.

Buteau J, Foisy S, Rhodes CJ, Carpenter L, Biden TJ and Prentki M. Protein kinase C zeta activation mediates glucagon-like peptide-1-induced pancreatic beta-cell proliferation. *Diabetes* 2001; 50(10): 2237-2243.

Butler AE, Janson J, Bonner-Weir S, Ritzel R, Rizza RA and Butler PC. Beta-cell deficit and increased beta-cell apoptosis in humans with type 2 diabetes. *Diabetes* 2003; 52: 102-110.

Cartailler J-P. Insulin – from secretion to action. *Beta Cell Biology Consortium* 2001; 1-4.

Cerf ME. Beta cell dynamics: beta cell replenishment, beta cell compensation and diabetes. *Endocrine* 2013; 44(2): 303-311.

Chellan N, De Beer D, Muller CJF, Joubert E and Louw J. A toxicological assessment of *Athrixia Phylicoides* aqueous extract following chronic ingestion in a rat model. Hum *Exp Toxicol.* 2008; 27(11): 819-825.

Chen J, Rogers SC and Kavdia M. Analysis of kinetics of dihydroethidium fluorescence with superoxide using xanthine oxidase and hypoxanthine assay. *Ann Biomed Eng.* 2013; 41(2): 327-37.

Chen WP, Chi TC, Chuang LM and Su MJ. Resveratrol enhances insulin secretion by blocking KATP and KV channels of beta cells. *Eur J Pharmacol.* 2007; 568: 269–277.

Cheng JT and Liu IM. Stimulatory effect of caffeic acid on alpha1A-adrenoceptors to increase glucose uptake into cultured C2C12 cells. *Naunyn Schmiedebergs Arch Pharmacol.* 2000; 362:122–127.

Chowdhury A, Dyachok O, Tengholm A, Sandler S and Bergsten P. Functional differences between aggregated and dispersed insulin-producing cells. *Diabetologia* 2013; 56(7): 1557-1568.

Cnop M, Welsh N, Jonas JC, Jorns A, Lenzen S and Eizirik DL. Mechanisms of pancreatic beta-cell death in type 1 and type 2 diabetes: many differences, few similarities. *Diabetes* 2005; 54(2): S97-S107.

Collins QF, Liu HY, Pi J, Liu Z, Quon MJ and Cao W: Epigallocatechin-3-gallate (EGCG), a green tea polyphenol, suppresses hepatic gluconeogenesis through 5′-AMP-activated protein kinase. J Biol Chem. 2007; 282: 30143–30149.

Cortas N and Wakid NW. Determination of inorganic nitrate in serum and urine by a kinetic cadmium-reduction method. *Clin Chem.* 1990; 36: 1440-1443.

Crouch S, Kozlowski R, Slater K and Fletcher J. The use of ATP bioluminescence as a measure of cell proliferation and cytotoxicity. *J Immunol Methods* 1993; 160(1): 81-88.

Cumaoglu A, Ari N, Kartal M and Karasu C. Polyphenolic extracts from *Olea europea L.* protect against cytokine-induced β-cell damage through maintenance of redox homeostasis. *Rejuvenation Res.* 2011; 14(3): 325-334.

Dandona P, Aljada A and Bandyopadhyay A. Inflammation: the link between insulin resistance, obesity and diabetes. *Trends Immunol.* 2004; 25(1): 4-7.

De Beer D and Joubert E. Development of HPLC method for *Cyclopia subternata* phenolic compound analysis and application to other *Cyclopia spp. J Food Comp Anal.* 2010; 23: 289–297.

De Leeuw van Weenen JE, Parlevliet ET, Maechler P, Havekes LM, Romijn JA, Ouwens DM, Pijl H and Guigas B. The dopamine receptor D2 agonist bromocriptine inhibits glucose-stimulated insulin secretion by direct activation of the alpha2-adrenergic receptors in beta cells. *Biochem Pharmacol.* 2010; 79(12): 1827-1836.

Del PS, Bianchi C and Marchetti P. Beta-cell function and anti-diabetic pharmacotherapy. *Diabetes Metab Res Rev.* 2007; 23(7): 518–527.

De Marchi U, Thevenet J, Hermant A, Dioum E and Wiederkehr A. Calcium co-regulates oxidative metabolism and ATP synthase-dependent respiration in pancreatic beta cells. *J Biol Chem.* 2014; 289(13): 9182-9194.

Deutschlander MS, Van de Venter M, Roux S, Louw J and Lall N. Hypoglycemic activity of four plant extracts traditionally used in South Africa for diabetes. *J Ethnopharmacol.* 2009; 124: 619-624.

Dimitrakoudis D, Vranic M and Klip A. Effects of hyperglycemia on glucose transporters of the muscle: Use of the renal glucose reabsorption inhibitor phlorizin to control glycemia. *J Am Soc Nephrol.* 1992; 3: 1078–1091.

Ding Y, Zhang Z, Dai X, Jiang Y, Bao L, Li Y and Li Y. Grape seed proanthocyanidins ameliorate pancreatic beta-cell dysfunction and death in low-dose streptozotocin- and high-carbohydrate/high-fat diet-induced diabetic rats partially by regulating endoplasmic reticulum stress. *Nutr Metab.* 2013; 10(51): 1-12.

Ding H, Zhang Y, Xu C, Hou D, Li J, Zhang Y, Peng W, Zen K, Zhang CY and Jiang X. Norathyriol reverses obesity- and high-fat-diet-induced insulin resistance in mice through inhibition of PTP1B. *Diabetologia* 2014. Epub ahead of print.

Dixit VD. Nlrp3 inflammasome activation in type 2 diabetes: is it clinically relevant? *Diabetes.* 2013; 62(1): 22–24.

Donath MY, Ehses JA, Maedler K, Schumann DM, Ellingsgaard H, Eppler E and Reinecke M. Mechanisms of beta-cell death in type 2 diabetes. *Diabetes* 2005; 54(2): S108-S113.

Dudhia Z, Louw J, Muller C, Joubert E, De Beer D, Kinnear C and Pheiffer C. *Cyclopia maculata* and *Cyclopia subternata* (honeybush tea) inhibits adipogenesis in 3T3-L1 pre-adipocytes. *Phytomedicine* 2013; 20: 401-408.

Efferth T and Koch E. Complex interactions between phytochemicals: The multi-target therapeutic concept of phytotherapy. *Curr Drug Targets* 2011; 12(1): 122-132.

Ehses JA, Perren A, Eppler E, Ribaux P, Pospisilik JA, Maor-Cahn R, Gueripel X, Ellingsgaard H, Schneider MK, Biollaz G, Fontana A, Reinecke M, Homo-Delarche F and Donath MY. Increased number of islet-associated macrophages in type 2 diabetes. *Diabetes.* 2007; 56(9): 2356–2370.

Elayat AA, el-Naggar MM and Tahir M. An immunocytochemical and morphometric study of the rat pancreatic islets. *J Anat.* 1995; 186(3): 629–637.

Elmore S. Apoptosis: a review of programmed cell death. *Toxicol Pathol.* 2007; 35(4): 495-516.

Elsner M, Guldbakke B, Tiedge M, Munday R, Lenzen S. Relative importance of transport and alkylation for pancreatic beta-cell toxicity of streptozotocin. *Diabetologia* 2000; 43: 1528-1533.

Emanuelli B, Glondu M, Filloux C, Peraldi P and Van Obberghen E. The potential role of Socs-3 in the interleukin-1β-induced desensitization of insulin signaling in pancreatic β-cells. *Diabetes* 2004; 53(3): S97-S103.

Fale PL, Ascensaob L and Serralheiro MLM. Effect of luteolin and apigenin on rosmarinic acid bioavailability in Caco-2 cell monolayers. *Food Funct.* 2013; 4: 426-431.

Feldman M, Friedman LS, Brandt LJ and Marvin H. Sleisenger & Fordtran's gastrointestinal and liver disease pathophysiology, diagnosis, management, 9th edition. *MD Consult* 2009.

Flodstrom M, Welsh N and Eizirik DL. Cytokines activate the nuclear factor kappa B and induce nitric oxide production in human pancreatic islets. *FEBS Letters* 1996; 385 (1-2): 4-6.

Fraga CG, Galleano M, Verstraeten SV and Oteiza PI. Basic biochemical mechanisms behind the health benefits of polyphenols. *Mol Aspects Med.* 2010; 31(6): 435-445.

Frei B. Efficacy of dietary antioxidants to prevent oxidative damage and inhibit chronic disease. *J Nutr.* 2004; 134(11): 3196S-3198S.

Fu Z, Zhang W, Zhen W, Lum H, Nadler J, Bassaganya-Riera J, Jia Z, Wang Y, Misra H and Liu D. Genistein induces pancreatic β-cell proliferation through activation of multiple signalling pathways and prevents insulin-deficient diabetes in mice. *Endocrinology* 2010; 151(7): 3026–3037.

Gao Y, Parker GJ and Hart GW. Streptozotocin-induced β-cell death is independent of its inhibition of O-GlcNAcase in pancreatic Min6 cells. *Arch Biochem Biophys.* 2000; 15; 383(2): 296-302.

Guo F, Huang C, Liao X, Wang Y, He Y, Feng R, Li Y and Sun C. Beneficial effects of mangiferin on hyperlipidemia in high-fat-fed hamsters. *Mol Nutr Food Res.* 2011; 55(12): 1809-1818.

Giannarelli R, Aragona M, Coppelli A and Del Prato S. Reducing insulin resistance with metformin: the evidence today. *Diabetes Metab.* 2003; 4(2): S28-S35.

Gilon P, Ravier MA, Jonas JC and Henquin JC. Control mechanisms of the oscillations of insulin secretion *in vitro* and *in vivo. Diabetes* 2002; 51(1): S144–S151.

Giorda CB, Nada E, Tartaglino B, Marafetti L and Gnavi R. A systematic review of acute pancreatitis as an adverse event of type 2 diabetes drugs. *Diabetes Obes Metab.* 2014; Epub ahead of print - doi: 10.1111/dom.12297.

Green LC, Wagner DA, Glogowski J, Skipper PL, Wishnok JS and Tannenbaum SR. Analysis of nitrate, nitrite and nitrate in biological fluids. *Anal Biochem.* 1982; 126: 131–138.

Grisham MB, Johnson GG and Lancaster JR Jr. Quantitation of nitrate and nitrite in extracellular fluids. *Methods Enzymol.* 1996; 268: 237-246.

Guidelines on ethics for medical research: use of animals in research and training. South African Medical Research Council (MRC) 2004.

Gurgul E, Lortz S, Tiedge M, Jorns A and Lenzen S. Mitochondrial catalase overexpression protects insulin-producing cells against toxicity of reactive oxygen species and proinflammatory cytokines. *Diabetes* 2004; 53(9): 2271-2280.

Gylfe E, Andersson T, Rorsman P, Abrahamsson H, Arkhammar P, Hellman P, Hellman B, Oie HK, Gazdar AF. Depolarization-independent net uptake of calcium into clonal insulin-releasing cells exposed to glucose. *Bioscience Reports* 1983; 3(10): 927-937.

Hanhineva K, Torronen R, Bondia-Pons I, Pekkinen J, Kolehmainen M, Mykkanen H and Poutanen K. Impact of dietary polyphenols on carbohydrate metabolism. *Int J Mol Sci.* 2010; 11: 1365-1402.

Hara Y, Fujino M, Takeuchi M and Li X-K. Green-tea polyphenol (-)-epigallocatechin-3-gallate provides resistance to apoptosis in isolated islets. *J Hepatobiliary Pancreat Surg* 2007; 14: 493–497.

Harkonen PL, Laaksonen EI, Valve EM, Solic N and Darbre PD. Temperature-sensitive mutants for steroid-sensitive growth of S115 mouse mammary tumour cells. *Exp Cell Res.* 1990; 186(2): 288-298.

Henningsson R, Salehi A and Lundquist I. Role of nitric oxide synthase isoforms in glucose-stimulated insulin release. *Am J Physiol Cell Physiol.* 2002; 283: C296-C304.

Henquin JC, Ravier MA, Nenquin M, Jonas JC and Gilon P.Hierarchy of the beta-cell signals controlling insulin secretion. *Eur J Clin Invest.* 2003; 33(9): 742-750.

Herchuelz A, Nguidjoe E, Jiang L and Pachera N. β-Cell preservation and regeneration in diabetes by modulation of β-cell Ca^{2+} homeostasis. *Diabetes Obes Metab.* 2012; 14(3): 136-142.

Herranz-Lopez M, Fernandez-Arroyo S, Perez-Sanchez A, Barrajon-Catalan E, Beltran-Debon R, Menendez JV, Alonso-Villaverde C, Segura-Carretero A, Joven J and Micol V. Synergism of plant-derived polyphenols in adipogenesis: Perspectives and implications. *Phytomedicine* 2012; 19(3-4): 253-261.

Hirosumi J, Tuncman G, Chang L, Gorgun CZ, Uysal KT, Maeda K, Karin M and Hotamisligil GS.. A central role for JNK in obesity and insulin resistance. *Nature* 2002; 420(6913): 333–336.

Hoehn KL, Hohnen-Behrens C, Cederberg A, Wu LE, Turner N, Yuasa T, Ebina Y and James DE. IRS1-independent defects define major nodes of insulin resistance. *Cell Metab.* 2008; 7:421-433.

Holt RI, Barnett AH and Bailey CJ. Bromocriptine: old drug, new formulation and new indication. *Diabetes Obes Metab.* 2010; 12: 1048–57.

Hou N, Torii S, Saito N, Hosaka M and Takeuchi T. Reactive oxygen species-mediated pancreatic beta-cell death is regulated by interactions between stress-activated protein kinases, p38 and c-Jun N-terminal kinase, and mitogen-activated protein kinase phosphatases. *Endocrinology* 2008; 149: 1654–1665.

Houstis N, Rosen DE and Lander ES. Reactive oxygen species have a causal role in multiple forms of insulin resistance. *Nature* 2006; 440: 944-948.

Hsu FL, Chen YC and Cheng JT. Caffeic acid as active principle from the fruit of *Xanthium strumarium* to lower plasma glucose in diabetic rats. *Planta Med.* 2000; 66: 228–230.

Hu Y-C, Hao D-M, Zhou L-X, Zhang Z, Huang N, Hoptroff M and Lu Y-H. 2′,4′-Dihydroxy-6′-methoxy-3′,5′-dimethylchalcone protects the impaired insulin secretion induced by glucotoxicity in pancreatic β‑cells. *J Agric Food Chem.* 2014; 62: 1602−1608.

Hunt JV, Dean RT and Wolff SP. Hydroxyl radical production and autoxidative glycosylation: glucose autoxidation as the cause of protein damage in the experimental glycation model of diabetes mellitus and ageing. *Biochem J.* 1988; 256: 205–212.

Hynes SO, McCabe C and O'Brien T. β-cell protection by inhibition of iNOS through lentiviral vector-based strategies. *Methods Mol Biol.* 2011; 704: 153-168.

Ichiki H, Miura T, Kubo M, Ishihara E, Komatsu Y, Tanigawa K and Okada M. New antidiabetic compounds, mangiferin and its glucoside. *Biol Pharm Bull.* 1998; 21: 1389-1390.

International Diabetes Federation. IDF Diabetes Atlas, 6th edition. Brussels, Belgium: International Diabetes Federation, 2013; http://www.idf.org/diabetesatlas.

International Federation of Clinical Chemistry. Provisional Recommendations on IFCC Methods for the Measurement of Catalytic Concentrations of Enzymes. *Clin Chem.* 1977; 23: 887.

Invitrogen, Countess™ Automated Cell Counter Manual, 2009.

Ishibashi T, Himeno M, Imaizumi N, Maejima K, Nakano S, Uchida K, Yoshida J and Nishio M. NOx contamination in laboratory ware and effect of countermeasures. *Nitric Oxide* 2000; 4: 516-525.

Iwata M, Haruta T, Usui I, Takata Y, Takano A, Uno T, Kawahara J, Ueno E, Sasaoka T, Ishibashi O and Kobayashi M. Pioglitazone ameliorates tumor necrosis factor-alpha-induced insulin resistance by a mechanism independent of adipogenic activity of peroxisome proliferator–activated receptorgamma. *Diabetes* 2001; 50: 1083–1092.

Jeng JY, Yeh TS, Chiu YH, Lee YC, Cheng HH and Hsieh RH. Linoleic acid promotes mitochondrial biogenesis and maintains mitochondrial structure for prevention of streptozotocin damage in RIN-m5F cells. *Biosci Biotechnol Biochem.* 2009; 73(6): 1262-1267.

Jin HM, Zhou DC, Gu HF, Qiao QY, Fu SK, Liu XL and Pan Y. Antioxidant N-acetylcysteine protects pancreatic β-cells against aldosterone-induced oxidative stress and apoptosis in female db/db mice and insulin-producing MIN6 cells. *Endocrinology* 2013; 154(11): 4068-4077.

Johansen JS, Harris AK, Rychky DJ and Erul A. Oxidative stress and the use of antioxidants in diabetes: Linking basic science to clinical practice. *Cardiovasc Diabetol.* 2005; 4(1): 5-16.

Johnston KL, Clifford MN and Morgan LM. Coffee acutely modifies gastrointestinal hormone secretion and glucose tolerance in humans: glycemic effects of chlorogenic acid and caffeine. *Am J Clin Nutr.* 2003; 78: 728–733.

Joubert E, Gelderblom WC, Louw A and de Beer D. South African herbal teas: *Aspalathus linearis, Cyclopia spp.* and *Athrixia phylicoides* – a review. *J Ethnopharmacol.* 2008a; 119: 376–412.

Joubert E, Joubert ME, Bester C, De Beer D and De Lange JH. Honeybush (*Cyclopia spp.*): From local cottage industry to global markets – the catalytic and supporting role of research. *S Afr J Bot.* 2011; 77: 887–907.

Joubert E, Muller CJF, De Beer D, Johnson R, Chellan N and Louw J. The potential role of phenolic acids in tea and herbal teas in modulating effects of obesity and diabetes. In: Phenolic Acids: Composition, Applications and Health Benefits (Edited by Munne-Bosch S). *Nova Science Publishers*, Inc. 2012; ISBN: 978-1-61942-032-82011.

Joubert E, Richards ES, Van der Merwe JD, De Beer D, Manley M and Gelderblom WCA. Effect of species variation and processing on phenolic composition and *in vitro* antioxidant activity of aqueous extracts of *Cyclopia spp.* (honeybush tea). *J Agric Food Chem.* 2008b; 56: 954–963.

Jung UJ, Lee MK, Jeong KS and Choi MS. The hypoglycemic effects of hesperidin and naringin are partly mediated by hepatic glucose-regulating enzymes in C57BL/KsJ-db/db mice. *J Nutr.* 2004; 134(10): 2499-2503.

Kacheva S, Lenzen S, Gurgul-Convey E. Differential effects of proinflammatory cytokines on cell death and ER stress in insulin-secreting INS1E cells and the involvement of nitric oxide*. Cytokine* 2011; 55: 195–201.

Kahn SE, Cooper ME and Del Prato S. Pathophysiology and treatment of type 2 diabetes: perspectives on the past, present, and future. *Lancet* 2014; 383(9922): 1068-1083.

Kahn SE, Hull RL and Utzschneider KM. Mechanisms linking obesity to insulin resistance and type 2 diabetes. *Nature* 2006; 444: 840-846.

Kaneto H, Kajimoto Y, Miyagawa J-I, Matsuoka T-A, Fujitani Y, Umayahara Y, Hanafusa T, Matsuzawa Y, Yamasaki Y and Hori M. Beneficial effects of antioxidants in diabetes – Possible protection of pancreatic β-cells against glucose toxicity. *Diabetes* 1999; 48: 2398 – 2406.

Kanter M, Coskun O, Korkmaz A and Oter S. Effects of *Nigella sativa* on oxidative stress and beta-cell damage in streptozotocin-induced diabetic rats. *Anat Rec A Discov Mol Cell Evol Biol.* 2004; 279(1): 685-691.

Karin M and Lin A. NF-κB at the crossroads of life and death. *Nat Immunol.* 2002; 3: 221–227.

Kawaguchi K, Mizuno T, Aida K and Uchino K. Hesperidin as an inhibitor of lipases from porcine pancreas and *Pseudomonas. Biosci Biotechnol Biochem.* 1997; 61: 102–104.

Kawano A, Nakamur H, Hat S-I, Minakawa M, Miura Y and Yagasaki K. Hypoglycemic effect of aspalathin, a rooibos tea component from *Aspalathus linearis*, in type 2 diabetic model *db/db* mice. *Phytomedicine* 2009; 16: 437–443.

Kelly C, Guo H, McCluskey JT, Flatt PR and McClenaghan NH. Comparison of insulin release from MIN6 pseudoislets and pancreatic islets of Langerhans reveals importance of homotypic cell interactions. *Pancreas 2*010; 39: 1016–1023.

Kharroubi I, Ladrie're L, Cardozo AK, Dogusan Z, Cnop M and Eizirik DL. Free fatty acids and cytokines induce pancreatic β-cell apoptosis by different mechanisms: role of nuclear factor-B and endoplasmic reticulum stress. *Endocrinology* 2004; 145(11): 5087–5096.

Kim H and Ahn Y. Role of peroxisome proliferator–activated receptor in the glucose-sensing apparatus of liver and β-cells. *Diabetes* 2004; 53(1): S60-S65.

Kirigia J, Sambo H, Sambo L and Barry S. Economic burden of diabetes mellitus in the WHO African region*. Int Health Hum Right.* 2009; 9(6): 1-12.

Knowler WC, Barrett-Connor E, Fowler SE, Hamman RF, Lachin JM, Walker EA and Nathan DM. Reduction in the incidence of type 2 diabetes with lifestyle intervention or metformin. *N Engl J Med.* 2002; 346: 393–403.

Kojima H, Urano Y, Kikuchi K, Higuchi T, Hirata Y and Nagano T. Fluorescent indicators for imaging nitric oxide production. *Angew Chem Int Ed Engl.* 1999; 38(21):3209-3212.

Kweon K-T, Ahn S-Y, Ham I-H, Lee K-J and Choi H-Y. Therapeutic effects of *Coptidis Rhizoma* and berberine in streptozotocin-induced diabetic rats. *J Korean Oriental Med.* 2011; 32(6): 1-9.

Kwon G, Corbett J, Rodi C, Sullivan P and McDaniel M. Interleukin-1β-induced nitric oxide synthase expression by rat pancreatic β-Cells: Evidence for the involvement of nuclear factor kappa B in the signalling mechanism. *Endocrinology* 1995; 136(11): 4790-4795.

Laakso M, Edelman SV, Brechtel G and Baron AD. Decreased effect of insulin to stimulate skeletal muscle blood flow in obese man. A novel mechanism for insulin resistance. *J Clin Invest.* 1990; 85: 1844–1852.

Lampe JW. Health effects of vegetables and fruit: Assessing mechanisms of action in human experimental studies. *Am J Clin Nutr.* 1999; 70: 475S–490S.

Lanuza-Masdeu J, Arevalo MI, Vila C, Barbera A, Gomis R and Caelles C. *In vivo* JNK activation in pancreatic β-cells leads to glucose intolerance caused by insulin resistance in pancreas. *Diabetes* 2013; 62(7): 2308–2317.

Laybutt DR, Preston AM, Akerfeldt MC, Kench JG, Busch AK, Biankin AV and Biden TJ. Endoplasmic reticulum stress contributes to β-cell apoptosis in type 2 diabetes. *Diabetologia* 2007; 50(4): 752-763.

Lee E, Ryu GR, Ko SH, Ahn YB, Yoon KH, Ha H and Song KH. Antioxidant treatment may protect pancreatic beta cells through the attenuation of islet fibrosis in an animal model of type 2 diabetes. *Biochem Biophys Res Commun.* 2011; 414(2): 397-402.

Lee JH, Nguyen KH, Mishra S and Nyomba BL. Prohibitin is expressed in pancreatic beta-cells and protects against oxidative and proapoptotic effects of ethanol. *FEBS J.* 2010; 277(2): 488-500.

Lee Y, Hirose H, Ohneda M, Johnson JH, McGarry J and Unger RH. Beta-cell lipotoxicity in the pathogenesis of non-insulin-dependent diabetes mellitus of obese rats: impairment in adipocyte-beta-cell relationships. *Proc Natl Acad Sci USA.* 1994; 91(23): 10878–10882.

Leighton F, Cuevas A, Guasch V, Perez DD, Strobel P, San Martin A, Urzua U, Diez MS, Foncea R, Castillo O, Mizon C, Espinoza MA, Urquiaga I, Rozowski J, Maiz A and Germain A. Plasma polyphenols and antioxidants, oxidative DNA damage and endothelial function in a diet and wine intervention study in humans. *Drugs Exp Clin Res.* 1999; 25: 133–141.

Leiro J, Arranz JA, Yanez M, Ubeira FM, Sanmartín ML and Orallo F. Expression profiles of genes involved in the mouse nuclear factor-kappa B signal transduction pathway are modulated by mangiferin. *Int Immunopharmacol* 2004; 4: 763–778.

Leiro JM, Alvarez E, Arranz JA, Siso IG and Orallo F. *In vitro* effects of mangiferin on superoxide concentrations and expression of the inducible nitric oxide synthase, tumor necrosis factor-alpha and transforming growth factor-beta genes. *Biochem Pharmacol.* 2003; 65: 1361-1371.

Lenzen S. The mechanisms of alloxan- and streptozotocin-induced diabetes. *Diabetologia* 2008; 51: 216–226.

Li Y, Schwabe RF, DeVries-Seimon T, Yao PM, Gerbod-Giannone MC, Tall AR, Davis RJ, Flavell R, Brenner DA and Tabas I. Free cholesterol-loaded macrophages are an abundant source of tumor necrosis factor-alpha and interleukin-6: model of NF-KB- and map kinase-dependent inflammation in advanced atherosclerosis. *J Biol Chem.* 2005; 280(23): 21763–21772.

Lin B, Zhang ZL, Yu LY and Guo LH. CMV-hFasL transgenic mice are sensitive to low doses of streptozotocin-induced type I diabetes mellitus. *Acta Pharmacol Sin.* 2003; 24(12): 1199-1204.

Lin Y and Sun Z. Current views on type 2 diabetes. *J Endocrin.* 2010; 204: 1–11.

Ling X, Nagai R, Sakashita N, Takeya M, Horiuchi S and Takahashi K. Immunohistochemical distribution and quantitative biochemical detection of advanced glycation end products in fetal to adult rats in rats with streptozotocin-induced diabetes. *Lab Invest.* 2001; 81: 845-861.

Lipson KL, Fonseca SG, Ishigaki S, Nguyen LX, Foss E, Bortell R, Rossini AA and Urano F. Regulation of insulin biosynthesis in pancreatic β-cells by an endoplasmic reticulum-resident proteinkinase IRE1. *Cell Metab.* 2006; 4: 245–254.

Liu IM, Hsu FL, Chen CF and Cheng JT. Antihyperglycemic action of isoferulic acid in streptozotocin-induced diabetic rats. *Br J Pharmacol.* 2000; 129: 631–636.

Liu JJ, Lee T and DeFronzo RA. Why Do SGLT2 inhibitors inhibit only 30–50% of renal glucose reabsorption in humans? *Diabetes* 2012; 61: 2199–21204.

Liu Z, Tanabe K, Bernal-Mizrachi E and Permutt MA. Mice with beta cell overexpression of glycogen synthase kinase-3beta have reduced beta cell mass and proliferation. *Diabetologia* 2008; 51(4): 623-631.

Locksley RM, Killeen N and Lenardo MJ. The TNF and TNF receptor superfamilies: integrating mammalian biology. *Cell* 2001; 104: 487–501.

Lofland HB Jr. A semiautomated procedure for the determination of triglycerides in serum. *Anal Biochem.* 1964; 9:393-400.

Logani MK and Davies RE. Lipid oxidation: biologic effects and antioxidants - a review. *Lipids* 1980; 15(6): 485-495.

Louw A, Joubert E and Visser K. Phytoestrogenic potential of *Cyclopia* extracts and polyphenols. *Planta Med*. 2013; 79(7): 580-590.

Louw J, Woodroof C, Seier J and Wolfe-Coote SA. The effect of diet on the Vervet monkey endocrine pancreas. *J Med Primatol.* 1997; 26(6): 307-311.

Loweth AC, Williams GT, James RF, Scarpello JH and Morgan NG. Human islets of Langerhans express Fas ligand and undergo apoptosis in response to interleukin-beta and Fas ligation. *Diabetes* 1998; 47: 727–732.

Lowry OH, Rosebrough NJ, Farr AL and Randall RJ. Protein measurement with the Folin phenol reagent. *J Biol Chem.* 1951; 193(1): 265-275.

Lupi R, Del Guerra S, Fierabracci V, Marselli L, Novelli M, Patanè G, Boggi U, Mosca F, Piro S, Del Prato S and Marchetti P. Lipotoxicity in human pancreatic islets and the protective effect of metformin. *Diabetes* 2002; 51(1): S134–S137.

Mabley JG, Suarez-Pinzon WL, Hasko G, Salzman AI, Rabinovitch A, Kun E and Szabo C. Inhibition of poly (ADP-ribose) synthetase by gene disruption or inhibition with 5-iodo-6-amino-1,2-benzopyrone protects mice from multiple-low-dose-streptozotocin-induced diabetes. *Br J Pharmacol.* 2001; 133(6): 909–919.

Maechler P, Kennedy ED, Wang H and Wollheim CB. Desensitization of mitochondrial Ca^{2+} and insulin secretion responses in the βcell. *J Biol Chem.* 1998; 273: 20770-20778.
Maedler K. Beta cells in type 2 diabetes - a crucial contribution to pathogenesis. *Diabetes Obes Metab.* 2008; 10(5): 408-420.

Maedler K, Carr RD, Bosco D, Zuellig RA, Berney T and Donath MY. Sulfonylurea induced beta-cell apoptosis in cultured human islets. *J Clin Endocrinol Metab.* 2005; 90(1): 501-506.

Maedler K, Sergeev P, Ris F, Oberholzer J, Joller-Jemelka HI, Spinas GA, Kaiser N, Halban PA and Donath MY. Glucose-induced beta-cell production of interleukin-1beta contributes to glucotoxicity in human pancreatic islets. *J Clin Invest.* 2002; 110: 851–860.

Maedler K, Spinas GA, Dyntar D, Moritz W, Kaiser N and Donath MY. Distinct effects of saturated and monounsaturated fatty acids on β-cell turnover and function. *Diabetes* 2001a; 50 (1): 69-76.

Maedler K, Spinas GA, Lehmann R, Sergeev P, Weber M, Fontana A, Kaiser N and Donath MY. Glucose induces β-cell apoptosis via upregulation of the Fas-receptor in human islets. *Diabetes* 2001b; 50: 1683–1690.

Mahmood T & Yang PC. Western blot: technique, theory, and trouble shooting. *N Am J Med Sci.* 2012; 49: 429-434.

Mahmoud AM, Ashour MB, Abdel-Moneim A and Ahmed OM. Hesperidin and naringin attenuate hyperglycemia-mediated oxidative stress and proinflammatory cytokine production in high fat fed/streptozotocin induced type 2 diabetic rats. *J Diabetes Complications* 2012; 26: 483–490.

Maioli E, Torricelli C, Fortino V, Carlucci F, Tommassini V and Pacini A. Critical appraisal of the MTT assay in the presence of rottlerin and uncouplers. *Biol Proced Online* 2009; 11: 227-40.

Malherbe CJ, Willenburg E, de Beer D, Bonnet SL, van der Westhuizen JH and Joubert E. Iriflophenone-3-*C*-glucoside from *Cyclopia genistoides*: isolation and quantitative comparison of antioxidant capacity with mangiferin and isomangiferin using on-line HPLC antioxidant assays. *J Chromatogr B* 2014; 951–952: 164–171.

Malinouski M, Zhou Y, Belousov VV, Hatfield DL and Gladyshev VN. Hydrogen peroxide probes directed to different cellular compartments. *PLoS One* 2011; 6(1): e14564.

Marchetti P, Del Guerra S, Marselli L, Lupi R, Masini M, Pollera M, Bugliani M, Boggi U, Vistoli F, Mosca F and Del Prato S. Pancreatic islets from type 2 diabetic patients have functional defects and increased apoptosis that are ameliorated by metformin. *J Clin Endocrinol Metab.* 2004; 89(11): 5535–5541.

Marshak S, Leibowitz G, Bertuzzi F, Socci C, Kaiser N, Gross DJ, Cerasi E and Melloul D. Impaired β-cell functions induced by chronic exposure of cultured human pancreatic islets to high glucose. *Diabetes* 1999; 48: 1230–1236.

Mazibuko SE, Muller CJ, Joubert E, de Beer D, Johnson R, Opoku AR and Louw J. Amelioration of palmitate-induced insulin resistance in C2C12 muscle cells by rooibos (*Aspalathus linearis*). *Phytomedicine* 2013; 20(10): 813-819.

McAuley KA, Williams SM, Mann JI, Walker RJ, Lewis-Barned NJ, Temple LA and Duncan AW. Diagnosing insulin resistance in the general population. *Diabetes Care* 2001; 24:460–464.

McCarthy DJ and Smyth GK. Testing significance relative to a fold-change threshold is a TREAT. *Bioinformatics* 2009; 25(6): 765–771.

McLellan KCP, Wyne K, Villagomez ET and Hsueh WA. Therapeutic interventions to reduce the risk of progression from prediabetes to type 2 diabetes mellitus. *Ther Clin Risk Manag.* 2014; 10:173–188.

Meerza D, Naseem I, Ahmed J. Pharmacology of signalling pathways: In type 2 diabetes. *Diabetes Metab Syndr.* 2013; 180–185.

Meidute Abaraviciene S, Lundquist I, Galvanovskis J, Flodgren E, Olde B, Salehi A. Palmitate-induced β-cell dysfunction is associated with excessive NO production and is reversed by thiazolidinedione-mediated inhibition of GPR40 transduction mechanisms. *PLoS ONE* 2008; 3(5): e2182.

Meier JJ and Bonadonna RC. Role of reduced β-cell mass versus impaired β-cell function in the pathogenesis of type 2 diabetes. *Diabetes Care* 2013; 36(2): S113-S119.

Mellado-Gil JM and Aguilar-Diosdado M. High glucose potentiates cytokine- and streptozotocin-induced apoptosis of rat islet cells: effect on apoptosis-related genes. *J Endocrinol.* 2004; 183(1): 155-162.

Miura T, Ichiki H, Hashimoto I, Iwamoto N, Kato M, Kubo M, Ishihara E, Komatsu Y, Okada M, Ishida T and Tanigawa K. Antidiabetic activity of a xanthone compound, mangiferin. *Phytomedicine* 2001; 8: 85-87.

Montane J, Cadavez L and Novials S. Stress and the inflammatory process: a major cause of pancreatic cell death in type 2 diabetes. *Diabetes Metab Syndr Obes.* 2014; 7: 25–34.

Moser B and Willimann K. New targets IV Chemokines: role in inflammation and immune surveillance. *Ann Rheum Dis.* 2004; 63(2): 84-89.

Mossman HMT. Rapid colorimetric assay for cellular growth and survival: application to proliferation and cytotoxic assays. *J Immunol Methods* 1983; 65: 55-63.

Muller CJ, Joubert E, de Beer D, Sanderson M, Malherbe CJ, Fey SJ and Louw J. Acute assessment of an aspalathin-enriched green rooibos (*Aspalathus linearis*) extract with hypoglycemic potential. *Phytomedicine* 2012; 20(1): 32-39.

Muller CJ, Joubert E, Pheiffer C, Ghoor S, Sanderson M, Chellan N, Fey SJ and Louw J. Z-2-(β-D-glucopyranosyloxy)-3-phenylpropenoic acid, an α-hydroxy acid from rooibos (*Aspalathus linearis*) with hypoglycemic activity. *Mol Nutr Food Res.* 2013; 57(12): 2216-2222.

Muller CJF, Joubert E, Gabuza K, De Beer D, Fey SJ and Louw J. Assessment of the antidiabetic potential of an aqueous extracts of honeybush (*Cyclopia intermedia*) in streptozotocin and obese insulin resistant Wistar rats. In: Phytochemicals/Bioactivities and Impact on Health (Edited by I. Rasooli). *Intech Publishers* 2011; ISBN: 978-953-307-424-5.

Muruganandan S, Gupta S, Kataria M, Lal J and Gupta PK. Mangiferin protects the streptozotocin-induced oxidative damage to cardiac and renal tissues in rats. *Toxicology* 2002; 176: 165-173.

Nakagawa K, Ninomiya M, Okubo T, Aoi N, Juneja LR, Kim M, Yamanaka K and Miyazawa T. Tea catechin supplementation increases antioxidant capacity and prevents phospholipid hydroperoxidation in plasma of humans. *J Agric Food Chem.* 1999; 47: 3967–3973.

Nedachi T and Kanzaki M. Regulation of glucose transporters by insulin and extracellular glucose in C2C12 myotubes. *Am J Physiol Endocrinol Metab.* 2006; 291: E817–E828.

Nesto RW, Bell D, Bonow RO, Fonseca V, Grundy SM, Horton ES, Le Winter M, Porte D, Semenkovich CF, Smith S, Young LH- and, Kahn R. Thiazolidinedione use, fluid retention, and congestive heart failure: a consensus statement from the American Heart Association and American Diabetes Association. *Circulation* 2003; 108: 2941–2948.

Newsholme P, Rebelato E, Abdulkader F, Krause M, Carpinelli A and Curi R. Reactive oxygen and nitrogen species generation, antioxidant defences, and β-cell function: a critical role for amino acids. *J Endocrinol.* 2012; 214: 11-20.

Nielsen DA, Welsh M, CasadabanII MJ and Steiner DF. Control of insulin gene expression in pancreatic β-cells and in an insulin-producing cell line, RIN-5F cells: Effects of glucose and cyclic AMP on the transcription of insulin mRNA. *J Biol Chem.* 1985; 260(25): 13585-13589.

Nolan CJ, Madiraju MSR, Delghingaro-Augusto V, Peyot M-L and Prentki M. Fatty acid signaling in the β-cell and insulin secretion. *Diabetes* 2006; 55(2): S16-S23.

Nukatsuka M, Yoshimura Y, Nishida M and Kawada J. Importance of the concentration of ATP in rat pancreatic β-cells in the mechanism of streptozotocin-induced cytotoxicity. *J Endocrinol.* 1990; 127: 161-165.

Oh YS, Lee YJ, Park EY and Jun HS. Interleukin-6 treatment induces β-cell apoptosis via STAT-3-mediated nitric oxide production. *Diabetes Metab Res Rev.* 2011; 27(8): 813-819.

Ohno T, Kato N, Ishii C, Shimizu M, Ito Y, Tomono S and Kawazu S. Genistein augments cyclic adenosine 3'5'-monophosphate (cAMP) accumulation and insulin release in MIN6 cells. *Endocr Res.* 1993; 19: 273–285.

Ortis F, Cardozo AK, Crispim D, Storling J, Mandrup-Poulsen T and Eizirik DL. Cytokine-induced proapoptotic gene expression in insulin-producing cells is related to rapid, sustained, and nonoscillatory nuclear factor-kappa B activation. *Mol Endocrinol.* 2006; 20(8): 1867-1879.

Pandey KB and Rizvi SI. Plant polyphenols as dietary antioxidants in human health and disease. *Oxid Med Cell Longev.* 2009; 2(5): 270-278.

Park CE, Kim MJ, Lee JH, Min BI, Bae H, Choe W, Kim SS and Ha J. Resveratrol stimulates glucose transport in C2C12 myotubes by activating AMP-activated protein kinase. *Mol Med.* 2007; 39: 222–229.

Perreault L, Pan Q, Mather KJ, Watson KE, Hamman RF and Kahn SE. Effect of regression from prediabetes to normal glucose regulation on long-term reduction in diabetes risk: results from the Diabetes Prevention Program Outcomes Study. *Lancet* 2012; 379: 2243–2251.

Petty RD, Sutherland LA, Hunter EM and Cree IA. Comparison of MTT and ATP-based assays for the measurement of viable cell number. *J Biolumin Chemilumin.* 2005; 10(1): 29–34.

Pheiffer C, Dudhia Z, Louw J, Muller C and Joubert E. *Cyclopia maculata* (honeybush tea) stimulates lipolysis in 3T3-L1 adipocytes. *Phytomedicine* 2013; 20(13): 1168-1171.

Pijl H, Ohashi S, Matsuda M, Miyazaki Y, Mahankali A, Kumar V, Pipek R, Iozzo P, Lancaster JL, Cincotta AH and DeFronzo RA. Bromocriptine: a novel approach to the treatment of type 2 diabetes. *Diabetes Care* 2000; 23(8): 1154–1161.

Porte D Jr. Banting lecture 1990. Beta-cells in type II diabetes mellitus. *Diabetes* 1991 40(2): 166-180.

Pospisilik JA, Martin J, Doty T, Ehses JA, Pamir N, Lynn FC, Piteau S, Demuth HU, McIntosh CH and Pederson RA. Dipeptidyl peptidase IV inhibitor treatment stimulates β-cell survival and islet neogenesis in streptozotocin-induced diabetic rats. *Diabetes* 2003; 52(3): 741-750.

Preedy VR. Diabetes: Oxidative stress and dietary antioxidants, First edition. *Academic Press* 2013; ISBN-13: 978-0124058859.

Purrello F, Rabuazzo AM, Anello M and Patane G. Effects of prolonged glucose stimulation on pancreatic β-cells: from increased sensitivity to desensitization. *Acta Diabetol.* 1996; 33(4): 253-256.

Qin C, Tan KL, Zhang CL, Tan CY, Chen YZ and Jiang YY. What does it take to synergistically combine sub-potent natural products into drug-level potent combinations? *PLoS One* 2012; 7(11): e49969.

Quan W, Jo EK and Lee MS, Role of pancreatic β-cell death and inflammation in diabetes. *Diabetes Obesity Metab.* 2013; 15(3): 141–151.

Rachman J, Payne MJ, Levy JC, Barrow BA, Holman RR and Turner RC. Changes in amylin and amylin-like peptide concentrations and (β-cell) function in response to sulfonylurea or insulin therapy in NIDDM. *Diabetes Care* 1998; 21(5): 810-816.

Rahimi R, Nikfar S, Larijani B and Abdollahi M. Dossier: Antioxidants in the prevention of human diseases. A review on the role of antioxidants in the management of diabetes and its complications. *Biomed Pharmacother.* 2005; 59: 365–373.

Rask-Madsen C and Kahn CR. Tissue-specific insulin signalling, metabolic syndrome, and cardiovascular disease. *Arterioscler Thromb Vasc Biol.* 2012; 32(9): 2052-2059.

Reddi AS and Jyothirmayi GN. Effect of chronic metformin treatment on hepatic and muscle glycogen metabolism in KK mice. *Biochem Med Metab Biol.* 1992; 47: 124-32.

Rendell M. The role of sulphonylureas in the management of type 2 diabetes mellitus. *Drugs* 2004; 64: 1339–58.

Rice-Evans CA, Miller NJ, Bolwell PG, Bramley PM and Pridham JB. The relative antioxidant activities of plant-derived polyphenolic flavonoids. *Free Radical Res.* 1995; 22: 375–383.

Robertson P, Harmon J, Tran PO, Tanaka Y and Takahashi H. Glucose toxicity in β-cells: Type 2 diabetes, good radicals gone bad, and the glutathione connection. *Diabetes* 2003; 52: 581–587.

Robertson RP, Harmon J, Tran PO and Poitout V. Beta-cell glucose toxicity, lipotoxicity, and chronic oxidative stress in type 2 diabetes. *Diabetes* 2004; 53(1): S119–S124.

Rorsman P, Braun M and Zhanga Q. Regulation of calcium in pancreatic α- and β-cells in health and disease. *Cell Calcium* 2012; 51(3-4): 300–308.

Rossetti L, Smith D, Shulman GI, Papachristou D and DeFronzo RA. Correction of hyperglycemia with phlorizin normalizes tissue sensitivity to insulin in diabetic rats. *J Clin Invest.* 1987; 79(5): 1510–1515.

Saelens X, Festjens N, Vande Walle L, Van Gurp M, Van Loo G and Vandenabeele P. Toxic proteins released from mitochondria in cell death. *Oncogene* 2004; 23: 2861–2874.

Sagrista ML, Garcia AE, Africa De Madariaga M and Mora M. Antioxidant and pro-oxidant effect of the thiolic compounds N-acetyl-L-cysteine and glutathione against free radical-induced lipid peroxidation. *Free Radic Res.* 2002; 36(3): 329-340.

Sakuraba H, Mizukami H, Yagihashi N, Wada R, Hanyu C and Yagihashi S. Reduced β-cell mass and expression of oxidative stress-related DNA damage in the islet of Japanese type II diabetic patients. *Diabetologia* 2002; 45: 85–96.

Sanchez GM, Re L, Giuliani A, Nunez-Selles AJ, Davison GP and Leon-Fernandez OS. Protective effects of *Mangifera indica* L. extract, mangiferin and selected antioxidants against TPA-induced biomolecules oxidation and peritoneal macrophage activation in mice. *Pharmacol Res.* 2000; 42: 565-573.

Sargsyan E, Ortsater H, Thorn K and Bergsten P. Diazoxide-induced β-cell rest reduces endoplasmic reticulum stress in lipotoxic β-cells. *J Endocrin.* 2008; 199(1): 41-50.

Sarkar A, Sreenivasan Y, Ramesh GT and Manna SK. Beta-D-glucoside suppresses tumor necrosis factor-induced activation of nuclear transcription factor kappaB but potentiates apoptosis. *J Biol Chem.* 2004; 279: 33768-33781.

Sarvazyan N, Swift L and Martinez-Zaguilan R. Effects of oxidants on properties of fluorescent calcium indicators. *Arch Biochem Biophys.* 1998; 350: 132–136.

Scalbert A and Williamson G. Dietary intake and bioavailability of polyphenols. *J Nutr.* 2000; 130: 2073S–2085S.

Scalbert A, Manach C, Morand C and Remesy C. Dietary Polyphenols and the Prevention of Diseases. *Crit Rev Food Sci Nutr.* 2005; 45: 287–306.

Schmitz O, Brock B and Rungby J. Amylin agonists: a novel approach in the treatment of diabetes. *Diabetes* 2001; 53(3): S233-S238.

Schuit FC. Is GLUT2 required for glucose sensing? Diabetologia 1997; 40: 104–111.

Schulz N, Kluth O, Jastroch M and Schurmann A. Minor role of mitochondrial respiration for fatty-acid induced insulin secretion *Int J Mol Sci.* 2013; 14: 18989-18998.

Schulze AE. HPLC method development for characterisation of the phenolic composition of *Cyclopia subternata* and *C. maculata* extracts and chromatographic fingerprint analysis for quality control. Stellenbosch University, Masters thesis 2013.

Sellamuthu PS, Arulselvan P, Kamalraj S, Fakurazi S and Kandasamy M. Protective nature of mangiferin on oxidative stress and antioxidant status in tissues of streptozotocin-induced diabetic rats. *Pharmacol.* 2013a; 1-10.

Sellamuthu PS, Arulselvan P, Muniappan BP, Fakurazi S and Kandasamy M. Mangiferin from *Salacia chinensis* prevents oxidative stress and protects pancreatic β-cells in streptozotocin-induced diabetic rats. *J Med Food* 2013b; 16: 719-727.

Seufert J, Libben G, Dietrich K and Bates PC. A comparison of the effects of thiazolidinediones and metformin on metabolic control in patients with type 2 diabetes mellitus. *Clin Ther.* 2004; 26 (6): 805-818.

Sharma RB and Alonso LC. Lipotoxicity in the pancreatic β-cell: not just survival and function, but proliferation as well? *Curr Diab Rep.* 2014 (6):492 Epub ahead of print - doi: 10.1007/s11892-014-0492-2.

Shaw JE, Sicree RA and Zimmet PZ. Global estimates of the prevalence of diabetes for 2010 and 2030. *Diabetes Res Clin Pract.* 2010; 87: 4-14.

Shoelson SE, Lee J, Goldfine AB. Inflammation and insulin resistance. *J Clin Invest.* 2006; 116(7): 1793-1801.

Smith U, Gogg S, Johansson A, Olausson T, Rotter V and Svalstedt B. Thiazolidinediones (PPARgamma agonists) but not PPARalpha agonists increase IRS-2 gene expression in 3T3–L1 and human adipocytes. *FASEB J.* 2001; 15: 215–220.

Smukler SR, Tang L, Wheeler MB and Salapatek AMF. Exogenous nitric oxide and endogenous glucose-stimulated β-cell nitric oxide augment insulin release. *Diabetes* 2002; 51: 3450–3460.

Son MJ, Minakawa M, Miura Y and Yagasaki K. Aspalathin improves hyperglycemia and glucose intolerance in obese diabetic ob/ob mice. *Eur J Nutr.* 2013; 52(6): 1607-19.

Son MJ, Miura Y and Yagasaki K. Mechanisms for antidiabetic effect of gingerol in cultured cells and obese diabetic model mice. *Cytotechnology* 2014; Epub ahead of print.

South African Honeybush Tea Associatian 2012; http://www.sahoneybush.co.za/. Accessed 5 May 2014.

South African National Treasury, http://www.treasury.gov.za/documents/national%20budget/2014/speech/speech.pdf. Accessed 08 May 2014.

Stassi G, Maria RD, Trucco G, Rudert W, Testi R, Galluzo A, Giordano C and Trucco M: Nitric oxide primes pancreatic beta cells for Fas-mediated destruction in insulin-dependent diabetes mellitus. *J Exp Med.* 1997; 186:1193–1200.

Strober W. Trypan blue exclusion test of cell viability. *Curr Protoc Immunol.* 2001; Appendix 3B - doi: 10.1002/0471142735.ima03bs21.

Stumvoll M, Goldstein BJ and W van Haeften T. Type 2 diabetes: principles of pathogenesis and therapy. *Lancet* 2005; 365: 1333–46.

Sun J, Zhang X, Broderick M and Fein H. Measurement of nitric oxide production in biological systems by using Griess reaction assay. *Sensors* 2003; 3: 276-284.

Szkudelska K and Szkudelski T. Resveratrol, obesity and diabetes. *Eur J Pharmacol.* 2010; 635: 1–8.

Szkudeleski T. The mechanism of alloxan and streptozotocin action in β-cells of the rat pancreas. *Physiol Res.* 2001; 50: 536-546.

Tabatabaie T, Graham KL, Vasquez AM, Floyd RA and Kotake Y. Inhibition of the cytokine-mediated inducible nitric oxide synthase expression in rat insulinoma cells by phenyl N-tert-butylnitrone. *Nitric Oxide* 2000; 4(2): 157–167.

Takaki R and Ono J. Preparation and culture of isolated islets and dissociated islet cells from rodent pancreas. *J Tissue Cult Methods.* 1985; 9(2): 61-66.

Takeda K and Akira S. Stat family of transcription factors in cytokine-mediated biological responses. *Cytokine Growth Factor Rev.* 2000; 11(3): 199-207.

Tanaka Y, Tran PO, Harmon J and Robertson RP. A role for glutathione peroxidase in protecting pancreatic beta cells against oxidative stress in a model of glucose toxicity. *Proc Natl Acad Sci US* 2002; A99: 12363–12368.

The National Diabetes Information Clearinghouse, National Institute of Diabetes and Digestive and Kidney Diseases, National Institutes of Health. http://diabetes.niddk.nih.gov/dm/pubs/pancreaticislet/images/PIT_islet.gif. Accessed: 22 April 2014.

The South African National Standard for the Care and Use of Animals for Scientific Purpose (SANS 10386:2008).

Tibaldi JM. Incorporating incretin-based therapies into clinical practice for patients with type 2 diabetes. *Adv Ther.* 2014; 31: 289–317.

Tiwari AK and Rao JM. Diabetes mellitus and multiple therapeutic approaches of phytochemicals: Present status and future prospects. *Curr Sci.* 2002; 83(1): 30-38.

Toft-Nielsen M, Madsbad S and Holst J. Determinants of the effectiveness of glucagon-like peptide-1 in type 2 diabetes. *J Clin Endocrinol Metab.* 2001; 86 (8): 3853–3860.

Tolosa L. Rodeiro I, Donato MT, Herrera JA, Delgado R, Castell JV, Gomez-Lechon MJ. Multiparametric evaluation of the cytoprotective effect of the *Mangifera indica L.* stem bark extract and mangiferin in HepG2 cells. J Pharm Pharmacol. 2013; 65(7): 1073-1082.

Tordjman K, Standley KN, Bernal-Mizrachi C, Leone TC, Coleman T, Kelly DP and Semenkovich CF. PPAR-alpha suppresses insulin secretion and induces UCP2 in insulinoma cells. *J Lipid Res.* 2002; 43: 936-943.

Toreson WE. Glycogen infiltration (so-called hydropic degeneration) in the pancreas of human and experimental diabetes mellitus. *Am J Pathol.* 1951; 27: 327–347.

Turner RC. The U.K. Prospective Diabetes Study: a review. *Diabetes Care* 1998; 21(3): C35–C38.

United Kingdom Prospective Diabetes Study Group. Intensive blood-glucose control with sulphonylureas or insulin compared with conventional treatment and risk of complications in patients with type 2 diabetes (UKPDS 33). *Lancet* 1998; 352 (9131): 837–853.

US Food and Drug Administration, Centre for Food Safety and Applied Nutrition, Office of Food Additive Safety Redbook 2000 – Toxicological Principles for the Safety Assessment of Food Ingredients. Revised 2007.

Valko M, Leibfritz D, Moncol J, Cronin MTD, Mazur M and Telser J. Free radicals and antioxidants in normal physiological functions and human disease. *Int J Biochem Cell Biol.* 2007; 39: 44-84.

Venables MC and Jeukendrup AE. Physical inactivity and obesity: links with insulin resistance and type 2 diabetes mellitus. *Int J Exp Diabetes Res.* 2009; 25: S18–S23.

Vermes I, Haanen C, Steffens-Nakken H and Reutelingsperger C. A novel assay for apoptosis flow cytometric detection of phosphatidylserine early apoptotic cells using fluorescein labelled expression on Annexin V. *J Immunol Methods* 1995; 184: 39-51.

Vetere A, Choudhary A, Burns SM and Wagner BK. Targeting the pancreatic β-cell to treat diabetes. *Nat Rev Drug Discov.* 2014; 13: 278–289.

Vincenz L, Szegezdi E, Jager R, Holohan C, O'Brien T and Samali A. Cytokine-induced β-cell stress and death in type 1 diabetes mellitus. In: Type 1 diabetes - complications, pathogenesis, and alternative treatments (Edited by Liu C-P). *InTech Publishers* 2011; ISBN 978-953-307-756-7.

Vinik A. Advancing therapy in type 2 diabetes mellitus with early, comprehensive progression from oral agents to insulin therapy. *Clin Ther.* 2007; 29: 1236-1253.

Waltner-Law ME, Wang XL, Law BK, Hall RK, Nawano M and Granner DK. Epigallocatechin gallate, a constituent of green tea, represses hepatic glucose production. *J Biol Chem.* 2002; 277: 34933–34940.

Wan L, Chen C, Xiao Z, Wang Y, Min Q, Yue Y and Chen J. In vitro and in vivo antidiabetic activity of *Swertia kouitchensis* extract. *J Ethnopharmacol.* 2013; 147: 622–630.

Wang P, Henning SM and Heber D. Limitations of MTT and MTS-based assays for measurement of antiproliferative activity of green tea polyphenols. *PLoS ONE* 2010; 5(4): e10202, 1-10.

Wang Z and Gleichmann H. Glucose transporter 2 expression: prevention of streptozotocin-induced reduction in β-cells with 5-thio-D-glucose. *Exp Clin Endocrinol Diabetes* 1995; 103: 83-97.

Warnotte C, Gilon P, Nenquin M and Henquin JC. Mechanisms of the stimulation of insulin release by saturated fatty acids: A study of palmitate effects in mouse β-cells. *Diabetes* 1994; 43: 703-711.

Weir GC and Bonner-Weir S. Five stages of evolving β-cell dysfunction during progression to diabetes. *Diabetes* 2004; 53(3): S210–S216.

West E, Simon OR and Morrison EY. Streptozotocin alters pancreatic β-cell responsiveness to glucose within six hours of injection into rats. *West Indian Med J.* 1996; 45: 60-62.

Wiernsperger NF and Bailey CJ. The antihyperglycaemic effect of metformin therapeutic and cellular mechanisms. *Drugs* 1999; 58 (1): 31-39.

World Health Organisation Traditional Medicine Strategy 2002-2005, World Health Organisation 2002; www.http://whqlibdoc.who.int/hq/2002/WHO_EDM_TRM_2002.1.pdf. Accessed: 25 March 2011.

Yang YH and Johnson JD. Multi-parameter single-cell kinetic analysis reveals multiple modes of cell death in primary pancreatic β-cells. *J Cell Sci.* 2013; 126(18): 4286-4295.

Yang Y, Zhang Z, Li S, Ye X, Li X and He K. Synergy effects of herb extracts: Pharmacokinetics and pharmacodynamic basis. *Fitoterapia* 2014; 92: 133–147.

Yki-Jarvinen H. Thiazolidinediones. *N Engl J Med.* 2004; 351: 1106–1118.

Yoshikawa M, Shimoda H, Nishida N, Takada M and Matsuda H. *Salacia reticulate* and its polyphenolic constituents with lipase inhibitory and lipolytic activities have mild antiobesity effects in rats. *J Nutr.* 2002; 132: 1819–1824.

Youl E, Bardy G, Magous R, Cros G, Sejalon F, Virsolvy A, Richard S, Quignard JF, Gross R, Petit P, Bataille D and Oiry C. Quercetin potentiates insulin secretion and protects INS-1 pancreatic b-cells against oxidative damage via the ERK1/2 pathway. *Br J Pharmacol.* 2010; 161: 799–814.

Young JF, Nielsen SE, Haraldsdottir J, Daneshvar B, Lauridsen ST, Knuthsen P, Crozier A, Sandstrom B and Dragsted LO. Effect of fruit juice intake on urinary quercetin excretion and biomarkers of antioxidative status. *Am J Clin Nutr.* 1999; 69: 87–94.

Younk LM, Mikeladze M and Davis SN. Pramlintide and the treatment of diabetes: a review of the data since its introduction. *Expert Opin Pharmacother* 2011; 12: 1439–51.

Yusta B, Baggio LL, Estall JL, Koehler JA, Holland DP, Li H, Pipeleers D, Ling Z and Drucker DJ. GLP-1 receptor activation improves β-cell function and survival following induction of endoplasmic reticulum stress. *Cell Metab.* 2006; 4(5): 391–406.

Zeiss CJ. The apoptosis-necrosis continuum: insights from genetically altered mice. *Vet Pathol.* 2003; 40: 481–495.

Zhang B, Kang M, Xie Q, Xu B, Sun C, Chen K and Wu Y. Anthocyanins from Chinese bayberry extract protect β cells from oxidative stress-mediated injury via HO-1 upregulation. *J Agric Food Chem.* 2011; 59: 537–545.

Zhang H-Y, Chen L-L, Li X-J and Zhang J. Evolutionary inspirations for drug discovery. *Trends Pharmacol Sci.* 2010; 31(10): 443-448.

Zhang Z, Jiang J, Yu P, Zeng X, Larrick JW and Wang Y. Hypoglycemic and β-cell protective effects of andrographolide analogue for diabetes treatment. *J Transl Med.* 2009; 62: 1-13.

ADDENDUM 1 - Outputs arising from this study

Peer-reviewed journal publication: <u>Chellan N</u>, Joubert E, Strijdom H, Roux C, Louw J and Muller CJF. Aqueous extract of unfermented Honeybush (*Cyclopia maculata*) attenuates STZ-induced diabetes and β-cell cytotoxicity. *Planta Medica* 2014; 80: 622-629 (appended; pages 245-252).

Peer-reviewed abstract publication: <u>Chellan N</u>, Muller CJF, Joubert E, Strijdom H and Louw J. Unfermented aqueous Honeybush extract (*Cyclopia maculata*) attenuates STZ-induced β-cell cytotoxicity. *Diabetologia* 2013; 56(1): S217-S218.

Conference/symposium presentations: <u>Chellan N</u>, Muller CJF, Joubert E, Strijdom H and Louw J. An *in vitro* model for the assessment of hyperglycemia-induced oxidative stress in RIN-5F pancreatic β-cells. Medical Research Council Early Career Scientists Conference, October 2012 (poster presentation).

<u>Chellan N</u>, Muller CJF, Joubert E, Strijdom H and Louw J. The effect of *Cyclopia maculata* extract on β-cell function, protection against oxidative stress and cell survival. Research Symposium, Diabetes Discovery Platform, Medical Research Council, March 2012 (oral presentation).

<u>Chellan N</u>, Muller CJF, Joubert E, Strijdom H and Louw J. An *in vitro* model for the assessment of hyperglycemia-induced oxidative stress in RIN-5F pancreatic β-cells. Physiology Society of Southern Africa (PSSA) Conference, September 2012 (oral presentation; second place in Wyndham competition).

<u>Chellan N</u>, Muller CJF, Joubert E, Strijdom H and Louw J. Unfermented aqueous honeybush extract (*Cyclopia maculata*) attenuates STZ-induced β-cell cytotoxicity. European Association for the Study of Diabetes Conference, September 2013 (poster presentation).

<u>Chellan N</u>, Joubert E, Strijdom H, Louw J and Muller CJF. The protective effect of an unfermented, aqueous *Cyclopia maculata* extract in pancreatic islets. Islet Society Meeting, July 2014 and Physiology Society of Southern Africa (PSSA) Conference, September 2014 (oral presentations).

622 | Original Papers

Aqueous Extract of Unfermented Honeybush (*Cyclopia maculata*) Attenuates STZ-induced Diabetes and β-cell Cytotoxicity

Authors Nireshni Chellan[1,3], Elizabeth Joubert[2,4], Hans Strijdom[3], Candice Roux[1], Johan Louw[1], Christo J. F. Muller[1]

Affiliations
[1] Diabetes Discovery Platform, Medical Research Council, Tygerberg, South Africa
[2] Post-Harvest and Wine Technology Division, Agricultural Research Council (ARC) Infruitec-Nietvoorbij, Stellenbosch, South Africa
[3] Division of Medical Physiology, Faculty of Medicine and Health Sciences, Stellenbosch University, Matieland, South Africa
[4] Department of Food Science, Stellenbosch University, Matieland, South Africa

Abstract
▼
New strategies, which include β-cell protection, are required in the treatment of T2D, as current drugs demonstrate little or no capacity to directly protect the vulnerable β-cell against diabetes-induced cytotoxicity. In this study we investigated the ameliorative effect of pre-treatment with an aqueous extract of unfermented *Cyclopia maculata* (honeybush) on STZ-induced diabetes and pancreatic β-cell cytotoxicity in Wistar rats after demonstrating a protective effect *in vitro* in RIN-5F cells. The amelioration of STZ-induced diabetes was seen in the reduction of the area under the curve, determined by the oral glucose tolerance test, as well as fasting glucose levels in extract-treated rats. Pre-treatment with extract also improved serum triglyceride levels and the glucose-to-insulin ratio. Pre-treatment with the extract or the drug, metformin, increased the β-cell area in islets, with a concomitant increase in β-cell proliferation at the higher extract dose (300 mg/kg/d), but not the lower dose (30 mg/kg/d). Subsequently, the *in vitro* tritiated thymidine incorporation assay showed that the extract was not mitogenic in RIN-5F cells. STZ-induced elevation of plasma nitrite levels was reduced in extract-treated rats, but no changes were observed in their serum catalase, serum glutathione, liver lipid perox-
idation and liver nitrotyrosine levels. Pre-treating the rats with extract ameliorated the diabetic effect of STZ in Wistar rats, with evidence of pancreatic β-cells protection, attributed to the presence of high levels of antioxidants such as the xanthones, mangiferin and isomangiferin.

Abbreviations
▼

ATP:	Adenosine triphosphate
AUC:	area under the curve
CAT:	catalase
C. mac.:	*Cyclopia maculata*
ELISA:	enzyme-linked immunosorbent assay
NAC:	N-acetyl cysteine
NO:	nitric oxide
PNK:	nitrotyrosine
NFκB:	nuclear factor kappa beta
OGTT:	oral glucose tolerance test
RPMI:	Roswell Park Memorial Institute medium
SEM:	standard error of the mean
STZ:	streptozotocin
TBARS:	thiobarbituric acid reactive substances
TNF-α:	tumor necrosis factor-alpha
T2D:	type 2 diabetes

Introduction
▼
Pancreatic β-cell dysfunction is well characterised as part of the disease progression of type 2 diabetes (T2D) [1]. Hyperglycemia and hypertriglyceridemia associated with T2D have been seen to further exacerbate β-cell dysfunction by increasing inflammation and oxidative stress [2,3]. Beta cells are particularly susceptible to inflammation and oxidative stress due to their low levels of antioxidant enzymes, with reduced levels of superoxide dismutase and glutathione peroxidase and no detectable levels of catalase [3]. As a consequence of T2D progression, pro-inflammatory cytokines and increased levels of intracellular reactive oxygen radicals increase β-cell apoptosis, leading to a reduction in β-cell mass [1]. Streptozotocin (STZ), a β-cell specific cytotoxin, is commonly used in rodent models of T2D. The cytotoxic effect of STZ involves mitochondrial and β-cell dysfunction with increased oxidative stress, ATP depletion, DNA alkylation, lipid peroxidation and apoptosis
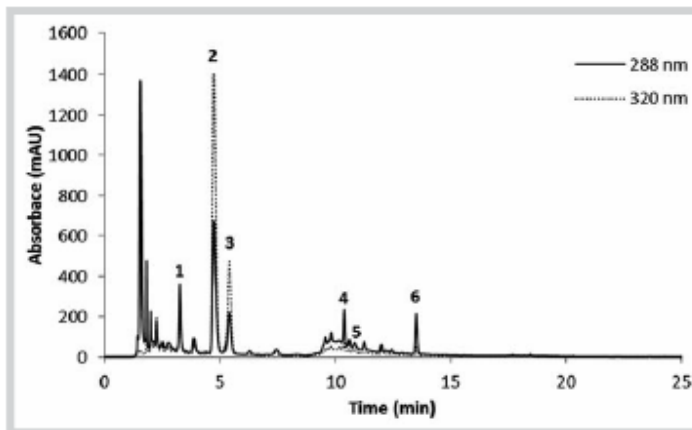
257

Fig. 1 HPLC chromatogram of unfermented *C. maculata* extract adapted from Dudhia et al. [16]. 1: iriflophenone-3-C-glucoside (1.13%); 2: mangiferin (6.19%); 3: isomangiferin (2.08%); 4: eriocitrin (0.42%); 5: phloretin-3',5'-di-C-glucoside (0.17%); 6: hesperidin.

[4]. The β-cell cytotoxicity induced by STZ has been shown to be ameliorated by substances with antioxidant activity [5]. Kaneto et al. demonstrated the ability of antioxidants (N-acetyl cysteine and vitamins C and E) to preserve β-cell function *in vivo* in C57BL/KsJ-*db/db* diabetic mice [6].

Glucose-lowering drugs currently used for the treatment of T2D mainly act by increasing insulin sensitivity and/or insulin secretion, with little or no capacity to directly protect the exceedingly vulnerable β-cell against T2D associated cytotoxicity [1,2,7]. Clearly, new strategies which include β-cell protection are needed for effective, long-term treatment of T2D. These strategies may include adjunctive alternative therapies with currently prescribed drugs. There is increased interest in the research and use of alternative therapies, particularly herbal therapies [1] such as the mangiferin-containing *Swertia kouitchensis* [8], *Salacia chinensis* [9] and *Mangifera indica* [10], all shown to have antidiabetic effects with potential β-cell protection. With increasing worldwide popularity, honeybush tea, brewed from several *Cyclopia spp.* (Fabaceae family), including *Cyclopia maculata* [11, 12], has been shown to have antidiabetic properties [13]. The xanthone mangiferin was shown to be one of the most active antioxidants of the major polyphenols present in *Cyclopia spp.* [14]. A recent study compared the peroxyl radical activity of mangiferin with that of two other major polyphenols found in the unfermented extract of *C. maculata* used in this study i.e. isomangiferin and the benzophenone, iriflophenone-3-C-glucoside, showing the relative order of activity to be isomangiferin > mangiferin > iriflophenone-3-C-glucoside [15]. The unfermented extract used in this study has been characterised by Dudhia et al. (○ **Fig. 1**) [16]. Several studies have investigated the antioxidant capacity [17] as well as antidiabetic actions [10,18] of mangiferin, likely contributing to the aforementioned effects observed for extracts of *Cyclopia spp.* Mangiferin has also been shown to have immunoregulatory capabilities, via the inhibition of NFκB [19, 20]. None of the current literature, however, includes the protective effect(s) of *Cyclopia spp.* extracts on pancreatic β-cells against chemically-induced cytotoxicity. In this study we propose that an aqueous extract of unfermented honeybush (*C. maculata*) protects against STZ-induced β-cell cytotoxicity.

Results

Cyclopia maculata extract improved cell viability in RIN-5F cells exposed to STZ and showed no mitogenic effect *in vitro*. Following 24 hour exposure of RIN-5F insulinoma cells to 10 mM STZ, the extract (0.001, 0.01, 1, 10, 100 and 1000 μg/mL) significantly increased cell viability as measured by cellular ATP content (52.67% ± 3.29 vs. 113.53% ± 7.07, 108.80% ± 8.20, 107.12% ± 6.37, 115.80% ± 10.92, 113.14% ± 5.61 and 89.92% ± 5.53, respectively) (○ **Fig. 2A**). These results were comparable to the NAC positive control (52.67% ± 3.29 vs. 95.77% ± 4.94) (○ **Fig. 2 A**). Increasing the extract concentration to 2000 μg/mL failed to ameliorate STZ-induced cytotoxicity in these cells (53.05% ± 3.32 vs. 36.82% ± 3.34) (○ **Fig. 2A**). Mangiferin failed to improve cell viability in STZ treated RIN-5F cells (○ **Fig. 2B**). Exposure of RIN-5F cells to the glucagon-like peptide 1 agonist liraglutide increased proliferation as determined by the incorporation of tritiated thymidine into these cells (271.36 Fmol ± 10.86 vs. 403.15 Fmol ± 27.90) (○ **Fig. 2C**). The range of *C. maculata* extract concentrations (0.01–1000 μg/mL) did not have any measurable mitogenic effects in RIN-5F cells (○ **Fig. 2C**). Compared to the normal control, the two highest extract concentrations (100 and 1000 μg/mL), however, reduced RIN-5F cell proliferation (271.36 Fmol ± 10.86 vs. 190.51 Fmol ± 1.99 and 13.38 Fmol ± 0.45, respectively) (○ **Fig. 2C**).

Cyclopia maculata extract improved glucose tolerance in STZ-induced diabetic rats. Pre-treatment with the extract (300 mg/kg/d) or metformin (125 mg/kg/d) decreased the percentage of diabetic rats (i.e. fasting plasma glucose greater than 7 mmol/L) following STZ injection to 25% (○ **Fig. 3A**). Pre-treatment with NAC or 30 mg/kg/d extract reduced the percentage to 50% (○ **Fig. 3A**). STZ injected control rats showed significantly increased fasting plasma glucose levels compared to the normal control rats (6.21 mmol/L ± 1.93 vs. 5.76 mmol/L ± 0.20) (○ **Fig. 3B**). Compared to the STZ controls, fasting plasma glucose levels were significantly reduced in metformin and the 300 mg/kg/d extract treated groups (16.21 mmol/L ± 1.93 vs. 6.30 mmol/L ± 0.66 and 6.70 mmol/L ± 1.17, respectively) (○ **Fig. 3B**). Compared to the normal control group, AUCs calculated from the OGTT were significantly increased in the STZ control and NAC treated groups (1461.251 ± 12.70 vs. 5264.38 ± 396.14 and 3896.00 ± 620.24, respectively) (○ **Fig. 3C**). However, compared to the STZ control,

Chellan N et al. Aqueous Extract of... Planta Med 2014; 80: 622–629

258
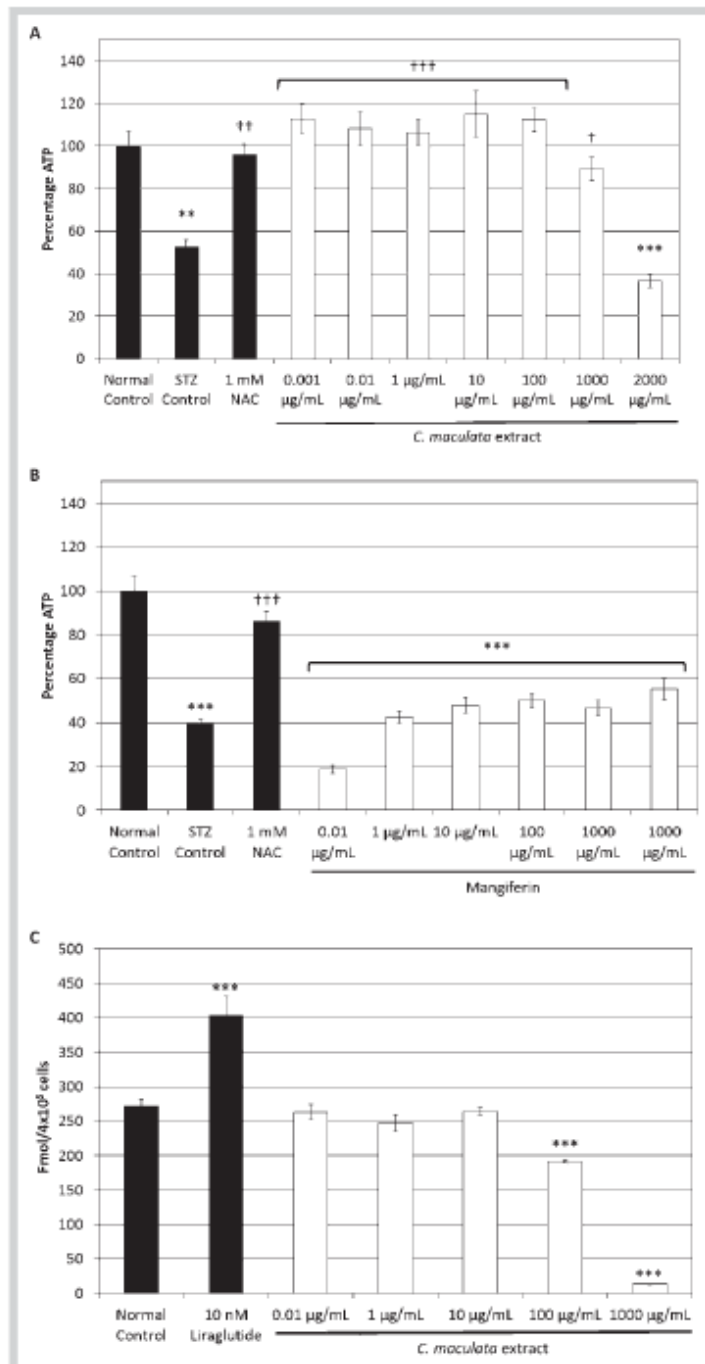
Fig. 2 RIN-5F cellular ATP content following exposure of cells to 10 mM STZ and increasing concentrations of *C. maculata* extract (**A**) or mangiferin (**B**) and ³H-thymidine incorporation (**C**) ** $p < 0.01$, *** $p < 0.001$ (vs. normal control, one-way ANOVA with Tukey post hoc); † $p < 0.05$, †† $p < 0.01$, ††† $p < 0.001$ (vs. STZ control).

treatment with metformin and the two extract concentrations (30 and 300 mg/kg) significantly reduced AUC values (5264.38 ± 396.14 vs. 2677.25 ± 483.80, 3114.13 ± 752.23 and 2824.38 ± 536.00, respectively) (⊙ **Fig. 3C**).

Cyclopia maculata extract improved the total serum triglyceride levels in STZ-induced diabetic rats. Total serum triglyceride levels were increased in control rats injected with STZ compared to the normal, non-diabetic controls (1.48 mmol/L ± 0.48 vs. 0.3 mmol/

Chellan N et al. Aqueous Extract of... Planta Med 2014; 80: 622–629

259

Fig. 3 Percentage diabetic (black bars) and non-diabetic (white bars) rats (A) and fasting plasma glucoses (B) of rats following induction of diabetes by STZ injection. Area under the curve of oral glucose tolerance test (C), total serum triglyceride levels (D), fasting serum insulin levels (E) and glucose-to- insulin ratio (F) in rats following 21 days treatment with metformin, NAC and *C. maculata* extract. * $P < 0.05$, ** $p < 0.01$, *** $p < 0.001$ (vs. normal control, one-way ANOVA with Tukey post hoc); † $p < 0.05$, †† $p < 0.01$ (vs. STZ control).

L ± 0.03) (○ **Fig. 3D**). The higher extract dose (300 mg/kg/d) reduced total triglyceride levels compared to the STZ control (1.48 mmol/L ± 0.48 vs. 0.40 mmol/L ± 0.04) (○ **Fig. 3D**).

STZ injection decreased the total serum insulin levels of the treated rats compared to normal, non-diabetic controls (3.00 ng/ mL ± 0.80 vs. 0.83 ng/mL ± 0.09) (○ **Fig. 3E**). The reduction in insulin in both of the extract treated groups, compared to the normal control rats, was not significant (3.00 ng/mL ± 0.80 vs. 1.70 ng/mL ± 0.50 and 1.50 ng/mL ± 0.14, respectively) (○ **Fig. 3E**). The glucose-to-insulin ratio (G:I) was increased in STZ control

rats compared to the normal controls (12.70 ± 2.34 vs. 1.49 ± 0.60) (○ **Fig. 3F**). Compared to the STZ control rats, *C. maculata* extract treated rats showed a reduction in the G:I ratio (12.70 ± 2.34 vs. 2.89 ± 0.70) (○ **Fig. 3F**).

An extract-induced increase in β-cell area to total islet area, as well as increased β-cell proliferation in STZ-induced diabetic rats was observed. The percentage β-cell to total islet area was reduced in STZ control rats compared to the normal, non-diabetic control rats (36.34% ± 5.01 vs. 81.30% ± 1.65) (○ **Fig. 4 A**). Compared to the STZ controls, rats treated with metformin or the

Fig. 4 Percentage β-cell area to total islet area (A), percentage MIB-5 positive β-cells (B) and total plasma nitrites (C) in rats following 21 days treatment with metformin, NAC and *C. maculata* extract. * P<0.05, ** p<0.01, *** p< 0.001 (vs. normal control, one-way ANOVA with Tukey post hoc); † p< 0.05, †† p<0.01 (vs. STZ control)
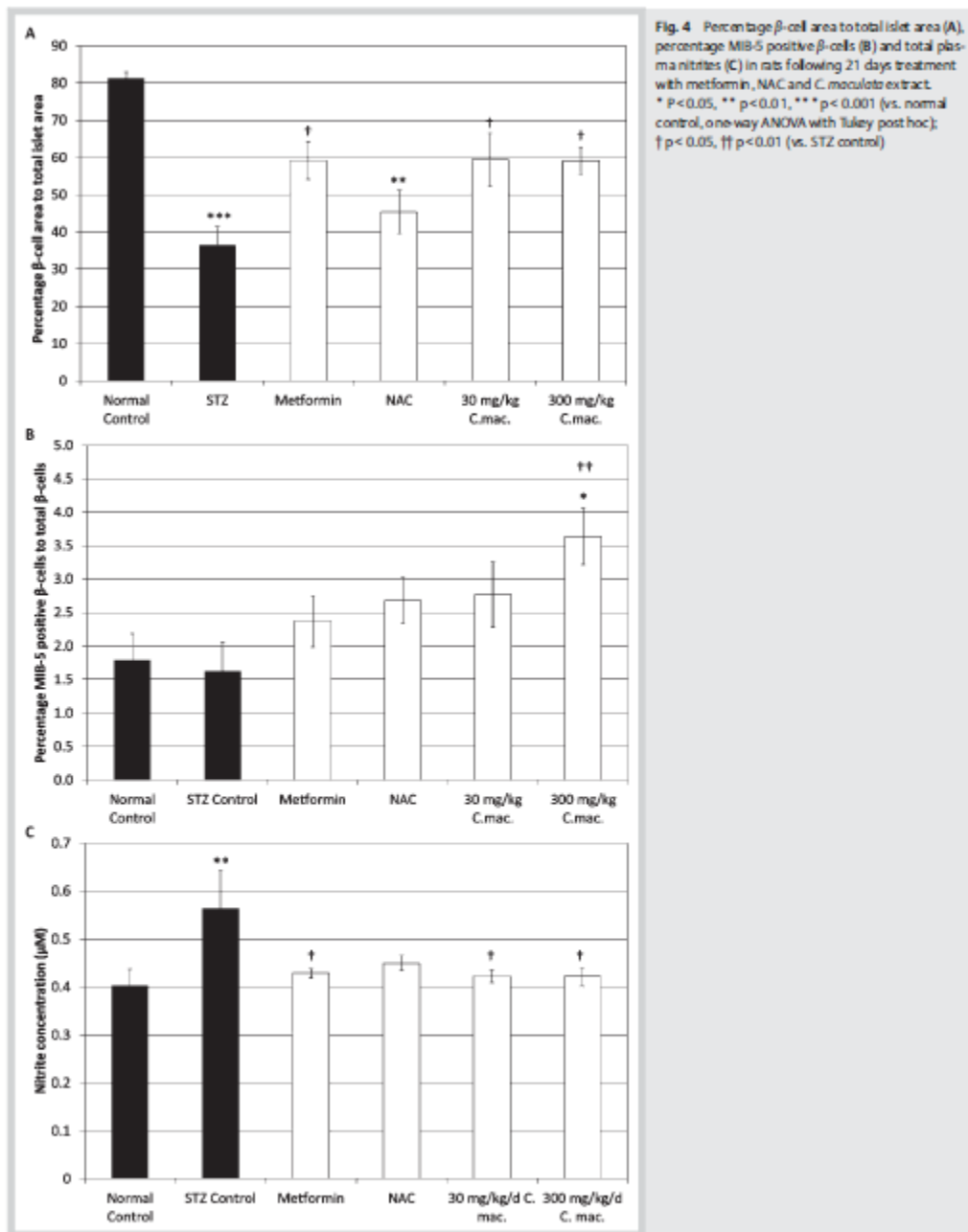
two extract doses (30 and 300 mg/kg/d), but not NAC showed significantly increased β-cell to total islet area (36.34% ± 5.01 vs. 59.22% ± 5.08, 59.38% ± 7.17 and 59.15% ± 3.56, respectively) (○ **Fig. 4 A**). The induction of diabetes by STZ injection had no ef- fect on β-cell proliferation, however, compared to both normal and STZ controls, treatment with 300 mg/kg/d of *C. maculata* extract increased the amount of proliferation in β-cells (1.78% ± 0.40 and 1.63% ± 0.43 vs. 3.64% ± 0.42) (○ **Fig. 4 B**).

Plasma nitrite levels were increased in control rats injected with STZ compared to the normal, non-diabetic control rats ($0.56\,\mu M \pm 0.08$ vs. $0.40\,\mu M \pm 0.03$) (○ **Fig. 4C**). Compared to the STZ control, rats treated with metformin or extract (30 or 300 mg/kg/d) showed reduced plasma nitrite levels ($0.56\,\mu M \pm 0.08$ vs. $0.43\,\mu M \pm 0.01$, $0.42\,\mu M \pm 0.01$ and $0.42\,\mu M \pm 0.02$, respectively) (○ **Fig. 4C**).

Discussion
▼

Based on the high mangiferin content (6.19%) and the presence of other bioactive phenolic compounds in our unfermented *C. maculata* extract such as isomangiferin (2.08%), iriflophenone-3-C-glucoside (1.13%), the dihydrochalcone, phloretin-3',5'-di-C-glucoside (0.17%) and the flavanones, hesperidin (0.80%) and eriocitrin (0.42%) [16], we anticipated that the extract used in this study would protect pancreatic β-cells from toxicity induced by STZ. At the extract concentration range tested (0.01–2000 μg/mL), we found that the extract did in fact protect RIN-5F rat insulinoma cells from STZ-induced toxicity up to the 1000 μg/mL concentration. With this promising result we investigated the *in vivo* effect of the extract in STZ-induced diabetic rats. By pre-treating the rats with extract, the toxic effect of STZ on β-cells was ameliorated as indicated by the reduced AUC of the OGTT and fasting glucose levels. Concomitantly, serum triglyceride levels were also reduced to within normal physiological ranges. This implies some benefit to hepatic function in these rats [21], which may potentially reduce the effects of long-term complications associated with hyperglycemia and hypertriglyceridemia, such as cardiovascular disease [22]. The improved hypertriglyceridemia may be attributed to the high mangiferin content of this extract, since Muruganandan et al. demonstrated the anti-lipidemic effect of mangiferin in STZ-induced diabetic rats [23]. Mangiferin also decreased fasting plasma glucose levels in the aforementioned study, and therefore may presumably play a role in the reduced fasting plasma glucose levels observed for *C. maculata* extract in this study [23]. Furthermore, we found that treatment with extract improved the glucose-to-insulin ratio of the rats, comparable with that of metformin. This could imply that the extract enhances insulin action, stimulates glucose uptake independent of insulin, or itself reduces blood glucose in an insulin mimetic manner. Additionally, treatment with extract, as well as metformin, increased the β-cell area in islets, with a concomitant increase in β-cell proliferation observed for the 300 mg/kg/d extract treated group. Similar improvement in pancreatic islet architecture with regeneration of β-cells was recently demonstrated in mangiferin treated STZ-induced diabetic rats by Sellamuthu et al. [17]. In our study we found no measurable effect on apoptosis, as assessed using TUNEL labelling of pancreatic tissue sections (data not shown). The increase in β-cell area indicates the extract offered some protection against the cytotoxicity of STZ. Increased proliferation of β-cells is an interesting observation since it may be an indirect adaptive response due to an extract-induced improved physiological status in these animals, or the extract may in fact be mitogenic. In order to exclude the mitogenic effect of the extract on β-cells, we assessed the incorporation of tritiated thymidine into RIN-5F cells exposed to a range of extract concentrations. This data revealed no detectable change in proliferation indicating no direct mitogenic effect of the extract *in vitro*. Pal et al. has demonstrated that mangiferin inhibits mitogen-activated protein kinases (MAPK) both *in vitro* and *in vivo* [24].

This finding provides further evidence that a direct extract-induced mitogenic effect is unlikely. Although mangiferin may be responsible for the indirect protection of β-cells by reducing STZ-induced diabetic parameters such as hyperglycemia and hypertriglyceridemia, *in vitro* data in this study suggest that direct protection of β-cells is not due to mangiferin. We demonstrated that the unfermented aqueous honeybush extract ameliorated STZ-induced cytotoxicity in RIN-5F cells, as measured by cellular ATP content. Mangiferin alone, however, did not have a similar effect. This suggests that other polyphenols present in the extract, either exclusively or synergistically, are mainly responsible for improved β-cell viability.

Plasma nitrite data indicated that there was an extract-induced reduction in rat serum nitrites elevated by STZ. Since these changes were very small and may in fact not be physiologically significant, we also assessed the levels of two antioxidant enzymes (catalase and glutathione), lipid peroxidation (TBARS assay) and liver nitrotyrosine (Western blot analysis). In this study we were not able to demonstrate that the extract had any effect on these parameters (data not shown). However, we cannot exclude that the extract could have had a pronounced antioxidant effect closer to the induction of diabetes by STZ.

We propose that pre-treatment with the extract may have had both pancreatic and extra-pancreatic effects. The extract may have induced a direct antioxidant protective effect on the β-cells as a result of antioxidants, such as mangiferin [23] and the flavanones, eriocitrin and hesperidin present in the extract [25,26]. Further protection of β-cells post STZ injection may in fact be indirect and rather as a result of a reduction in both hyperglycemia and hypertriglyceridemia. Reduction of inflammation induced by STZ, particularly in the pancreatic islets [27], may also play a significant role in the ameliorative effect of the extract since mangiferin is seen to reduce TNF-α induced activation of NFκB in human histiocytic lymphoma cells [20], as well as inhibits NFκB and downstream pro-inflammatory cytokines in macrophages [19]. Anti-inflammatory properties of the *C. maculata* extract have yet to be explored.

In this study we demonstrate that pre-treatment of Wistar rats with an aqueous extract of unfermented *C. maculata* reduces harmful effects of STZ such as hyperglycemia and hypertriglyceridemia, with evidence of β-cell preservation.

Materials and Methods
▼

Preparation and analysis of *C. maculata* extract
The same unfermented extract previously described and analysed for major phenolic compounds by Dudhia et al. was used for this study [16]. Briefly, preparation entailed extraction of unfermented plant material ("tea bag cut") with purified water in a ratio of 1 : 10 (m/v) at 93 °C for 30 min. The extract was filtered, cooled to room temperature and freeze-dried. The dried extract was stored under desiccation at room temperature, in a dry environment at the Diabetes Discovery Platform.

In vitro studies
RIN-5F viability: RIN-5F cells (Cat no. 95090402, European Collection of Cell Cultures, Salisbury, UK) were cultured under standard conditions in Roswell Park Memorial Institute medium (RPMI) 1640 (Lonza) containing 11 mM glucose and supplemented with 10% fetal bovine serum (HyClone, Thermo Fisher Scientific Inc.). These rat islet tumour cells have been shown to be susceptible to

262

STZ-induced toxicity [28]. Cells were seeded into 96 well plates at 1.2×10^4 cells per well. Upon confluence, cells were exposed to 10 mM STZ (Sigma) in RPMI1640 media containing 2% BSA (Roche) for 24 hours with or without *C. maculata* extract (0.01–2000 µg/mL) and mangiferin (Sigma) (≥ 98% purity by TLC) (0.001–1000 µg/mL). N-acetyl cysteine (NAC) (≥ 99% purity by TLC), used at 1 mM, served as positive control. Thereafter, a bioluminescent ViaLight® Plus cell proliferation and cytotoxicity assay kit (Lonza) was used to quantify cellular ATP according to the manufacturer's instructions.

Tritiated thymidine (^{3}H-thymidine) incorporation in RIN-5F cells: Following 20 hours exposure of RIN-5F cells to a range of extract concentrations (0.01–1000 µg/mL) and the positive control liraglutide at 10 nM (Victoza®, Novo Nordisk) (> 99% purity by HPLC), 1 µCi of ^{3}H-thymidine (Perkin Elmer) was added to each well for a further 4 hours. The amount of ^{3}H-thymidine incorporated into proliferating cells was determined by lysing the cells and measuring ^{3}H radioactivity on a scintillation counter (Perkin Elmer).

In vivo studies

Forty-eight male Wistar rats were bred at the Primate Unit and Delft Animal Centre of the South African Medical Research Council (Parow, South Africa) and individually housed in cages under constant temperature (23–25 °C) and humidity (± 50%), with a 12 hour light and dark cycle and 15–20 air changes per hour. The rats were fed standard rodent pellets (laboratory chow) (Afresh Vention) *ad libitum* with free access to drinking water (fresh tap water). All procedures were performed in accordance with the principles and guidelines of the South African Medical Research Council as outlined in Guidelines on Ethics for Medical Research: Use of Animals in Research and Training, 2004 (http://www.mrc.ac.za/ethics/ethicsbook3.pdf), as well as the South African National Standard for the Care and Use of Animals for Scientific Purpose (SANS 10386:2008). Ethical approval was obtained from the Stellenbosch University Research Ethics Committee on 3 August 2011 (11GK_CHE01). At three months of age, rats were randomised into the following six groups (n = 8 per group): Normal control (distilled water daily), STZ control (distilled water daily), metformin (Sigma) (≥ 97% purity by TLC) (125 mg/kg daily), NAC (125 mg/kg daily) and two *C. maculata* treated groups (30 and 300 mg/kg daily). Rats were treated for 15 days and were then injected with STZ. Treatment continued for a further 6 days (21 days in total), after which the rats were sacrificed.

Streptozotocin-induced diabetes in the Wistar rat

Wistar rats were injected intra-peritoneally with STZ (Sigma; 40 mg/kg body weight) following 8 hours fasting after 15 day pre-treatment with extract, metformin or NAC. STZ was dissolved in 0.1 M sterile filtered citric acid (Sigma) buffer (pH 4.5) at a concentration of 40 mg/3 mL. STZ was administered immediately after dissolution.

Treatment administration

All treatments were administered in a gelatine jelly cube as described by Chellan et al. [29]. Each cube contained the kilogram dose equivalent of NAC, metformin or *C. maculata* extract per 3 mL gelatine jelly.

Blood glucose monitoring

Five days post STZ injection, after a 4 hour fast, a drop of blood was collected from the tail. Blood glucose concentration was determined using a handheld glucometer (OneTouch Select®, Johnson and Johnson).

Oral glucose tolerance test (OGTT)

The procedure was performed following an overnight fast (16 hours). A 50% dextrose solution (IntraMed) was gavaged (2 g/kg) 2 hours after the rats received their respective treatments. Blood glucose was determined at the following time points: 0, 15, 30, 60, 120, 180 and 240 minutes.

Blood and tissue collection at post-mortem

Following 21 days of treatment, rats were anaesthetised using isoflurane gas (Forane® Liquid, Abbott Laboratories Pty Ltd.) administered at 2% with 100% oxygen (Afrox, Linde Group). A laparotomy was performed and 10 mL of blood was collected from the abdominal vena cava of each rat into two serum-separating gel tubes (BD Biosciences) and one K_2 EDTA tube (BD Biosciences). Following blood collection, pancreata were excised and fixed in 10% buffered formalin. Pancreata were processed according to a standard protocol and embedded in paraffin wax. Snap frozen liver samples were collected for the measurement of thiobarbituric acid reactive substances (TBARS) and nitrosylated proteins.

Serum triglyceride quantification

Serum triglyceride concentrations were determined by PathCare Medical Diagnostic Laboratories, using a modified method of Lofland [30].

Serum insulin quantification

Serum insulin was quantified using an ELISA kit according to manufacturer's instruction (Millipore).

Plasma nitrite determination

Griess reagent (Sigma) was used to determine the nitrite concentration in rat plasma, according to a method modified from Grisham et al. [31]. Briefly, equal amounts of plasma and Griess reagent were incubated for 15 minutes and the absorbance read at 540 nm on a BioTek® ELx 800 plate reader, using Gen 5® software for data acquisition (BioTek Instruments Inc.).

Immunohistochemistry

Paraffin wax embedded pancreatic tissue was sectioned at approximately 8 µm thickness. Prior to immunolabeling, sections were dewaxed, using xylene and hydrated in decreasing concentrations of ethanol (rinsed in distilled water). Sections were labelled with insulin monoclonal antibody (Cat. No. 12018, Sigma) at a 1:10000 dilution and glucagon polyclonal antibody (Cat No. G2654, Sigma) at a 1:100 dilution. Following overnight incubation at 4°C with the primary antibody, either a biotinylated anti-mouse or biotinylated anti-rabbit secondary link anti-body was applied, respectively (DAKO). Envision system (DAKO) and chromogen diaminobenzidine (DAKO) were used to detect and visualise antibody labelling. Image analysis was performed on captured images, using Leica QWinPro software (Leica Microsystems Cambridge Ltd.).

263

Statistical analysis

In vitro data are expressed as mean of three independent experiments ± standard error of the mean (SEM), with six repeats per treatment. *In vivo* data are expressed as the mean per group ± SEM. Microsoft Excel (Microsoft Corporation) and GraphPad Prism v.5.01 (GraphPad Software Inc.) were used for data compilation and statistical analysis. Significant differences between groups were determined using a one-way ANOVA with a Tukey post hoc test if $p < 0.05$.

Acknowledgements
▼

Conflict of Interest
▼

The authors report no conflicts of interest and are responsible for the content and writing of this paper.

References

1 Hassan Z, Yam MF, Ahmad M, Yusof AP. Antidiabetic properties and mechanism of action of *Gynura procumbens* water extract in streptozotocin-induced diabetic rats. Molecules 2010; 15: 9008–9023

2 Marchetti P, Prato SD, Lupi R, Guerra SD. The pancreatic beta-cell in human type 2 diabetes. Nutr Metab Cardiovasc Dis 2006; 16: 3–6

3 Bonora E. Protection of pancreatic beta-cells: is it feasible? Nutr Metab Cardiovasc Dis 2008; 18: 74–83

4 Szkudelski T. The mechanism of alloxan and streptozotocin action in beta cells of the rat pancreas. Physiol Res 2001; 50: 537–546

5 Ho E, Chen G, Bray TM. Alpha-phenyl-tert-butylnitrone (PBN) inhibits NFkappaB activation offering protection against chemically induced diabetes. Free Radic Biol Med 2000; 28: 604–614

6 Kaneto H, Kajimoto Y, Miyagawa JI, Matsuoka TA, Fujitani Y, Umayahara Y, Hanafusa T, Matsuzawa Y, Yamasaki Y, Hori M. Beneficial effects of antioxidants in diabetes – possible protection of pancreatic β-cells against glucose toxicity. Diabetes 1999; 48: 2398–2406

7 Robertson RP. Antioxidant drugs for treating beta-cell oxidative stress in type 2 diabetes: Glucose-centric versus insulin-centric therapy. Discovery Medicine. Available at http://www.discoverymedicine.com. Accessed September 28, 2010

8 Wan L, Chen C, Xiao Z, Wang Y, Min Q, Yue Y, Chen J. In vitro and in vivo antidiabetic activity of Swertia kouitchensis extract. J Ethnopharmacol 2013; 147: 622–630

9 Anitha S, Rose AML. Comparative evaluation of antihyperglycaemic effect of various parts of *Salacia chinensis* L. J Med Sci (Pakistan) 2013; 13: 493–496

10 Muruganandan S, Gupta S, Kataria M, Lal J, Gupta PK. Mangiferin protects the streptozotocin-induced oxidative damage to cardiac and renal tissues in rats. Toxicology 2002; 176: 165–173

11 Joubert E, Gelderblom WC, Louw A, De Beer D. South African herbal teas: Aspalathus linearis, Cyclopia spp. and Athrixia phylicoides – a review. J Ethnopharmacol 2008; 119: 376–412

12 Joubert E, Joubert ME, Bester C, De Beer D, De Lange JH. Honeybush (Cyclopia spp.): From local cottage industry to global markets – the catalytic and supporting role of research. S Afr J Bot 2011; 77: 887–907

13 Muller CJF, Joubert E, Gabuza K, De Beer D, Fey SJ, Louw J. Assessment of the antidiabetic potential of an aqueous extracts of honeybush (Cyclopia intermedia) in streptozotocin and obese insulin resistant Wistar rats. In: Rassoli I, ed. Phytochemicals/bioactivities and impact on health. Rijeka, Croatia: Intech-Open Acess Publisher; 2011: 313–332

14 Joubert E, Richards ES, Van der Merwe JD, De Beer D, Manley M, Gelderblom WCA. Effect of species variation and processing on phenolic composition and in vitro antioxidant activity of aqueous extracts of Cyclopia spp. (honeybush tea). J Agric Food Chem 2008; 56: 954–963

15 Malherbe CJ, Willenburg E, de Beer D, Bonnet SL, van der Westhuizen JH, Joubert E. Iriflophenone-3-C-glucoside from Cyclopia genistoides: isolation and quantitative comparison of antioxidant capacity with mangiferin and isomangiferin using on-line HPLC antioxidant assays. J Chromatogr B Analyt Technol Biomed Life Sci 2014; 951–952: 164–171

16 Dudhia Z, Louw J, Muller C, Joubert E, De Beer D, Kinnear C, Pheiffer C. Cyclopia maculata and Cyclopia subternata (honeybush tea) inhibits adipogenesis in 3T3-L1 pre-adipocytes. Phytomedicine 2013; 20: 401–408

17 Sellamuthu PS, Arulselvan P, Muniappan BP, Fakurazi S, Kandasamy M. Mangiferin from Salacia chinensis prevents oxidative stress and protects pancreatic β-cells in streptozotocin-induced diabetic rats. J Med Food 2013; 16: 719–727

18 Miura T, Ichiki H, Hashimoto I, Iwamoto N, Kato M, Kubo M, Ishihara E, Komatsu Y, Okada M, Ishida T, Tanigawa K. Antidiabetic activity of a xanthone compound, mangiferin. Phytomedicine 2001; 8: 85–87

19 Leiro J, Arranz JA, Yáñez M, Ubeira FM, Sanmartín ML, Orallo F. Expression profiles of genes involved in the mouse nuclear factor-kappa B signal transduction pathway are modulated by mangiferin. Int Immunopharmacol 2004; 4: 763–778

20 Sarkar A, Sreenivasan Y, Ramesh GT, Manna SK. Beta-D-glucoside suppresses tumor necrosis factor-induced activation of nuclear transcription factor kappaB but potentiates apoptosis. J Biol Chem 2004; 279: 33768–33781

21 Mahmoud AM, Ashour MB, Abdel-Moneim A, Ahmed OM. Hesperidin and naringin attenuate hyperglycemia-mediated oxidative stress and proinflammatory cytokine production in high fat fed/streptozotocin-induced type 2 diabetic rats. J Diabetes Complications 2012; 26: 483–490

22 Ceriello A, Taboga C, Tonutti L, Quagliaro L, Piconi L, Bais B, Da Ros R, Motz E. Evidence for an independent and cumulative effect of postprandial hypertriglyceridemia and hyperglycemia on endothelial dysfunction and oxidative stress generation: effects of short- and long-term simvastatin treatment. Circulation 2002; 106: 1211–1218

23 Muruganandan S, Srinivasan K, Gupta S, Gupta PK, Lal J. Effect of mangiferin on hyperglycemia and atherogenicity in streptozotocin diabetic rats. J Ethnopharmacol 2005; 97: 497–501

24 Pal PB, Sinha K, Sil PC. Mangiferin, a natural xanthone, protects murine liver in Pb (II) induced hepatic damage and cell death via MAP kinase, NFκB and mitochondria dependent pathways. PLoS One 2013; 8: e56894 (DOI: 10.1371/journal.pone.0056894)

25 Miyake Y, Yamamotoi K, Osawa T. Isolation of eriocitrin (eriodictyol 7-rutinoside) from lemon fruit (Citrus limon BURM. f.) and its antioxidative activity. Food Sci Technol Int Tokyo 1997; 3: 84–89

26 Garg A, Garg S, Zaneveld LJD, Singla AK. Chemistry and pharmacology of the citrus bioflavonoid hesperidin. Pytother Res 2001; 15: 655–669

27 Fujimoto H, Hirase T, Miyazaki Y, Hara H, Ide-Iwata N, Nishimoto-Hazuku A, Saris CJM, Yoshida H, Node K. IL-27 Inhibits hyperglycemia and pancreatic islet inflammation induced by streptozotocin in mice. Am J Pathol 2011; 179: 2327–2336

28 Mabley JG, Suarez-Pinzon WL, Hasko G, Salzman AL, Rabinovitch A, Kun E, Szabo C. Inhibition of poly (ADP-ribose) synthetase by gene disruption or inhibition with 5-iodo-6-amino-1, 2-benzopyrone protects mice from multiple-low-dose-streptozotocin-induced diabetes. Br J Pharmacol 2001; 133: 909–919

29 Chellan N, De Beer D, Muller CJF, Joubert E, Louw J. A toxicological assessment of Athrixia phylicoides aqueous extract following chronic ingestion in a rat model. Hum Exp Toxicol 2008; 27: 819–825

30 Maurad N, Zager R, Neveu P. Semi-automated enzymatic method for determining serum triglycerides by use of the Beckman DSA 560. Clin Chem 1973; 19: 116–118

31 Grisham MB, Johnson GG, Lancaster jr. JR. Quantitation of nitrate and nitrite in extracellular fluids. Methods Enzymol 1996; 268: 237–246

264

ADDENDUM 2 - Animal ethical clearance

UNIVERSITEIT·STELLENBOSCH·UNIVERSITY
jou kennisvennoot • your knowledge partner

4 August 2011

Miss N Chellan (15268322)
Diabetes Discovery Platform
South African Medical Research Council
Francie van Zijl Drive
Parow Valley, 7505, Cape Town

E-MAILED and **MAILED**

Dear Miss Chellan

Application for Ethical Clearance:
The effect of *Cyclopia maculate* extract on B-cell function, protection against oxidative stress
and cell survival.
Ref: 11GK_CHE01

Your application for ethics clearance has been approved by the Research Ethics Committee:
Animal Care and Use (REC: ACU). Please note that this clearance is only valid for a period of
twelve months. Ethics clearance of protocols spanning more than one year must be renewed
annually through submission of a progress report, up to a maximum of three years.

Applicants are reminded that they are expected to comply with accepted standards for
the use of animals in research and teaching as reflected in the South African National
Standards 10386: 2008. The SANS 10386: 2008 document is available on the Division for
Research Development's website www.sun.ac.za/research .

Please feel free to contact me if any additional information is needed.

Kind regards

Mr. WA Beukes (Secretary: REC: ACU)

APPROVED
0 3 AUG 2011

DIE UNIVERSITEIT VAN STELLENBOSCH
THE UNIVERSITY OF STELLENBOSCH
0 4 AUG 2011

Mr · Mnr WA Beukes
Afdeling: Navorsingsontwikkeling • Division: Research Development
Privaat Sak/Private Bag·Matieland 7602·Suid-Afrika/ South Africa
Tel +27 21 808 9003 • E-mail wabeukes@sun.ac.za • Faks/Fax: +27 021 808 4537

265

UNIVERSITEIT·STELLENBOSCH·UNIVERSITY
jou kennisvennoot · your knowledge partner

13 September 2011

Miss N Chellan
Diabetes Discovery Platform
South African Medical Research Council
Francie van Zijl Drive
Parow Valley, 7505, Cape Town

E-MAILED and **MAILED**

Dear Miss Chellan

Application for an Amendment to study:
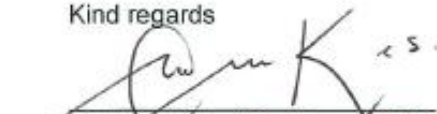The effect of *Cyclopia maculate* extract on B-cell function, protection against oxidative stress and cell survival.
Ref: 11GK_CHE01

Your application for amendments to your study has been approved by the Research Ethics Committee: Animal Care and Use (REC: ACU). Please note that this approval in conjunction with your original clearance certificate is only valid for a period of twelve months. Ethics clearance of protocols spanning more than one year must be renewed annually through submission of a progress report, up to a maximum of three years.

Below please find the approved amendments as requested by you:

1. On p 10, "the animals will be fasted for four hours (from 07h00)" – it should be noted by the applicant that this is not a fasting value, but rather a fed value as the animals feed during the night. Changed to a 16-hour overnight fast.

2. On p10, it is advised that the oral glucose tolerance test should include time points at 5 min and 15 min as well; otherwise the changes in the curve may be missed. Included 5 and 15 min time points.

APPROVED
1 3 SEP 2011
Approval date
for amendments.
WAB

UNIVERSITEIT VAN STELLENBOSCH
1 3 SEP 2011
THE UNIVERSITY OF STELLENBOSCH
DIE

Mr · Mnr WA Beukes
Afdeling: Navorsingsontwikkeling · Division: Research Development
Privaat Sak/Private Bag·Matieland 7602·Suid-Afrika/ South Africa
Tel +27 21 808 9003 · E-mail wabeukes@sun.ac.za · Faks/Fax: +27 021 808 4537

ADDENDUM 3 - Reagents and equipment

1. Citrate buffer

588 mg sodium citrate (Cat no. W302600, Sigma-Aldrich) + 20 ml distilled water (pH to 4.5 with concentrated HCl).

2. Gelatine jelly cubes

Pick 'n Pay® brand raspberry flavoured jelly (Pick 'n Pay Retailers Pty Ltd., Gauteng, South Africa) was used. Ingredients listed on the package were: sugar, bovine gelatine, acidity regulators, artificial flavourant (raspberry) and colourant (No added vitamin C). Eighty grams of Pick 'n Pay® brand raspberry flavoured jelly was supplemented with 7 g of bovine gelatine (Sheridans Gelatine, Libstar Manufacturing Solutions Pty Ltd, Gauteng, South Africa). Gelatine jelly powder was dissolved in 300 ml of distilled water.

3. Krebs's-Ringer bicarbonate HEPES buffer (all reagents from Sigma-Aldrich)

Component	mmol/L
NaCl (Cat No. S5886)	115
$NaHCO_3$ (Cat No. S3817)	24
KCl (Cat No. P5405)	5
$MgCl_2$ (Cat No. M4880)	1
$CaCl_2$ (Cat No. C5670)	2.5
2% BSA (Cat No. A4919)	
10 mM HEPES Buffer (Cat No. H3375)	

4. Sorensen's glycine buffer

0.751 g glycine (0.1M) (Cat no. 2139410, AnalaR Laboratories, Poole, England) + 0.584 g NaCl (0.1M) (Cat no. AB006404.500, Merck Millipore) in 100 ml cell culture tested water.

4 g NaOH (1M) (Cat no. 10252, AnalaR Laboratories) in 100 ml cell culture tested water (to equilibrate buffer to pH 10.5).

5. Transfer buffer

25 mM Tris (Cat no. 93352, Sigma-Aldrich) + 192 mM glycine (Cat no. 50046, Sigma-Aldrich) + 200 mL made up to 1 L in distilled water.

6. Tris buffered saline Tween

20 mM Tris (Cat no. 93352, Sigma-Aldrich) + 137 mM NaCl (Cat no. S3014, Sigma-Aldrich)

+ 1 mL Tween20 made up to 1 L in distilled water.

List of equipment

Description	Manufacturer
Absorbance microplate reader (ELX800)	Bio-Tek Instruments; Friedrichshall, Germany
Automated tissue processer (TP1020)	Leica Biosystems; Nussloch, Germany
Benchtop centrifuge (SL 16R)	Thermo Fisher Scientific
Benchtop microfuge (5415 R)	Eppendorf
Benchtop microfuge (5810 R)	Eppendorf
Biohazard safety cabinet, class II	Airvolution; Johannesburg, South Africa
Bio-Rad ChemiDoc imaging device (170-8265)	Bio-Rad
Cell/tissue homogeniser (85600)	Retsch Technology; Haan, Germany
Countess™ automated cell counter (C10227)	Invitrogen
Fluorometric microplate reader (FLX800)	Bio-Tek Instruments
Heating block	Labnet International Inc.; NJ, USA
Incubator (Galaxy R)	RS Biotech; West Lothian, United Kingdom
Inverted fluorescent microscope (Eclipse Ti)	Nikon; NY, USA
Inverted microscope (CKX 41)	Olympus; NY, USA
Liquid scintillation analyser (ParkardTricarb series 2810 TR)	Perkin Elmer
PowerPac™ HC	Bio-Rad
Quantity One Software	Bio-Rad
Rotary microtome (Leica RM 2125RT)	Leica Biosystems
Stereo microscope (Wild)	Wild, Heerbrugg, Johannesburg, South Africa
Waterbath	Memmert; Heilbronn, Germany
Software	**Manufacturer**
Gen5 software (version 1.05)	Bio-Tek Instruments
Graphpad Prism® (version 5.0)	Graphpad Software; CA, USA
Leica Qwin Software	Leica Microsystems; Nussloch, Germany
Microsoft Excel 2013	Microsoft Corporation; WA, USA
Quantity One 1-D software (version 1.02)	Bio-Rad

List of reagents

Description	Catalogue No.	Manufacturer
3-(4,5-dimethylthiazol-2-yl)-2,5-diphenyltetrazolium (MTT)	M5655	Sigma-Aldrich; St Louis, MO, USA
Annexin-v conjugate	A9210	Sigma-Aldrich
Anti-rabbit IgG	sc-2317	Santa Cruz Biotechnology; CA, USA
Assay plate (96 well, clear)	655101	Greiner Bio-One; Frickenhausen, Germany
Beta-mercaptoethanol	60-24-2	Sigma-Aldrich
Beta-tubulin antibody	2146	Cell Signalling Technology; Danvers, MA, USA
Bovine serum albumin (BSA)	A4919	Sigma-Aldrich
Bovine serum albumin (BSA) - free fatty acid free	A1302-25G	Sigma-Aldrich
Bradford protein assay kit	500-0203	Bio-Rad; CA, USA
Buffered formalin (10 %)	-	KIMIX Chemicals; South Africa
Carbon dioxide (CO_2)	K239C	Air Products; Centurion, Cape Town, South Africa
Cell culture 24 well plate (clear)	662160	Greiner Bio-One
Cell culture 96 well plate (black)	655077	Greiner Bio-One
Cell culture 96 well plate (clear)	655160	Greiner Bio-One
Cell culture 96 well plate (white)	22915	Porvair; Leatherhead, UK
Cell culture flask (75 cm^2)	658975	Greiner Bio-One
Cell scrapers	P0500	Sigma-Aldrich
Collagenase P type I from *Clostridium histolyticum*	C0130	Sigma-Aldrich
Commercial cell lysis buffer	FNN0011	Life Technologies; CA, USA
Countess™ chamber slides	C10228	Invitrogen; CA, USA
Cruz marker	sc-2035	Santa Cruz Biotechnology
Cryogenic vial (2 mL)	122279	Greiner Bio-One
Crystal violet	C3886	Sigma-Aldrich
Diaminobenzidine Plus kit	K3468	DAKO; Glostrupt, Denmark
Dextrose-Fresenius 50% solution	-	Intramed; Port Elizabeth, South Africa
Diaminofluorescein-FM diacetate (DAF)	292648	Sigma-Aldrich
Dihydroethidium	37291	Sigma-Aldrich
Dimethyl sulfoxide (DMSO)	D4540	Sigma-Aldrich
Dulbecco's phosphate buffered saline (DPBS)	17-513	Lonza; MD, USA

Description	Catalogue No.	Manufacturer
Envision kit	K5355	DAKO
Eppendforf tube (2 mL)	22363344	Eppendorf, Hamburg, Germany
Ethanol	E7023	Sigma-Aldrich
Fermentas PageRuler prestained marker	26616	Thermo Fisher Scientific; MA, USA
Fetal bovine serum (FBS)	SH3007903HI	Thermo Fisher Scientific
Fluo-3AM	F14218	Invitrogen
Geneticin	11464990	Roche Diagnostics; IN, USA
Glucometer (OneTouch Select)	-	Johnson and Johnson Medical; Johannesburg, South Africa
Glucose (cell culture tested)	G7021	Sigma-Aldrich
Griess reagent	G4410	Sigma-Aldrich
Haematoxylin	MHS1	Sigma-Aldrich
Hank's balanced salt solution (HBSS)	14025	Invitrogen
Histopaque 1077	10771	Sigma-Aldrich
Histopaque 1083	10831	Sigma-Aldrich
Histopaque 1119	1191	Sigma-Aldrich
Homogenising beads (steel)	69989	Qiagen; Hilden, Germany
Hydrochloric acid	320331	Sigma-Aldrich
Hydrogen peroxide	107209	Merck Millipore; MA, USA
Immobilon-P polyvinylidene difluoride (PVDF) membrane	IPVH00010	Merck Millipore
Insulin ELISA kit	EZRMI-13K	Merck Millipore
Interferon gamma (IFN-γ)	I3275	Sigma-Aldrich
Interleukin-1 beta (IL-1β)	I2393	Sigma-Aldrich
K_2 ethylenediaminetetraacetic acid (EDTA) tube	368861	BD Biosciences; Woodmead, South Africa
Laemmli sample buffer (4 x concentrate)	161-0747	Bio-Rad
LumiGLO® chemiluminescent substrate	54-71-01	Kirkegaard & Perry Laboratories (KPL); MD, USA
Mangiferin	M3547	Sigma-Aldrich
Metformin	D150959	Sigma-Aldrich
Methanol	67-56-1	Sigma-Aldrich
MIB-5 antibody	M7248	DAKO
Milk powder (non-fat)	2082054	Clover; Johannesburg, South Africa
N-acetyl cysteine (NAC)	A9165	Sigma-Aldrich

Description	Catalogue No.	Manufacturer
Neonatal 26 G canula	NM126	Neotec Medical Industries; Jalan Bukit Merah, Singapore
Palmitic acid (PA)	P0500	Sigma-Aldrich
Penicillin and streptomycin	17602	Lonza
Phenylmethanesulfonyl fluoride (PMSF)	78830	Sigma-Aldrich
Ponceau S stain	P23295	Sigma-Aldrich
Pre-cast sodium dodecyl sulphate polyacrylamide gels	161-0993	Bio-Rad
Propidium iodide	P4170	Sigma-Aldrich
Protease inhibitors	11206893001	Roche Diagnostics
Pure Harvest rat/mouse pellets	-	Afresh Vention (PTY) LTD; Durbanville, South Africa
RC DC protein kit	500-0119	Bio-Rad
RIN-5F rat insulinoma cells	95090402	European Collection of Cell Cultures; Salisbury, UK
Roswell Park Memorial Institute 1640 (RPMI1460)	12-702F	Lonza
Running buffer (electrophoresis)	161-0772	Bio-Rad
Scintillation fluid (Ultima Gold)	6013329	Perkin Elmer; CA, USA
Serum separating tube (SST)	367955	BD Biosciences
Sodium dodecyl sulfate	L3771	Sigma-Aldrich
Sodium hydroxide	S5881	Sigma-Aldrich
Sodium pentobarbital euthanase	-	Bayer Pty. Ltd., Animal Health Division; Isando, South Africa
Sterile tube (15 mL)	188261	Greiner Bio-One
Sterile tube (50 mL)	227261	Greiner Bio-One
Strepavidin ABC	SA-5704	Vector Labs; CA, USA
Streptozotocin (STZ)	S0130	Sigma-Aldrich
Stripping buffer	46430	Thermo Fisher Scientific
Syringe-driven sterile filter	SLGP033RS	Merck Millipore
Tris	93352	Sigma-Aldrich
Triton X-100	648465	Merck Millipore
Trypan blue	T10282	Invitrogen;
Trypsin-versene	17-161F	Lonza
Tumour necrosis factor alpha (TNF-α)	PMC3014	Invitrogen
Tween20	58980C	Sigma-Aldrich
ViaLight™ plus ATP kit	LT07-321	Lonza
Water (cell culture tested)	W3500	Sigma-Aldrich

ADDENDUM 4 - Supplementary data

Table 9. Liver enzyme levels of treated (A**) and pretreated (**B**) diabetic Wistar rats.**

A.

	S-AP (u/L)	S-AST (u/L)	S-ALT (u/L)
Normal Control	86.00 ± 15.36	48.38 ± 2.24	110.25 ± 5.65
STZ Control	240.00 ± 58.03	87.00 ± 13.70	157.38 ± 37.34
Metformin	467.67 ± 124.43	93.50 ± 11.49	181.00 ± 11.31
NAC	238.86 ± 97.19	70.00 ± 14.76	192.29 ± 23.63
30 mg/kg/d C. mac.	482.86 ± 171.73	86.29 ± 13.86	218.29 ± 22.46
300 mg/kg/d C. mac.	330.86 ± 84.10	64.14 ± 8.15	167.29 ± 14.29

B.

	S-AP (u/L)	S-AST (u/L)	S-ALT (u/L)
Normal Control	86.00 ± 15.36	48.38 ± 2.24	110.25 ± 5.65
STZ Control	125.91 ± 22.86	65.63 ± 10.07	127.75 ± 14.99
Metformin	85.25 ± 23.82	52.00 ± 6.34	130.25 ± 7.44
NAC	137.57 ± 35.96	85.43 ± 26.78	172.43 ± 37.78
30 mg/kg/d C. mac.	143.88 ± 56.18	57.63 ± 10.13	141.13 ± 15.01
300 mg/kg/d C. mac.	71.75 ± 7.57	46.38 ± 5.42	127.13 ± 11.08

Table 10. Pancreas and islet area measurements (A) and β- and α-cell counts (B).

A.

	Total tissue area	Total islet area	Total α-cell area	Total β-cell area	Total islet: Total tissue area
Normal Control	62520715.70 ± 6092136.21	546541.19 ± 67240.48	74250.94 ± 8903.44	447078.83 ± 61441.42	0.91 ± 0.15
STZ Control	58245134.43 ± 8338433.03	241945.74 ± 64012.38	92403.34 ± 22426.53	100056.91 ± 34244.34	0.40 ± 0.06
Metformin	64881248.73 ± 4599052.32	396617.75 ± 49964.07	96116.29 ± 13674.33	246239.47 ± 49034.11	0.64 ± 0.10
NAC	68275082.58 ± 13433310.98	322881.19 ± 100407.09	91416.21 ± 28913.93	163050.88 ± 68016.94	0.46 ± 0.12
30 mg/kg C.mac.	53295925.94 ± 6712864.26	361136.25 ± 84212.37	72078.30 ± 11871.57	240458.52 ± 75524.90	0.72 ± 0.13
300 mg/kg C.mac.	64202644.21 ± 5560970.04	289844.49 ± 67671.21	71589.56 ± 23542.55	170353.20 ± 37193.37	0.45 ± 0.09

B.

	Total no. α-cells	Total no. β-cells	Total β-cell area: Total no. β-cells
Normal Control	435.50 ± 36.38	1156.25 ± 115.65	381.71 ± 18.64
STZ Control	457.63 ± 122.01	240.25 ± 71.74	374.45 ± 38.10
Metformin	530.29 ± 67.02	598.71 ± 163.96	458.71 ± 42.76
NAC	290.00 ± 23.10	336.38 ± 187.72	640.66 ± 155.98
30 mg/kg C.mac.	373.50 ± 67.01	550.38 ± 169.53	728.72 ± 246.42
300 mg/kg C.mac.	348.29 ± 98.99	388.14 ± 74.76	433.08 ± 29.73

ADDENDUM 5 - Digital copy of dissertation